The morphology, growth and metabolic state of *Fusarium venenatum* in cation modified media

Jeffrey McGeorge

PhD

2018

The morphology, growth and metabolic state of *Fusarium venenatum* in cation modified media

Jeffrey McGeorge B.Sc. M.Sc.

A thesis submitted in partial fulfilment
of the requirements of the
University of Northumbria at Newcastle
for the degree of
Doctor of Philosophy

Research undertaken in the
Faculty of Applied Sciences
in collaboration with
Quorn foods.
December 2018

Abstract

Fusarium venenatum is a filamentous ascomycete fungus that is currently used in the production of Quorn™ food products. This is an important organism for research as there is scope for increasing our knowledge of the fungus in order to develop and improve production methods. This research involved investigating the morphology and metabolic responses of *F. venenatum* when grown in media modified in the amounts of iron and calcium, and in recycled growth medium. This type of analysis has not been attempted before in this fungus.

Methods were developed for the analysis of the intracellular metabolites and proteins using LC-MS/MS technology, along with software and database searches. Targeted analysis of amino acids by GC-MS was also carried out. The morphology of the fungus was measured using light-microscopy and software.

Increases in the length of the hyphae and decreases in branching were observed in iron-limited cultures, and the branching was increased in calcium-limited medium. These results could be significant for Quorn™ production as the morphology could affect the texture and quality of the product.

In the iron-limited condition there was a downregulation of amino acid synthesis, with a 31% reduction of total amino acids without any reduction in biomass. The metabolome and proteome results revealed that many diverse pathways were affected. For example, respiration was downregulated in the iron-limited cultures but upregulated in excess iron cultures. Knowledge of changes in metabolites such as amino acids and nucleotides could lead to the development of ways to control the flavour of the product.

The growth of the fungus in recycled medium showed a significant increase in biomass, although there were changes to the morphology. This is a significant result as the use of recycled media would reduce expensive wastewater treatment, decrease waste, and a higher biomass would increase profitability.

Table of Contents

List of abbreviations

2SM	2 stage medium
3-ADN	3-acetyldeoxynivalenol
α-IPM	α-isopropylmalate
ACP	Acid phosphatase
AGC	Automatic gain control
AICRP	5-aminoimidazole-4-carboxamide ribonucleotide phosphate
AIR	5-aminoimidazole ribonucleotide
AMP	Adenosine monophosphate
ANOVA	Analysis of variance
APS	Ammonium persulfate
ATP	Adenosine triphosphate
ACN	Acetonitrile
CAT	Carnitine acetyltransferase
CCD	Conserved domain search
cDNA	Complimentary DNA
CHAPS	3-[(3-cholamidopropyl)dimethylammonio]-1-propanesulfonate
CoA	Coenzyme A
CSI	Compound structure identification
DDA	Data dependent analysis
dH_2O	deionised H_2O
DNA	Deoxyribonucleic acid
DNS	Dinitrosalicylic acid
DTT	Dithiothreitol
EDTA	Ethylenediaminetetraacetic acid
EGTA	Ethylene glycol-bis(β-aminoethyl ether)-N,N,N′,N′-tetraacetic acid
EI	Electron impact
ESI	Electrospray ionisation
EST	Expressed sequence tags
FADH	Flavin adenine dinucleotide (reduced)
FGAM	Formylglycinamidine ribonucleotide
G	Hyphal growth unit (G= length ÷ number of tips)
GABA	γ-aminobutyric acid
GAR	Glycinamide ribonucleotide
GC	Gas chromatography
GC-MS	Gas chromatography - Mass spectrometry
GMP	Guanosine monophosphate
GTP	Guanosine triphosphate
HACS	High-affinity calcium uptake system
HESI	Heated electrospray ionisation
HFBII	Hydrophobin II
HIV	Human immunodeficiency virus
HPLC	High performance liquid chromatography
IAA	Iodoacetamide
IMP	Inosine monophosphate

InGP	Indole-3-glycerol phosphate
KEGG	Kyoto encyclopaedia of genes and genomes
LACS	low-affinity calcium uptake system
LC	Liquid chromatography
LC-MS	Liquid chromatography - mass spectrometry
LC-MS/MS	Liquid chromatography - tandem mass spectrometry
leu1	Isopropylmalate isomerase
MAP	Mitogen-activated protein
MM	Minimal medium
mRNA	Messenger ribonucleic acid
MS	Mass spectrometry
MS/MS	Tandem mass spectrometry
MSG	Monosodium glutamate
MW	Molecular weight
NADH	Nicotinamide adenine dinucleotide (reduced)
NCBI	National centre for biotechnology information
NCE	Normalised collision energy
NMR	Nuclear magnetic resonance
NO	Nitric oxide
NRP	Non-ribosomal peptide
NRPS	Non-ribosomal peptide synthetase
PCA	Principle component analysis
PDA	Potato dextrose agar
PIPES	Piperazine-N,N′-bis(2-ethanesulfonic acid)
PK	Polyketide
PMSF	Phenylmethane sulfonyl fluoride
PRA	N-(5’-phosphoribosyl)-anthranilate
PSA	Potato sucrose agar
QC	Quality control
RCF	Relative centrifugal force
RNA	Ribonucleic acid
ROS	Reactive oxygen species
RSD	Relative standard deviation
SDS	Sodium dodecyl sulfate
SDS-PAGE	sodium dodecyl sulfate polyacrylamide gel electrophoresis
SIRIUS	Sum formula identification by ranking isotope patterns using mass spectrometry
SOM	soil organic matter
SPK	Spitzenkörper
SPSS	Statistical package for the social sciences
SREB	Siderophore biosynthesis repressor
TCA (cycle)	Tricarboxylic acid (cycle)
TCA	Trichloroacetic acid
TEMED	Tetramethylethylenediamine
TFA	Tetrafluoroacetic acid
TIC	Total ion count
TML	6-N-trimethyllysine

TMSI:TMCS	Trimethylsilylimidazole: Trimethylchlorosilane
Tris	Tris(hydroxymethyl)aminomethane
tRNA	Transfer RNA
UDP	Uridine diphosphate
UGP	UDP-glucose pyrophosphorylase
UHPLC-DAD	Ultra high performance liquid chromatography - diode array detector
XMP	Xanthosine monophosphate
YES	Yeast extract agar
ZEA	Zearalenone

Acknowledgements

I would like to thank my supervisor Prof. Georgios Koutsidis for his help, support and guidance during my project, and my other supervisors Prof. Gary Black and Dr Lynn Dover who have also provided advice and assistance. I would also like to acknowledge the advice and support of my supervisors from Quorn foods, Dr Tim Finnigan and Dr Rob Johnson, and also Rachel Marsh at Quorn foods for providing me with samples of the fungus and materials for media preparation.

I would like to thank all of the technical staff in the department who gave me help during this project, as well as my colleagues in the laboratory, especially Matthew Knight who helped in the set-up and use of the instruments.

Declaration

I declare that the work contained in this thesis has not been submitted for any other award and that it is all my own work. I also confirm that this work fully acknowledges opinions, ideas and contributions from the work of others. The work was done in collaboration with Quorn foods.

Any ethical clearance for the research presented in this thesis has been approved. Approval has been sought and granted by the Faculty Ethics Committee on 31/3/2015.

I declare that the Word Count of this Thesis is 49,132 words

Name: Jeffrey McGeorge

Signature:

Date: 30/5/2019

1. Review of the taxonomy, growth characteristics and important metabolites in *Fusarium venenatum*

1.1 Introduction

1.1.1 Fungi of the genus *Fusarium.*

The *Fusaria* belong to the *Ascomycota* phylum of fungi, which are characterised by their having an ascus, a reproductive structure containing ascospores (Ingold, 1984). The genus itself is characterised by having elongate, curved macroconidia that are septate (Moss & Thrane, 2004). These fungi are widespread, and as well as dwelling in the soil, they can grow on plant surfaces as well as within plants as pathogens and endophytes (Postic *et al.*, 2012).

Most *Fusarium* species are harmless saprotrophs that live in the soil, but some members of this genus are significant plant pathogens (Lowe *et al.*, 2010). Based on the characteristics of some species the *Fusaria* have also been described by Geiser et al. (2004) as the single most important toxigenic fungi genus. This is due to the fact that along with *Aspergillus* and *Penicillium, Fusarium* is one of the main three genera of fungi that produce mycotoxins (Gong *et al.*, 2015). Mycotoxins are a substantial problem for agriculture as pathogenic *Fusarium* species infect crop plants and the grain becomes contaminated with these toxic compounds (Browne & Brindle, 2007). The mycotoxins can remain in plant material that is destined for human or animal consumption, even after processing and chemical treatment (Postic *et al.*, 2012).

The toxigenic and pathogenic species have made *Fusarium* a significant fungi genus for study, and their economic importance has been demonstrated by a number of *Fusarium*-caused plant diseases that have impacted world agriculture (Leslie & Summerell, 2006). *Fusarium* head blight affects small grain cereals such as wheat and barley (Ito *et al.*, 2012), and is caused by *Fusarium graminearum* and *Fusarium culmorum*, along with other species (Browne & Brindle, 2007). Other pathogenic species include *Fusarium oxysporum*, which causes vascular wilt, and *Fusarium verticillioides*, which causes stalk rot (Lowe *et al.*, 2010). Mycotoxins

cause annual losses of millions of dollars due to their effects on human and animal health, and contaminated food products (Edlayne *et al.*, 2009). In humans, *Fusarium* infections have a high mortality rate, and HIV patients are susceptible (Leslie & Summerell, 2006).

Fusarium venenatum is a species with no known sexual reproductive stage (Leslie & Summerell, 2006). Its macroconidia are short, slender and falcate with a pointed apical cell and foot shaped basal cell, and they mostly have 5 septa (Leslie & Summerell, 2006). The species can be found in Europe both in the soil and on various plant species (Leslie & Summerell, 2006).

A study by King *et al.* (2018) tested the pathogenicity of *F. venenatum* on plants but found that it was not able to cause disease symptoms on wheat and mycelia only grew on tomatoes after a prolonged period of 12 days. It was concluded that *F. venenatum* only had a limited ability to grow on living plant material, which was in contrast to its related species *F. graminearum* which caused significant bleaching of the wheat and produced mycelia on the tomato within only 4 days (King *et al.*, 2018).

1.1.2 *Fusarium venenatum*.

The fungus used to produce Quorn™ products was originally identified as *Fusarium graminearum* A3/5, but a study by O'Donnell *et al.* (1998) reclassified it as *Fusarium venenatum*. Molecular techniques were employed in this study, which used sequence data from 28S ribosomal DNA, and the β-tubulin gene to explore the phylogeny of the *Fusarium* genus (O'Donnell *et al.*, 1998). The results showed that the *Fusarium* strains used to produce Quorn™ products form a clade with the reference strains of *F. venenatum*, whereas *F. graminearum* strains were part of an outgroup (O'Donnell *et al.*, 1998). The assertion that the Quorn™ producing strains are *F. venenatum* is further supported by the mycotoxin analysis that showed that they were able produce type A trichothecenes while *F. graminearum* produces only type B trichothecenes and zearalenone (ZEA) (O'Donnell *et al.*, 1998).

A study of the *F. venenatum* genome by Berka *et al.* (2004) found evidence to suggest that the fungus contains four large (>10Mbp) chromosomes. In this study, *F. venenatum* mRNA was used to construct several cDNA libraries from cultures grown in different carbon sources and media (Berka *et al.*, 2004). These were sequenced to give expressed sequence tags (ESTs) that represented *F. venenatum* gene sequences (Berka *et al.*, 2004). The EST collection was then used to identify enzymes such as lysophospholipase and triacylglycerol lipase (Berka *et al.*, 2004).

The full genome of the related species *Fusarium graminearum* was revised and completed in a study by King *et al.*, (2015). This species also has 4 chromosomes and the sequence contains 36,563,796 bp, with a GC content of 48% (King *et al.*, 2015). In a more recent study, the full genome of *Fusarium venenatum* was sequenced and compared to that of *Fusarium graminearum* by King *et al.* (2018). The genomes of both species were found to be similar in length, completeness, number of chromosomes, and centromere position (King *et al.*, 2018). *F. venenatum* had a GC content of 47.6%, which was also similar to *F. graminearum* (King *et al.*, 2018). The chromosomes were 2.8% larger in *F. venenatum*, with chromosome 3 being 7% larger, and this was explained by an increase in repetitive elements and transposon sequences in this species (King *et al.*, 2018). The authors state that the *F. venenatum* genome is the most closely related to *F. graminearum* of a non-pathogenic species (King *et al.*, 2018). *Fusarium venenatum* A3/5 is the strain used to produce myco-protein for use in Quorn™ food products, which were first marketed in 1985 (Wiebe, 2004). It was developed as a protein source due to concerns that animal protein sources would eventually be insufficient to feed the population (Wiebe, 2002a), and a filamentous fungus was chosen because the morphology of the hyphae gives a texture similar to that of meat (Wiebe, 2004). It is grown in 120-150 m^3 air-lift bioreactors with a completely defined growth medium, based on glucose and ammonium and supplemented with biotin, with a culture temperature of 28-30 °C and pH 6.0 (Figure 1) (Wiebe, 2004). The fermentation is run as a continuous flow culture with a constant input of nutrients in which the level of residual glucose is kept constant – a type of fermentation

known as a nutrient-unlimited glucose-stat (Simpson et al., 1998). This type of cultivation is used because it maintains a higher level of biomass production, as opposed to batch culture (Trinci, 1994), and this gives a production rate of 300 to 350 kg h^{-1} of biomass (Wiebe, 2004).

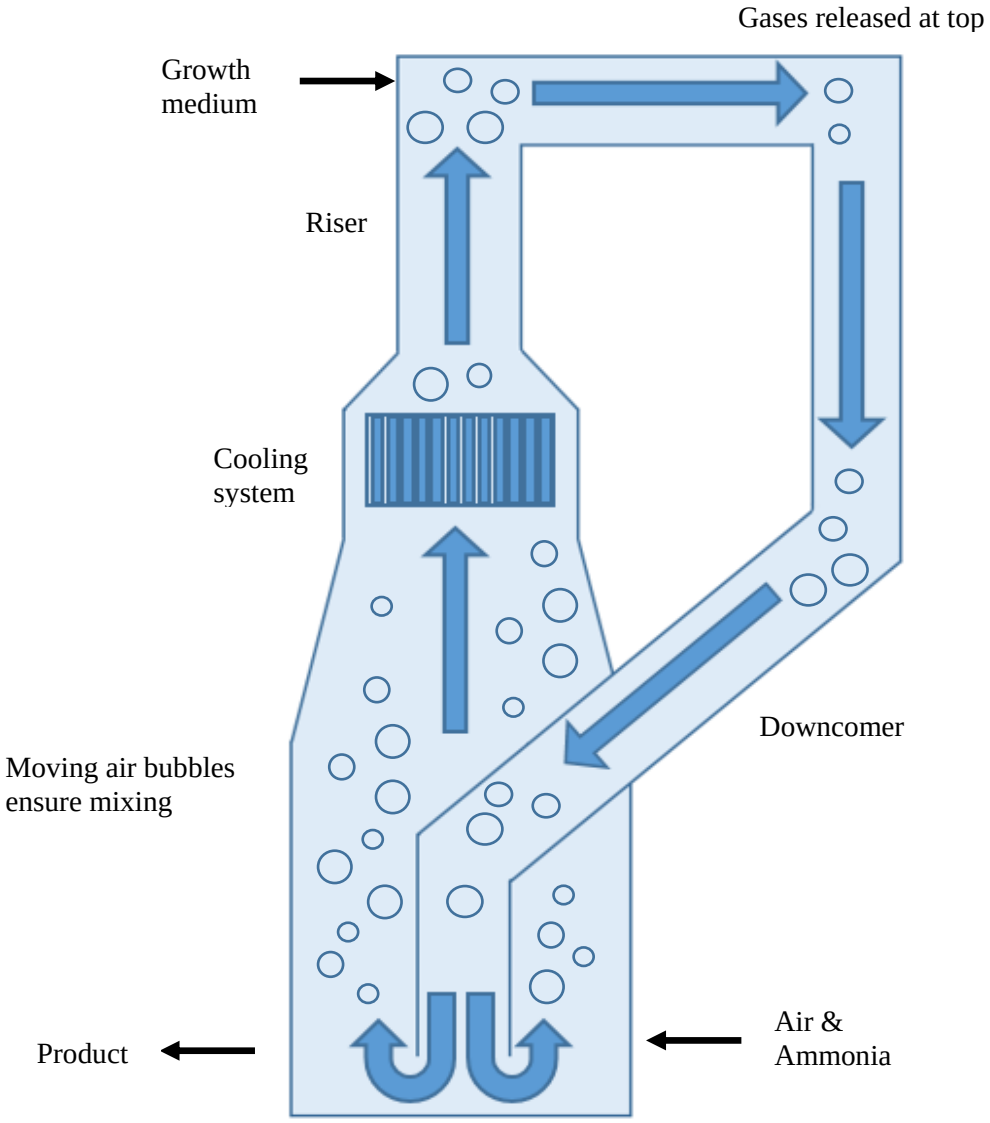

Figure 1: Diagram showing the Quorn fermentation system in an air-lift bioreactor (Wiebe, 2004).

Once the biomass is released from the fermenter it is then heated above 68 °C for 20-30 min in order to reduce the RNA content so that it complies with food safety standards (Wiebe, 2002). The RNA-reduced biomass is then mixed with either egg albumin or potato starch before being rolled to produce fibres that resemble meat (King et al., 2018). Although it is known that *F. venenatum* is capable of producing trichothecenes such as diacetoxyscirpenol (Lowe *et al.*, 2010), it has been shown using regular testing that these production conditions do not lead to the production of mycotoxins by this strain (Wiebe, 2004).

Quorn Foods currently sells its meat-substitute products in 16 countries and had sales of £150.3 million in 2014, with ambitions of creating a business worth $1 billion (Grandhi, 2015). The Quorn Foods company was recently sold to Monde Nissin, a Philippines-based company, for £550 million, which more than doubled the £205 million investment of its previous owner Exponent, which acquired the business in 2011 (Grandhi, 2015).

1.1.3 Growth and morphology of filamentous fungi

Ascomycete fungi grow by extension of their cells at the tips of hyphae, and by doing so can produce networks of hyphae known as mycelia that cover vast areas, which can take advantage of nutrients that they can transport within the network from nutrient-rich areas to nutrient-poor areas (Jennings, 1996). The hyphae are essentially tubes surrounded by cell wall material which is composed of a mixture of glycoproteins, polysaccharides (mainly β-1,3-glucan), and chitin (Bowman & Free, 2006). Chitin is a polymer of β-1,4-linked N-acetyl glucosamine, and makes up around 10-20% of the cell wall (Bowman & Free, 2006). The cells of the hyphae are not divided by cross walls, but instead septa are formed with pores that allow the movement of water and dissolved compounds, as well as organelles (Jennings, 1996).

Filamentous fungal growth begins from the spore, which first produces a germ tube that utilises materials from the spore itself and continues its growth by the uptake of medium components (Papagianni, 2004). The growth of the hyphae is polarised, with elongation

occurring at the tips (Grimm *et al.*, 2005); the rate of wall synthesis at the tip of the hyphae can be as much as 50 times greater than the region behind it (Papagianni, 2004). The initial period of growth is exponential, using material reserves that were held in the spore, but eventually the growth slows to a constant rate (Papagianni, 2004). The rate of growth at the tip is dependent on the supply of materials from other regions, and this can be limited by transport of these materials (Papagianni, 2004).

In order for the growing apex of the hyphae to produce new material, wall-building vesicles are delivered to this region (Dijksterhuis & Molenaar, 2013). The vesicles provide the materials to manufacture new cell membrane and enzymes for the synthesis of the chitin and glucans that will become new cell wall (Brand & Gow, 2009). These wall-building vesicles travel to the tip via the microtubules of the cytoskeleton, helped by motor proteins (Dijksterhuis & Molenaar, 2013). At the growing tip is the hyphal tip complex which consists of the spitzenkörper (SPK), the polarisome and the exocyst (Lin *et al.*, 2014). The SPK has been described as a vesicle supply centre for wall-building vesicles (Dijksterhuis & Molenaar, 2013), and is composed of vesicles (such as chitosomes and calcium-containing vesicles), proteins (such as F-actin, tubulin, formins and calmodulin), and ribosomes (Meyer *et al.*, 2009). The polarisome is a collection of proteins that mark a region for polarised growth that includes Ras-GTPase and Rho-GTPase (Brand & Gow, 2009). It is thought the polarisome has a role in nucleation of actin filaments and ensuring maximum growth rate (Meyer *et al.*, 2009). The exocyst is a group of 8 proteins that are responsible for the docking and fusion of vesicles with the membrane for exocytosis (Lipschutz & Mostov, 2002). Research by Dijksterhuis & Molenaar (2013) investigated the flow of vesicles from the cytoplasm to the SPK at the apical plasma membrane in *Rhizoctonia solani* and showed the turnover time of vesicles at the SPK was 1.3–2.5 min and that the rate of membrane addition to the tip (53 $\mu m^2\ min^{-1}$) is consistent with its extension rate (1.8 $\mu m\ min^{-1}$). At intervals, the growing hypha produces lateral branches, which also grow by extension at their tips (Papagianni, 2004).

1.1.4 Hydrophobins and their expression in filamentous fungi.

Filamentous fungi are uniquely responsible for the production of hydrophobins (Cox & Hooley, 2009), which are proteins that are able to self-assemble at hydrophilic-hydrophobic interfaces into monolayers (Bayry *et al.*, 2012). Bioinformatic analysis of fungal genomes has revealed that many distinct forms exist, and these may have been overlooked in the past (Bayry *et al.*, 2012). The hydrophobins are important to the fungi as they have significant roles at varying points in the fungal life cycle, for example: they allow the formation of an aerial mycelium by decreasing the surface tension of water; and they form layers on the conidia and hyphae to allow dispersal into the air or water (Minenko *et al.*, 2014). They can also form gas channels to provide gas exchange for the fungus in wet conditions (Scholtmeijer *et al.*, 2002). These functions are based on the highly surfactant properties of the hydrophobins (Bayry *et al.*, 2012). Sequencing of the genome of *F. graminearum* has revealed 5 hydrophobin genes (Minenko *et al.*, 2014). It has been found that if brewing malt is infected by *F. graminearum* then the beer produced will be affected by gushing (over-foaming, caused by hydrophobins) (Minenko *et al.*, 2014).

Hydrophobins are of great interest as they have numerous potential uses in biotechnology such as the production of emulsions for low fat foods, improving biocompatibility of medical implants, and nanotechnology (Cox & Hooley, 2009). Hydrophobins are not toxic, making them safe for use with foods or drugs (Valo *et al.*, 2010).

The reduction of lipid in low-fat food production could be aided by using small air bubbles that resemble fat droplets (Tchuenbou-Magaia *et al.*, 2009). These bubbles are unstable however, which reduces their shelf life but the use of hydrophobins as a stabilising molecule is proposed by the authors (Tchuenbou-Magaia *et al.*, 2009).

Nanoparticles can be used to increase the bioavailability of drugs that would otherwise have poor solubility, poor permeation, and stability problems in the digestive system (Valo *et al.*, 2010). Surfactants need to be used with nanoparticle systems to allow them to be delivered into the body without aggregation (Valo *et al.*, 2010). Class II hydrophobin HFBII from

Trichoderma reesei was used successfully to coat drug nanoparticles and it is suggested that this will improve bioavailability and targeting of the drug (Valo *et al.*, 2010).

The expression of hydrophobins in different growth conditions was investigated by Nakari-Setala *et al.* (1997). It was found that the carbon source affected the expression of hydrophobin genes, for example the *hfb2* gene was expressed on cellobiose, lactose, cellulose, xylan and plant material whereas the *hfb1* gene was not expressed with these media (Nakari-Setälä *et al.*, 1997). The authors also suggested that *hfb2* expression is triggered in conditions of starvation of carbon and nitrogen (Nakari-Setälä *et al.*, 1997).

1.1.5 Sulfur and fungal biochemistry.

Sulfur is an essential nutrient for fungal cells, due to its inclusion in the structures of the amino acids cysteine and methionine (Marzluf, 1997). Cysteine is important for the structure and function of many proteins, for example the hydrophobins, which contain a conserved pattern of eight cysteine residues, involved in the formation of disulfide bridges to stabilise the structure (Bayry *et al.*, 2012). Sulfur also forms part of a number of enzymes as part of an iron-sulfur complex, for example in cytochrome c oxidoreductase, which is responsible for transferring electrons from ubiquinol to cytochrome c, in the mitochondrial respiratory chain (de Paulo Martins *et al.*, 2011) (Figure 2).

Inorganic sulfate is utilised by filamentous fungi via a pathway in which it is first phosphorylated to 3'phosphoadenosine-5'phosphosulfate, then it is reduced to sulfite and afterwards to sulfide (Marzluf, 1997). The resulting sulfide is then used with *o*-acetyl serine to produce cysteine, which can then be used to make methionine and S-adenosylmethionine (Marzluf, 1997).

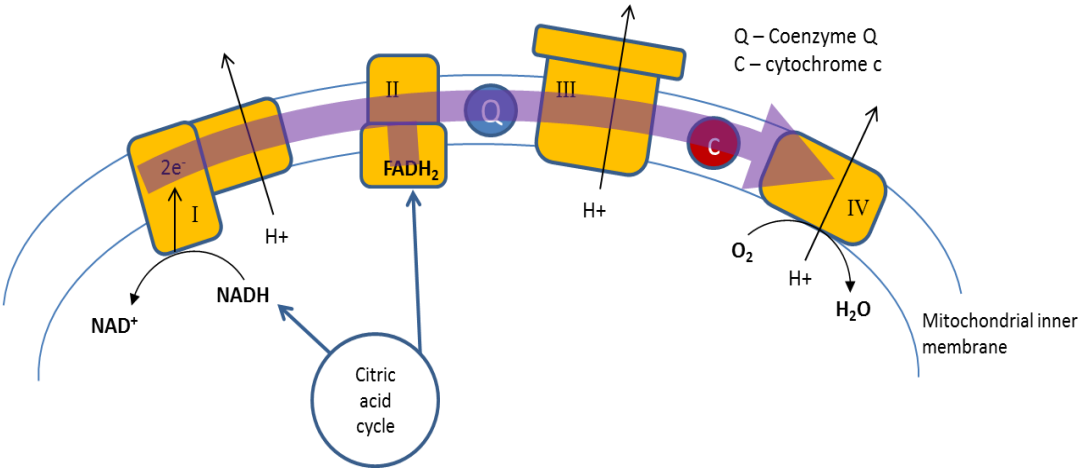

I - NADH-Q oxidoreductase: 2 electrons are transferred from NADH to FMN ($FMNH_2$), and then the Fe-S cluster passes these to coenzyme Q (QH_2).

II- Succinate Q reductase: $FADH_2$ passes 2 electrons to the Fe-S cluster, and then to coenzyme Q (QH_2).

III- Q – cytochrome c oxidoreductase: each QH_2 transfers 2 electrons to 2 cytochrome c molecules (1 electron to each) via the Fe-S cluster and haem groups.

IV - Cytochrome c oxidase: 2 cytochrome c molecules each pass 1 electron through the copper centre and haem group to the final Fe and Cu ions which then bind O_2 (O_2^{2-}); 2 further cytochrome c molecules each pass 1 electron to the O_2^{2-} ; and then $4H^+$ ions are added to produce H_2O.

Figure 2: Respiratory chain. Adapted from Berg et al., (2006)

In yeast, there are two transporters for moving sulfate into the cell, Sul1p and Sul2p (Cherest *et al.*, 1997). The transport system allows the cells to regulate their sulfate uptake, as has been shown in a study by Jennings & Cui (2012), which found that Sul2p is inactivated by an increase in extracellular sulfate. As well as sulfate, cysteine can also be transported directly into the cell both via non-specific transporters that function at high levels of cysteine, and Yct1p, a high-affinity specific cysteine transporter that can function at lower levels of cysteine (Kaur & Bachhawat, 2007).

1.1.6 Metabolites and flavour in food products

For organisms used in the food industry, another important consideration is how certain metabolites will affect the flavour of the final product, as metabolites such as amino acids, 5'-nucleotides and sugars contribute to the flavour of food products (Mau *et al.*, 2001).

The umami taste is described as a savoury or meat-like flavour and is accepted as the fifth basic taste alongside sweet, salty, bitter and sour (Zhang *et al.*, 2013). The precursor chemicals of the umami flavour are inosinic acid, glutamic acid and guanylic acid, which are metabolised to become inosine monophosphate disodium salt (IMP), glutamic acid monosodium salt (MSG) and guanosine monophosphate disodium salt (GMP), respectively, which are the three main umami flavour substances, alongside xanthosine monophosphate (XMP) (Zhang *et al.*, 2013). Although GMP and IMP themselves do not activate umami receptors, they act to intensify the effect of glutamate by up to 8 times, and thus there is a synergy between the nucleoside monophosphate salts and glutamate that increases the umami taste (Zhang *et al.*, 2013).

Amino acids can also affect flavour, and they have been classified based on their contribution: aspartic acid gives monosodium glutamate-like (MSG-like) flavour; alanine, glycine, serine and threonine give a sweet flavour; arginine, histidine, isoleucine, leucine, methionine,

phenylalanine, tryptophan, and valine give a bitter flavour; and lysine and tyrosine are categorised as tasteless (Mau *et al.*, 2001).

Amino acids are also important in cooked foods due to the Maillard reaction, in which they form condensation products with reducing sugars (Ames, 1998). The condensation products then go through further complex reactions to produce further compounds (Ames, 1998). The products of these reactions include volatile aroma compounds that affect the flavour of the food (Xu *et al.*, 2013), and the colour of the food can also be affected as these reactions lead to brown compounds called melanoidins (Ames, 1998).

1.2 The effect of growth medium components and inorganic ions on the growth and metabolism of filamentous fungi.

Most fungi only have simple nutritional requirements; they require an energy source such as glucose, a source of nitrogen such as ammonium or nitrate, phosphate ions, and trace amounts of minerals (Deacon, 2009). From these simple nutrients, most fungi can synthesise the components that they need (Deacon, 2009). The lifestyle of many fungi as immobile soil-dwelling organisms, however, dictates that they must use their growing mycelium to spread out and seek these required resources (Winkelmann, 2007). Life in the soil therefore means that these fungi are subject to changes in phenotype in response to interactions with the minerals available in their immediate environment (Cuero *et al.*, 2003).

One change in phenotype that has been shown to be affected by environmental factors is the production of secondary metabolites (Yin & Keller, 2011). These include factors such as carbon and nitrogen sources, temperature, light, and pH, and since secondary metabolism is costly to the fungus in terms of energy and resources, the production of secondary metabolites is switched on and off according to these conditions (Yin & Keller, 2011). Global transcription factors are used by the fungus to control secondary metabolite production, in accordance with signals from the environment, e.g. CreA for carbon signalling, AreA for nitrogen signalling

and PacC for pH signalling (Yin & Keller, 2011). The concentrations of inorganic ions are also known to affect fungal growth and mycotoxin production (Cuero *et al.*, 2003).

The exact environmental conditions used to grow the fungus are therefore very important, and variations in the growth medium have been shown to affect growth (Lowe *et al.*, 2010), protein production (Hosseini *et al.*, 2009), enzyme production (Panagiotou *et al.*, 2003), and secondary metabolite production (Hestbjerg *et al.*, 2002).

1.2.1 The effect of varying growth medium components on fungal growth & metabolism.

The primary metabolism of fungi was studied by Panagiotou *et al.* (2003), who investigated the production of xylanolytic enzymes by *F. oxysporum* under growth conditions that varied and optimised the nitrogen source, the moisture level, the temperature and pH of the culture (Panagiotou *et al.*, 2003). The results showed that an initial moisture level of 80% led to the highest enzyme activity, along with an optimal pH of 7, and a temperature of 27 °C (Panagiotou *et al.*, 2003). The optimum concentration of the nitrogen source varied according to the enzyme produced e.g. 7% was optimal for xylanase production (Panagiotou *et al.*, 2003).

The metabolome of *F. oxysporum* was investigated when the fungus was grown in aerobic/anaerobic conditions, different carbon sources, and different nitrogen sources (Panagiotou *et al.*, 2005a). It was found that the specific growth rate of the fungus varied according to the carbon source chosen (Panagiotou *et al.*, 2005a). The analysis of intracellular amino and non-amino acids showed that the carbon source in the growth medium affects the amounts of these metabolites (Panagiotou *et al.*, 2005a). The conclusion of this study was that the metabolite profile is affected by the carbon source, the O_2 supply and the cultivation phase of the fungus (Panagiotou *et al.*, 2005a). In a further study the aeration of the culture was shown to affect the metabolite profile, specifically in oxygen-limited fermentation of *F.*

oxysporum it was found that sedoheptulose-7-P accumulated revealing a block in the pentose phosphate pathway and resulted in the production of acetate (Panagiotou *et al.*, 2005b).

A study by Hestberg *et al.* (2002) compared the production of mycotoxins by *Fusarium* species in laboratory conditions and media prepared from soil organic matter. Results of GC-MS and HPLC analysis of selected metabolites showed that there was variation in secondary metabolite production between the 2 species tested (*F. culmorum* and *F. equiseti*) grown on the 3 types of media (yeast extract sucrose agar (YES), potato sucrose agar (PSA), and soil organic matter agar (SOM)) (Hestbjerg *et al.*, 2002). For example, most isolates of *F. culmorum* made ZEA on YES but only one isolate made ZEA on PSA, while some *F. equiseti* isolates made ZEA on PSA but none made ZEA on YES (Hestbjerg *et al.*, 2002). It was also found that most metabolites that were analysed are produced on the laboratory media, which was high in energy and nutrients, while only one of the known metabolites tested (chrysogine) was made when the SOM media was used (Hestbjerg *et al.*, 2002).

1.2.2 The effect of varying growth medium components on *Fusarium venenatum* growth & metabolism.

There have been few published studies so far on the effects of changing growth conditions on *F. venenatum*. One example is the study by Hosseini *et al.* (2009), which investigated protein production by *F. venenatum* grown in varying conditions. In particular the use of date sugar containing glucose, fructose, and sucrose as the carbon source to modify the medium defined by Vogel (1956) was investigated (Hosseini *et al.*, 2009). Results revealed that the concentration of the carbon and nitrogen sources were significant factors that had positive effects on the yield of protein (Hosseini *et al.*, 2009). In this study, only the protein production was measured, and the metabolome of the fungus was not analysed. The carbon source tested (date sugar) was a complex medium containing 3 sugars, and therefore there would be difficulty in isolating these variables to identify which was causing the changes in protein production.

The production of acid phosphatase (ACP) enzymes in *F. venenatum* in differing phosphate concentrations was investigated in a study by Hidayat *et al.* (2007). Results showed that ACP production was repressed by phosphate and de-repressed in phosphate-limited conditions (Hidayat *et al.*, 2007). ACP production was also affected by pH, since the highest production was at pH 3.3, and it is suggested that the PacC transcription factor is active in neutral or alkaline conditions and represses ACP gene expression, whereas in acidic conditions PacC is deactivated (Hidayat *et al.*, 2007).

A study by Lowe *et al.* (2010) investigated the basal metabolism of *Fusarium* species, which included *F. venenatum*, when they were grown in different culture conditions. Direct injection electrospray ionisation-mass spectrometry, and ^{1}H nuclear magnetic resonance (NMR) spectroscopy were used to examine the intracellular metabolomes of 9 isolates of the 4 chosen species: *F. graminearum*; *F. culmorum*; *F. pseudograminearum*; and *F. venenatum* A3/5 (Lowe *et al.*, 2010). The growth conditions were chosen to reflect the conditions that encourage the production of mycotoxins, and those that do not lead to mycotoxin production (Lowe *et al.*, 2010).

Initial results showed that the *F. graminearum*, *F. culmorum* and *F. pseudograminearum* isolates grew similarly on potato dextrose agar (PDA), but *F. venenatum* A3/5 grew slowest and had a yellow pigmentation (Lowe *et al.*, 2010). The isolates were grown on minimal medium (MM) for 48h, and 2 stage medium (2SM) for 48h and the intracellular metabolomes for each growth condition were compared (Lowe *et al.*, 2010). The MM contained lower concentrations of sucrose compared with 2SM, 2SM contained glycerol and NaCl, in MM the nitrogen source is nitrate rather than ammonia, and the MM does not induce mycotoxin production, whereas the 2SM does (Lowe *et al.*, 2010). The nutrient conditions were shown to affect the metabolites produced, e.g. when grown in the 2SM condition, it was found that the *Fusarium* metabolomes had higher concentrations of glycerol, mannitol and trehalose (Lowe *et al.*, 2010). In addition, the γ-aminobutyric acid (GABA) concentration was increased in all 2SM cultures (Lowe *et al.*, 2010). Comparisons between the isolates also showed variation,

e.g. in MM *F. venenatum* was found to accumulate less trehalose, glycerol, and glycine-betaine and more tyrosine, phenylalanine and tryptophan than the other isolates (Lowe *et al.*, 2010).

In summary, this study detected differences in metabolites between the isolates, and these differences were altered according to the culture conditions, which shows that the fungi intracellular metabolome can be changed in response to the environment (Lowe *et al.*, 2010). Overall, it was discovered that the nutrients supplied in the media influenced the metabolome more than the variation in the organism's genotypes (Lowe *et al.*, 2010). The authors suggest that fingerprinting the metabolome in this way could aid research that aims to compare the phenotype of an organism with the genome in order to identify the genes responsible for novel metabolites (Lowe *et al.*, 2010). However, this study aimed to analyse the intracellular metabolome only, and the extracellular metabolites measured were restricted to mycotoxins, which were investigated in only one of the growth conditions tested. The media chosen had variations in the nitrogen source, carbon source, and one condition had added glycerol and salts; this meant that there was no isolation of these variables to enable comparison.

1.2.3 Metal ions and fungal biochemistry.

Metal ions are an essential component of fungal nutrition; they are required for the structure of some proteins, and the catalytic activity of enzymes that are involved in a number of important biological processes (Bailão *et al.*, 2012). For example, cytochrome c oxidase enzyme, which catalyses the final step of respiration in the mitochondria contains both iron and copper ions as part of prosthetic groups in the active site (de Paulo Martins *et al.*, 2011) (Figure 2). Magnesium is required for the activity of nucleotide monophosphate kinases, for example adenosine triphosphate: guanosine monophosphate phosphotransferase (Miech & Parks, 1965). Hydrogen carbonate ions are an important substrate for many reactions, and the enzyme responsible for producing them from CO_2, carbonic anhydrase, requires Zn^{2+} ions (Elleuche & Poggeler, 2010).

Fungi grow by extension of the hyphal tips, and a high concentration of Ca^{2+} in the hyphal tip has been shown to have a role in tip morphogenesis and growth (Jackson & Heath, 1993). This tip-high gradient is maintained by its influx at calcium channels in the membrane, and it is suggested that Ca^{2+} controls hyphal morphogenesis via interactions with the actin network (Jackson & Heath, 1993). Calcium signalling in fungi has been shown to be involved in cell motility and contraction, as well as gene expression and cell division (Cavinder *et al.*, 2011). Calcium ions work in the cell through proteins such as calmodulin, which is a calcium-binding protein that once bound to Ca^{2+} can activate other proteins, and remodel active sites (Clapham, 2007). Hundreds of proteins have sites to interact with calmodulin (Clapham, 2007), and calmodulin has been found in fungi (Hallen & Trail, 2008). A study by Meyer *et al.* (2009) included a transcriptome analysis of an *A. niger* mutant (*ramosa – 1*, a temperature sensitive hyperbranching mutant) that was induced for apical branching. Among other genes, it was found that genes responsible for Ca^{2+} signalling were upregulated, for example Ca^{2+}/calmodulin dependent protein kinases, and vacuolar Ca^{2+} pumps, which implicates calcium signalling in the process of apical branching (Meyer *et al.*, 2009).

In addition to their importance in enzyme activity, investigations have shown that cations such as magnesium, calcium, zinc and copper are bound to polynucleotides, and it has been found that some transition metals such as zinc stabilise RNA tertiary structure (Cuero *et al.*, 2003). For example, the Zinc finger proteins are DNA-binding transcription factors that contain Zn^{2+} ions as part of their structure (MacPherson *et al.*, 2006). It is suggested therefore that metal ions are important in nucleic acid structure (Cuero *et al.*, 2003).

1.2.3.1 Metal ion homeostasis in fungi.

Adaptation to an environment that is often very low in metal ions such as iron has led to strategies for the uptake of these ions (Kosman, 2003), and transport mechanisms exist in both high-affinity and low-affinity forms to cope with situations of high and low nutrient availability (Bailão *et al.*, 2012). For example, it has been shown in *Saccharomyces cerevisiae* that a low affinity iron transport system exists that begins with a reductase enzyme in the cell membrane for reducing Fe^{3+}, making the more soluble Fe^{2+} available for uptake (Kosman, 2003) (Figure 3). This Fe^{2+} can then be taken in by ferrous permease or by non-specific divalent ion transporters (Kosman, 2003).

Many fungi also produce siderophores, which bind Fe^{3+} for uptake via plasma membrane permeases (Kosman, 2003) (Figure 3). The optimum conditions for siderophore production in *F. venenatum* were investigated in a study by Wiebe, (2002b). It was discovered that siderophore production was repressed if iron was added to the medium, soluble iron had a greater repressing effect than insoluble iron, and the highest production of siderophores occurred at pH 4.7 (Wiebe, 2002b).

Copper ions are reduced from Cu^{2+} to Cu^{+} by a plasma membrane metalloreductase enzyme, and these are taken into the fungus either via high-affinity Cu transporters, CTR1 and CTR3, or the low-affinity transporter Fet4 (Festa & Thiele, 2011) (Figure 4). Zinc ions are taken into fungi cells via ZRT2, the low-affinity transporter, and ZRT1, the high-affinity transporter (Claus & Chavarría-Krauser, 2012).

Calcium uptake in fungi takes place via the high-affinity calcium uptake system (HACS) and the low-affinity calcium uptake system (LACS) (Cavinder *et al.*, 2011). The calcium channels Cch1 and Mid1 are part of the HACS, and Fig1 makes up the LACS (Cavinder *et al.*, 2011). In a study of *Gibberella zeae* calcium channel mutants, it was shown that these channels are required for calcium signalling and that these mutants had slowed growth and reduced ascospore discharge, but they are rescued by calcium supplementation (Cavinder *et al.*, 2011).

These uptake mechanisms also allow fungi to control their uptake of metal ions according to their availability, for example, the genes for the copper transporters CTR1 and CTR3 are activated in low copper conditions by a transcriptional regulator (Festa & Thiele, 2011). Additionally, in high copper conditions uptake is controlled by the endocytosis and degradation of the CTR1 protein (Festa & Thiele, 2011). The zinc transporters are controlled by reducing the expression of their genes in situations of high zinc availability, and ZRT1 can also be post-translationally modified so that it is inactive, and endocytosed (Claus & Chavarría-Krauser, 2012). The high-affinity uptake pathways for iron are also regulated at the level of gene transcription (Kosman, 2003).

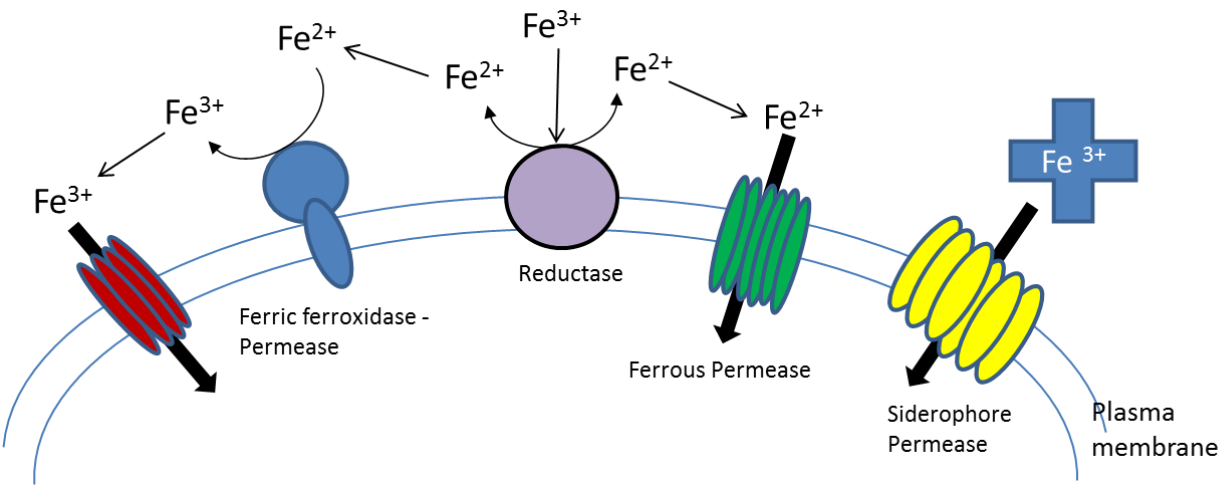

Reductase enzymes in the plasma membrane reduce Fe^{3+} to Fe^{2+} making it available for uptake as Fe^{2+} is more soluble. Fe^{2+} can be oxidised to Fe^{3+} by ferroxidation. This is coupled to a high-affinity permease. Fe^{2+} can be taken in by ferrous permease or by non-specific divalent ion transporters (low-affinity). Siderophore proteins e.g. ferrichrome bind to Fe^{3+} and this complex enters the cell through siderophore permease (high-affinity). (Kosman, 2003).

Figure 3: Iron transport systems in fungi. Adapted from Kosman (2003).

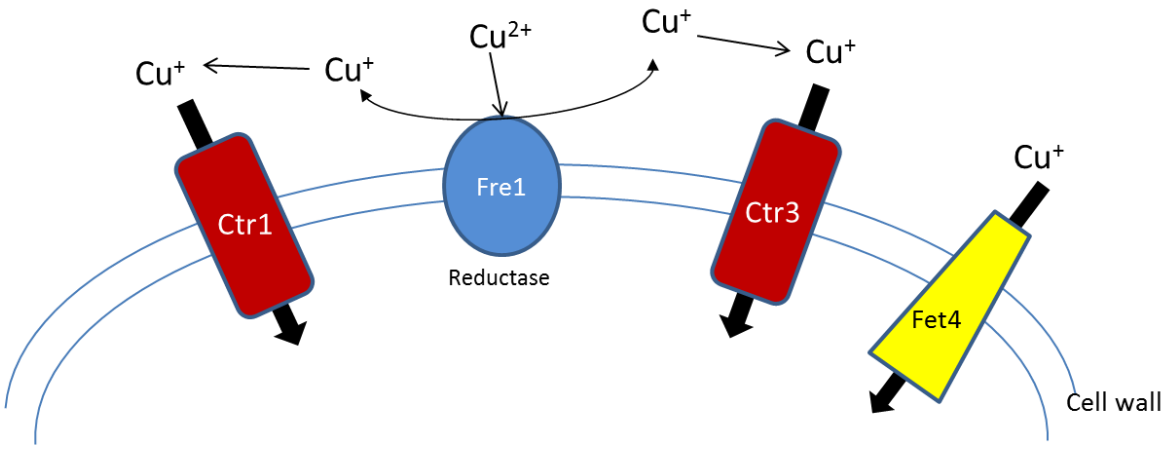

The plasma membrane metalloreductase Fre1 first reduces Cu^{2+} to Cu^{+} for uptake. The high-affinity uptake system is made up of CTR1 and CTR3, which are activated along with Fre1 by a Cu sensing transcriptional regulator. The low-affinity uptake system is Fet4. (Festa & Thiele, 2011).

Figure 4: Copper transport mechanisms in yeast. Adapted from Festa & Thiele (2011).

1.2.3.2 The effect of varying the concentration of metal ions in the growth medium on fungal growth & metabolism.

The presence of inorganic ions in the growth medium of fungi has been shown in some species to affect the production of mycotoxins. For example, a study by Vasavada & Hsieh (1988), investigated growth and the production of the mycotoxin 3-acetyldeoxynivalenol (3-ADN) in *F. graminearum*. Sulfate salts of Mg^{2+}, Mn^{2+}, Zn^{2+}, and Fe^{2+} were used to supplement a metal-free defined medium, in varying concentrations from 5 µM to 50 mM (Vasavada & Hsieh, 1988). Increased Mg^{2+} up to 50 mM led to increased growth; Mn^{2+} stimulated growth at some concentrations; Fe^{2+} gave increased growth in concentrations up to 5 mM, beyond which growth was slowed; and Zn^{2+} stimulated growth up to 100 µM but growth was decreased at higher concentrations (Vasavada & Hsieh, 1988). The production of 3-ADN was also affected by the ions, for example, Mg^{2+} encouraged 3-ADN production with a maximum yield at 1.0 mM Mg^{2+} (Vasavada & Hsieh, 1988). Zn^{2+} caused a decrease in 3-ADN production but only for those concentrations where it was increasing growth, when it inhibited growth at higher concentrations, Zn^{2+} caused an increase in 3-ADN production (Vasavada & Hsieh, 1988). Fe^{2+} stimulated 3-ADN production at 5 to 10 µM, and Mn^{2+} was found to inhibit 3-ADN production at all concentrations (Vasavada & Hsieh, 1988). The authors suggest that the production of 3-ADN is decreased when growth is increased, as faster metabolism prevents the build-up of the precursors needed for secondary metabolite production (Vasavada & Hsieh, 1988).

An investigation into inorganic ions and fungal growth, using *Aspergillus flavus*, showed that a mixture of Zn^{2+}, Cu^{2+} and Fe^{2+} ions stimulated growth, as did Zn^{2+} with Cu^{2+} and Zn^{2+} with Fe^{2+} mixtures, while Zn^{2+} on its own had a greater effect on growth than the other two ions on their own (Cuero *et al.*, 2003). The total RNA was also compared in *A. flavus* grown with differing metal ion treatments and it was found that the Zn^{2+}, Fe^{2+} and Cu^{2+} ion mixture enhanced RNA accumulation, as did the Zn^{2+} with Cu^{2+} and Zn^{2+} with Fe^{2+} mixtures, and the single ion treatments (Cuero *et al.*, 2003).

In the study by Cuero *et al.* (2003), it was found that an increase in growth of the fungus *A. flavus* when treated with mixed metal ions was correlated with an increase in aflatoxin production. It was also found that expression of the aflatoxin pathway gene, *omtA*, was increased when the fungus was treated with metal ions, and this increase was consistent with the increase in total RNA (Cuero *et al.*, 2003). The authors suggest that increases in the total RNA may be due to increased expression when metal ions are added to the culture, and the upregulated genes could be related to growth and secondary metabolism (Cuero *et al.*, 2003).

The effect of metal ions Zn^{2+}, Cu^{2+} and Fe^{2+} on growth and mycotoxin production was further investigated in *Aspergillus flavus* and *Fusarium graminearum* in a study by Cuero & Ouellet (2005). Results showed that the growth of both species was stimulated in media supplemented with all three ions (Cuero & Ouellet, 2005). Mycotoxin production was also affected by the presence of the ions, as results showed that zearalenone accumulation in *F. graminearum* was increased when all three ions were used, and in the Cu^{2+} with Fe^{2+} mixture (Cuero & Ouellet, 2005). Aflatoxin production in *A. flavus* was stimulated by the presence of both single ions Cu^{2+} and Fe^{2+} and the triple ion mixture (Cuero & Ouellet, 2005). These increases in mycotoxin production were found to be above the increases in biomass (Cuero & Ouellet, 2005).

Expression of genes related to fungal growth was also shown to be increased in *F. graminearum* grown in media containing all three ions (Cuero & Ouellet, 2005). For example, genes for GDP-mannose pyrophosphorylase, neutral amino acid permease, and GTPase Ras2p, all associated with growth, and alcohol dehydrogenase, mitochondrial ribosomal protein S5, and phosphoketolase, all associated with energy production, were all upregulated (Cuero & Ouellet, 2005).

The authors of this study explain that zinc affects the gene expression of alcohol dehydrogenases and their structural stability in yeast, and zinc can affect other synthesis enzymes such as fatty acid synthetase (Cuero & Ouellet, 2005). Enzymes such as synthetase require Mg^{2+} to bind the substrate to the active site, and it is suggested that the metal ions could

be stimulating enzymes such as synthetases, and alcohol dehydrogenases during the growth phase, and this increased activity then leads to the subsequent production of secondary metabolites (Cuero & Ouellet, 2005).

The presence and absence of Ca^{2+} in the culture medium was studied by Pera & Callieri (1997) in *Aspergillus niger*, and the growth, citric acid production, and morphology of the fungus were investigated. It was found that adding $CaCl_2$ at a concentration of 2 g L^{-1} led to a 35% decrease in biomass, and an increase in citric acid production when compared with the culture lacking in Ca^{2+} (Pera & Callieri, 1997). The morphology of the fungus was shown to be affected by a lack of Ca^{2+}, with these cultures showing the presence of both the pelleted and free-hyphae form, and hyphae with a lower number of branches (Pera & Callieri, 1997). In the culture with added Ca^{2+}, the growth was predominated by the pelleted form and hyphae with a greater number of branches (Pera & Callieri, 1997). Cellular morphology was also seen to be affected by Ca^{2+}, with the appearance of bulbous cells when the Ca^{2+} was present, but none were seen in its absence (Pera & Callieri, 1997).

Ca^{2+} concentrations in *F. venenatum* cultures were investigated by Robson *et al.* (1991b), and it was found that a low concentration of Ca^{2+} (1.4×10^{-8} M) led to more highly branched hyphae with larger diameters, whereas a higher concentration (5×10^{-4} M) gave less branches, narrower hyphae and a longer G measurement (G = total hyphal length ÷ number of tips). A similar study by the same group used a Ca^{2+} ionophore (A23187), and calcium channel blockers to study the effects of a reduction in Ca^{2+} concentration on *F. venenatum* morphology (Robson *et al.*, 1991a). It was found that a high concentration of the ionophore, and therefore a low Ca^{2+} concentration, led to more highly branched hyphae and decreased extension rate (Robson *et al.*, 1991a). The use of calcium channel blockers also caused an increase in branching and reduced extension, showing that it is the intracellular Ca^{2+} concentration in particular that is involved in the control of branching and growth (Robson *et al.*, 1991a).

1.3 Morphology and evolution of morphological defects in *F. venenatum* cultivation

The growth of *F. venenatum* A3/5 for the production of Quorn™ food products occurs in an air-lift bioreactor with a continuous flow system (Trinci, 1994). This system operates as a nutrient unlimited glucose-stat so that the concentration of residual glucose is kept constant (Simpson *et al.*, 1998). This type of cultivation is used because it maintains a higher level of biomass production, as opposed to batch culture (Trinci, 1994).

The disadvantage of these continuous flow conditions is that they encourage a strong selection pressure that leads to evolution of the organism (Wiebe *et al.*, 1996b). The continuous flow cultures therefore cannot be run indefinitely as these selection pressures eventually favour the growth of a variant strain, known as 'colonial mutants' (Wiebe *et al.*, 1996b). These variants appear after approx. 400 h, which corresponds to around 107 generations (Wiebe *et al.*, 1996b). They show a different morphology to the parent strain, with much shorter hyphae and a greater number of branches (Wiebe *et al.*, 1996a). When using measurements of the hyphal growth unit (G), higher G values belong to the parent strain with long hyphae and fewer branches e.g. 334 µm, and lower G values belong to the variant with short hyphae and numerous branches e.g. 56 µm (Wiebe *et al.*, 1996a).

The morphology of the mutant strain decreases the viscosity of the culture, and this increases the mass transfer of O_2 (Wiebe & Trinci, 1991). The mutant strain presents a problem in Quorn™ production as the highly branched phenotype results in a more crumbly structure which is undesirable for the final product, and the filters used to harvest the biomass from the fermenter are not so effective at separating the mutant organism from the broth (Trinci, 1994). The appearance of these variants therefore necessitates the shut-down of the fermenter after approx. 6 weeks, and it therefore causes a significant loss of biomass production for the company (Trinci, 1994).

The industrial growth conditions with constant glucose are not the only conditions that encourage mutant strains to develop (Simpson *et al.*, 1998). In other studies, highly branched colonial mutants of *F. venenatum* A3/5 have been discovered in continuous glucose-limited

chemostat cultures (Simpson *et al.*, 1998). These particular mutants have a selective advantage over the wild type only in glucose-limited conditions, and mutations were found to have occurred in genes relating to glucose metabolism (Simpson *et al.*, 1998). In addition, other mutants have also been found during Quorn™ production that confer no selective advantage, along with some others that have unchanged morphology but are still able to out-compete the wild-type (Simpson *et al.*, 1998).

The mutations that lead to colonial mutants in Quorn™ production are recessive (Wiebe *et al.*, 1996a). In the Quorn™ fermenter, the fungal mycelium produces fragments due to shearing forces, and it will also produce macroconidia (spores), both giving rise to new hyphae (Wiebe *et al.*, 1996a). The nuclei contained in the fragments that are produced by shearing may not be identical to each other, and so the fragments are heterokaryotic, but the macroconidia are formed on structures known as phialides, which are uninucleate and give rise to homokaryotic mycelia (Wiebe *et al.*, 1996a) (Trinci, 1994). If the macroconidia contain the recessive mutations that confer a selective advantage, or the heterokaryotic fragments contain a high enough proportion of nuclei with these mutations, the colonial mutants are then able to spread through the culture (Wiebe *et al.*, 1996a).

A study by Wiebe et al., (1996b) reasoned that chemostat cultures with constant conditions were allowing the mutant strain to thrive due to the competitive exclusion principle (two complete competitors cannot coexist). They decided therefore to investigate the growth of the mutant in conditions of oscillating pH so that mutants with a selective advantage at a certain pH would be at a disadvantage when the pH is periodically changed (Wiebe *et al.*, 1996b). This was proposed to be a viable strategy since the morphology of the parent strain *F. venenatum* remains unchanged over a wide range of pH values (Wiebe *et al.*, 1996b). Two strains of the colonial mutants were investigated, each with a different optimum pH, and they had a reduced selective advantage over the parent strain when the pH was changed (Wiebe *et al.*, 1996b). It was ultimately found that the appearance of the colonial mutants can be delayed

to 712 h with a constant low pH of 4.5, rather than oscillating pH, as this was sub-optimal for both mutants (Wiebe *et al.*, 1996b).

In another investigation, the nutrient composition of the medium was investigated by supplementing the medium with the complex nitrogen source, peptone (Wiebe *et al.*, 1998). In glucose-limited cultures, this supplementation of the medium with peptone was shown to affect the variant, diminishing their ability to supplant the original strain even after 528 h (Wiebe *et al.*, 1998). The authors suggest the small concentrations of peptone added to the growth medium during Quorn^{TM} production could help to delay the appearance of colonial mutants, thus allowing greater productivity for the fermentation (Wiebe *et al.*, 1998).

These studies have found that varying the nutrients supplied, such as peptone, or changing the pH can affect the selection pressures in the fermenter, which delays the appearance of these variants. This suggests that changes made to medium could have an effect on the morphology of the fungus or the production of unwanted variants with a different morphological phenotype. The morphology of *F. venenatum* in cultures with altered levels of metal ions has not yet been carried out and so this is an important area for study.

1.4 Important secondary metabolites, structural proteins, and mycotoxins in *Fusaria*

Secondary metabolites are compounds that are not essential for the life of the organism (Brown *et al.*, 2012). These compounds are thought to have evolved as signals for communication, self-defence or to eliminate competitors (Brakhage & Schroeckh, 2011). Mycotoxins are just one example of these secondary metabolites (Desjardins & Proctor, 2007); filamentous fungi also produce a great number of useful compounds, with 42% of known bioactive microbial products e.g. antifungals, antibacterials, antivirals, and immunosuppressants being produced by fungi (Brakhage & Schroeckh, 2011). Fungal secondary metabolites are therefore of great significance to the biotechnology and pharmaceutical industries (Nguyen *et al.*, 2012), but there are many that remain as yet undiscovered (Brakhage & Schroeckh, 2011).

An example of this is a study by Prakash et al. (2015), in which the culture broth from *F. venenatum* was investigated for insecticidal metabolites. An extract of the culture broth was tested for cytotoxicity with Sf-21 (*Spodoptera frugiperda*-21) cells, and the results showed a dose dependent effect on the viability of the cells with cytotoxicity increasing with higher concentrations (Prakash *et al.*, 2015). This study demonstrated the potential for producing insecticidal metabolites in *F. venenatum* cultures (Prakash *et al.*, 2015).

1.4.1 Polyketide synthases and non-ribosomal peptide synthetases.

Many of the secondary metabolites produced by fungi are polyketides (PKs) (Brown *et al.*, 2012). Polyketides are manufactured by polyketide synthases (PKSs) which are multi-enzyme complexes containing multiple functional domains (Brown *et al.*, 2012). Functional domain analysis revealed that the *Fusarium* PKSs can be organised into 34 groups that synthesise different metabolites (Brown *et al.*, 2012). A PKS uses an iterative process to synthesise these large compounds from the small molecules acetyl-CoA and malonyl-CoA (Brown *et al.*, 2012). Polyketide derived secondary metabolites include compounds such as fumonisin, fusarin, zearalenone, aurofusarin and penicillin (Brown *et al.*, 2012).

Aside from the polyketides, some other natural compounds that are biologically useful e.g. in clinical applications, such as antibiotics, immunosuppressants, or antitumour drugs are non-ribosomal peptides (NRPs), that are produced by non-ribosomal peptide synthetases (NRPSs) (Strieker *et al.*, 2010). NRPSs synthesise peptides by the consecutive addition of amino acids, but are able to utilise more monomers than the usual 20 proteinogenic amino acids, making use of 500 different potential building blocks such as nonproteinogenic amino acids, fatty acids, and α-hydroxy acids (Strieker *et al.*, 2010). Their ability to use a much greater variety of monomers allows the NRPS to produce compounds with greater structural versatility than peptides produced by the ribosomal system (Strieker *et al.*, 2010). Bioinformatic tools exist that can predict the substrates of NRPSs in bacteria and fungi (Hansen *et al.*, 2012).

1.4.2 Mycotoxins of *Fusarium* species.

Fungal species of the genera *Aspergillus*, *Penicillium* and *Fusarium* are the main producers of mycotoxins (Gong *et al*., 2015). The mycotoxins produced by *Fusarium* species are the trichothecenes, fumonisins, zearalenones, beauvericin, enniatins, butenolide, equisetin, and the fusarins (Desjardins & Proctor, 2007). The most significant of the *Fusarium* mycotoxins in terms of public health and agriculture are the trichothecenes, zearalenone, and the fumonisins (Hussein & Brasel, 2001).

Zearalenone (ZEA) is produced by a number of *Fusarium* species including *F. graminearum*, *F. culmorum*, and *F. semitectum* (Zinedine *et al.*, 2007). The production of zearalenone is influenced by nutrient availability, as starvation of carbon, nitrogen or phosphorous was discovered to lead to reduced transcription of the zearalenone pathway genes in *Gibberella zeae* (Kim *et al.*, 2005). The pH also has an effect on zearalenone, with highest transcription at pH 4 and a reduction in transcription with increased pH (Kim *et al.*, 2005).

1.4.3 Mycotoxins of *F. venenatum.*

Mycotoxin analysis of the Quorn™ producing strain of *F. venenatum* has shown that it is capable of producing the type A trichothecenes: scirpentriol; 15-acetoxyscirpenol; diacetoxyscirpenol; and 4-monoacetoxyscirpenol (O'Donnell *et al.*, 1998). A gene responsible for fusarin biosynthesis has been discovered in *F. venenatum*, which codes for a polyketide synthase (Song *et al.*, 2004). However, current production conditions for Quorn™ do not lead to the production of mycotoxins (Wiebe, 2004).

Eight different strains of *F. venenatum* that are not used in Quorn™ production, some with the trichodiene synthase gene deleted, were tested for mycotoxin production in a study by Miller & MacKenzie (2000). The growth conditions were optimised for trichothecene production by using a two-step fermentation that started with 48 h at 28 °C in 50 mL of medium composed of 20 g L^{-1} molasses, 30 g L^{-1} glucose, 15 g L^{-1} fish meal, 15 g L^{-1} pharmamedia (Miller &

MacKenzie, 2000). This was followed by 4 weeks of fermentation at 28 °C, pH 6.5, in 1 L of medium containing glucose 10 g L^{-1}, yeast extract 1 g L^{-1}, and peptone 1 g L^{-1} (Miller & MacKenzie, 2000). It was found that those strains with the trichodiene synthase gene removed did not produce diacetoxyscirpenol, scirpentriol, tricodermol or apotrichothene (Miller & MacKenzie, 2000). It was also found that strains subjected to repeated culturing had lower secondary metabolite production (Miller & MacKenzie, 2000).

The trichothecenes (tricyclic sesquiterpenes) have been linked to several serious toxicoses of both animals and humans (Desjardins & Proctor, 2007). The trichothecene family contains a number of end-products and derivatives but the most common are type A (e.g. 4,15-diacetoxyscirpenol) and type B (e.g. deoxynivalenol and nivalenol, and their derivatives 3-acetyldeoxynivalenol, 15-acetyldeoxynivalenol, and 4-acetylnivalenol) (Figure 5) (Suzuki & Iwahashi, 2012). Deoxynivalenol and nivalenol have an established regulatory value since they are major contaminants in food (Suzuki & Iwahashi, 2012). The toxicity of trichothecenes is due to their inhibition of translation by binding to the 60S ribosome, leading to apoptosis, cell cycle arrest, mitochondrial oxidative stress and immunotoxic effects (Suzuki & Iwahashi, 2012). These effects lead to the symptoms of intestine inflammation, and anorexia or diarrhoea (Suzuki & Iwahashi, 2012).

Biosynthesis of the trichothecenes begins with the trichodiene synthase enzyme, which catalyses the cyclisation of a sesquiterpene (Desjardins & Proctor, 2007). Genes for trichothecene biosynthesis belong to a cluster of 12 genes, 10 of which have been shown to be essential for the process (Desjardins & Proctor, 2007). The gene for trichodiene synthase enzyme, *tri5* has been deleted in *F. venenatum* and it was found that the deletion strain did not produce a detectable level of 4,15-diacetoxyscirpenol even when the growth conditions were optimised for its production (Royer *et al.*, 1999).

A study by Miller & Blackwell (1986), investigated the production of the type B trichothecene 3-acetyldeoxynivalenol (ADON) (Figure 5) during the growth of *F. culmorum* in a stirred fermenter and found that its production was linked to nitrogen availability. It was discovered

that ADON biosynthesis began when the ammonium concentration had been reduced to trace amounts, which was 36h after inoculation, and the highest rate of its production was between 48h and 108h after inoculation (Miller & Blackwell, 1986). Adding less $(NH_4)_2HPO_4$ to the medium led to the detection of ADON earlier in the fermentation, and addition of $(NH_4)_2HPO_4$ at 36h reduced the yield (Miller & Blackwell, 1986).

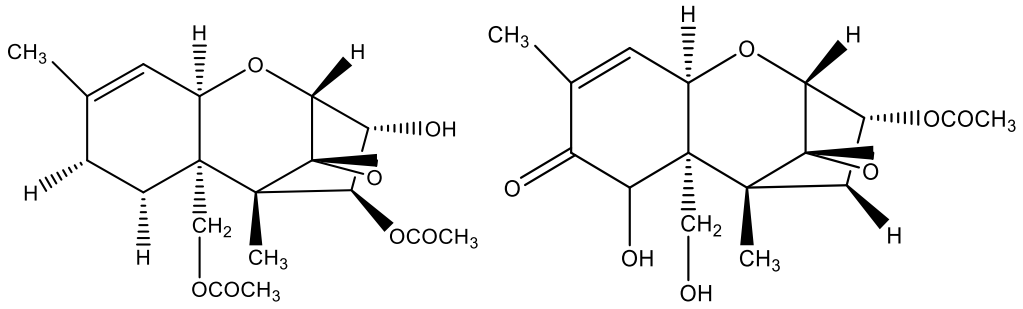

4, 15-Diacetoxyscirpenol 3-Acetyldeoxynivalenol

Figure 5: Trichothecene mycotoxins. Structure of 4, 15-Diacetoxyscirpenol, a type A trichothecene (Gottschalk *et al.*, 2007), and structure of 3-Acetyldeoxynivalenol, a type B trichothecene (Suzuki & Iwahashi, 2012). Type A trichothecenes differ from type B as they do not have a carbonyl group at the C8 position (Klötzel *et al.*, 2005).

1.5 The potential to re-use wastewater from fermentation to grow *F. venenatum*.

The industrial fermentation of microorganisms requires the input of immense volumes of water, and it produces a substantial amount of wastewater that has to be released into the environment once it is treated (Hsiao *et al.*, 1994). The processing and disposing of this wastewater are expensive and require dedicated facilities and high energy input (Hsiao & Glatz, 1996). This currently adds millions every year to the cost of production of *F. venenatum* for Quorn™ foods. Reducing the amount of this fermenter effluent is therefore of economic benefit to this industry and could help to make *F. venenatum* production more cost-effective

and efficient while at the same time reducing the environmental impact (Hsiao & Glatz, 1996). Fermentations that require large amounts of nutrients such as carbon or nitrogen sources can also benefit from broth recycling as this reduces wastage of these substrates, which would also help to increase profitability (Wang *et al.*, 2012).

A number of previous studies have illustrated the possibility of wastewater recycling for the growth of microorganisms, but so far there have been no studies published that have investigated the use of recycled wastewater in *F. venenatum*, and so investigation is therefore necessary into its feasibility. Wastewater recycling during *F. venenatum* cultivation could potentially lead to a reduction in production costs, and additionally, it could decrease the amount of waste that would otherwise have to be treated and released into the environment.

Babu & Panda (1991) investigated broth recycling in the fermentation of *E. Coli* for penicillin amidase production. The supernatant from centrifugation of used broth had nutrients replaced up to initial concentrations and this was mixed with fresh medium in varying ratios between 0.1 and 1.0 for 8 consecutive batch fermentations (Babu & Panda, 1991). It was found that the specific growth rate increased with greater recycle ratio, for up to 3 consecutive fermentations, but for a greater number of fermentations this did not happen (Babu & Panda, 1991). Results also showed that the specific growth rate increased with batch number for lower recycle ratios (0.1 and 0.2), but an optimum growth rate was achieved at batch number 7 for a ratio of 0.4, batch number 5 for a ratio of 0.8 and batch number 3 for a ratio of 1.0 (Babu & Panda, 1991). The authors suggest that it is therefore possible to reuse 40-60% of the broth water in fermentations for penicillin amidase production (Babu & Panda, 1991).

A study by Hsiao & Glatz (1996) investigated the possibility of wastewater reuse during the production of L-lysine in *Corynebacterium glutamicum* ATCC 21253. The broth effluent from this process can either be sent for treatment, or the water is evaporated to produce a concentrated by-product; therefore recycling this effluent would both reduce the volume of wastewater for treatment as well as possibly reducing its solid content (Hsiao & Glatz, 1996). Before the broth was recycled, cation-exchange resin was first used to remove L-lysine, the

amounts of glucose, citric acid and minerals in the broth were replenished, and the required amino acids were replaced in full (Hsiao & Glatz, 1996). When used with a defined medium, the broth was then recycled at a ratio of 75% (ratio of recycled effluent to the total volume) for 3 consecutive fermentations and it was found to be successful, with the fermentations closely matching the control (a batch fermentation with fresh medium) (Hsiao & Glatz, 1996).

1.6 Conclusions

In summary, the growth and production of secondary metabolites in fungi has been shown to be affected by environmental factors such as temperature, light, pH and availability of carbon and nitrogen (Yin & Keller, 2011). The type of media used (Hestbjerg *et al.*, 2002) (Lowe *et al.*, 2010) and specific inorganic ions added to the media can affect the production of mycotoxins, and fungal growth (Cuero & Ouellet, 2005). Calcium signalling is an important factor in fungal gene expression, cell division and motility, and therefore calcium availability is an important factor for growth (Cavinder *et al.*, 2011).

Gene expression, particularly for enzymes involved with the production of energy, and growth has been shown to be altered in *F. graminearum* by the concentrations of inorganic ions (Cuero & Ouellet, 2005), and the production of ACP enzymes in *F. venenatum* was shown to be affected by phosphate availability and pH (Hidayat *et al.*, 2007). These studies suggest that the production of enzymes, some of which may be of commercial use, could be encouraged in *F. venenatum* with changes in the medium composition.

Studies have also shown that there is potential for altering the growth and metabolism of fungal species by altering the components of the growth medium (Cuero & Ouellet, 2005) (Lowe *et al.*, 2010). However, the scarcity of literature in this area, and the specifics of the methods used in the studies mentioned above, mean that this is an important area for further study. In addition, the use of *F. venenatum* in the food industry for the production of Quorn^{TM} products makes this fungus a significant candidate for a study of its metabolome and proteome. While

the production of some metabolites may be of benefit to the final food product in terms of flavour and other characteristics, the production of mycotoxins would be detrimental and must be avoided, therefore an increase in our knowledge of the effects of different medium components on the *F. venenatum* metabolome is necessary. This knowledge could allow further research into the use of alternative growth media for *F. venenatum* cultivation. Investigation of the *F. venenatum* metabolome and proteome under varying growth conditions may also lead to discovery of novel secondary metabolites, or enzymes that are useful to the food, pharmaceutical or biotechnology industries.

Another important aspect of *F. venenatum* growth that could be affected by the nutrients in the medium is its morphology. Studies have shown that the morphology of the fungus is affected by selection pressures in the fermenter, which eventually encourages the growth of variants with a more highly branched phenotype (Wiebe *et al.*, 1996a). This is a significant area for further study since it can affect the productivity of the fermentation, influencing the economic viability of the process. An investigation into *F. venenatum* growth and morphology in varying nutrient conditions could therefore lead to further knowledge in this area. In addition, changes in the morphology of the fungus may have an impact on the texture and quality of the final product, and so investigating the ways that nutrient conditions affect fungal morphology could inform ways to improve the production process to yield the best product possible, and it may be possible to find ways of delaying the onset of the variant morphology.

Knowledge of the effects of altering the growth medium on *F. venenatum* growth and biochemistry could help devise ways of producing the fungus in a more environmentally sustainable way that could also save money and improve profitability. Several studies have illustrated the possibility of wastewater recycling in industrial microorganism cultivation, and this would be of great benefit since it would reduce the need for the disposal and treatment of large amounts of wastewater. So far there have been no studies published that have investigated effluent recycle in *F. venenatum* cultures and the procedures used in the examples above were specific to the process and microorganisms investigated, which don't reflect the

growth conditions used for *F. venenatum* cultivation in industry. Investigation is therefore necessary into the feasibility of effluent reuse in *F. venenatum* culture. Wastewater recycling during *F. venenatum* cultivation could potentially lead to a reduction in production costs, and additionally, it could decrease the amount of waste that would otherwise have to be treated and released into the environment.

The aim of this investigation is to conduct a thorough analysis of the morphology, metabolome and proteome of *F. venenatum* when it is grown in media that contains iron and calcium ions in limiting amounts and in excess, and when grown in recycled media. This will reveal how these metal ions influence the growth and biochemistry of the fungus, and this knowledge could inform new ways to grow the fungus in a more sustainable way that provides a higher biomass, aids the production of beneficial metabolites, such as those that influence flavour, and which does not encourage the growth of mycotoxins. Further knowledge of how the growth medium affects morphology could help to devise ways to produce the fungus with properties that favour a better texture for the final product, and it could help to find a way to delay the onset of the variant strains with a detrimental highly branched phenotype.

2. Effect of calcium and iron of the morphology and biomass of *Fusarium venenatum* cultures.

2.1 Introduction

2.1.1 Growth and morphology of filamentous fungi

Fungi grow by the elongation of the cells at the hyphal tips (Jackson & Heath, 1993). This process is made possible by the transport of wall-building vesicles to the tip, which contain the materials required to synthesis new cell membrane and cell wall, along with the necessary enzymes (Brand & Gow, 2009). The SPK is a structure found at the hyphal tip which is the vesicle supply centre for wall-building vesicles (Dijksterhuis & Molenaar, 2013), and it is composed of vesicles, proteins and ribosomes (Meyer *et al.*, 2009).

In order to quantitatively measure the growth of filamentous fungus, while taking into account its complex growth pattern, the 'hyphal growth unit' (G), which is the total length of all of the branches divided by the number of tips, is used (Wiebe & Trinci, 1991). This is measured using digital imaging and analysis software (Wiebe *et al.*, 1996a).

As filamentous fungi grow, G increases as both the number of tips and hyphal length increase (Grimm *et al.*, 2005). Eventually G reaches a maximum and is constant while the length increase is linear, and tips increase exponentially (Grimm *et al.*, 2005). This effect is theorised to be due to the wall-building vesicles being manufactured at a faster rate as the hyphae increase in length (Grimm *et al.*, 2005). Once the hyphae reach a certain length the vesicles cannot be transported quickly enough to the tip and so new branches form making use of the vesicles that accumulate in the regions further away from the tip (Grimm *et al.*, 2005).

2.1.2 The role of calcium ions in fungal morphology

Calcium ions are known to have an important role in fungal morphogenesis, as they are involved in growth at the tips of the hyphae (Jackson & Heath, 1993). In support of this, hyphal tips have been found to contain highly polarised concentrations of calcium ions, as have cells

in other organisms that are highly polarised, such as pollen tubes in plants (Jackson & Heath, 1993). This phenomenon has been photographed in the hyphae of *Saprolegnia ferax* with the use of fluorescent dyes that have a high affinity for free Ca^{2+}, such as Fluo-3 (Jackson & Heath, 1993). In addition, measurements of calcium concentration have shown a typical average concentration of 350 nM in the cytoplasm of fungi in non-apical regions, but a range of 100-2,600 nM in the apical tip (Jackson & Heath, 1993).

Work by Takeshita *et al.* (2017) investigated the link between Ca^{2+} influxes and growth of the fungal cell wall. It was found that pulses of Ca^{2+} into the cell caused oscillations between slow and faster growth through the control of actin polymerisation and depolymerisation (Takeshita *et al.*, 2017). Actin is important in cell growth as it forms a major part of the system for transporting secretory vesicles to the cell membrane at the hyphal tip (Takeshita *et al.*, 2017). The vesicles are moved along the cell by microtubules, passed onward to actin cables and from there reach the apex of the growing tip (Takeshita *et al.*, 2017). When the tip is growing slowly, the actin filaments in their polymerised form build-up at the tip, along with the secretory vesicles (Takeshita *et al.*, 2017). An increase in Ca^{2+} concentration in the cell causes de-polymerisation of the actin, which then leads to exocytosis of the vesicles, allowing the cell membrane to extend (Takeshita *et al.*, 2017). Calcium uptake in filamentous fungi consists of a high-affinity and low-affinity system, with calcium channels Cch1 and Mid1 making up the high-affinity system, and Fig1 the low-affinity system (Cavinder *et al.*, 2011). The increase in Ca^{2+} concentration in the tip was shown in *Aspergillus nidulans* to be due to the activation of their CchA and MidA channels, allowing the influx of Ca^{2+} (Takeshita *et al.*, 2017).

Calcium ion channels have been investigated in *Gibberella zeae* (the sexual stage or teleomorph of *F. graminearum*) by Cavinder *et al.* (2011). The importance of the mid1 and Cch1 channels (high-affinity calcium uptake system) was demonstrated in this study, as mutants lacking either only mid1 or lacking both channels had slowed growth, reduced production of conidia, abnormal ascospores and reduced discharge of ascospores (Cavinder *et al.*, 2011). Growth and spore discharge were able to be rescued by the addition of Ca^{2+}, which

led the authors to conclude that calcium signalling had been disrupted by the lack of mid1 and Cch1 channels (Cavinder *et al.*, 2011).

Aside from growth, calcium ions are also known to be involved in signalling pathways, cell motility and contraction, and cell division and gene expression (Cavinder *et al.*, 2011). Calcium ions exert an effect in the cell through calcium binding proteins such as calmodulin that can activate other proteins and remodel active sites (Clapham, 2007). The target proteins that calmodulin interacts with form a large and diverse group, including serine/threonine kinases, calcineurin (a protein phosphatase) and NO (nitric oxide) synthases (Hoeflich & Ikura, 2002). The binding of Ca^{2+} to calmodulin causes a change in structure that exposes hydrophobic surfaces and triggers its ability to bind to its targets (Clapham, 2007). Calmodulin can activate proteins such as serine/threonine kinases by binding a part of the protein that acts as an autoinhibitory site and causing a conformational change, which then allows restoration of enzyme activity (Hoeflich & Ikura, 2002). Calmodulin can exert its effects by either directly activating enzymes in this way, or by activating kinases that go on to phosphorylate other enzymes (Robson *et al.*, 1991a).

A study by Meyer *et al.* (2009) investigated a hyperbranching mutant of *Aspergillus niger* that was induced for apical branching. The process of apical branching (new branches formed by the tip splitting) includes: contraction of the cytoplasm; retraction and disappearance of the SPK; and the formation of two new SPK that then lead to two new branches (Meyer *et al.*, 2009). This type of branching is thought to be a result of the build-up of too many vesicles at the tip (Meyer *et al.*, 2009). The mutation that leads to hyperbranching in this organism is a single-point mutation in the *rmsA* gene that regulates actin polarity (Meyer *et al.*, 2009). Gene profiling of the transcriptome showed upregulation of cell wall biosynthesis genes including the chitin synthase gene, linking apical branching with reorganisation of the cell wall (Meyer *et al.*, 2009). Genes for the synthesis of phospholipid signalling molecules were also upregulated, and this showed a link between apical branching and actin polarisation, calcium signalling and cell wall integrity (Meyer *et al.*, 2009). Genes directly responsible for Ca^{2+}

signalling were also upregulated, for example Ca^{2+}/calmodulin dependent protein kinases, and vacuolar Ca^{2+} pumps, further implicating calcium in the control of apical branching (Meyer *et al.*, 2009).

2.1.3 The role of iron ions in fungal growth and morphology

Iron ions often form an integral part of enzyme structure as cofactors or prosthetic groups, thus taking part in essential biochemical reactions, such as respiration, which consists of glycolysis, the tricarboxylic acid (TCA) cycle, and oxidative phosphorylation (Tavsan & Ayar Kayali, 2015). Much of the ATP required by the cell is generated by ATP synthase enzyme in the mitochondria, which is driven by a flow of protons across the inner mitochondrial membrane down the electrochemical gradient generated by the electron carrier system (de Paulo Martins *et al.*, 2011). The electron carrier system consists of 4 multi-enzyme complexes which transfer electrons from $FADH_2$ and NADH to oxygen via ubiquinone and cytochrome c (de Paulo Martins *et al.*, 2011). These multi-enzyme complexes contain haem and Fe/S clusters, which are the prosthetic groups necessary for electron transfers from one electron carrier to the next (Philpott *et al.*, 2012). The final enzyme complex in the system contains both copper and iron ions, for electron transfer from cytochrome c to oxygen (de Paulo Martins *et al.*, 2011). As well as these enzyme complexes, two of the key enzymes of the citric acid cycle, aconitase and succinate dehydrogenase, which is also part of the electron carrier system, contain Fe/S clusters (Philpott *et al.*, 2012). The substrate for aconitase is the citrate produced in the first step of the TCA cycle (Tavsan & Ayar Kayali, 2015), and succinate dehydrogenase produces fumarate from succinate, and also transfers electrons to ubiquinone (de Paulo Martins *et al.*, 2011).

Any changes or disruption to glucose metabolism can also have wider consequences in other areas of cellular biochemistry, such as biosynthesis of amino acids, as some amino acids rely on precursor molecules that are produced in glycolysis or the TCA cycle (Tavsan & Ayar Kayali, 2015). An example of this is serine, whose biosynthesis begins with 3-

phosphoglycerate from glycolysis (Xie *et al.*, 2017), and the branched chain amino acids leucine, isoleucine and valine, are made from pyruvate, another glycolysis intermediate (Liu *et al.*, 2014).

In addition, the enzymes containing Fe/S clusters are not only confined to the process of respiration, they also play an important and direct role in amino acid biosynthesis, nucleotide biosynthesis, protein translation, and the regulation of telomere length (Netz *et al.*, 2014). Enzymes involved in DNA metabolism which have been discovered to contain Fe/S clusters include DNA helicases, nucleases, primase and polymerases, further illustrating the importance of iron ions in the most fundamental aspects of cellular metabolism (Netz *et al.*, 2014).

Altering the levels of iron in the media is therefore likely to cause disruption to the central biochemical processes of carbon metabolism and ATP generation, and it is possible that this could have consequences for the cells including changes to the growth and morphology. The involvement of iron ions in other biochemical pathways of fungal cells such as amino acid biosynthesis, as well as crucial DNA synthesis and repair mechanisms are further possible routes through which altered concentrations of iron in the medium could have an effect on both the growth and possibly also the morphology of the fungus.

Studies of other *Fusarium* species have shown that varying the amount of inorganic ions in the culture broth affects both growth and mycotoxin production (Vasavada & Hsieh, 1988), (Cuero & Ouellet, 2005). These studies have demonstrated that there is scope for altering the growth and metabolism of *F. venenatum* by treating the growth medium with varying amounts of metal ions.

The study by Vasavada & Hsieh (1988) looked at the effects of several metal ions on growth and mycotoxin production in *F. graminearum*. Cultures were supplemented with sulfate salts of Mg^{2+}, Mn^{2+}, Zn^{2+}, and Fe^{2+} in concentrations from 5 µM to 50 µM (Vasavada & Hsieh, 1988). It was found that an increased concentration of Fe^{2+} ions increased the growth of the fungus, but only up to a maximum concentration of 5 mM, after which a toxic effect was

observed (Vasavada & Hsieh, 1988). Lower concentrations of Fe^{2+} ions (5 to 10 µM) affected mycotoxin production in this species, leading to a higher production of 3-acetyldeoxynivalenol, but concentrations above 10 µM reduced production of the mycotoxin, while causing an increase in dry weight (Vasavada & Hsieh, 1988). This suggested that production of 3-acetyldeoxynivalenol was inversely proportional to the growth, which could be explained by strong growth using up the precursors from various pathways that would otherwise be used in biosynthesis of secondary metabolites (Vasavada & Hsieh, 1988).

Metal ions in combination were investigated by Cuero & Ouellet (2005) who used media supplemented with sulfate salts of Fe^{2+}, Zn^{2+}, and Cu^{2+} singly and in combination. They discovered that Fe^{2+} added to a culture of *F. graminearum* had the largest effect on biomass production compared to the addition of Zn^{2+} and Cu^{2+}, and combinations of these two ions with Fe^{2+}, with a twofold increase in biomass (Cuero & Ouellet, 2005). As well as affecting biomass, metal ions also affected the production of zearalenone by *F. graminearum*, as this was shown to be stimulated most by the addition of the ions in combination (Cuero & Ouellet, 2005). Zinc ion supplementation alone only caused a twofold increase in zearalenone production, but treatment with iron or copper alone, or mixtures of the ions caused much greater increases (11 - 25-fold) (Cuero & Ouellet, 2005). The biggest increase in zearalenone production was caused by iron and copper together (25 fold), while a combination of all three ions caused a 16-fold increase (Cuero & Ouellet, 2005).

The importance of iron ions in fungi is underlined by the fact that mechanisms have evolved for their uptake in situations of low supply (high-affinity), and increased supply (low-affinity) (Kosman, 2003). For example, an iron transport system has been found in *Saccharomyces cerevisiae* consisting of a reductase enzyme in the membrane to reduce Fe^{3+} to Fe^{2+}, and ferrous permease for uptake of Fe^{2+} (low-affinity) (Kosman, 2003). The high-affinity transport system for iron consists of siderophores, which are molecules that bind Fe^{3+} and are then taken in by permeases in the membrane (Kosman, 2003).

Siderophore production has been investigated by Wiebe (2002b), who looked at the growth of *F. venenatum* in conditions of limited iron in shake flask cultures. The results showed a reduction of specific growth rate (μ) from 0.22 h^{-1} seen in iron supplemented media down to 0.12 h^{-1} in the media without iron (Wiebe, 2002b). The siderophores were produced in iron-depleted cultures and the addition of soluble or insoluble iron to the medium caused a reduction in siderophore production (Wiebe, 2002b).

The aim of this investigation was to determine whether there were any changes in the biomass production or morphology of the fungus when grown in shake flask cultures with media containing excess iron and calcium ions, and with limited iron and calcium ions, when compared with the control.

It is important to consider the morphology in these experiments as the growth of filamentous fungi is complex, involving differentiated cells such as conidia and the production of branches by the growing hyphae (Grimm *et al.*, 2005). In the production of Quorn™, the morphology of the fungus could affect the texture of the product and so it would be useful to understand how to affect the morphology so that it can be controlled.

2.2 Methods

The fungus was initially grown in each condition, iron-limited and calcium-limited and excess iron and excess calcium in baffled conical flasks. There were 4 repeats for each culture to allow statistical tests to be carried out. This initial experiment was followed up with further cultures in a 1 L fermenter which allowed greater control over pH and aeration, which could have affected the results.

2.2.1 Fungal growth in conical flasks in a shaking incubator

F. venenatum A3/5 (obtained from Quorn Foods) cultures were maintained on oatmeal agar at 4 °C. Starter cultures for each strain were begun by transferring a small piece of hyphae from

the edge of the growing fungus into 50 mL Oxoid nutrient broth in a 250 mL baffled conical flask. The starter culture was incubated at 28 °C with shaking at 150 rpm for 3 days. Fifty millilitres of RHM medium and modified RHM medium cultures in 250 mL baffled conical flasks were inoculated using 500 µL of the starter culture, and these were incubated for various time periods at 28 °C with shaking at 150 rpm. RHM medium consisted of potassium dihydrogen phosphate (20 g L^{-1}), ammonium chloride (4.4 g L^{-1}), potassium sulfate (0.3 g L^{-1}), magnesium sulfate heptahydrate (0.25 g L^{-1}), 50% glucose soln. (4 mL L^{-1}), 0.3 g L^{-1} biotin soln. (1 mL L^{-1}), trace metal soln. (5 mL L^{1}), and deionised H_2O (dH_2O). The trace metal soln. consisted of iron sulfate heptahydrate (2.8 g L^{-1}), zinc chloride (1 g L^{-1}), manganese chloride tetrahydrate (1 g L^{-1}), copper chloride (0.2 g L^{-1}), cobalt chloride (0.2 g L^{-1}), sodium molybdate (0.2 g L^{-1}), calcium chloride dihydrate (2 g L^{-1}), citric acid (1.5 g L^{-1}), and dH_2O. The modifications to RHM medium were made by altering the trace metal soln. as follows: TR1 (as above); TR2 - iron sulfate heptahydrate x0; TR3 - iron sulfate heptahydrate x10 (28 g L^{-1}); TR4 - calcium chloride dihydrate x0; TR5 - calcium chloride dihydrate x10 (20 g L^{-1}). All RHM cultures were brought up to pH 6 using 1 M NaOH solution, before autoclaving and the 50% glucose soln. was autoclaved separately and added to the cultures just before they were inoculated.

A sample of each culture was examined under the microscope for evidence of morphological changes and the hyphae in the resulting images were measured using Media Cybernetics Image-Pro Analyser 7.0 software. This software (calibrated using a photograph of a stage micrometer) allows measurements to be made by simply tracing a line with the mouse over the hyphae, with a new line for each branch. The results for each measured hyphae were then exported to excel and the total length (length of main hyphae added to the length of all of its branches) and number of tips were calculated, along with the hyphal growth unit (G), which was calculated using the formula: G = total hyphal length ÷ number of tips.

Four repeat cultures were used. These consisted of 2 identical experiments with 2 repeats in each. For the length, tips and G measurements, an average was calculated from 80

measurements; 20 from each of 4 cultures per condition, and for diameters an average was calculated from 400 measurements; 100 from each of the 4 cultures.

Assessment of the biomass production of filamentous fungi in liquid culture is made difficult by the fact that they do not form a homogenous culture, as in bacteria, but instead a more complex and heterogeneous culture is formed from differentiated cells such as conidia and hyphae (Grimm *et al.*, 2005). Multicellular hyphae form numerous branches, which can result in different growth forms ranging from dispersed hyphae and inter-connected hyphal networks to densely packed pellets (Grimm *et al.*, 2005). Therefore, to obtain a more accurate measurement of the biomass it was necessary in this experiment to use the cells from an entire 50 mL culture rather than take smaller samples. The dry mass of the fungal cells in the culture was therefore determined by centrifugation of full 50 mL cultures at 3,500 rpm for 10 min (Beckman Allegra 6R centrifuge), careful removal of the supernatant with a pipette and lyophilisation (Virtis SP Scientific, Sentry 2.0) of the cell pellet for 4-5 d at -63 °C.

Statistical tests were performed using SPSS. The data were transformed by calculating the Log^{10} of the G value and length in order to give normally distributed data, which were then tested for statistical significance using the t test for two independent samples. Repeatability of the method for sampling and measuring the cells was checked by taking four 500 µL samples from one *F. venenatum* A3/5 culture and subjecting this to the same measurements described below. Statistical analysis showed no significant difference between the 4 repeats.

2.2.2 Fungal growth in a 1 L fermenter

F. venenatum A3/5 (obtained from Quorn Foods) cultures were maintained on oatmeal agar at 4 °C. Starter cultures for each strain were begun by transferring a small piece of hyphae from the edge of the growing fungus into 50 mL Oxoid nutrient broth in a 250 mL baffled conical flask and this was incubated at 28 °C with shaking at 150 rpm for 3 days. One hundred microliters of the starter culture were then used to inoculate 600 mL of the medium in the

fermenter, and the fermenter was set to maintain a temperature of 28 °C, a pH of 6.0, the impeller speed was 100 rpm, and air was introduced to the culture at an approximate rate of 0.5 L h^{-1}. The medium consisted of 800 mL fermenter medium added to 200 mL iron sulfate solution, which were autoclaved separately. The fermenter medium consisted of potassium sulfate (3.33 g L^{-1}), magnesium sulfate heptahydrate (1.5 g L^{-1}), calcium acetate (0.33 g L^{-1}), glucose monohydrate (60.498 g L^{-1}), 85% orthophosphoric acid (1.93 mL L^{-1}), polypropylene glycol 2000 grade (0.83 mL $^{-1}$), fermenter trace elements solution (2.5 mL $^{-1}$), and dH_2O. The fermenter trace elements solution consisted of manganese sulfate tetrahydrate (40 g L^{-1}), zinc sulfate heptahydrate (50 g L^{-1}), copper sulfate pentahydrate (5 g L^{-1}), biotin (0.05 g L^{-1}), concentrated sulfuric acid (5 mL L^{-1}), and dH_2O. The iron sulfate solution consisted of iron sulfate heptahydrate (0.102 g L^{-1}) and concentrated sulfuric acid (0.408 mL L^{-1}), and for the iron-limited condition the same solution was prepared omitting the iron sulfate. The pH of the fermenter was controlled at pH 6 automatically by the fermenter control system using inputs of 2 M ammonium hydroxide solution and 5% sulfuric acid solution.

Six repeat cultures were grown in the control condition and iron-limited condition, 3 samples were taken from each culture at the end of the 3-day culture period and 20 images of hyphae were photographed from each sample. Measurements of 50 hyphal diameters per sample were also taken. The hyphae in the resulting images were measured using Media Cybernetics Image-Pro Analyser 7.0 software in the same way as described above. The Hyphal growth unit (G) was calculated using the formula G = total hyphal length ÷ number of tips.

Statistical tests were performed using SPSS. The data were not normally distributed even after transformation, and so the Mann-Whitney U test was used to compare the length, tips and G measurements between the two conditions. The Kruskal-Wallis test was used to test whether there were any significant differences between the repeats. This analysis showed that there was not a significant difference between repeat cultures of each condition for the length, tips and G measurements. However, analysis did show that there were significant differences

between repeats for diameter measurements and so this data could not be used to compare diameters between the conditions.

2.3 Results

2.3.1 Growth conditions

In this experiment, the fungus was grown in batch conditions either in conical flasks in an incubator or in a 1 L stirred fermenter. Batch conditions are set up so that sufficient nutrients and glucose to meet the needs of the fungus for the duration of the experiment are provided in the medium at the start. The pH was controlled in the fermenter cultures (by the input of either ammonium hydroxide or sulfuric acid) but was not controlled in the conical flask cultures. This is in contrast to the production process for Quorn™, used in industry which is a nutrient-unlimited glucose-stat continuous flow culture in which the nutrients and glucose are constantly added during the fermentation (Simpson *et al.*, 1998). This ensures that the nutrients do not fall to limiting amounts and the glucose is kept at a constant concentration (Simpson *et al.*, 1998). The industrial process uses an air-lift system that both adds air to the fermenter and aids mixing, rather than using an impeller for stirring (Wiebe, 2004). The Quorn™ production process is therefore different to the conditions used here and so the initial results found here would need to be confirmed in continuous flow conditions that more closely match the industrial process.

2.3.2 Growth of *F. venenatum* A3/5 in conical flask cultures

The growth curve for *F. venenatum* A3/5 (Figure 6) has shown that the peak of growth is at the 2nd and 3rd day, after which growth slows due to depletion of nutrients.

The analysis of biomass produced in each condition has shown some differences of statistical significance. There was a 30.3% increase with limited iron ($P<0.05$), a 19.8% increase with

excess iron (P<0.05), and a 25.1% increase with excess calcium (P<0.001), when each was compared to the control. (Figure 7).

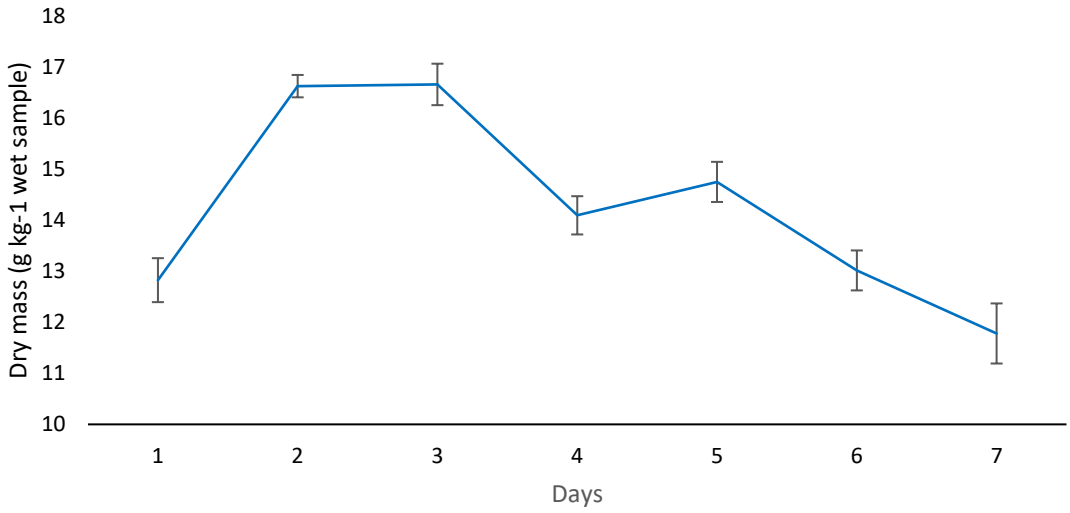

Figure 6: *F. venenatum* A3/5 growth curve for the control culture, grown in shake flasks, calculated from daily measurement of dry mass (g kg^{-1} wet sample). Calculated as an average of 3 cultures. Error bars represent one standard deviation.

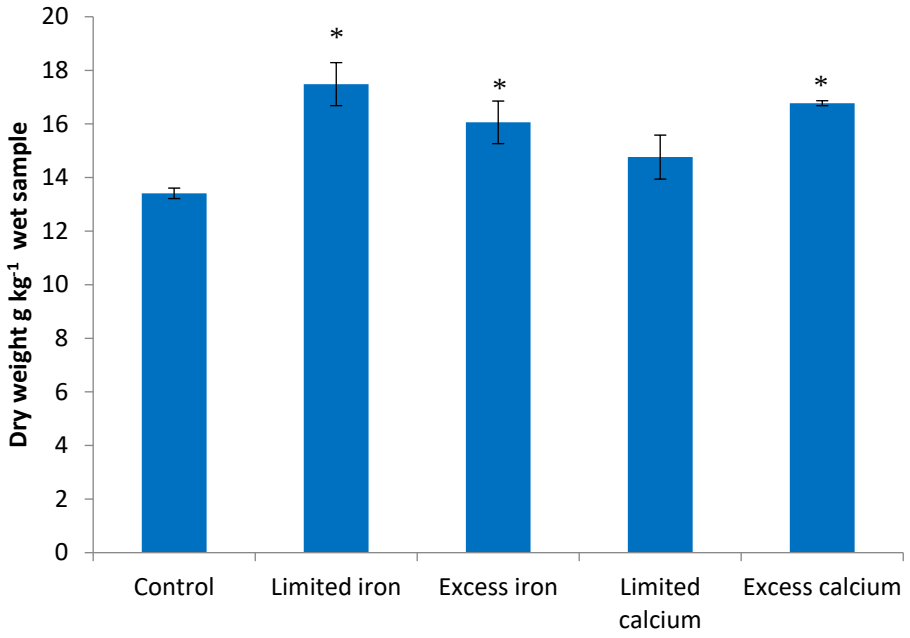

Figure 7: *F. venenatum* A3/5 dry mass of cultures after 3 d growth (g kg^{-1} wet sample). Calculated as an average of 3 cultures for each treatment. Error bars represent one standard deviation. * indicates statistical significance.

2.3.3 Morphology of *F. venenatum* A3/5 grown in conical flask cultures

The results for *F. venenatum* A3/5 morphology have shown that the G value decreased with time after day 4 in all cultures (Figure 8a). The average G value was found to be 35% higher than the control in the iron-limited culture for measurements taken after 2 days (Figure 8a). This result was very highly statistically significant ($P<0.001$). There were also some differences in the other conditions, but these results were not statistically significant. An example photograph for the morphology observed in the control and the low iron conditions is shown in Figure 9 and Figure 10.

The average length for all cultures showed a decrease from the 4^{th} day to the 14^{th} day of culture, which is likely to be due to the depletion of nutrients reducing the growth of the fungus (Figure 8b). After 2 days of culture, the average length measurements showed that the hyphae in the iron-limited culture were 35% longer than in the control culture, and these results were highly

statistically significant for 2 days (P<0.01). Other conditions did not show a significantly altered length.

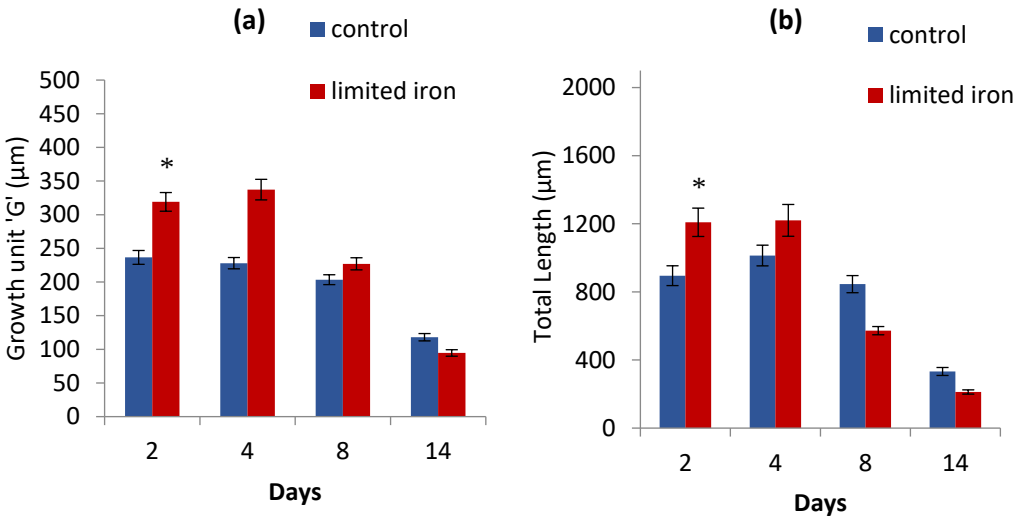

Figure 8: (a) *F. venenatum* A3/5 Hyphal Growth Unit (G) (µm) (G = total hyphal length ÷ number of tips) for iron-limited cultures compared to the control. G was calculated from 80 measurements, 20 from each of 4 cultures for each treatment. Error bars represent the standard error. (b) *F. venenatum* A3/5 average total hyphal length (µm) for iron-limited cultures compared to the control. Length was calculated from 80 measurements, 20 from each of 4 cultures for each treatment. Error bars represent the standard error. * indicates statistical significance.

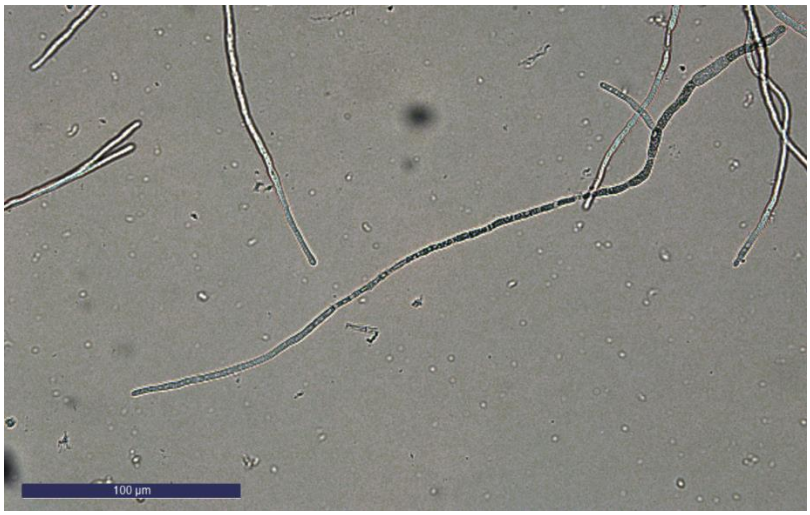

Figure 9: Example photograph of *Fusarium venenatum* A3/5 hyphae (x200 magnification) when grown in shake flask cultures with the control growth medium (unmodified RHM medium). Photographed with Leica Application Suite software (version 4.3.0) connected to a Leica DM5000B microscope.

Figure 10: Example photograph of *Fusarium venenatum* A3/5 hyphae (x200 magnification) when grown in shake flask cultures with limited iron medium (RHM medium with no added iron). Photographed with Leica Application Suite software (version 4.3.0) connected to a Leica DM5000B microscope.

The number of tips showed a decrease with time in all cultures, over the 14 days of culture (Figure 11). There was a lower number of tips in the iron-limited culture, when compared to the control (Figure 11a). This was a statistically significant difference for 4 days (24% decrease) and 8 days (37% decrease) of culture ($P<0.05$). There was also a statistically significant difference in the number of tips in the low calcium culture; there was a greater number of tips after 2 days, with a 26% increase ($P<0.05$) (Figure 11b). This result is in agreement with the research by (Robson *et al.*, 1991b) that linked low calcium conditions with more branches in *F. venenatum* A3/5. Other slight differences in the number of tips were not statistically significant.

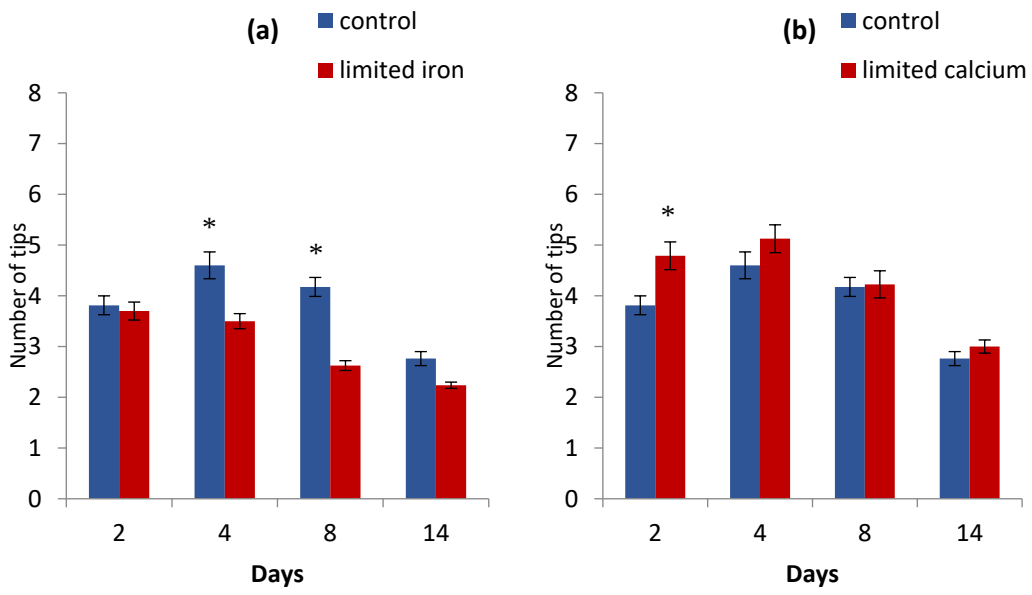

Figure 11: *F. venenatum* A3/5 average number of tips, calculated from 80 measurements, 20 from each of 4 cultures for each treatment. (a) Limited iron compared to control. (b) Limited calcium compared to control. Error bars represent the standard error. * indicates statistical significance.

Average measurements suggest that cells in the iron-limited culture had smaller diameters compared to the control at every time point (Figure 12). However, the results for diameter measurements in the modified media were not statistically significant. A study by (Robson *et al.*, 1991b) did find significant differences, however, with increased diameters in *F. venenatum* A3/5 when the calcium concentration was reduced.

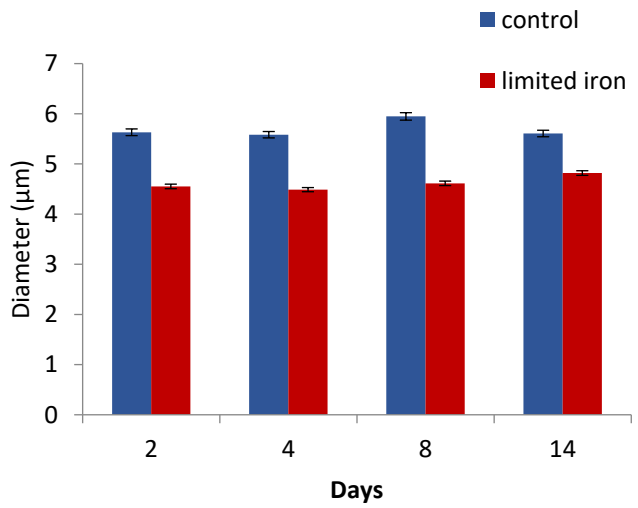

Figure 12: *F. venenatum* A3/5 average diameter of hyphae (µm) for iron-limited cultures compared to control, calculated from 400 measurements, 100 from each of 4 cultures for each treatment. Error bars represent the standard error. These results were not statistically significant.

2.3.4 Morphology of *F. venenatum* A3/5 grown in 1 L fermenter

The fermenter was chosen for a second experiment as it allowed the growth of the cultures with control of pH and air input. This was carried out for the iron depleted condition in order to compare with the shake flask data and investigate whether the same effect would be seen with greater control of the culture environment.

When grown in the 1 L fermenter, the fungus has shown the same morphology effect of limited iron compared with the control, with longer hyphae and larger G after 3 days of culture (Figure 13). In the iron-limited culture, the hyphae were 21% longer, with a 13% larger G value, and these results were statistically significant ($P<0.05$). Results suggested a slight increase in the number of tips by 8%, but this was not a statistically significant change. There was not a significant difference in diameter measurements between the two conditions.

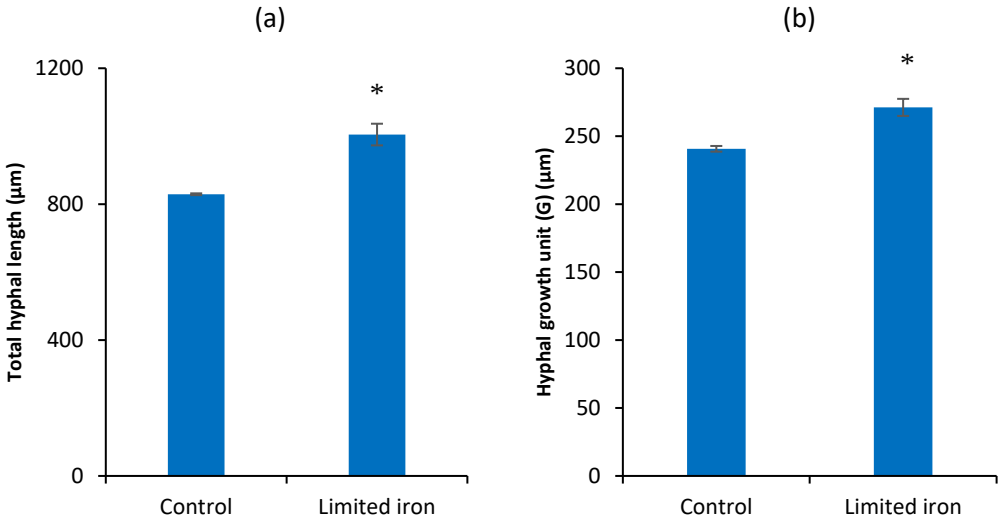

Figure 13: Morphology measurements from *F venenatum* A3/5 cultures grown in 1 L fermenter, averages calculated from 6 cultures for each treatment, from samples taken after 3 days of fermentation. (a) Total hyphal length (µm). (b) Hyphal Growth Unit (G) (µm) (G = total hyphal length ÷ number of tips). * indicates statistical significance.

2.4 Discussion

The biomass results have shown a significant increase in biomass for iron-limited and excess iron, when compared to the control. Other studies in closely related fungi have found differences in dry mass with increased amounts of iron, for example the study by Vasavada & Hsieh (1988) which discovered increased dry cell mass with increased concentrations of Fe^{2+} ions in the range 0.01 mM to 5 mM in *F. graminearum*. Cuero & Ouellet (2005) also found an increase in fungal dry mass when Fe^{2+} ions were added to *F. graminearum* cultures at a concentration of 5 mg L^{-1}. The study by Cuero & Ouellet (Cuero & Ouellet, 2005) looked at gene expression in media supplemented by a mixture of Fe^{2+}, Zn^{2+}, and Cu^{2+} and found that genes associated with cell growth and energy production were upregulated in the supplemented cultures. This lends weight to the suggestion by Vasavada & Hsieh (1988) that the supplementation of metal ions to the growth medium could cause an increase in growth by causing an increased stimulation of enzymes belonging to essential metabolic pathways.

Increased calcium caused an increase in biomass when compared to the control, but limited calcium did not cause a significant change. It's possible that the limited calcium medium didn't have a significant effect here due to the difficulty of eliminating all calcium ions from the media, since it is likely present as a contamination from the other nutrients added or from the glassware (Robson *et al.*, 1991b). A significantly decreased growth yield (biomass produced per g glucose utilised) with lower calcium concentrations in *F. venenatum* was however described in the investigation by Robson *et al.*, (1991b), and they explain this effect by suggesting that the calcium concentration affects glucose metabolism, which has been found to be the case in other organisms. It is also possible that a lower concentration of calcium affected the processes at the growing hyphal tip that are known to require calcium, i.e. actin polymerisation/depolymerisation and vesicle exocytosis, and so influenced growth (Takeshita *et al.*, 2017).

In this present investigation, after 2 days the number of tips was higher in the limited calcium culture when compared to the control (Figure 11b). Two studies of morphology in *F.*

venenatum A3/5 by Robson *et al.* (1991b) and Robson *et al.* (1991a) also found a relationship between Ca^{2+} concentration and hyphal branching. In the first study a chelating agent (EGTA) was used to reduce the Ca^{2+} concentration to very low levels in the growth media (10^{-9} to 10^{-7} M). Calcium chloride was then added to certain cultures to investigate the effects of various concentrations of Ca^{2+} in the range of 10^{-5} to 10^{-2} M (Robson *et al.*, 1991b). It was found that a low concentration of Ca^{2+} (1.4×10^{-8} M) encouraged hyphae with more branches and larger diameters, but a higher Ca^{2+} concentration (5×10^{-4} M) resulted in less branches, and smaller diameters (Robson *et al.*, 1991b).

The second study used a Ca^{2+} ionophore and calcium channel blockers to confirm this effect, and to demonstrate that it is the intracellular Ca^{2+} concentration that is involved in the control of hyphal branching (Robson *et al.*, 1991a). Higher concentrations of the ionophore A23187 led to a decrease in growth unit length, with a progressive increase in branching frequency as the ionophore increased (Robson *et al.*, 1991a). The authors suggest that the low concentration of A23187 is affecting the fungus by increasing the release of Ca^{2+} from intracellular storage, but higher concentrations of A23187 cause Ca^{2+} uptake from the medium, thus triggering a different response (Robson *et al.*, 1991a). This investigation also used a calmodulin antagonist to indicate that Ca^{2+} affects the growth of the hyphae and the production of branches in *F. venenatum* via calmodulin (Robson *et al.*, 1991a). The authors suggest that this may be due to the increased activation of chitin synthase enzyme, an essential enzyme for cell wall biosynthesis, as it has been demonstrated that calmodulin stimulates this enzyme in other filamentous fungi (Robson *et al.*, 1991a).

The results of the iron-limited cultures showed that after 2 days, when grown in a medium with limited iron, the hyphae are longer, and had a larger G value for iron-limited cultures. In addition, the number of tips was lower for iron-limited cultures after 4 days and 8 days. The other altered concentrations of iron and calcium did not produce significant variations in length, tips or diameter when compared with the control. A very similar result was found when the fungus was grown in the fermenter with iron-limited medium, which gave a significant

increase in length and G value compared to the control, but no significant change in the number of tips.

These results suggest that a low concentration of iron has affected the morphology of the fungus, with changes in both the length and branching. The length has increased, but this may be accompanied by a decrease in the number of branches. The production of new fungal biomass is dependent on the production of the cell wall, along with cell membrane, organelles and cytoplasm, and the fungal cell wall consists of chitin and glucans, which are polymers of N-acetylglucosamine and glucose, respectively (Bowman & Free, 2006). Other constituents of the cell wall include glycoproteins, carbohydrates and glycosylphosphatidylinositol (Bowman & Free, 2006). The central biochemical processes such as amino acid biosynthesis and glucose metabolism, which are necessary for the production of the precursor molecules, and the enzymes required for production of new hyphae could be disrupted by altered concentrations of iron ions due to their dependence of their biosynthesis on numerous enzymes that contain Fe/S clusters (Netz *et al.,* 2014). Hyphal growth and branching could therefore be affected by altered availability, either by depletion or accumulation of these precursor molecules.

A study by Li et al., (2015) looked at a possible link between the control of hyphal branching in filamentous fungi and glucose metabolism. This study investigated the enzyme UDP-glucose pyrophosphorylase (UGP), which catalyses the conversion between glucose-1-phosphate and UDP-glucose, an important precursor in cell wall biosynthesis due to its incorporation in lipopolysaccharides, extracellular polysaccharides and glycolipids, among others (Li *et al.,* 2015). The results showed that there was a decrease in intracellular Ca^{2+} concentration when there was an accumulation of glucose-1-phosphate, and vice versa, and this affected hyphal branching (Li *et al.,* 2015). It was found that in the fungus with increased glucose-1-phosphate, there was a 30% reduction in the distance between branches, but this was reversed with addition of $CaCl_2$ (Li *et al.,* 2015). This study has demonstrated that there could be a mechanism that links glucose metabolism with hyphal branching, via Ca^{2+}

concentration (Li *et al.*, 2015). A disruption of glucose metabolism and build-up of precursor molecules caused by low iron concentration could therefore be affecting the morphology of the fungus by affecting Ca^{2+} levels, which have an essential role at growing tips, and possibly by disrupting calcium signalling pathways that control growth and morphology (Li *et al.*, 2015).

Alternatively, the iron-limited conditions could be affecting morphology by causing a disruption of DNA metabolism. Since critical elements of DNA metabolism, including its repair, also depend on Fe/S clusters, a lack of iron could also be disrupting these processes (Netz *et al.*, 2014). This could lead to far-ranging and unpredictable effects on the cell, including the changes in morphology shown here (Netz *et al.*, 2014).

2.5 Conclusions

The biomass results have shown an increase in growth for limited iron, excess iron and excess calcium cultures, when compared to the control. At the peak of its growth, after 2 days when grown in a medium with limited iron, the hyphae are longer, and had a larger G value for iron-limited cultures. The number of tips was lower for iron limited cultures after 4 days and 8 days, and the number of tips was higher after 2 days in the limited calcium culture. The other altered concentrations of iron and calcium did not produce significant variations in length, tips or diameter when compared with the control. A very similar result was found when the fungus was grown in the fermenter with iron-limited medium, which gave a significant increase in length and G value compared to the control, but no significant change in the number of tips.

2.6 Further work

The results shown here were based on batch cultures, which differ from the continuous flow fermentation used to produce Quorn™. This investigation will therefore need to be scaled up

to a continuous flow fermentation that more closely replicates the industrial process, in order to determine if the same changes to morphology are observed in these conditions.

In addition to this, further work will also be necessary to find the mechanism behind the increase in length in iron-limited conditions in order to increase our understanding of the control of morphology in filamentous fungi. Further investigations could include a proteome and transcriptome analysis in each condition so that the proteins and genes upregulated or downregulated can be found. This could be targeted towards genes that are already known to affect morphology and branching frequency in fungi. This could reveal transcripts of genes that are responsible for controlling this change in morphology and this knowledge could help to optimise the fermentation to achieve the best morphology for the Quorn^{TM} product. In addition, growth of the fungus in a range of varying concentrations of iron ions could reveal the threshold for iron that initiates the change in morphology.

3. Changes in the amounts of free intracellular amino acids in response to altered concentration of iron and calcium ions in *F. venenatum*

3.1 Introduction

Amino acid biosynthesis is one of the cell's essential processes, producing the building blocks of proteins necessary for growth and metabolism, with the pathways for the synthesis of many amino acids occurring universally in modern species (Hernandez-Montes *et al.*, 2008). Iron cofactors are required for enzymes involved with many of the major pathways in the cell, including those for amino acid production and respiration (Philpott *et al.*, 2012), and so it is likely that changes to the concentration of iron in the medium would affect amino acid production. Calcium acts as messenger which in combination with proteins such as calmodulin is able to activate enzymes from a variety of pathways (Hoeflich & Ikura, 2002), and so it is possible that altering the amount of calcium supplied to the fungus may also have an effect on amino acid production.

The levels of amino acids in response to limiting iron and calcium or supplying these cations in excess has not yet been studied in *F. venenatum*. The use of this fungus in the food industry make this an important area for study as the levels of amino acids such as glutamate and aspartate can affect the umami flavour of the product (Zhang *et al.*, 2013), and other amino acids may also contribute to flavour by imparting a sweet or bitter taste (Mau *et al.*, 2001), or contributing to the development of aroma upon cooking via the Maillard reaction (Ames, 1998). Changes to amino acid synthesis could also have far-ranging effects on the biochemistry of the fungus as they are the precursors for protein synthesis and provide intermediates necessary for the production of many other essential compounds, for example the production of purine nucleotides requires the input of glycine, glutamate and aspartate (Zhang *et al.*, 2008).

In this investigation *Fusarium venenatum* cultures were subjected to altered levels of iron and calcium ions and the levels of free amino acids were measured in order to ascertain whether amino acid metabolism was significantly altered by the availability of these ions.

3.1.1 Amino acid biosynthesis

Fungi possess the necessary biosynthetic pathways to synthesise all amino acids required for their metabolism (Feldmann, 2012). Their production begins with ammonium ions, which are first incorporated into glutamate which can then donate the amino group for the production of other amino acids (Shakoury-Elizeh *et al.*, 2010). The biosynthesis of glutamate also requires the TCA cycle intermediate, α-ketoglutarate, along with the ammonium ions, and this reaction is catalysed by glutamate dehydrogenase (Sieg & Trotter, 2014). Glutamate can be converted to glutamine by the enzyme glutamine synthetase, which requires the addition of ATP and a further molecule of ammonia (Sieg & Trotter, 2014). In conditions of low ammonium, glutamate can be made from glutamine and α-ketoglutarate using glutamate synthase enzyme, which has an Fe/S cluster (Philpott & Protchenko, 2008), (Figure 14).

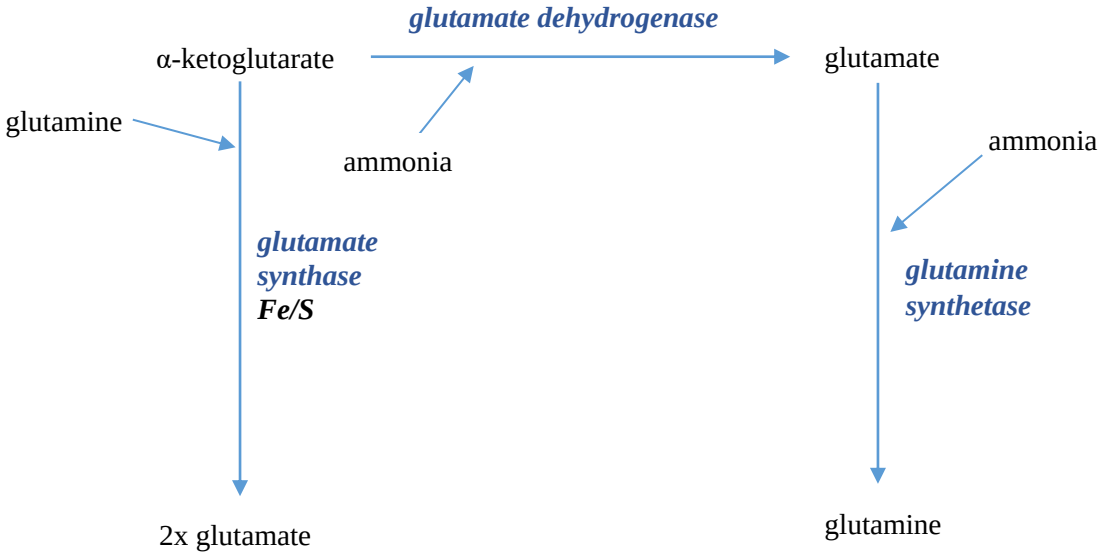

Figure 14: Pathways for the production of glutamate and glutamine (Sieg & Trotter, 2014), (Philpott & Protchenko, 2008).

Alanine is made by the transfer of an amino group from glutamate to pyruvate by alanine transaminase enzyme, and this is accompanied by the production of α-ketoglutarate (Peñalosa-Ruiz *et al.*, 2012). In a similar alternative reaction, glutamine is used in place of glutamate, and α-ketoglutaramate is produced (Peñalosa-Ruiz *et al.*, 2012). (Figure 15).

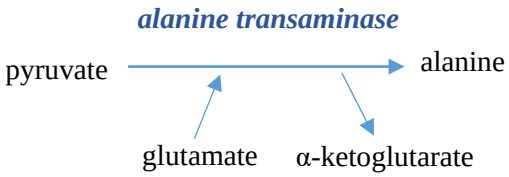

Figure 15: Pathway for the synthesis of alanine from pyruvate (Peñalosa-Ruiz et al., 2012).

Proline is formed from glutamate in a process requiring 3 enzymes: glutamate kinase, γ-glutamyl phosphate reductase, and pyrroline-5-carboxylate reductase (Liang *et al.*, 2014). (Figure 16). In yeast, arginine biosynthesis also begins with glutamate and several reactions are required, leading to the production of ornithine and citrulline, before resulting in arginine (Abadjieva *et al.*, 2001), (Figure 16).

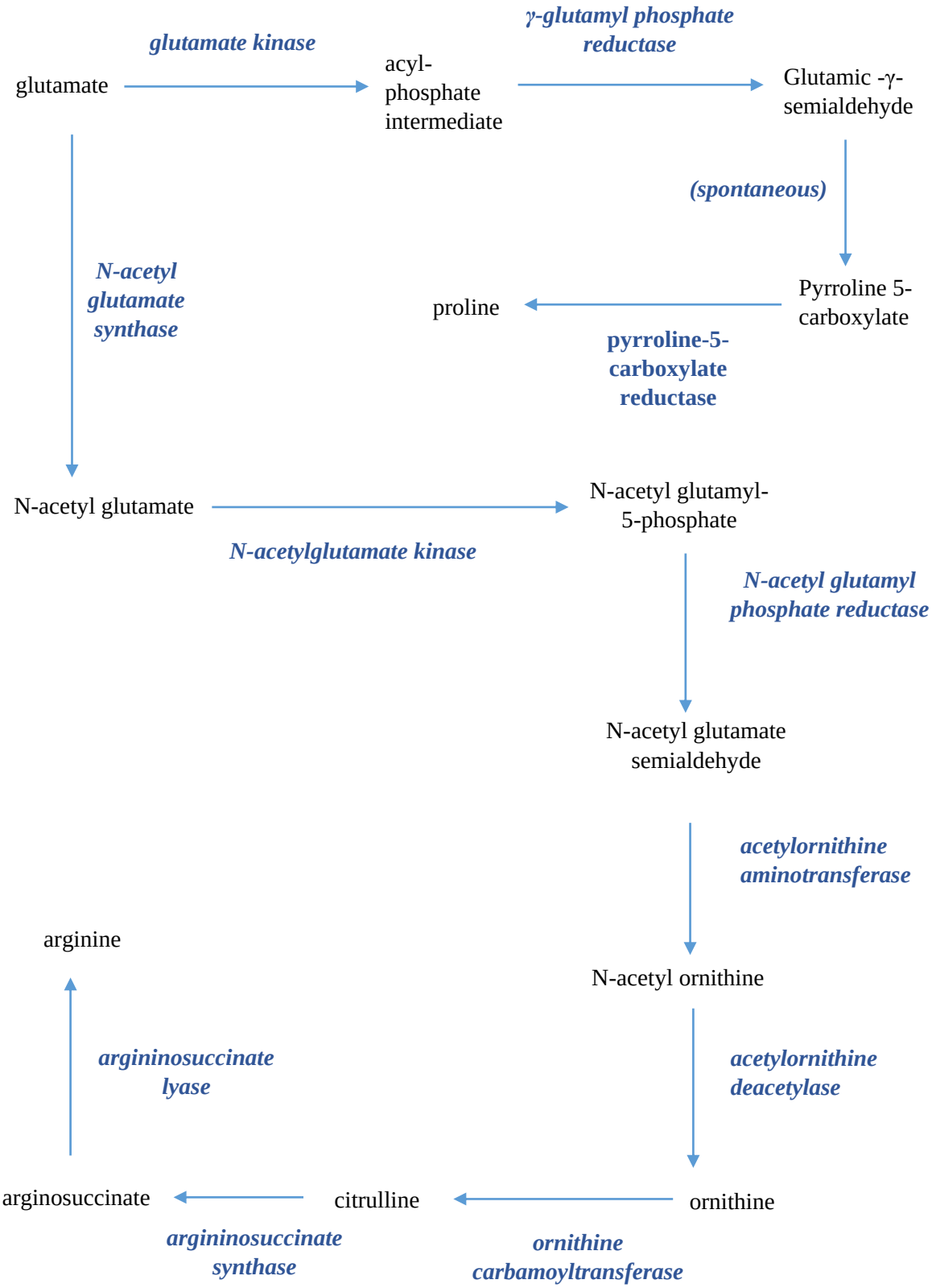

Figure 16: Pathways for the synthesis of proline (Liang et al., 2014), and arginine (Abadjieva et al., 2001).

The biosynthesis of the aromatic amino acids; phenylalanine, tyrosine and tryptophan occurs though a linked series of pathways. The first seven reactions of the shikimate pathway convert erythrose-4-phosphate and phosphoenolpyruvate to chorismate (Braus, 1991). This compound can then be converted to each of the amino acids in this group (Braus, 1991). Tyrosine and phenylalanine can both be made in three steps from chorismate, but tryptophan requires five reactions with the input of glutamine in the first reaction and a serine molecule is used in the final reaction (Braus, 1991), (Figure 17).

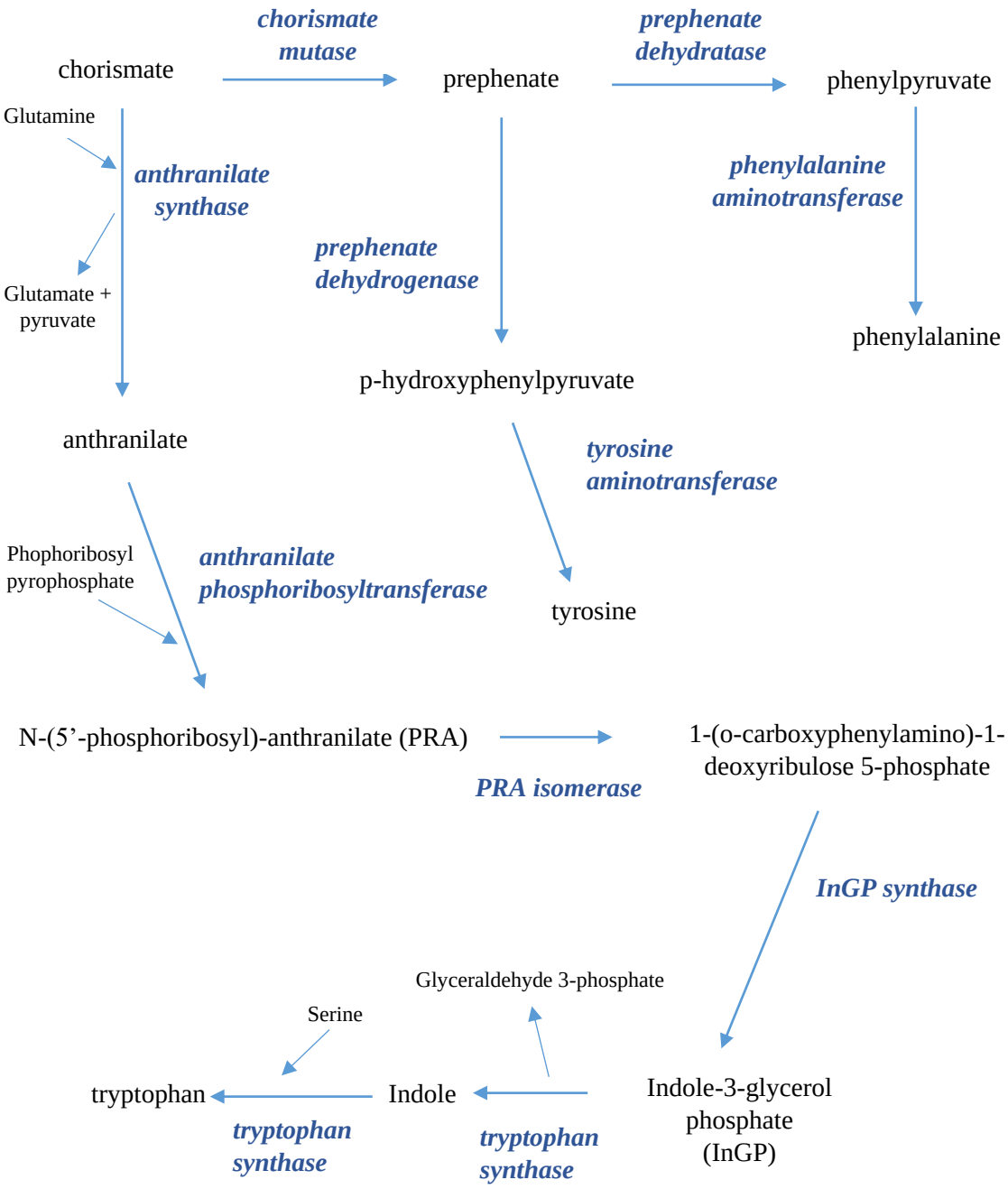

Figure 17: Pathways for the synthesis of aromatic amino acids tyrosine, phenylalanine, and tryptophan (Braus, 1991).

Higher fungi possess the α-aminoadipate pathway for lysine biosynthesis, which is not present in other organisms (Xu *et al.*, 2006). In this pathway α-ketoglutarate is combined with acetyl-CoA to produce homocitrate, which once converted to homoisocitrate is combined with nitrogen from glutamate to form α-ketoadipate, which is then converted to α-aminoadipate (Xu *et al.*, 2006). α-aminoadipate is converted to α-aminoadipate-δ-semialdehyde, which then reacts with a molecule of glutamate to produce saccharopine, which is then converted to lysine with the release of α-ketoglutarate (Xu *et al.*, 2006), (Figure 18).

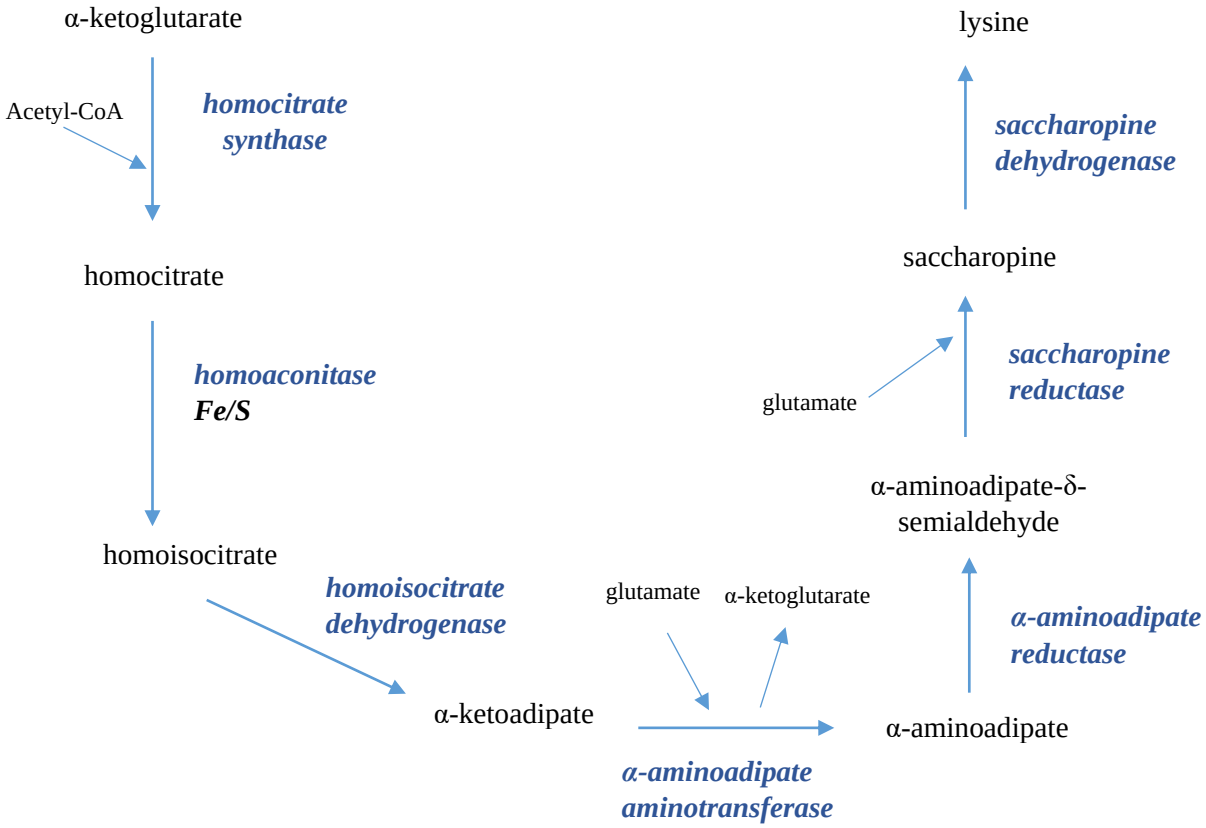

Figure 18: α-aminoadipate pathway for the synthesis of lysine (Xu et al., 2006).

Asparagine is synthesised from oxaloacetate via aspartate (Jastrzębowska & Gabriel, 2015). First, oxaloacetic acid from the TCA cycle is converted to aspartate with the addition of an amino group from glutamine (Jastrzębowska & Gabriel, 2015). The aspartate is then converted to asparagine by asparagine synthetase, and this reaction is accompanied by the conversion of glutamine to glutamate, which donates another amino group (Jastrzębowska & Gabriel, 2015). Threonine is produced in 5 steps from aspartate, with the production of homoserine as an intermediate, which can be converted to methionine (Farfán & Calderón, 2000), (Figure 19).

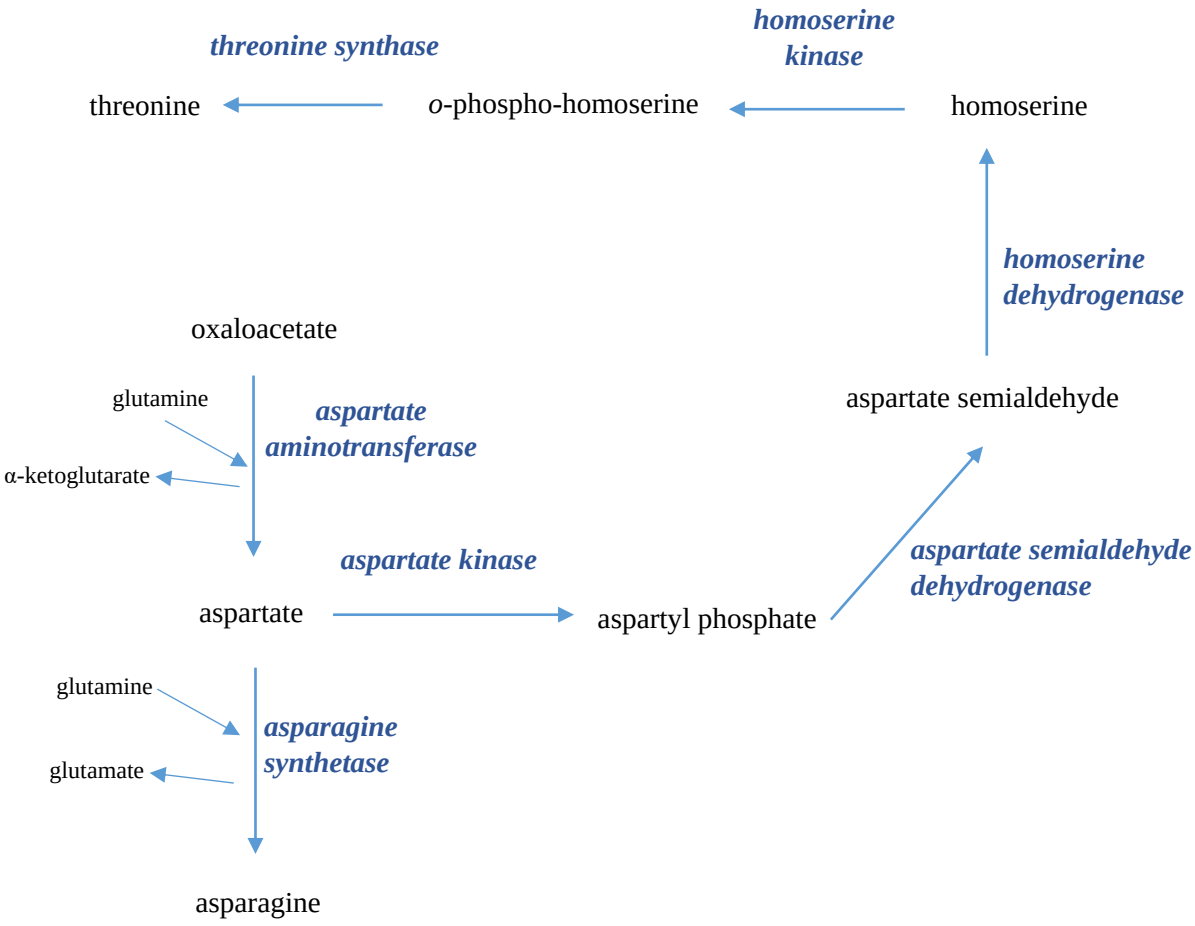

Figure 19: Pathways for the synthesis of asparagine and threonine (Jastrzębowska & Gabriel, 2015).

The branched-chain amino acids, leucine, isoleucine and valine all begin with a common pathway in fungi (Shimizu *et al.*, 2010). The valine and isoleucine pathways both lead directly from pyruvate and they share a set of four enzymes (Shimizu *et al.*, 2010), (Figure 20).

The Leucine pathway begins with 2-oxoisovalerate, the precursor of valine, and this is converted to α-isopropylmalate (Bedekovics et al., 2011). The α-isopropylmalate is then converted to β-isopropylmalate by α-isopropylmalate isomerase, which contains an Fe/S cluster (Bedekovics et al., 2011). The β-isopropylmalate then converts to α-ketoisocaproate, and branched-chain aminotransferase uses this to produce leucine, using glutamate in the process (Bedekovics et al., 2011), (Figure 21).

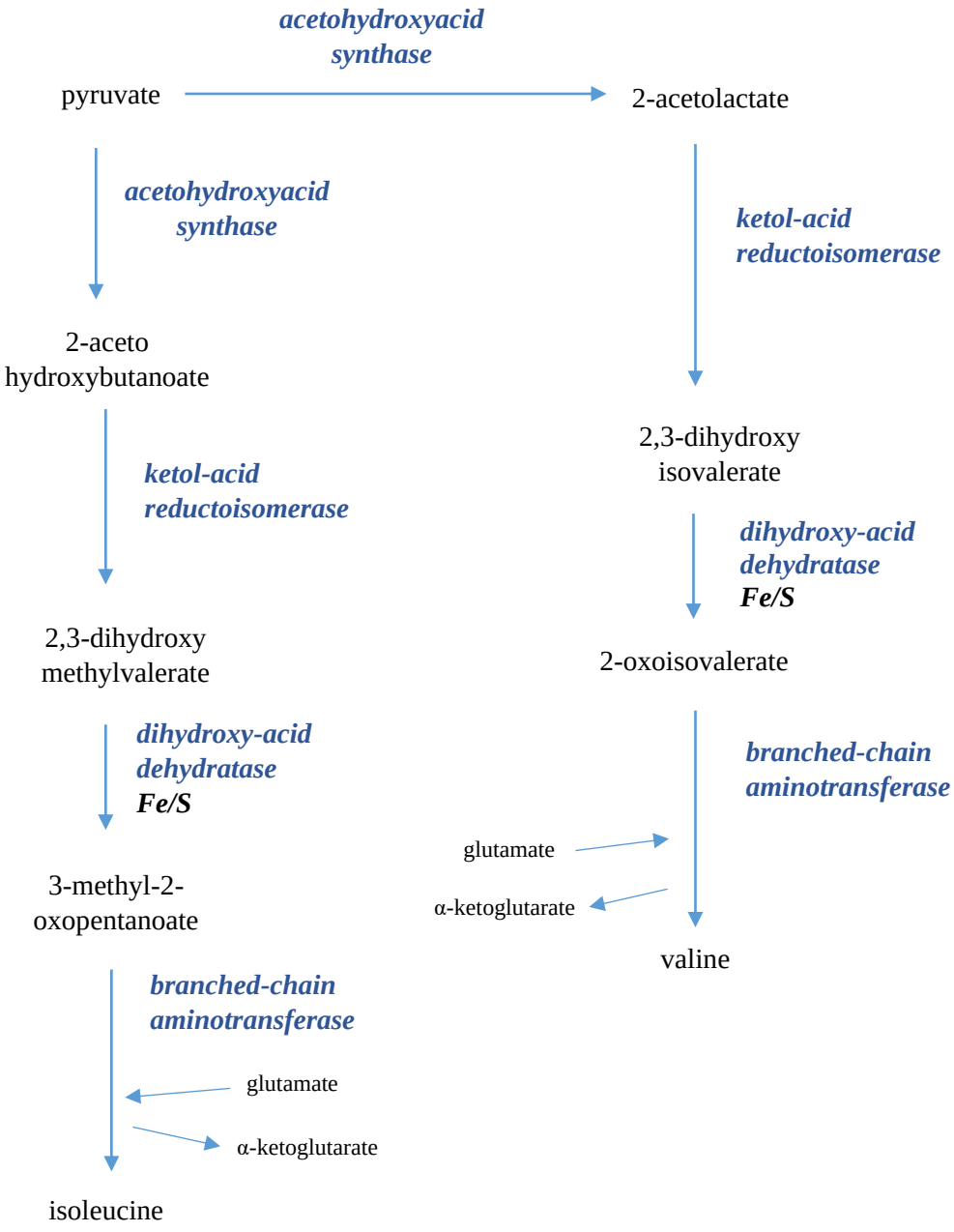

Figure 20: Pathway for the synthesis of the branched-chain amino acids isoleucine and valine (Shimizu et al., 2010).

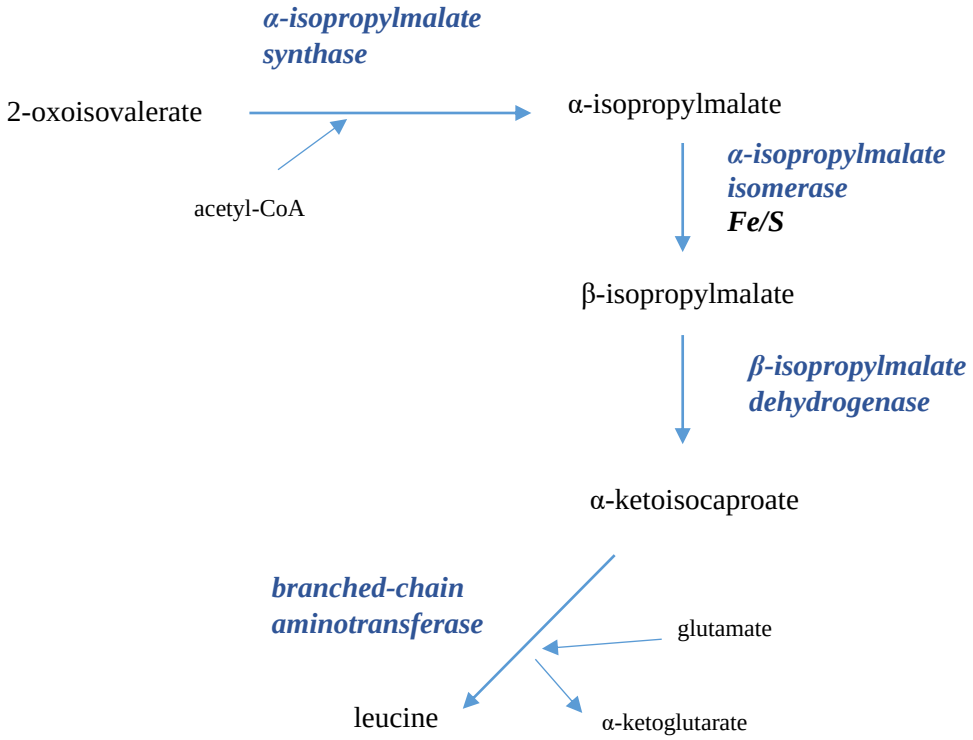

Figure 21: Pathway for the production of the branched-chain amino acid leucine from the intermediate 2-oxoisovalerate (also known as α-ketoisovalerate) (Bedekovics *et al.*, 2011).

The biosynthesis of Methionine and cysteine is linked to the assimilation of sulfur into the cell (Saint-Macary *et al.*, 2015). In sulfur assimilation, sulfate ions are activated and then reduced to sulfite and then to sulfide, which can then be incorporated into the amino acids (Thomas & Surdin-Kerjan, 1997). The sulfide combines with *o*-acetylserine to make cysteine, and this is catalysed by cysteine synthase (Brzywczy *et al.*, 2002). The cysteine can then be converted to cystathionine and subsequently to homocysteine, which can then be converted to methionine (Saint-Macary *et al.*, 2015), (Figure 22).

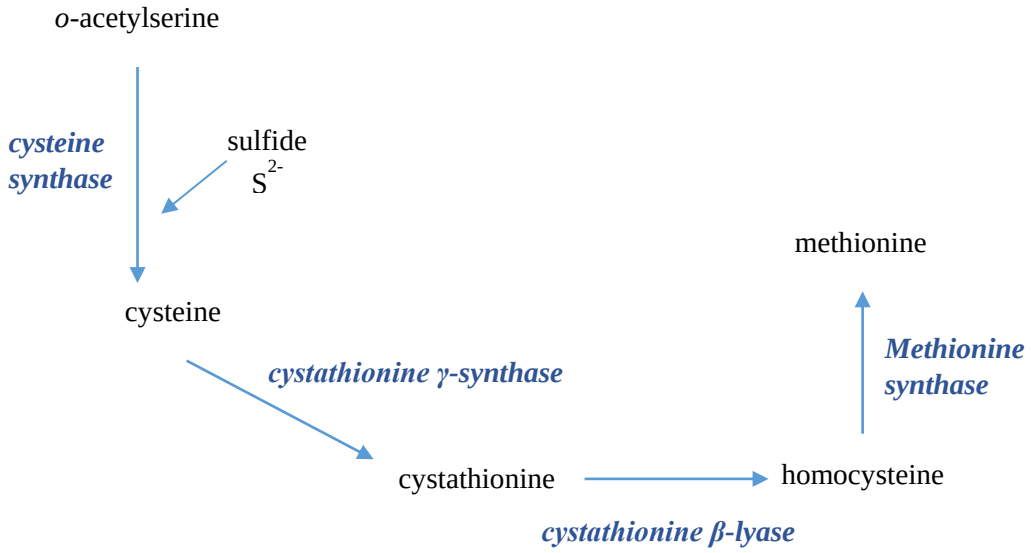

Figure 22: Pathway for the production of cysteine and methionine (Brzywczy et al., 2002), (Saint-Macary et al., 2015).

Histidine is made in a series of 10 reactions (Jastrzębowska & Gabriel, 2015). The pathway starts with phosphoribosylpyrophosphate, which is converted in 4 reactions to phosphoribulosyl-formimino-5-aminoimidazole-4-carboxamide ribonucleotide phosphate (phosphoribulosyl-formimino-AICRP), which after 2 further reactions becomes imidazoleacetol-phosphate, which is converted in 3 reactions to histidinal, and this is then converted to histidine (Jastrzębowska & Gabriel, 2015), (Figure 23) and (Figure 24).

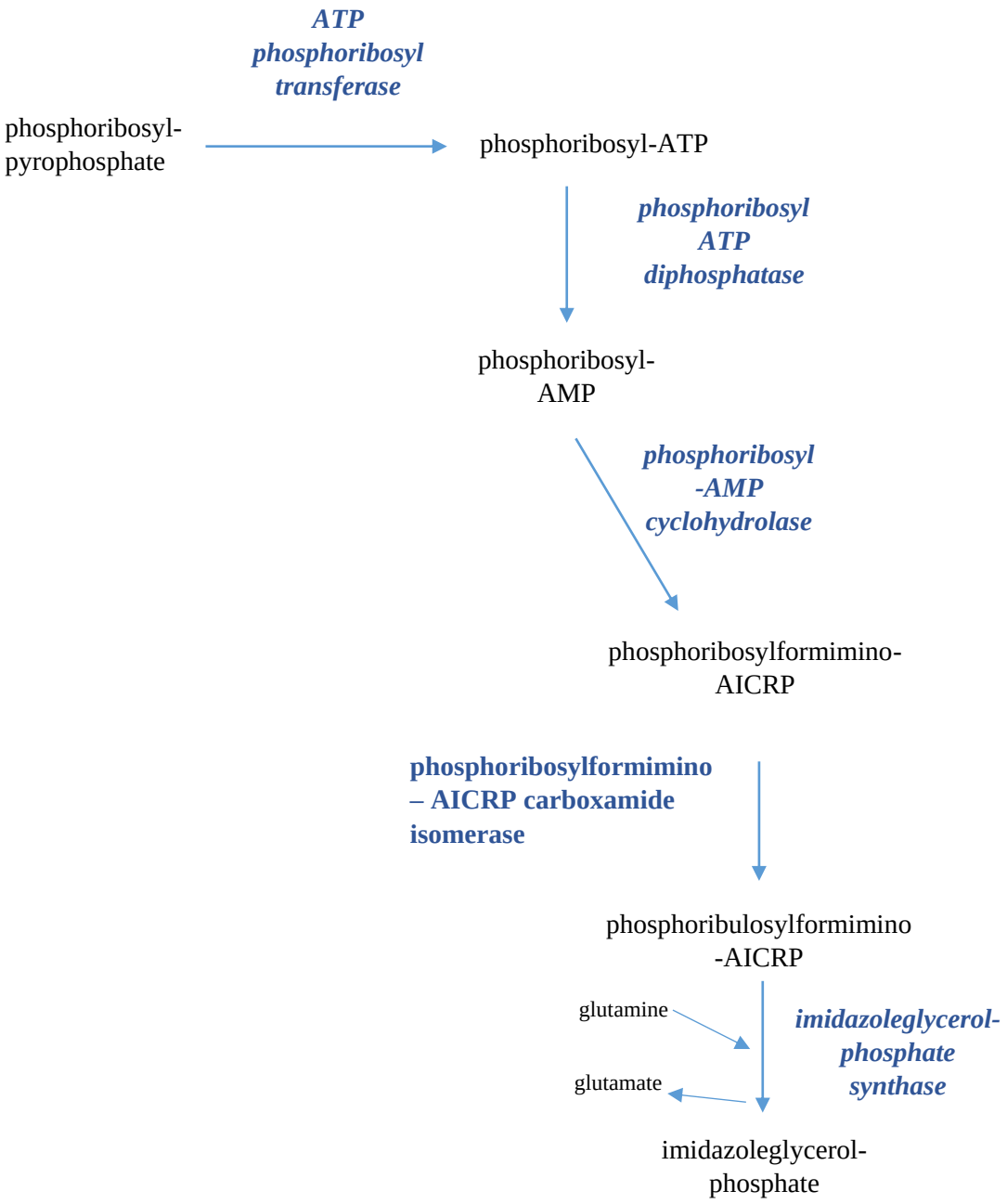

Figure 23: Pathway for the production of histidine *pt1* (Jastrzębowska & Gabriel, 2015).

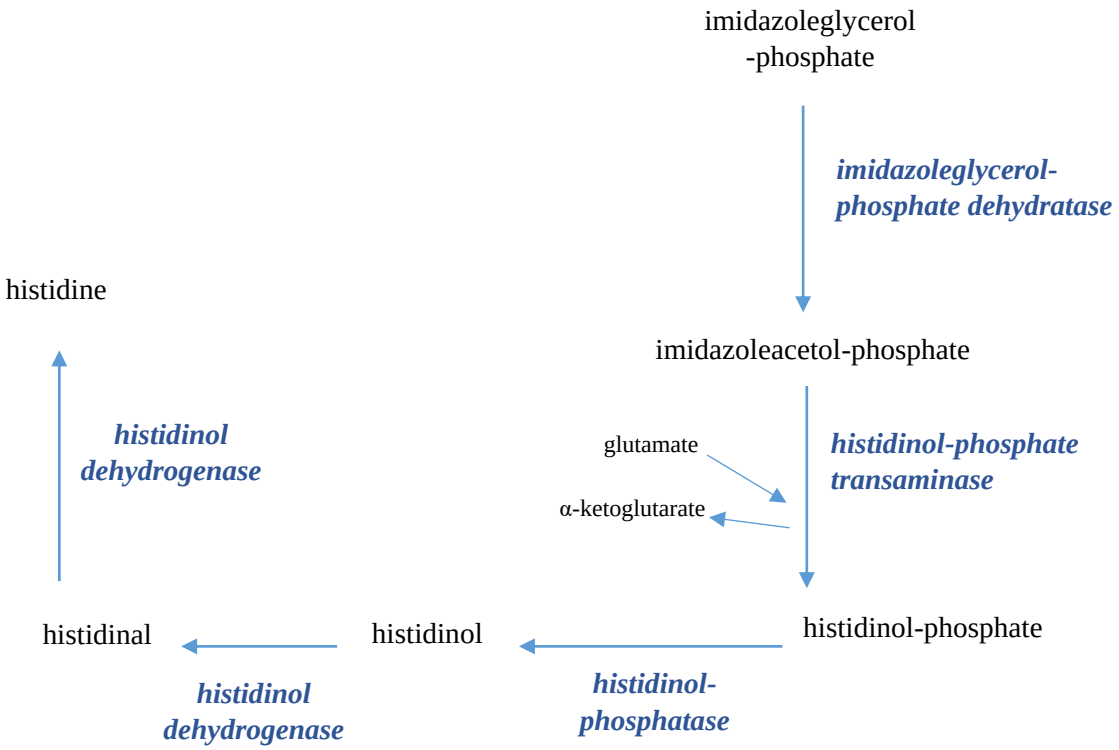

Figure 24: Pathway for the production of histidine *pt2* (Jastrzębowska & Gabriel, 2015).

Serine is produced from 3-phosphoglycerate, an intermediate of glycolysis (Xie *et al.*, 2017). This is converted to serine in 3 reactions by phosphoglycerate dehydrogenase, 3-phosphoserine aminotransferase, and 3-phosphoserine phosphatase (Xie *et al.*, 2017). Serine can also be made from glyoxylate by glyoxylate aminotransferase enzyme (Xie *et al.*, 2017), (Figure 25).

Glycine is produced from serine in one reaction, catalysed by serine hydroxymethyltransferase enzyme (Liu *et al.*, 2015). The reaction requires pyridoxal 5'-phosphate as a cofactor (Liu *et al.*, 2015). An alternative pathway for glycine synthesis via the cleavage of threonine by threonine aldolase enzyme, a reaction that also uses the pyridoxal 5'-phosphate cofactor, and produces glycine with acetaldehyde (Liu *et al.*, 2015), (Figure 25).

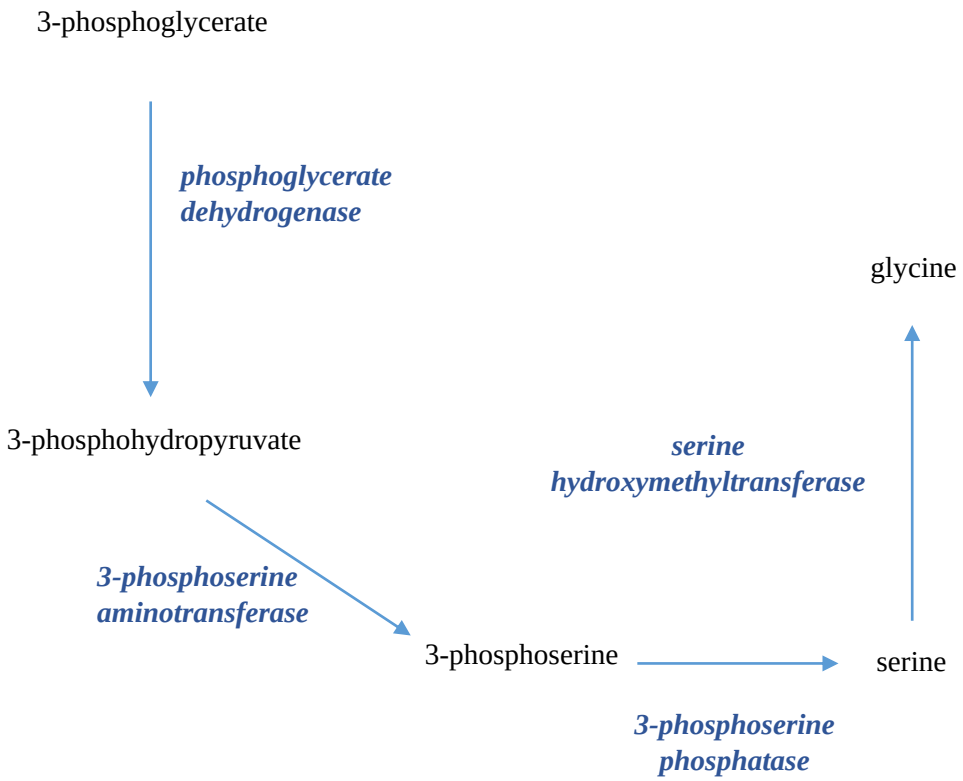

Figure 25: Pathway for the production of serine (Xie et al., 2017) and glycine (Liu et al., 2015).

3.1.2 Amino acid degradation pathways

Alanine, serine, glycine, threonine and cysteine can all be broken down to pyruvate, which links amino acid pathways to carbon metabolism. Alanine can be simply converted back to pyruvate by alanine transaminase enzyme (Peñalosa-Ruiz *et al.*, 2012). Serine can also be broken down directly to pyruvate (Donofrio *et al.*, 2006). Glycine is first converted to serine and then to pyruvate (Zhao *et al.*, 2012). Threonine can be converted to glycine by threonine aldolase (van Maris *et al.*, 2003).

Cysteine can be converted to serine (El-Sayed *et al.*, 2015). Methionine degradation produces cysteine, via homocysteine and cystathionine, (Gerke *et al.*, 2012). Asparagine is converted to aspartate and ammonia (Patro *et al.*, 2014), and aspartate is converted directly to oxaloacetate (Huss *et al.*, 1996).

Glutamine, arginine, proline and histidine, can all be broken down to glutamate. Glutamine is converted to glutamate by glutamate synthase (Lara *et al.*, 1982). Arginine is converted to glutamate via ornithine and glutamate-5-semialdehyde (Goodman & Weiss, 1986). Proline is converted to pyrroline-5-carboxylate, before becoming glutamate (Arst *et al.*, 1981). Histidine can be converted to glutamate, by a series of reactions with intermediates urocanic acid, imidazolone propionate, and formiminoglutamate (Polkinghorne & Hynes, 1982).

Leucine, isoleucine, and valine are degraded by a complex set of reactions. Valine and isoleucine are both ultimately broken down to propionyl-CoA (Maggio-Hall *et al.*, 2008). Leucine is first converted to 4-methyl-2-oxovaleric acid, then to 3-methylbutanoyl-CoA, which is ultimately broken down by a series of reactions to acetyl-CoA and acetoacetate (Rodríguez *et al.*, 2004).

Lysine catabolism is a complex pathway that is not well researched in species of filamentous fungi, and the pathway follows a number of different routes in different organisms (Zabriskie & Jackson, 2000). In different species of yeast there are alternative pathways, one of which begins with the conversion of lysine to 2-aminoadipate-6-semialdehyde (Zabriskie & Jackson, 2000).

In *F. graminearum*, Tryptophan is converted to acetyl-CoA by a series of 13 reactions, although not every enzyme has been confirmed in this species (KEGG, 2017) (Kanehisa *et al.*, 2017). Tyrosine can be converted to fumarate and acetoacetate in 5 reactions, with all but one enzyme confirmed in *F. graminearum* (KEGG, 2017) (Kanehisa *et al.*, 2017).

In most fungi there are enzymes that convert phenylalanine to cinnamic acid and phenylpyruvic acid (Kishore *et al.*, 1976). The cinnamic acid can then be converted to

protocatechuate, and the phenylpyruvic acid can be converted to homogentisate, which then undergoes further degradation (Kishore *et al.*, 1976).

3.1.3 Iron & amino acid biochemistry

Iron is an essential nutrient for eukaryotic cells due to its inclusion in cofactors such as Fe/S clusters that form part of enzymes (Netz *et al.*, 2014). The Fe/S clusters allow electron transfer during reactions and Fe/S proteins take part in many areas of biochemistry, such as DNA synthesis and repair, protein translation, amino acid biosynthesis and nucleotide metabolism (Netz *et al.*, 2014). The reliance of the cell on these essential processes means that iron is an absolute requirement for cells, and thus mechanisms exist for its uptake, and its use is carefully regulated (Philpott *et al.*, 2012).

Transport mechanisms for iron exist in both high-affinity and low-affinity forms to cope with situations of high and low iron availability (Bailão *et al.*, 2012). In *Saccharomyces cerevisiae*, a low affinity iron transport system exists which involves a reductase enzyme in the cell membrane for reducing Fe^{3+} to Fe^{2+}, and a ferrous permease or non-specific divalent ion transporter for uptake of the Fe^{2+} (Kosman, 2003). Siderophores are chemicals which bind Fe^{3+} for entry to the cell via plasma membrane permeases, and many fungi use these for iron uptake (Kosman, 2003). The iron transporters can be controlled both at the transcriptional and post-transcriptional level, so that iron concentrations are tightly regulated (Kaplan & Kaplan, 2009). As well as iron acquisition from the extracellular matrix, iron can also be stored in and retrieved from the vacuole (Kaplan & Kaplan, 2009). In *S. cerevisiae*, transport systems at the vacuole membrane are homologous to those at the cell surface membrane (Kaplan & Kaplan, 2009). Vacuolar iron transporters can be activated when the cytosol concentration of iron rises, so that iron is sequestered (Kaplan & Kaplan, 2009). This allows the organism to mitigate the effects of growth in iron-limited conditions.

Iron cofactors are required for respiration, they are present in the TCA cycle enzymes aconitase and succinate dehydrogenase, and the enzyme complexes in the electron carrier chain for oxidative phosphorylation contain many haem and Fe/S centres (Shakoury-Elizeh *et al.*, 2010). This could have an effect on amino acid biosynthesis as many pathways require precursors that are produced during respiration e.g. oxaloacetic acid is needed for asparagine and aspartate production (Jastrzębowska & Gabriel, 2015). Furthermore, in yeast, several enzymes that require iron are known that are directly involved in amino acid metabolism: isopropylmalate isomerase (leucine biosynthesis); sulfite reductase (methionine biosynthesis); glutamate synthase; dihydroxyacid dehydratase (branched chain amino acids); and homoaconitase (lysine biosynthesis) (Philpott *et al.*, 2012), and so these particular amino acids could be expected to be directly affected by a lack of iron.

3.1.4 Amino acids and flavour

The study of amino acid amounts in *F. venenatum* is of particular importance due to its use in the food industry for Quorn™ production. This is because amino acids, along with certain nucleotides contribute to the flavour of the final product (Zhang *et al.*, 2013). The word umami describes a savoury taste found in foods such as mushrooms, meat, and fish (Zhang *et al.*, 2013). This is in addition to the well-known basic tastes of sour, sweet, bitter and salty (Beluhan & Ranogajec, 2011). The umami taste has been revealed to be due to a combination of amino acids such as aspartic acid and glutamic acid, and the nucleotide monophosphates: guanosine monophosphate (GMP); inosine monophosphate (IMP); and xanthosine monophosphate (XMP) (Zhang *et al.*, 2013). The nucleotides alone do not have a taste, but instead they act synergistically with glutamate to intensify the umami taste up to 8 times (Zhang *et al.*, 2013). The main three chemicals thought to be responsible for umami taste are therefore IMP, GMP, and monosodium glutamate (MSG) (Zhang *et al.*, 2013). Other amino acids can also affect flavour, e.g. some such as alanine give a sweet flavour, while others such as arginine give a bitter flavour (Mau *et al.*, 2001).

The Maillard reaction is an extremely complex reaction that is important in the food industry for generating colour and flavour of cooked foods (Ames, 1998). When food is cooked, amino groups from compounds such as amines and free amino acids or amino acids as part of peptides and proteins react with reducing sugars to produce volatile aroma compounds (Xu *et al.*, 2013). Changes in the amounts of amino acids available for these reactions will therefore affect the production of these compounds, and alongside impacting the umami flavour, this is another way that affecting the amino acids could potentially affect the quality of the Quorn™ product in terms of flavour and colour (Ames, 1998).

The potential, therefore, for altering or controlling the amounts of amino acids by altering the cations in the medium would certainly be of interest to Quorn™ producers as a way to improve the flavour of their product.

3.2 Methods

3.2.1 Fungal cultures and media

F. venenatum A3/5 (obtained from Quorn Foods) cultures were maintained on oatmeal agar at 4 °C. Starter cultures for each strain were begun by transferring a small piece of hyphae from the edge of the growing fungus into 50 mL Oxoid nutrient broth in a 250 mL baffled conical flask. The starter culture was incubated at 28 °C with shaking at 150 rpm for 3 days. Fifty millilitres of RHM medium and modified RHM medium cultures in 250 mL baffled conical flasks were inoculated using 500 µL of the starter culture, and these were incubated for various time periods at 28 °C with shaking at 150 rpm. RHM medium consisted of potassium dihydrogen phosphate (20 g L^{-1}), ammonium chloride (4.4 g L^{-1}), potassium sulfate (0.3 g L^{-1}), magnesium sulfate heptahydrate (0.25 g L^{-1}), 50% glucose soln. (4 mL L^{-1}), 0.3 g L^{-1} biotin soln. (1 mL L^{-1}), trace metal soln. (5 mL L^{1}), and dH_2O. The trace metal soln. consisted of iron sulfate heptahydrate (2.8 g L^{-1}), zinc chloride (1 g L^{-1}), manganese chloride tetrahydrate (1 g L^{-1}), copper chloride (0.2 g L^{-1}), cobalt chloride (0.2 g L^{-1}), sodium

molybdate (0.2 g L^{-1}), calcium chloride dihydrate (2 g L^{-1}), citric acid (1.5 g L^{-1}), and dH_2O. The modifications to RHM medium were made by altering the trace metal soln. as follows: TR1 (as above); TR2 - iron sulfate heptahydrate x0; TR3 - iron sulfate heptahydrate x10 (28 g L^{-1}); TR4 - calcium chloride dihydrate x0; TR5 - calcium chloride dihydrate x10 (20 g L^{1}). All RHM cultures were brought up to pH 6 using 1 M NaOH solution, before autoclaving and the 50% glucose solution was autoclaved separately and added to the cultures just before they were inoculated.

3.2.2 Quantitation of amino acids

The cells from each culture were separated from the broth by centrifugation for 10 min at 3,500 rpm (Beckman Allegra 6R centrifuge). The cell pellets were then lyophilised (Virtis SP Scientific, Sentry 2.0), and the dry cell pellets were frozen in liquid nitrogen and then ground to a fine powder (IKA analytical batch mill). The samples were prepared by weighing 25 mg of dry powdered cells from each sample into a 2 mL Eppendorf tube. 1 mL of 50:50 methanol and 0.01 M hydrochloric acid solution was then added to each tube and these were shaken for 25 min, followed by centrifugation at 12,500 rpm for 10 min (Fisherbrand bench-top centrifuge). The supernatant was used for analysis.

The presence of amino acids in the samples was determined by gas chromatography-mass spectrometry (GC-MS) using the materials and method supplied with the Phenomenex EZ:Faast™ amino acids kit (Phenomenex). A Zebron ZB-AAA GC column (10 mm x 250 um x 0.25 mm) was used with a GC sampler 80 (Agilent Technologies) injector. A standard split injection mode and a 2 µL injection volume was used with the injector temperature set at 250 °C and the split ratio at 15:1. The oven programme had an initial temperature of 110 °C for 1 min followed by a ramp of 30 °C min^{-1} up to 320 °C, which was held for 2 min. The carrier gas was helium with a 1.5 mL min^{-1} constant flow. The solvent delay was 1 min. The total ion count (TIC) scanning mode was used with an m/z range of 45-460, and a gain factor of 2. Results were calculated from 6 repeats of each condition and quantitation was performed

using the formula below, which uses the amino acid norvaline added to samples as an internal standard.

$$Amount\ AA\ (nmol/g) = \frac{Area\ AA/_{Area\ norvaline}}{Rf\ x\ mass\ (g)}\ x\ amount\ norvaline\ (nmol)$$

3.2.3 Statistical analysis

The statistical tests were performed using SPSS. The data for amino acids were tested for normal distribution using the Shapiro-Wilk test and those data points that were not normally distributed were compared using the Mann Whitney U test, and the rest were compared to the control using t tests. The data for biomass were found to be normally distributed and so were compared to the control using t tests.

3.3 Results and Discussion

An analysis of the dry mass produced by this set of cultures showed that there was not a statistically significant difference between any of the altered ion conditions and the control cultures, although the average mass for iron limited cultures was slightly higher than the control (Figure 26).

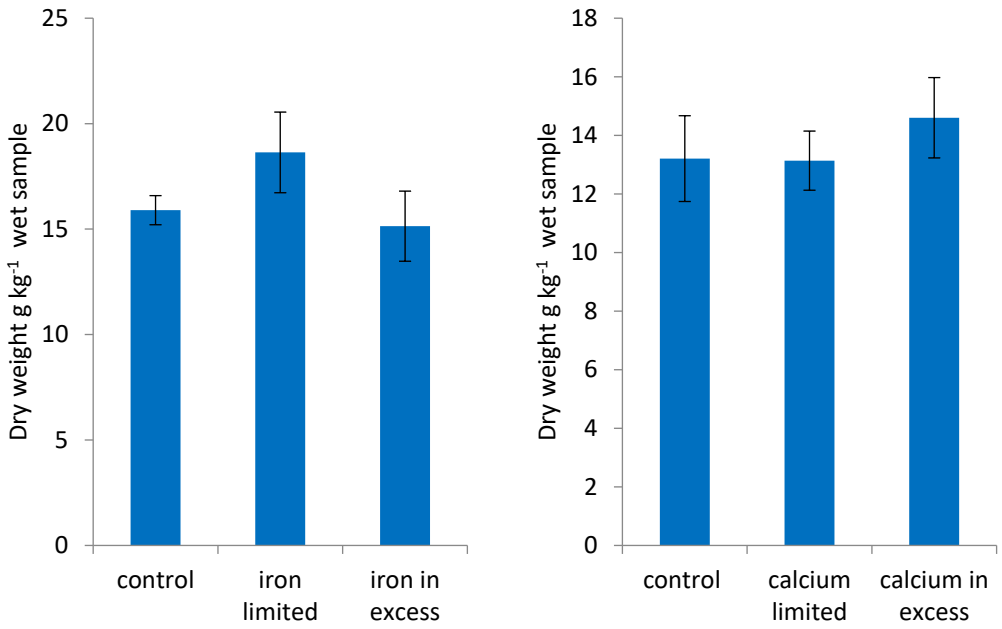

Figure 26: Dry mass of cultures after 3 d growth (g kg^{-1} wet sample). Calculated as an average of 6 cultures for each treatment. Error bars represent one standard deviation. The results did not show a statistically significant difference in dry mass for any of the cultures.

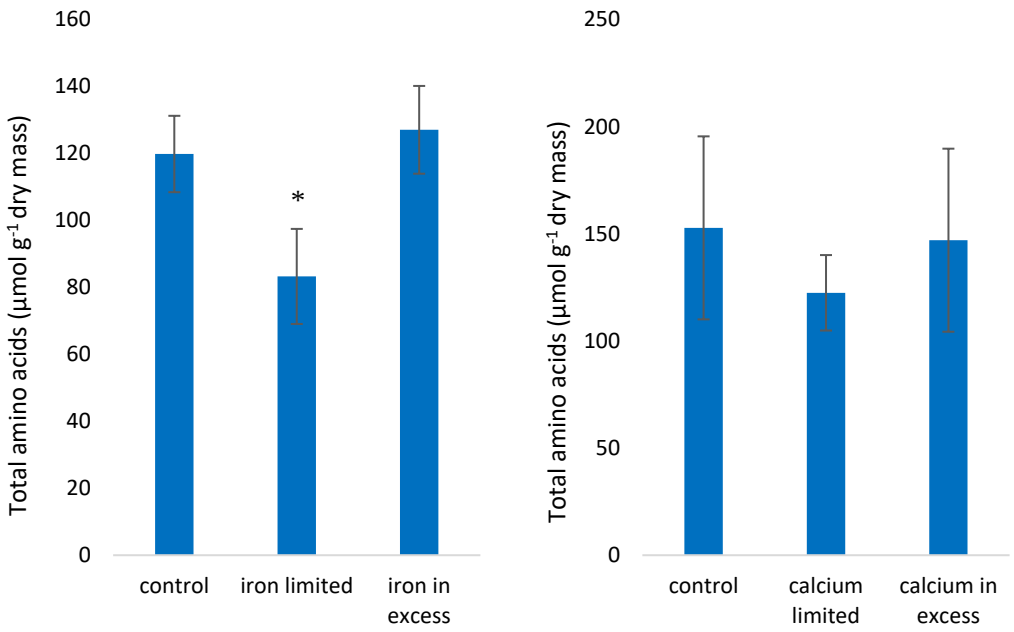

Figure 27: Total free amino acids for each culture (µmol g^{-1} of dry mass). The result for the iron limited culture was statistically significant ($P<0.05$). * indicates statistical significance.

The results have shown that the amounts of most amino acids have been decreased in iron limited conditions (Figure 28). In iron limited cultures the total free amino acids content was significantly lower than the control (31% decrease) ($P<0.05$) (Figure 27). All amino acids, except leucine, histidine, and phenylalanine had a statistically significant change ($P<0.05$) compared to the control in the iron limited condition. Most showed a decrease compared to the control, but glutamate showed a significant increase (54%), which was the largest difference of all the amino acids.

The pathway for the production of glutamate does require an Fe/S enzyme, but an alternative pathway exists so that its production can be independent of iron (Philpott *et al.*, 2012). The breakdown product of a number of other amino acids is glutamate, and so glutamate levels could be increased as these amino acids are being broken down; in fact one such compound is proline (Arst *et al.*, 1981), and this was decreased in these results, so this could be an explanation for the increase in glutamate. Alternatively, the increase in glutamate levels in iron-limited conditions could also be due to the downregulation of enzymes in pathways for the amino acids that require molecules of glutamate for the donation of the amino group: glutamine; alanine; proline; lysine; and leucine, and all of these except leucine were significantly decreased.

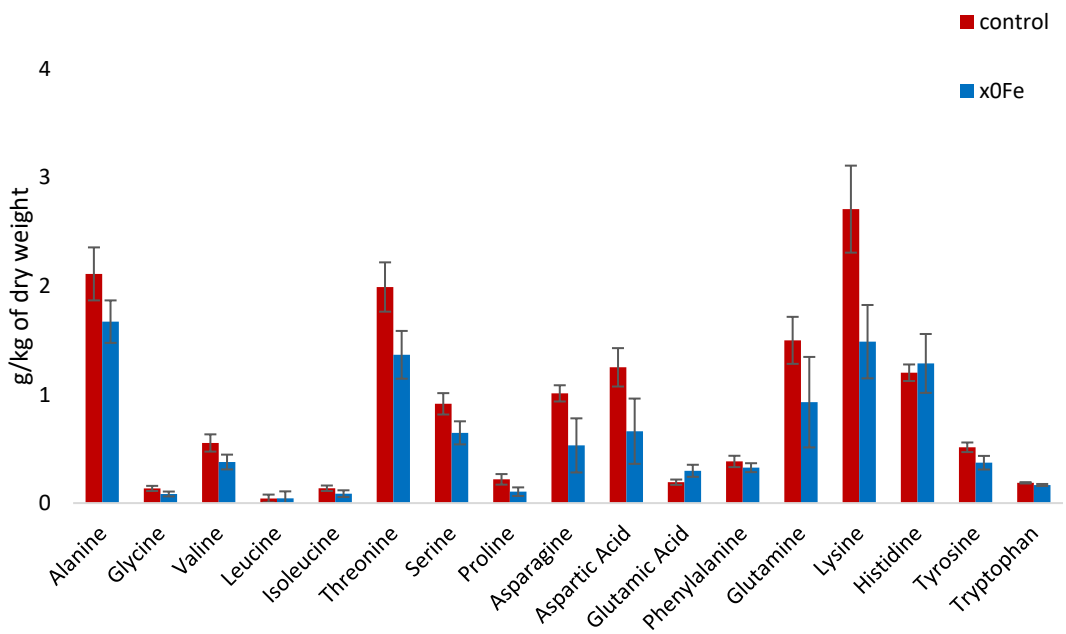

Figure 28: Amount of each free amino acid in intracellular matrix of culture grown in a medium with depleted iron, compared to the control (g kg^{-1} dry weight). Error bars represent one standard deviation. Results based on 6 repeat cultures. All results shown were statistically significant ($P<0.05$) except for leucine, histidine, and phenylalanine.

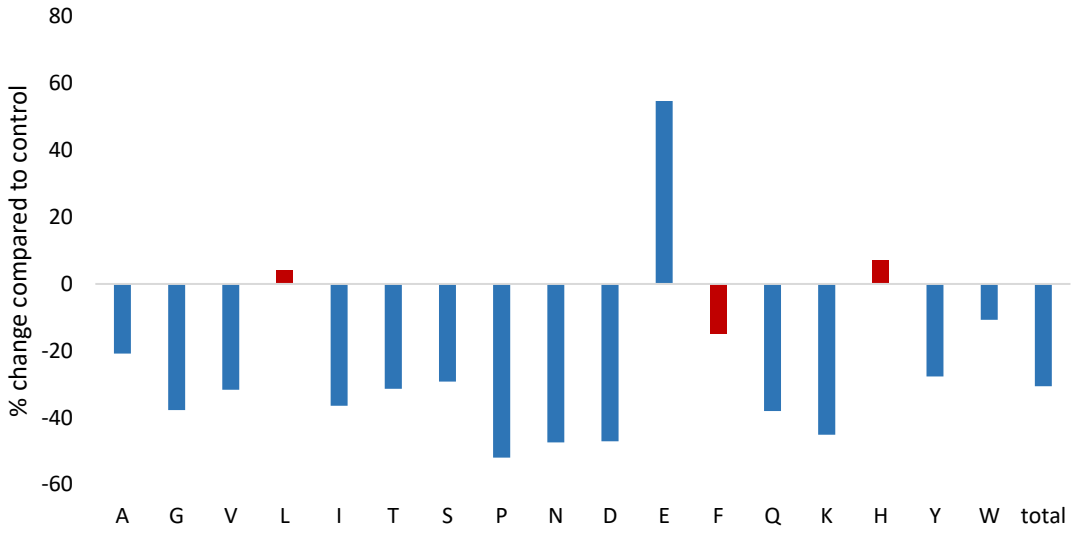

Figure 29: Differences in amino acid amounts in *F. venenatum* when grown in iron-limited conditions. Percentage change compared to the control. A) alanine G) glycine V) valine L) leucine I) isoleucine T) threonine S) serine P) proline N) asparagine D) aspartic acid E) glutamic acid F) phenylalanine Q) glutamine K) lysine H) histidine Y) tyrosine W) tryptophan. Note: changes seen in leucine, phenylalanine, and histidine (shaded red) were not found to be statistically significant.

Large significant decreases were seen in proline (52%), asparagine (47%), aspartic acid (47%), and lysine (45%) ($P<0.05$). Aspartic acid biosynthesis relies on the input of oxaloacetate, a TCA cycle intermediate which could be reduced in iron-limited conditions if respiration reactions are downregulated (Philpott *et al.*, 2012), and asparagine requires aspartic acid as a precursor (Jastrzębowska & Gabriel, 2015). The production of lysine requires an Fe/S enzyme, homoaconitase, and so it could be the case that this pathway is downregulated in iron-limited conditions (Xu *et al.*, 2006). In addition, lysine production also requires α-ketoglutarate, an intermediate of the TCA cycle which may be decreased in these conditions (Shakoury-Elizeh *et al.*, 2010).

Smaller significant decreases were seen with the aromatic amino acids phenylalanine (15%), tyrosine (27%), and tryptophan (11%) ($P<0.05$). The production of this group of amino acids

involves complex pathways that are energetically costly to the cell, requiring the input of ATP (Braus, 1991). The reduction in these amino acids could be consistent with iron-limited conditions since low iron concentration could lead to a downregulation of the TCA cycle (Philpott *et al.*, 2012), which would lower the availability of ATP for biosynthesis. In addition, the production of tryptophan requires the input of glutamine and serine, which were also reduced, which could have affected this pathway (Braus, 1991).

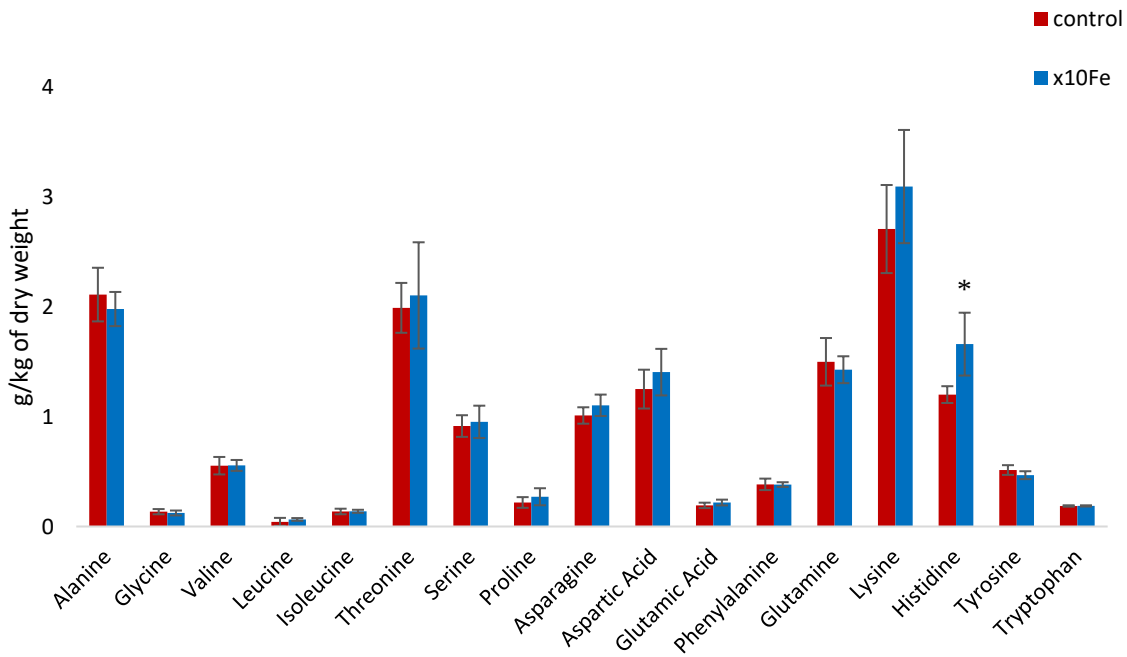

Figure 30: Amount of each free amino acid in intracellular matrix of culture grown in a medium with excess iron, compared to the control (g kg^{-1} dry weight). Error bars represent one standard deviation. Results based on 6 repeat cultures. * indicates statistical significance.

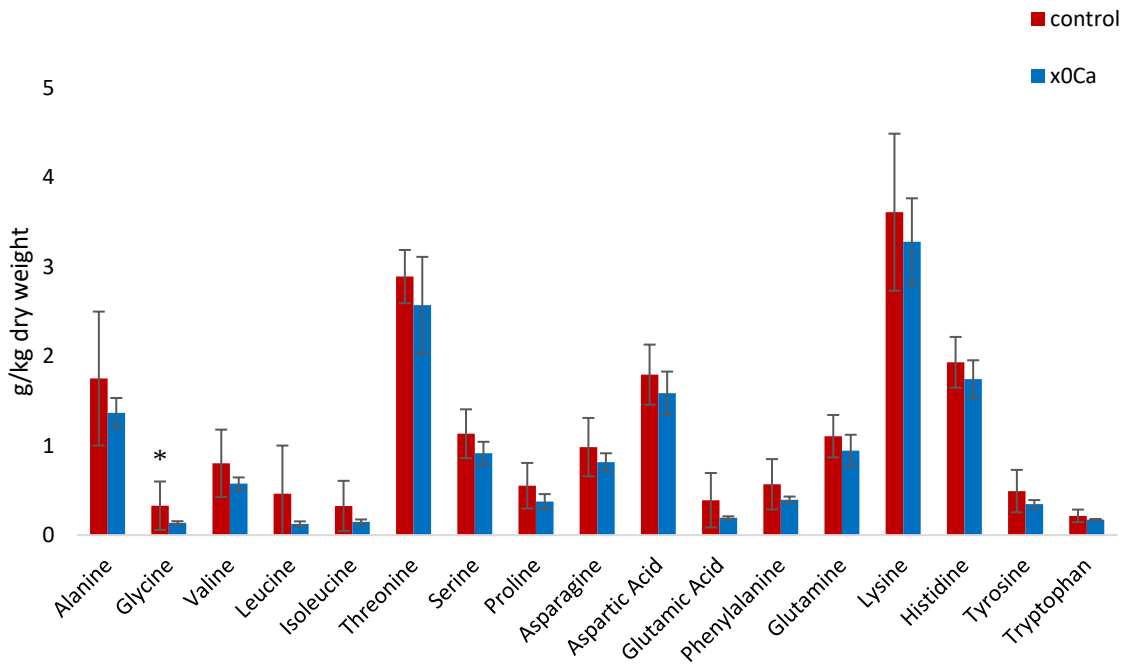

Figure 31: Amount of each free amino acid in intracellular matrix of culture grown in a medium with depleted calcium, compared to the control (g kg^{-1} dry weight). Error bars represent one standard deviation. Results based on 6 repeat cultures. * indicates statistical significance.

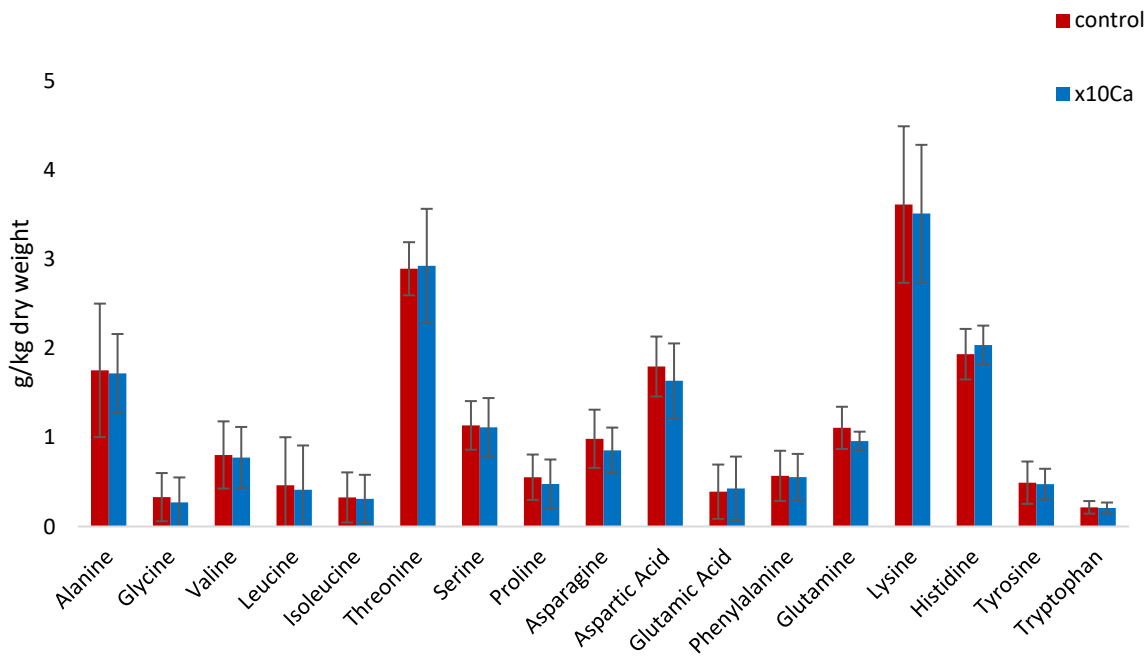

Figure 32: Amount of each free amino acid in intracellular matrix of culture grown in a medium with excess calcium, compared to the control (g kg^{-1} dry weight). Error bars represent one standard deviation. Results based on 6 repeat cultures. None of these results were statistically significant.

The other conditions tested did not make such a noticeable change to amino acid levels. When iron was increased, there were no significant changes to most amino acids, except histidine (38% increase) ($P<0.05$) (Figure 30). With low calcium, only glycine showed a significant change, with a 13% increase compared to the control ($P<0.05$) (Figure 31). There were no significant differences at all in the amounts of amino acids in the culture with increased calcium (Figure 32).

Previous studies of iron deficiency in yeast have identified that the organism responds by increasing its uptake of iron from outside of the cell, releasing iron from intracellular stores, and by adjusting its metabolism via transcription factors that downregulate non-essential iron-requiring pathways (Shakoury-Elizeh *et al.*, 2010). For example, enzymes in the pathways for the production of leucine, glutamate and lipoic acid are downregulated, along with the

enzymes succinate dehydrogenase and aconitase (Shakoury-Elizeh *et al.*, 2010). It has been shown in *S. cerevisiae* that cells under iron deprivation conditions reduce levels of mRNAs that encode proteins from the TCA cycle and respiration (Puig *et al.*, 2005). This has the effect of decreasing metabolites of glycolysis in iron-depleted cells, while increasing levels of pyruvate, showing that glycolysis is used more than respiration for energy production in these cells (Shakoury-Elizeh *et al.*, 2010). In addition, α-ketoglutarate levels were reduced in low-iron cells and as this intermediate is important in the production of amino acids such as lysine it may become depleted as it is used for these pathways (Shakoury-Elizeh *et al.*, 2010).

Despite changes in the levels of enzymes in some iron-requiring pathways, levels of important metabolites may not necessarily be affected; for example, glutamate which is an important amino acid as the majority of cellular nitrogen is derived from the amino group of either glutamate or glutamine (Shakoury-Elizeh *et al.*, 2004). In the case of glutamate production, an iron-requiring pathway can be substituted by a non iron-requiring pathway (Philpott *et al.*, 2012). In yeast grown in iron-limited conditions, glutamate synthase (contains Fe/S) is downregulated while glutamate dehydrogenase (no iron requirement) is upregulated, and thus iron is preserved for more essential pathways without a detriment to glutamate metabolism (Philpott *et al.*, 2012).

It is possible that even amino acid pathways that have no alternative route can be downregulated without significantly changing their output (Shakoury-Elizeh *et al.*, 2010). It has been found in yeast that amino acid metabolism is not greatly affected by iron deficiency, despite an apparent reduction in the metalation and activity of Fe/S enzymes (12-33 fold reduction), but lipid biosynthesis and carbon utilisation are more noticeably altered (Shakoury-Elizeh *et al.*, 2010). This was explained by the authors who state that amino acid homeostasis is able to cope with this reduction in enzyme activity, and that the Fe/S enzymes are normally present in such excess that amino acid biosynthesis is not detrimentally effected (Shakoury-Elizeh *et al.*, 2010). The authors suggest that this is because protecting amino acid homeostasis is imperative, as depletion of amino acids would seriously impede protein synthesis

(Shakoury-Elizeh *et al.*, 2010). However, in the study by Shakoury-Elizeh *et al.*, (2010) the cultures were grown for only 18-24 h and after more prolonged growth in iron-limited media deficiencies did begin to develop, with a decrease in lysine of 55% compared to iron replete media. Alternatively, levels of amino acids can also be maintained in the cell during conditions of iron deficiency by the break-down of proteins in autophagosomes that release their amino acids into the vacuole that can then be exported back into the cytosol (Philpott *et al.*, 2012).

The pathways for isoleucine and valine both contain the enzyme dihydroxyacid dehydratase, which contains an Fe/S cluster (Philpott *et al.*, 2012). These have both been reduced in the iron limited media, which is possibly a result of these pathways being downregulated due to a lack of iron. The results of this present study do not show a significant change in the level of leucine, but another study has shown that iron deficiency can affect the leucine biosynthetic pathway (Philpott *et al.*, 2012). In order to produce leucine, its intermediate α-isopropylmalate (α-IPM) must first be made in the mitochondria, and subsequently the Fe/S enzyme isopropylmalate isomerase (leu1) begins the reactions to convert this to leucine (Philpott *et al.*, 2012). In iron-limited conditions it has been found that α-IPM accumulates due to a loss of leu1 activity, which has been found to be due to a loss of the Fe/S cofactors (Philpott *et al.*, 2012). Elsewhere it has been suggested that the activity of leu1 can be increased at the expense of aconitase enzyme in the citric acid cycle (also an Fe/S enzyme) (Bedekovics *et al.*, 2011). These authors explain that leu1 is transcriptionally up-regulated when α-isopropylmalate levels are increased, while there is a reduction in the transcription of aconitase (Bedekovics *et al.*, 2011). This effect was not investigated in iron-limited conditions, but this mechanism could be used to mitigate the effects of limited iron on leucine biosynthesis by sacrificing the activity of the TCA cycle. However, this is not clear in the results of this present investigation as the change in the amount of leucine in iron-limited conditions was not statistically significant, although the level of leucine was already very low in control conditions (0.04 g kg^{-1} dry weight).

3.4 Conclusions

Growth of *F. venenatum* A3/5 in iron limiting conditions has led to a significant decrease in the level of almost all the amino acids measured, with glutamic acid, conversely showing a significant increase. This has occurred without a significant decrease in biomass production. Potential loss of Fe/S cofactors in enzymes that are required for their biosynthesis, e.g. in the case of amino acids such as lysine or leucine, as has been suggested in previous studies (Shakoury-Elizeh *et al.*, 2010) (Philpott *et al.*, 2012) could explain the effects observed. Other amino acids are reliant on either ATP or intermediates produced by the TCA cycle, and these could be expected to be reduced in iron-limited conditions due to the downregulation of the Fe/S enzymes in the TCA cycle. Changes in the amounts of amino acids could be significant for the use of *F. venenatum* in Quorn™ production as this could affect the flavour of the product, particularly aspartic acid and glutamic acid which contribute to the umami taste (Zhang *et al.*, 2013). Iron limited conditions may have a significant effect on the umami taste as the amount of glutamic acid was actually increased, while the majority of other amino acids were decreased. Furthermore, the significant reduction of the concentration of total free amino acids (31% decrease) could significantly affect the formation of aroma compounds via the Maillard reaction upon cooking.

3.5 Further work

This study has shown that most pathways for amino acid biosynthesis have been decreased by a reduction of iron ions in the media, without a decrease in biomass, however the reasons behind this are not yet established. Other studies have suggested that this is due to iron-requiring enzymes in both the amino acid pathways and other pathways that contribute intermediates. This could be confirmed by a targeted analysis of the transcriptome in iron-limited conditions to determine exactly which enzymes are up or downregulated as a result. A series of cultures grown with varying concentrations of iron ions could also be investigated to

reveal the threshold level of iron needed by the fungus to protect amino acid biosynthesis from this effect.

This could be a significant finding for Quorn™ production since amino acids are known to affect flavour either by acting with nucleotides to enhance the umami flavour (Zhang *et al.*, 2013), or in the Maillard reaction by forming aroma compounds with sugars when the food is cooked (Ames, 1998). The fact that the biomass has not been reduced by the iron-limited conditions is also significant because it suggests that the medium could be manipulated for flavour while still maintaining maximum production. It is not yet known exactly how this reduction will affect flavour, or whether the changes are beneficial, and so further investigation would be required, for example quantitation of the volatile compounds produced by the Maillard reaction could be carried out.

Note: Biochemical pathways for the biosynthesis of the amino acids and their degradation were researched for *Fusarium graminearum* (*Fusarium venenatum* was not available in the database) using the KEGG website. (KEGG, 2017), (Kanehisa & Goto, 2000), (Kanehisa *et al.*, 2016), (Kanehisa *et al.*, 2017).

4. Optimisation of metabolite and protein extraction protocols

4.1 Introduction

4.1.1 Extraction of *Fusarium venenatum* metabolites

In order to carry out metabolome analysis of intracellular metabolites it is necessary first to extract such compounds into a suitable solvent (Villas-Boas *et al.*, 2005). This extraction can be problematic for quantitation, however, due to the diversity in compound characteristics such as polarity, and differences in abundance and stability, as metabolites will inevitably be lost due to their diverse chemical properties (Villas-Boas *et al.*, 2005). Moreover, cell lysis could be problematic and a source of errors in quantitation, requiring the development of robust methodologies with standardised protocols and enhanced recovery of intracellular material.

Many studies use grinding of the cells followed by the addition of methanol or other solvents and centrifugation to lyse the cells and separate the lipophilic and hydrophilic phases (Matheus *et al.*, 2014). A study by Matheus *et al.*, (2014) investigated two protocols for cell extraction, the first used a sonication probe for periods of 30 – 60 s, and the second used an automated sonicator (Bioruptor®Pico) using various numbers of cycles (30 s on and 30 s off) (Matheus *et al.*, 2014). The automated sonicator had the advantage of a more standardised procedure and the ability to sonicate a number of samples at once, although a longer time was needed (20 – 30 min) (Matheus *et al.*, 2014). The profile given by the automated sonicator was similar to that given by the probe (Matheus *et al.*, 2014).

The solvent chosen will affect the metabolites available for analysis and so a study by Villas-Bôas et al., (2005) compared sample preparation methods for yeast metabolomics, and this included the choice of solvent. Six methods were tested, and results were compared using GC-MS to evaluate the recovery of spiked metabolites (Villas-Boas *et al.*, 2005). One of the methods used methanol (-40 °C), chloroform (-40 °C) and buffer (PIPES, 3 mM; EDTA, 3 mM; pH 7.2) (ice-cold), the upper aqueous phase after centrifugation was taken and this

process was repeated for a second extraction (Villas-Boas *et al.*, 2005). It was found that this method resulted in recovery of sugars and sugar phosphates but poor recovery of nucleotides and fatty acids (Villas-Boas *et al.*, 2005). In another method, cold 50% methanol (-40 °C) solution was added followed by freeze-thaw with liquid nitrogen and centrifugation, after which further methanol was added with shaking (Villas-Boas *et al.*, 2005). The final method used pure methanol with the same procedure as the 50% methanol (Villas-Boas *et al.*, 2005). The 50% methanol extraction was found to give a good recovery of most of the metabolite classes, with particularly good recovery of nucleotides, but the pure methanol gave outstanding recoveries for most of the metabolites (Villas-Boas *et al.*, 2005). The pure methanol also gave the best repeatability of all the methods and gave the best recovery for nucleotides and α-keto acids, although it still had poor recovery of sugars and sugar phosphates (Villas-Boas *et al.*, 2005). The authors also state that an advantage of using the methanol extraction is that it uses a less toxic solvent than chloroform and can be easily removed by evaporation (Villas-Boas *et al.*, 2005).

An untargeted plant metabolomics study by De Vos *et al.*, (2007) used a 75% acidified (0.1% formic acid) methanol solution, which was added to frozen plant powder to extract metabolites. The authors concluded that this was the most suitable solvent for extraction of secondary metabolites from different plant species, after testing a number of solvents such as methanol, ethanol and acetone with different ratios of added water (De Vos *et al.*, 2007). Adding the solvent to the frozen plant powder was assumed to inactivate any enzymes in the sample. The samples were then sonicated in a sonication bath (Branson 3510, 40 kHz) for 15 min, and it was found that recovery of standards was > 90 %, and sonication times longer than 15 min up to 2 h did not change the metabolite profile (De Vos *et al.*, 2007). Sample concentration by lyophilisation and solvent extraction were compared and it was found that organic acids, nucleotides, sugars and peptide had >80% recovery, fatty acid had poor recovery, and sugar alcohols and sugar phosphates had <75% recovery with lyophilisation (Villas-Boas *et al.*, 2005). Solvent evaporation gave excellent recoveries for amino acids,

organic acids, nucleotides, sugars and sugar alcohols, but it is only available for methods using organic solvents (Villas-Boas *et al.*, 2005).

Based on this research, and before starting the main investigation, it was necessary to test the method for metabolite extraction to ensure the most reliable and repeatable results. A preliminary investigation was therefore carried out to evaluate the use of solvents and sonication protocol for LC-MS analysis of *Fusarium venenatum* metabolites. A solvent mixture of methanol and water (3:1) was compared to a mixture of methanol, chloroform and water (3:1:1). Sonication using a sonication probe (soniprep 150) was compared to sonication using a sonication bath (Grant Ultrasonic Bath XUBA1).

4.1.2 Extraction of *Fusarium venenatum* proteins

The aim of a proteomics study is to compare the different sets of proteins present at different developmental stages or when the organism is subjected to different external conditions (González-Fernández et al., 2010). The information given by this kind of study can reveal the interactions between proteins and metabolites that work together to control growth, development, and interactions between the organism and its environment (González-Fernández et al., 2010).

The most widely used technology for proteomics study is LC-MS/MS, which is used to identify peptides derived from the digestion of proteins by endoprotease enzymes (Hildonen *et al.*, 2014). The digestion of proteins generates molecules with masses and charges which can be separated and analysed by MS/MS (Hildonen *et al.*, 2014). Trypsin is the most commonly used endoprotease due to its specificity; it cleaves peptide bonds between the specific amino acid residues lysine and arginine and their following residue, except when the following amino acid is proline (Brownridge & Beynon, 2011). This fragmentation results in peptide fragments (limit peptides) that are about 10-15 amino acids long, that are detectable by the MS (between 1000 Da /~8 amino acids and 3000 Da /~25 amino acids) (Brownridge &

Beynon, 2011). Smaller peptide fragments of only 6 amino acids or less are not well detected by LC-MS (Hildonen *et al.*, 2014). This process doesn't require prior separation of proteins since the MS/MS data derives from individual peptide fragments which are then used to infer the proteins that were present (Cottrell, 2011). The peptides are allocated to their protein by database searches; this works because the LC-MS/MS fragmentation only breaks the peptide at certain points (Cottrell, 2011). It is possible, however that multiple proteins could be identified from one peptide fragment, leading to ambiguous results (Cottrell, 2011), but this can be mitigated for during the data analysis by manually choosing the best match based on criteria such as the mass error.

In order to release the proteins into solution for digestion and subsequent LC-MS/MS analysis several steps of sample preparation are necessary. The first step is the physical breaking of cell walls and cell membranes to release the cell contents, this is achieved by freezing the cells in liquid nitrogen, followed by mechanical blending (Cañas *et al.*, 2007). The dry cell powder is then added to the lysis buffer, which contains compounds that help to disrupt the cell membranes and transfer the proteins into solution (Pasquali *et al.*, 2010). The ingredients of the lysis buffer aid the release of proteins from the cells, helps them to dissolve, and protects them from break-down. The addition of sodium dodecyl sulfate (SDS) to the buffer, along with heating to 95 °C helps to dissolve cell walls and hydrophobic proteins, and prevents proteins from joining together in insoluble oligomers (Pasquali *et al.*, 2010). The process of releasing the cell contents into the lysis buffer will also unfortunately release protease enzymes that will start to digest the proteins to be analysed, and so in order to prevent this as much as possible, the lysis buffer must also contains compounds that act as protease inhibitors (Cañas *et al.*, 2007). Phenylmethane sulfonyl fluoride (PMSF) and ethylenediaminetetraacetic acid (EDTA) both achieve this effect, along with heating the solution to high temperatures (Cañas *et al.*, 2007). To ensure the highest solubilisation of the proteins, tris(hydroxymethyl)aminomethane (tris) base is used so that the correct pH is achieved, and dithiothreitol (DTT) is used to remove the disulfide bonds between cysteine residues (Cañas

et al., 2007). Before the trypsin digestion, the sulfidryl groups released by the DTT are protected by alkylation so that the disulfide bonds can't reform; this is achieved by using Iodoacetamide (IAA) (Cañas *et al.,* 2007). Once the proteins are obtained from the cells in sufficient concentration they are separated by sodium dodecyl sulfate polyacrylamide gel electrophoresis (SDS-PAGE) (Cañas *et al.,* 2007). The gel pieces containing the separated proteins are then cut into pieces and the proteins are digested in the gel, a process known as in-gel digestion (Cañas *et al.,* 2007). Alternatively the gel step can be omitted and the proteins can be digested in the solution (in-solution digestion) (Cañas *et al.,* 2007).

4.2. Extraction procedure for intracellular metabolomics

4.2.1 Method

The methods were tested using lyophilised material from a single 50 mL culture that used the RHM medium containing an increased concentration of iron described previously (see chapter 2 for details of media). Two extraction solvents were tested, along with two methods of sonication – sonication probe and sonication bath. Twenty-five milligrams of the freeze-dried material were added to twelve 2 mL Eppendorf tubes. To six tubes 500 µL of distilled water were added along with 1500 µL of methanol. To another six of the tubes 1200 µL of methanol, 400 µL of chloroform and 400 µL of water were added. Three tubes for each solvent were then sonicated either using the sonication bath for 25 minutes or the sonication probe for 1 cycle of 30 s on, 30 s off, and 30 s on. The sonication bath (Grant Ultrasonic Bath XUBA1) had a frequency of 44 kHz, the sonication probe (Soniprep 150) had a frequency of 23 KHz. Twelve sample blanks were also produced using identical methods but containing 25 µL distilled water rather than the sample. The samples were then subjected to LC-MS analysis by the same method used for the final samples (described in chapter 5).

The number of peaks produced by MS was reduced by first subtracting the areas of peaks found in the blanks from the peak areas found in the samples and any compounds that were

found in the blanks were therefore removed. Repeatability of results was calculated using the relative standard deviation (RSD) expressed as a percentage for each compound. All peaks that had an RSD greater than 15% across the three repeats were removed as these peaks would have poor repeatability. Small peaks with an area of less than 10,000 were also removed. The data was then assembled into pairs for comparison, and the Mann Whitney U test for non-parametric data was used to compare the peak areas, as the data was not normally distributed.

4.2.2 Results and Discussion

The statistical analysis revealed only a small number of peaks that were significantly different ($P<0.05$) when the sonication probe was compared with the sonication bath regardless of which solvent was used. When the methanol, chloroform and water mixture was used, only 10% of the peaks were significantly different, and when methanol and water was used only 19% of the peaks were significantly different between the two sonication methods. This suggests that the choice of sonication method has not made a significant difference to the peak areas. This agrees with the finding by Matheus et al., (2014) who compared a sonication probe with an automated sonicator (Bioruptor system) and found that the profiles from each method were similar. It was therefore decided to use the sonication bath for the main samples due to ease of use and the ability to process multiple samples at once thereby ensuring identical conditions for as many samples as possible to ensure the highest repeatability possible.

When comparing the different solvents using the sonication bath there were 47% of peaks that were significantly different between the two ($P<0.05$). Of these peaks, the RSD was lower in 57% of the peak areas when methanol and water was used, which suggests that this data had slightly better repeatability. It was therefore decided to use the methanol and water mix as the solvent for the metabolomics investigation described in chapter 5.

4.3 Extraction and separation of proteins by SDS-PAGE for in-gel trypsin digestion

4.3.1 Protein extraction and precipitation

Before the proteomics investigation could be attempted it was first necessary to test methods that allowed the highest possible concentration of proteins to be extracted, and then validate this using SDS-PAGE gels which enabled visualisation of the separated proteins. Once the gels showed that the extraction procedure had been successful, the next step of in-gel trypsin digestion could be attempted (see chapter 6).

The first method for protein extraction was based on that described by Pascali *et al.* (2010). The first part of the procedure was as follows: 50 mg of dried cells were added to 2 mL lysis buffer, this was vortexed for 10 s, Sonicated with ice for 20 min, and shaken for 20 min. Lysis buffer consisted of 50 mL L^{-1} tris(hydroxymethyl)aminomethane (Tris)-HCl pH 8, 20 g L^{-1} sodium dodecyl sulfate (SDS), 5 mL L^{-1} 2M dithiothreitol (DTT), 800 µL L^{-1} ethylenediaminetetraacetic acid (EDTA), 0.17 g L^{-1} phenylmethane sulfonyl fluoride (PMSF). Samples were then placed in a water bath at 95 °C for 10 min. The tubes were centrifuged for 15 min at 15,000 rpm and the supernatant was kept to be pooled later. The resulting pellet was retained, and the same method was repeated twice – pooling all 3 supernatants together and finally discarding the pellet.

The second part of the procedure was to precipitate the proteins from the solution so that they could be separated from the other compounds in the solution. 15 mL precipitation buffer was added to the protein supernatants and these were left at -20 °C overnight so that the proteins would precipitate out of the solution. Precipitation buffer consisted of 200 g L^{-1} trichloroacetic acid (TCA), 1 mL L^{-1} 2 M DTT, in acetone.

After being left overnight, the second part of the procedure was as follows: The solution containing precipitated proteins was centrifuged at 18,000 rpm for 30 min (Sorvall centrifuge). The resulting protein pellet was transferred to a 2 mL Eppendorf tube and the supernatant was discarded. The protein pellet was then washed three times with washing buffer by adding 2 mL

of the buffer followed by centrifugation at 15,000 rpm (Harrier centrifuge). Washing buffer consisted of 1 mL L^{-1} 2 M DTT in acetone. The final protein pellet was dried using a sample pre-concentrator (Christ RVC 2-18) and resuspended in labelling buffer. Labelling buffer consisted of 140 g L^{-1} Urea, 50 g L^{-1} thiourea, 40 g L^{-1} CHAPS, and 30 mL L^{-1} 1 M Tris. Before use the pellet was sonicated for 10 s using a sonication probe (Soniprep 150) to re-dissolve the proteins.

4.3.2 SDS-PAGE

All gels were prepared using the following method: 12% SDS PAGE gels were prepared by making solutions to the following recipes. Resolving gel: 3 mL acrylamide (40%); 4.5 mL dH_2O; 2.5 mL buffer B; 50 µL 10% ammonium persulfate (APS); 10 µL tetramethylethylenediamine (TEMED). Stacking gel: 0.5 mL acrylamide (40%); 2.5 mL dH_2O; 1 mL buffer C; 30 µL 10% APS; 10 µL TEMED. 300 mL of SDS buffer B was prepared by combining 225 mL 2M Tris HCl pH 8.8, 12 mL 10% SDS soln., and 63 mL dH_2O. 300 mL of SDS buffer C was comprised of 150mL 1 M Tris-HCl pH 6.8, 12 mL 10% SDS soln., and 138 mL dH_2O. The resolving gel was added to the glass plates and left to set for approx. 20 min before the stacking gel was added and the comb was inserted, and this was allowed to set for a further 20 min. The SDS running buffer was comprised of 3.039 g L^{-1} Tris-HCl pH 8, 14.4 g glycine, and 10 g L^{-1} SDS. The gels were stained in the Coomassie Brilliant Blue stain for 10 mins in square petri dishes while being slowly rocked, they were then placed in destain solution overnight. The Coomassie Brilliant Blue stain was comprised of Coomassie Brilliant Blue R250 1 g L^{-1}, 400 mL L^{-1} methanol, and 100 mL L^{-1} acetic acid. The destain solution was comprised of 400 mL L^{-1} methanol, and 100 mL L^{-1} acetic acid.

The method for loading the gel was as follows: 20 µL of each sample was added to 5 µL SDS loading dye (loading dye consisted of: 4% SDS, 10% 2-mercaptoethanol, 20% glycerol, 0.004% bromophenol blue, 0.125 M Tris-HCl, pH adjusted to 6.8). These were boiled for 10

min and 10 µL of each were loaded onto the gel along with 5 µL of the MW marker. Gels were run at 180V for 45 min.

4.3.3 Modification and optimisation of protocols for SDS-PAGE

The first method resulted in poor separation of protein on the SDS-PAGE gel (Figure 33).

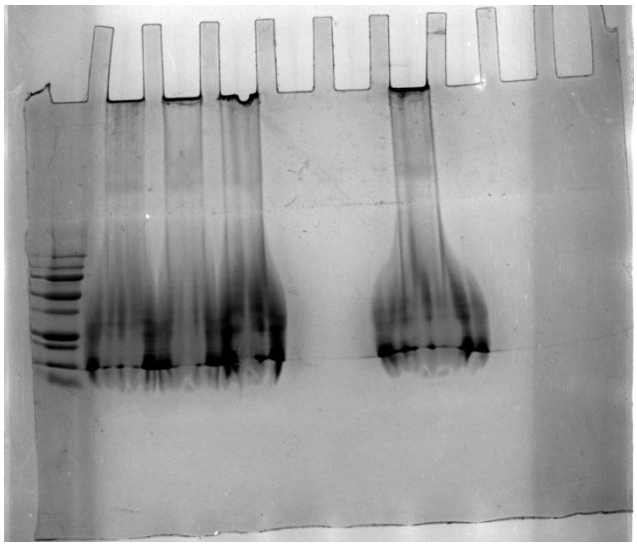

Figure 33: SDS-PAGE gel showing separation of proteins. Proteins were loaded in the following order: marker (Biorad prestained SDS-PAGE standards, low range), 1a1, 1a2, 1a3, empty, 1a1 (20 µL of each sample were loaded, 5 µL of the marker were added).

The method was then adjusted to use only 2 washes in the washing buffer after the precipitation. This was followed by 3 washes in dH_2O to fully remove the washing buffer. dH_2O was then used instead of the labelling buffer to re-dissolve the proteins, and the samples were tried in a range of dilutions in dH_2O. This method resulted in better separation with less smearing (Figure 34).

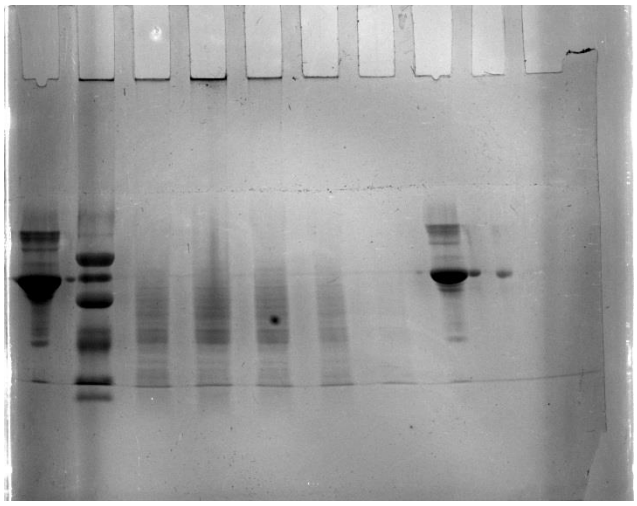

Figure 34: SDS-PAGE gel showing separation of proteins. Proteins were loaded in the following order: BSA protein standard, marker (Biorad prestained SDS-PAGE standards, low range), 2c2 (10%), 2c3 (10%), 2c1 (5%), 2c2 (5%), 2c3 (5%), BSA protein standard (20 µL of each sample were loaded, 5 µL of the marker were added).

Further modification of the method included re-dissolving and diluting using lysis solution rather than dH_2O. The lysis solution consisted of: 48 g L^{-1} urea, 4 g L^{-1} 3-[(3-cholamidopropyl)dimethylammonio]-1-propanesulfonate (CHAPS). The gel showed that the proteins were smearing, possibly due to undissolved protein (Figure 35).

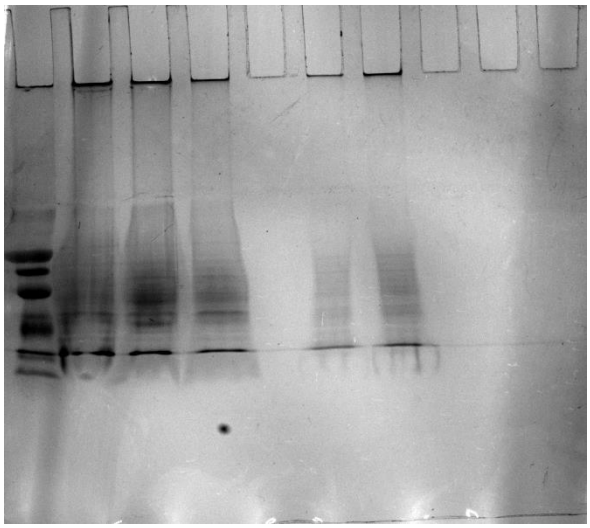

Figure 35: SDS-PAGE gel showing separation of proteins. Proteins were loaded in the following order: marker (Biorad prestained SDS-PAGE standards, low range), 2c1, 2c2, 2c3, empty, 2c1 (10%), 2c2 (10%) (10 µL of each sample were loaded, 5 µL of the marker were added).

Since previous methods have shown problems with insoluble proteins it was decided to attempt a method using the raw protein extracts rather than proceeding with the protein precipitation, which may be causing the difficulty in re-dissolving the proteins.

4.3.4 Raw protein extraction and direct application without protein precipitation

The protein extraction method was used without continuing to the protein precipitation. Samples of the raw protein extract were not diluted and were centrifuged at 18,000 rpm (Harrier centrifuge) before the loading dye was added. The sample and loading dye mixture was also centrifuged at 12,500rpm for 2 min (Fisherbrand bench-top centrifuge) before loading onto the gel. This method gave clear separation of proteins with strong bands in the control and high iron conditions, although the proteins were less clear for the iron-limited condition (Figure 36) (Figure 37) (Figure 38).

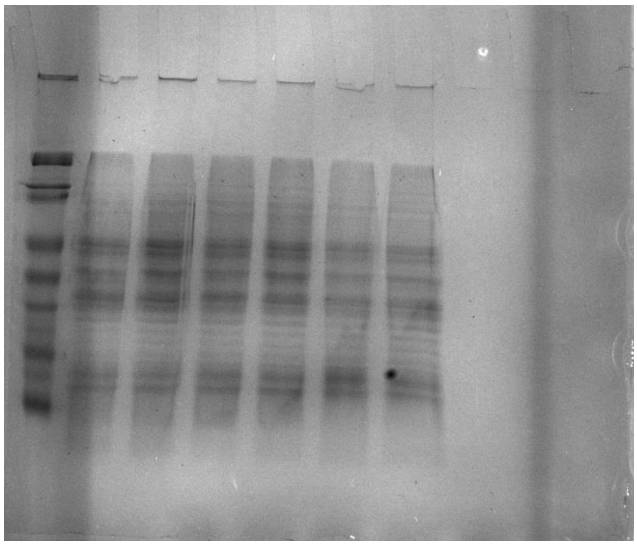

Figure 36: SDS-PAGE gel showing separation of proteins for samples from control cultures. Samples were loaded in the following order: marker (Biorad prestained SDS-PAGE standards, low range), 1a, 1b, 1c, 1d, 1e, 1f.

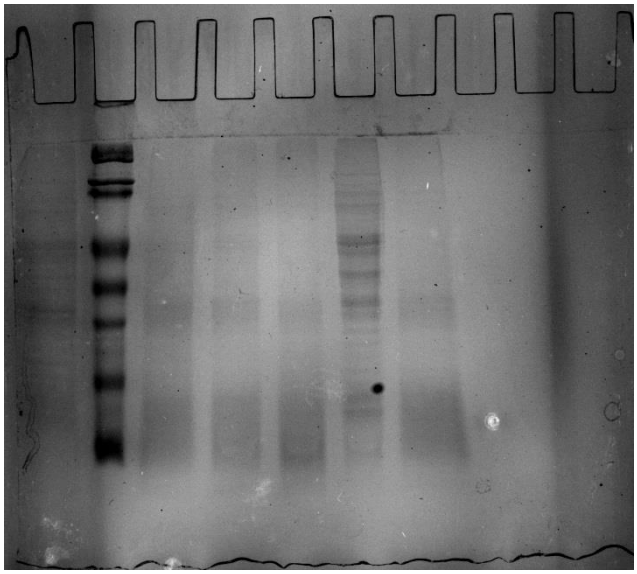

Figure 37: SDS-PAGE gel showing separation of proteins for samples from cultures grown in iron-limited conditions. Samples were loaded in the following order: 2a, marker (Biorad prestained SDS-PAGE standards, low range), 2b, 2c, 2d, 2e, 2f.

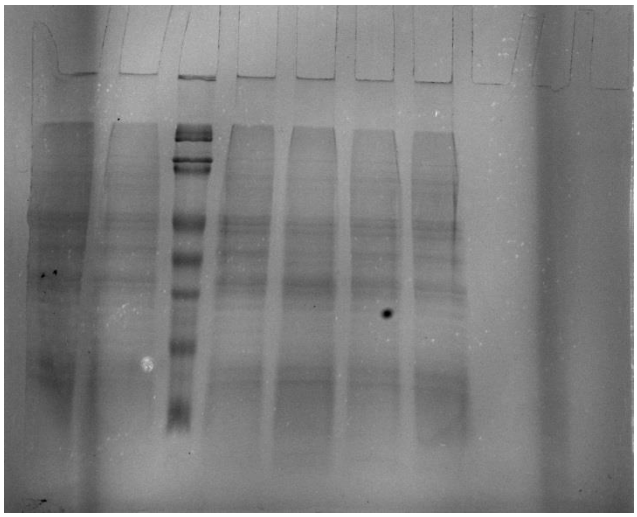

Figure 38: SDS-PAGE gel showing separation of proteins for samples from cultures grown in high iron conditions. Samples were loaded in the following order: 3a, 3b, marker (Biorad prestained SDS-PAGE standards, low range), 3c, 3d, 3e, 3f.

4.3.5 Conclusions

Raw protein extraction without using a protein precipitation step gave clear separation of proteins with strong bands in the control and high iron conditions, although the proteins were less clear for the iron-limited condition (Figure 36) (Figure 37) (Figure 38). This was judged to be sufficient to proceed to the next step, and so this method was then used to process the samples for the final proteomics results (see chapter 6).

5. Comparison of metabolite profiles of *F. venenatum* grown in iron limited, excess iron, calcium limited and excess calcium media.

5.1 Introduction

5.1.1 Fungal metabolomics

Metabolites are substrates, intermediates or products of the cell's biochemistry that are not encoded by the DNA (Jewett *et al.*, 2006). Metabolome analysis aims to quantitatively profile the metabolites that correspond to a particular genotype, phenotype or environmental condition, using analytical techniques such as liquid chromatography - mass spectrometry (Putri *et al.*, 2013). A metabolomics study may comprise: targeted analysis and quantification of a small number of metabolites; metabolite profiling which seeks to investigate all metabolites possible with a given analytical technique, thus producing a profile of known and unknown metabolites (Jewett *et al.*, 2006); or metabolite fingerprinting which does not identify individual compounds but rather produces a biochemical fingerprint that can be used for comparison (Putri *et al.*, 2013). A study of the metabolome can therefore lead to a biochemical profile that allows an organism's responses and gene functions to be assessed (Bedair & Sumner, 2008).

Members of the fungi kingdom have previously been the subject of metabolomics investigations due to their use in biotechnology applications (Smedsgaard & Nielsen, 2005), and as producers of many useful bioactive compounds, as well as being implicated in diseases of humans, and spoilage of food (Nielsen & Larsen, 2015).

A targeted metabolomics approach was used by Gold et al., (2015) who evaluated a metabolic engineering strategy for improving the yield of L-tyrosine in *Saccharomyces cerevisiae*. In all, 19 metabolites relevant to tyrosine production were monitored over time and researchers were able to compare engineering strategies that increased tyrosine yield using feedback resistant enzymes (Gold *et al.*, 2015).

Untargeted metabolomics has been used in a study that identified metabolites induced in co-cultures of *Aspergillus* and *Fusarium* species (Bertrand *et al.*, 2014). The study discovered metabolites that were found earlier in co-culture than pure culture and were increased in co-culture rather than pure culture (Bertrand *et al.*, 2014). Five compounds were identified as substances that are thought to possess antimicrobial properties (Bertrand *et al.*, 2014).

Metabolite fingerprinting was used in a study by Tylová *et al.*, (2011), which used this technique to examine extracellular metabolites of filamentous fungi species of the genus *Geosmithia*. The production of secondary metabolites was related to ecological or taxonomic differences using ultra high performance liquid chromatography - diode array detector (UHPLC-DAD) fingerprints (Tylová *et al.*, 2011). The method allows comparisons to be made between species using the chromatograms that include not only marker compounds but also many unidentified compounds, and the authors explain that this approach could also be used in taxonomic studies, and could aid research on flavour (Tylová *et al.*, 2011).

A previous study of the metabolome of *F. venenatum* compared two growth conditions, with variations in the medium that either encouraged or discouraged the production of mycotoxins (Lowe *et al.*, 2010). Four related *Fusarium* species including *venenatum* were investigated and H^1 nuclear magnetic resonance (NMR) spectroscopy was used along with direct injection mass spectrometry to produce a metabolic fingerprint that could be compared in the different conditions (Lowe *et al.*, 2010). The study showed that growth conditions had an effect on the metabolome of each species that was greater than the differences seen between species (Lowe *et al.*, 2010). The authors assert that the external environment therefore was critical in determining the internal metabolome of these fungi (Lowe *et al.*, 2010).

5.1.2 Current methods for metabolomics studies

Studies that investigate metabolomics are not restricted to one technology or methodology, but rather a range of approaches have been used, depending on the aims of the researchers.

This is necessary because given the large amount of variation in chemical or physical properties of metabolites, it is not possible to measure all metabolites with one method (Putri *et al.*, 2013). Current methods in use for identification and measurement of metabolites include nuclear magnetic resonance (NMR) spectroscopy, Liquid chromatography – mass spectrometry (LC-MS), liquid chromatography - tandem mass spectrometry (LC-MS/MS), and gas chromatography mass spectrometry (GC-MS) (Putri *et al.*, 2013). These methods can then be followed by data analysis and library searches to identify the unknown compounds (Nielsen & Larsen, 2015).

NMR has been used for compound identification in studies of metabolomics. NMR works by detecting the magnetic resonance absorption profiles of the compounds, which depends on their chemical structure (Putri *et al.*, 2013). This technique is advantageous over other methods as it does not require separation, and it is non-destructive to the compounds tested (Wishart, 2008). However, a disadvantage is its relative insensitivity, and it therefore requires larger sample sizes (~500 µL) (Wishart, 2008). NMR spectroscopy can be used for metabolite fingerprinting as it allows simultaneous analysis of a wide range of compounds (Larive *et al.*, 2015). In addition, it is also possible to use this technique for metabolic profiling of a smaller number of metabolites that belong to a few pathways (Larive *et al.*, 2015). Identification of compounds is possible by comparing the spectra to a library of reference spectra of known compounds (Wishart, 2008). ^{1}H NMR was used in a study by Son *et al.*, (2009) to investigate a number of metabolites produced by yeast during the winemaking process. PCA plots from NMR spectra were used to show differences in fermentation activity between different strains of *Saccharomyces cerevisiae* in terms of fast and slow changes in metabolites during the process (Son *et al.*, 2009).

Gas chromatography mass spectrometry (GC-MS) can be advantageous for some metabolomics applications as it can give good separation, and uses reproducible electron impact (EI^{+}) ionisation (Nielsen & Larsen, 2015). However it is only suited to volatile chemicals or those that can be made volatile by derivatisation (Nielsen & Larsen, 2015). GC-

MS was used in a study by Zheng *et al.* (2012) in order to produce a targeted metabolite profile of compounds produced in osmoregulation mutants of *F. graminearum* (Zheng *et al.*, 2012). In the wild type, it was found that the sugar alcohols glycerol, mannitol, arabitol and the sugar sucrose were induced by NaCl treatment (Zheng *et al.*, 2012). In mutants of the FgHog1 mitogen-activated protein (MAP) kinase pathway these metabolites were still accumulated but at a lower level (Zheng *et al.*, 2012). The target compounds had to be first derivatised for GC-MS using TMSI:TMCS (Trimethylsilylimidazole: Trimethylchlorosilane) (Zheng *et al.*, 2012).

Liquid chromatography – mass spectrometry (LC-MS) is in widespread use in metabolomics applications (Theodoridis *et al.*, 2008). High performance liquid chromatography (HPLC) is used for separation of compounds prior to MS analysis, which generally uses reverse-phase gradients for compounds of medium or low polarity (Theodoridis *et al.*, 2008). In reverse-phase liquid chromatography, the mobile phase used is a mixture of polar solvents, and the stationary phase consists of silica particles with octadecyl silane groups (C_{18}) attached (Rafferty *et al.*, 2011). The analytes are separated based on physical differences e.g. molecular weight or polarity, which affect their retention in the column, with more polar molecules being released more quickly from the column as they have higher affinity to the polar mobile phase than the non-polar stationary phase (Rafferty *et al.*, 2011).

5.1.3 Metabolite identification

In an untargeted metabolomics investigation, the metabolites whose amounts have been altered significantly between conditions must be identified accurately (Xiao *et al.*, 2012). Identification begins by searching the accurate mass for the compound given by the initial LC-MS in mass spectra databases such as METLIN (Xiao *et al.*, 2012) (Metlin, 2017). These initially identified compounds are then subjected to fragmentation in a second MS analysis (Xiao *et al.*, 2012). The data resulting from the retention time and m/z of the precursor ions together with the second MS analysis of the fragmented ions is then used to produce structural

information for identification, which can be compared to the same data from authentic compound standards for confirmation (Xiao *et al.*, 2012). Unfortunately, the high number of detected compounds in an untargeted investigation and the likelihood of multiple initial identifications for each one (one ion can have 100 putative identifications) make this process extremely time consuming and costly (Xiao *et al.*, 2012). In fungal studies this can be especially difficult due to the large structural diversity of compounds present in the sample, and reference standards for secondary metabolites such as mycotoxins may not be easily available (Nielsen & Larsen, 2015).

Instead of using standards and making comparisons, computational methods exist that can interpret LC-MS/MS data and use this to suggest possible molecular formulas which can be searched in databases so that the compound can be identified. One example of this is SIRIUS (Lehrstuhl-Bioinformatik, 2018) (Böcker & Dührkop, 2016).

5.1.4 Using Sirius for metabolite identification

SIRIUS (Sum formula Identification by Ranking Isotope patterns Using mass Spectrometry) is a web-based tool for the identification of compounds from LC-MS (Lehrstuhl-Bioinformatik, 2018). The SIRIUS system first uses isotope patterns and database searches to enable an accurate chemical formula to be deduced from the LC-MS data (Böcker *et al.*, 2009). This is because the distribution of isotopes in the elements that make up the compound mean that there will be several peaks in the LC-MS chromatogram which correspond to the same type of sample molecule, this is its isotope pattern (Böcker *et al.*, 2009). The monoisotopic mass is the mass that corresponds to the molecule made up the isotopes that have the lowest possible mass (Böcker *et al.*, 2009). The SIRIUS procedure first takes the monoisotopic mass of the input compound and computes all the possible formulas that could have that mass (Böcker *et al.*, 2009). Each of these possible formulas will each have a possible isotope pattern that can be simulated and then compared with the isotope pattern of the input compound (Böcker *et al.*, 2009). This method allows the reduction of the number of possible formulas to

a much smaller number and can give the correct formula in many cases (Böcker *et al.*, 2009). Next, the SIRIUS system uses fragmentation trees to analyse the fragmentation data from LC-MS/MS, which further narrows down the number of choices for the predicted molecular formula (Dührkop *et al.*, 2013). A fragmentation tree consists of nodes that represent the chemical formula or structure of a particular fragment and shows the relationship between them (Vaniya & Fiehn, 2015). The computer generates a fragmentation tree for each parent peak that shows a predicted fragmentation pathway that can be expected in the LC-MS/MS data for that compound (Dührkop *et al.*, 2013). The combination of the isotope pattern score and the fragmentation tree score (weighted towards the isotope pattern score due to its higher reliability) is applied to each possible molecular formula and these are then ranked by this score (Dührkop *et al.*, 2013). This fragmentation tree data can then be used to search spectral libraries to obtain an identification of the compound, by using the CSI:FingerID (CSI – Compound Structure Identification) program (Dührkop *et al.*, 2015). This system incorporates a learning phase in which all known compounds in the library are processed to produce a fragmentation tree and molecular properties (Dührkop *et al.*, 2015). The fragmentation tree from the unknown compound is then compared to the fragmentation trees from the library to find the best match, for which a score is given (Dührkop *et al.*, 2015). The authors claim that searching databases using the CSI:FingerID method is more effective than other techniques, and it gave a 2.5 fold increase in correct identification over the next best method (Dührkop *et al.*, 2015).

This software therefore provides a good indication of the identity of the metabolite but it is not 100% accurate. These identifications would still need to be followed up with comparison between the LC-MS/MS fragmentation data obtained from the samples and LC-MS/MS fragmentation data from verified standards to achieve a more positive identification.

5.1.5 Non-targeted metabolomics analysis of *F. venenatum* intracellular metabolites

In the case of *F. venenatum*, it is important to assess its metabolic response to growth conditions as it is used in the food industry in the production of Quorn™ meat substitute products, and it may become beneficial to alter growth conditions if they confer an advantage, for example producing a better quality product in terms of either morphology, or production of flavour compounds. The analysis of the metabolites that are increased or decreased in media modified with differing amounts of iron and calcium could reveal more about the biochemistry of the organism and how it may be optimised in future to produce a different flavour profile, commercially relevant secondary metabolites or it could reveal the production of unwanted compounds such as mycotoxins or their intermediates that we would want to avoid. As has already been discussed in previous chapters, metal ions such as iron and calcium are essential in biochemistry and changing the amounts of these is likely to cause a response in the organism e.g. the morphology was changed in iron limited conditions. Iron is important due to its use as cofactors for some of the enzymes responsible for essential cellular reactions (Bailão *et al.*, 2012). For example, enzymes with Fe/S clusters are involved in diverse reactions of the cell including amino acid biosynthesis, production of nucleotides, DNA synthesis and repair, and respiration (Netz *et al.*, 2014). Calcium is involved in many cellular processes including cell signalling, cell motility, cell division, gene expression (Cavinder *et al.*, 2011), growth at the tip (Jackson & Heath, 1993), and studies have shown that *F. venenatum* changes its morphology in response to calcium levels (Robson *et al.*, 1991b). Other organisms grown in iron-free or iron limited media show changes in their metabolism, and this has been found to be the case in species such as *Saccharomyces cerevisiae* (Shakoury-Elizeh *et al.*, 2010). It is likely therefore that these altered metal ion conditions will also produce a change in the metabolite profile of *F. venenatum* and this investigation aims to discover these changes.

5.2 Methods

5.2.1 Sample preparation

F. venenatum A3/5 (obtained from Quorn Foods) cultures were maintained on oatmeal agar at 4 °C. Starter cultures for each strain were begun by transferring a small piece of hyphae from the edge of the growing fungus into 50 mL Oxoid nutrient broth in a 250 mL baffled conical flask. The starter culture was incubated at 28 °C with shaking at 150 rpm for 3 days. Fifty millilitres of RHM medium and modified RHM medium cultures in 250 mL baffled conical flasks were inoculated using 500 µL of the starter culture, and these were incubated for 3 days at 28 °C with shaking at 150 rpm. RHM medium consisted of potassium dihydrogen phosphate (20 g L^{-1}), ammonium chloride (4.4 g L^{-1}), potassium sulfate (0.3 g L^{-1}), magnesium sulfate heptahydrate (0.25 g L^{-1}), 50% glucose soln. (4 mL L^{-1}), 0.3 g L^{-1} biotin soln. (1 mL L^{-1}), and trace metal soln. (5 mL L^{-1}). The trace metal soln. consisted of iron sulfate heptahydrate (2.8 g L^{-1}), zinc chloride (1 g L^{-1}), manganese chloride tetrahydrate (1 g L^{-1}), copper chloride (0.2 g L^{-1}), cobalt chloride (0.2 g L^{-1}), sodium molybdate (0.2 g L^{-1}), calcium chloride dihydrate (2 g L^{-1}), and citric acid (1.5 g L^{-1}). The modifications to RHM medium were made by altering the trace metal soln. as follows: TR1 (as above); TR2 - iron sulfate heptahydrate x0; TR3 - iron sulfate heptahydrate x10 (28 g L^{-1}); TR4 - calcium chloride dihydrate x0; TR5 - calcium chloride dihydrate x10 (20 g L^{-1}). All RHM cultures were brought to pH 6 using 1 M NaOH solution, before autoclaving and the 50% glucose soln. was autoclaved separately and added to the cultures just before they were inoculated.

The cells from each culture were separated from the broth by centrifugation for 10 min at 3,500 rpm (Beckman Allegra 6R centrifuge). The cell pellets were then lyophilised (Virtis SP Scientific, Sentry 2.0), and the dry cell pellets were frozen in liquid nitrogen and then ground to a fine powder (IKA analytical batch mill). Twenty-five milligrams of the powdered cells were then added to 2 mL of 75% methanol in dH_2O. These samples were then sonicated for 25 min in iced water. The sonication bath (Grant Ultrasonic Bath XUBA1) had a frequency of 44 kHz. The tubes were inverted several times and vortexed to mix before and after sonication.

The sonicated samples were then centrifuged at 12,500 rpm (17,469 g RCF) with the temperature set to 0 °C (Sigma 3-18KS centrifuge). The supernatant was then dried to a powder in a sample pre-concentrator (Christ RVC 2-18). Three hundred microliters of 75% methanol in dH_2O was then added to each tube, and they were shaken for 20 min at full speed (Scientific Industries Vortex Genie 2). Finally, the samples were filtered through a 35 mm nylon 0.2 µm filter and were analysed by LC-MS using the method described below.

5.2.2 LC-MS analysis

The samples were analysed using a Dionex UltiMate 3000 UHPLC system (Dionex, Sunnyvale, CA) connected to a Thermoscientific Q-Exactive mass spectrometer system (Thermo, Loughborough, UK). The UHPLC system used a Waters T3 high strength silica (HSS) C18 UHPLC column (150 x 1.8 mm, 1.7 µm) (Waters, Elstree, UK). The flow rate was 0.4 mL min^{-1}, with an oven temperature of 45 °C and an injection volume of 5 µL. Samples were held in the autosampler at 4 °C while waiting to be injected. Buffer A consisted of dH_2O with 0.1% formic acid. Buffer B consisted of LC-MS Optima grade acetonitrile with 0.1% formic acid. The buffers were used in the UHPLC with the following gradient system: 0 min (5% B) hold for 1 min and then a linear gradient to 100% B up to 12 mins, hold for further 2 min (wash period) and return to the starting condition at 14 min with a column stabilization time of a further 4 mins.

The heated electrospray ionisation (HESI) introduction source had a capillary temperature of 325 °C and 3.8 KV (Positive mode). The nitrogen sheath flow was set to 45 and an auxiliary flow was set to 15 (arbitrary units). The radio frequency of the S-lens was set to 50. For the first MS scan the mass spectrometer was set to 17.5K mass resolution with 13.2 scan s^{-1} and automatic gain control (AGC) at 1^{e6}. The maximum injection time was 100 ms.

For MS/MS profiling the mass spectrometer was operating at 35K mass resolution with a scan rate of 8 scan s^{-1} and AGC of 5^{e5}. The maximum injection time was 50 ms. The mass ranges were set to 100-950.

The peaks were chosen for MS/MS fragmentation using chromatograms from the first MS analysis, after statistical analysis had shown the metabolites with significantly altered peak areas. Peaks were chosen whose mass was within 10 ppm of the selected metabolite. MS/MS scans were carried out at 10, 30, 50 and 70 NCE (normalised collision energy).

5.2.3 Data reduction, statistical analysis and metabolite searches

Six quality control (QC) (pooled) samples were made by pooling all the samples together. Repeatability of the results was calculated using the relative standard deviation (RSD) of the peak area totals of these QC (pooled) sample expressed as a percentage. Metabolites that had an RSD value of 16% or greater for the QC samples were removed from the data as this indicated poor repeatability. Metabolites that had an average peak area across the 6 repeat cultures in each condition that was less than 100,000 were discounted from the data as compounds with low abundance would not be suitable for MS/MS analysis.

SPSS statistics software (IBM SPSS Statistics version 24) was used to perform statistical analysis on the data. The Mann Whitney U test was used to compare the data in pairs, as the data were not normally distributed. Each condition was compared to the control. Compounds that were shown to be significantly altered in each growth condition compared to the control were given initial identifications using the metlin online database (Metlin, 2017).

Data from the MS/MS chromatograms was converted into text files using Xcalibur software, and these were converted to .mgf files to be fed into the SIRIUS program. The SIRIUS program was set up to analyse only $[M + H]^+$ ions, the instrument was set to Orbitrap, and the ppm window was set to 10.

5.3 Results & Discussion

The Mann-Whitney U test result ($P<0.05$) gave a number of significantly altered compounds for each condition. From the significant compounds as many as possible were given putative identifications from the Metlin database, based only on their accurate mass measurement. From this group, MS/MS was attempted for each compound that could be reliably found in the chromatograms, with a peak area above 100,000. The resulting MS/MS data were processed, and searches were carried out by the SIRIUS programme. The numbers of compounds for each condition are given in Table 1.

Table 1: Number of compounds identified for each condition

Condition	Total compounds	Statistically significant effect	% increased peak areas	% decreased peak areas	MS/MS data	SIRIUS ID (>70% score)
Iron (-)	1617	347	58	42	35	9
Iron (+)	1617	110	45	55	17	2
Calcium (-)	1617	42	14	86	5	3
Calcium (+)	1617	58	66	34	5	0

5.3.1 Identified metabolites

The compounds identified by the SIRIUS software are given in the tables below.

Table 2: Summary of identified metabolites and pathways with significantly altered peak areas in the **iron limited** condition, compared to the control. P values refer to the Mann-Whitney U test for non-parametric data, based on data from 6 repeat cultures.

Cell constituent	**Pathway**	**Iron cofactor in pathway**	**Metabolite Name**	**Fold-change**	**P value**	**SIRIUS score %**
Energy metabolism	Carnitine pathway	Yes	Acetyl carnitine	0.4	0.006	88
			Propionylcarnitine	0.3	0.006	90
Amino Acids	Histidine pathway	No	Histidine	0.7	0.016	94
	Lysine pathway	Yes	Lysine	0.6	0.010	94
Dipeptide	glutamate/valine pathway	Yes	Valylglutamate	7.3	0.004	80
Benzaldehyde	Benzaldehyde	No	Benzaldehyde	0.7	0.037	82
Nucleic acids	Purine nucleotides	No	2-*o*-methyladenosine	4.0	0.006	91
	Purine nucleotides	No	Hypoxanthine	0.6	0.016	90
Cell membrane	Phospholipids	No	Lysophosphatidylcholine	0.3	0.037	76

Table 3: Summary of identified metabolites and pathways with significantly altered peak areas in the **calcium limited** condition, compared to the control. P values refer to the Mann-Whitney U test for non-parametric data, based on data from 6 repeat cultures.

Cell constituent	**Pathway**	**Metabolite Name**	**Fold change**	**P value**	**SIRIUS score %**
Energy metabolism	Carnitine pathway	Acetyl carnitine	1.5	0.01	87
Amino Acids	Histidine pathway	Histidine	0.7	0.037	94
Dipeptide	Threonine/valine pathway	Threonylvaline	0.2	0.034	86

Table 4: Summary of identified metabolites and pathways with significantly altered peak areas in the **excess iron** *condition* compared to the control. P values refer to the Mann-Whitney U test for non-parametric data, based on data from 6 repeat cultures.

Cell constituent	**Pathway**	**Metabolite Name**	**Fold change**	**P value**	**SIRIUS score %**
Oxylipins	Lipoxygenase	9-Octadecadienoic acid-10,12-odda	0.67	0.037	81
Oxylipins	Lipoxygenase	9-Octadecadienoic acid-10,12-odda	0.45	0.016	80

5.3.2 Metabolites identified in iron limited conditions

5.3.2.1 Carnitine pathway

5.3.2.1.1 Acetylcarnitine, fold change: 0.4, P value: 0.006, SIRIUS score: 88%

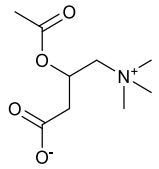

Figure 39: Acetlycarnitine.

5.3.2.1.2 Propionylcarnitine, fold change: 0.3, P value 0.006, SIRIUS score 90%

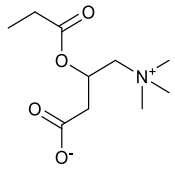

Figure 40: Propionylcarnitine.

Acetyl carnitine has been reduced to 0.4 times the peak area of the control. Acetyl carnitine is involved with the transport of acetyl-CoA into the mitochondria, a process known as the carnitine shuttle (Strijbis *et al.*, 2010). Acetyl-CoA is produced by the breakdown of fatty acids, and this needs to be transported into the mitochondria for oxidation (Franken *et al.*, 2008). The acetyl group is transferred to carnitine by the enzyme carnitine acetyltransferase (CAT), and the acetyl carnitine then enters the mitochondrion through carnitine acetyl-carnitine translocase Crc1p (Franken *et al.*, 2008). Once inside the mitochondrion, the reverse reaction is catalysed by mitochondrial CAT to release the acetyl-CoA so that it can take part in the TCA cycle (Franken *et al.*, 2008). Carnitine is therefore highly important in both fatty acid metabolism and in respiration due to the use of acetyl-CoA in the TCA cycle.

The first step of the biosynthesis of carnitine is the conversion of 6-N-trimethyllysine (TML) to 3-hydroxy-TML and this reaction requires the enzyme TML dioxygenase (Strijbis *et al.*, 2010). TML dioxygenase is an enzyme that requires Fe^{3+} as a cofactor, and so the production of carnitine could be affected by iron limited conditions, which could explain the reduction of acetyl carnitine (Strijbis *et al.*, 2010). Propionylcarnitine has also been reduced in iron limited conditions, which may be due to the same effect.

5.3.2.2 Amino acid metabolism

5.3.2.2.1 Lysine, fold change: 0.6, P value: 0.01, SIRIUS score: 94%

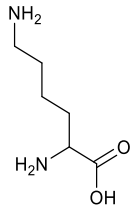

Figure 41: Lysine.

Results show a decrease in average peak area of lysine to 0.6 times the control value. Lysine is produced in higher fungi using the α-aminoadipate pathway, which has been demonstrated in species such as *S. cerevisiae*, *Neurospora crassa* and *Aspergillus fumigatus* (Xu *et al.*, 2006). The pathway has 8 steps and is catalysed by 7 enzymes (Xu *et al.*, 2006). Homocitrate synthase first converts α-ketoglutarate and acetyl-CoA to homocitrate, which is the rate-limiting step of the pathway (Xu *et al.*, 2006). The second reaction requires an Fe/S enzyme: homoaconitase which converts the homocitrate to homoisocitrate (Xu *et al.*, 2006). The homoisocitrate is then converted to α-ketoadipate by homoisocitrate dehydrogenase (Xu *et al.*, 2006). The α-ketoadipate is then acted upon by an aminotransferase to become α-aminoadipate, which uses the amino group from glutamate (Xu *et al.*, 2006). α-aminoadipate-δ-semialdehyde is the next intermediate, formed by α-aminoadipate reductase (Xu *et al.*, 2006). The α-aminoadipate-δ-semialdehyde is then converted to saccharopine, using a

molecule of glutamate by saccharopine reductase (Xu *et al.,* 2006). The final step is the conversion of saccharopine to lysine (Xu *et al.,* 2006).

This result is consistent with reduced iron conditions as the pathway begins with α-ketoglutarate, which could be decreased due to a downregulation of the TCA cycle as two of its enzymes are dependent on Fe/S enzymes, and the production of lysine also depends on an Fe/S enzyme in its second reaction – homoaconitase (Xu *et al.,* 2006). This pathway is therefore likely to have been downregulated when the fungus is starved of iron.

5.3.2.2.2 Histidine, fold change: 0.7, P value: 0.016, SIRUS score 94%

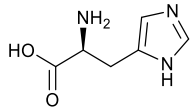

Figure 42: Histidine.

Histidine biosynthesis requires a total of 10 reactions (Jastrzębowska & Gabriel, 2015). The pathway starts with phosphoribosylpyrophosphate from the pentose phosphate pathway (Jastrzębowska & Gabriel, 2015). This is first converted to phosphoribosyl-ATP by ATP phosphoribosyl transferase (Jastrzębowska & Gabriel, 2015). Phosphoribosyl ATP diphosphatase enzyme then converts this to phosphoribosyl-AMP (Jastrzębowska & Gabriel, 2015). The phosphoribosyl-AMP then becomes phosphoribosylformimino-5-aminoimidazole-4-carboxamide ribonucleotide (phosphoribosylformimino-AICRP) due to the action of phosphoribosyl-AMP cyclohydrolase (Jastrzębowska & Gabriel, 2015). The phosphoribosylformimino-AICRP is then converted to phosphoribulosylformimino-5-aminoimidazole-4-carboxamide ribonucleotide by phosphoribosylformimino-5-amino-1-phosphoribosyl-imidazole carboxamide isomerase (Jastrzębowska & Gabriel, 2015). The phosphoribulosylformimino-5-aminoimidazole-4-carboxamide ribonucleotide is then converted to imidazoleglycerol-phosphate by imidazoleglycerol-phosphate synthase, while converting a molecule of glutamine to glutamate (Jastrzębowska & Gabriel, 2015). The next

step is the conversion of imidazoleglycerol-phosphate to imidazoleacetol-phosphate by imidazoleglycerol-phosphate dehydratase (Jastrzębowska & Gabriel, 2015). The conversion of glutamine to α-ketoglutarate accompanies the next step which is the conversion of imidazoleacetol-phosphate to histidinol-phosphate by histidinol-phosphate transaminase (Jastrzębowska & Gabriel, 2015). The histidinol-phosphate then becomes histidinol by the action of histidinol-phosphatase (Jastrzębowska & Gabriel, 2015). The histidinol is then converted to histidine by histidinol dehydrogenase first converting it to histidinal and finally to histidine (Jastrzębowska & Gabriel, 2015).

This pathway is linked to glucose metabolism via the pentose phosphate pathway, via the intermediates glucose-6-phosphate and glyceraldehyde-3-phosphate (Stincone *et al.,* 2015). Glucose metabolism is likely to be affected by iron limited conditions due to the use of Fe/S enzymes in the TCA cycle (Philpott *et al.*, 2012). It has been found in yeast that low levels of iron results in lower levels of intermediate compounds from glycolysis, and genes required for respiration were downregulated (Philpott *et al.*, 2012). Reduction of respiration would result in a reduction of ATP synthesis, which could also affect histidine production as this is required for the second reaction of the pathway. Another reaction in the pathway requires the input of a glutamine molecule, which was found to be reduced in iron limited conditions in my results (see chapter 3). Together, these consequences of iron limited growth conditions are likely to reduce histidine biosynthesis.

5.3.2.2.3 Valylglutamate, fold change 7.3, P value: 0.004, SIRIUS score 80%

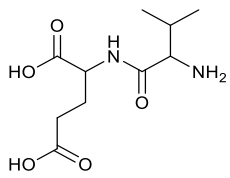

Figure 43: Valylglutamate.

In contrast to the above amino acids, the dipeptide valylgluatmate appears to have been increased in iron limited conditions, with a 7.3 times greater peak area. As a dipeptide, valyl glutamate is a product of protein catabolism in the cell (Wishart *et al.*, 2018a) (Wishart *et al.*, 2018b). This suggests that iron limitation may have affected the breakdown of dipeptides, or it may be that valine and glutamate levels have increased or were unaffected by iron limited.

It is possible that therefore that glutamate production was not be affected by iron limited conditions, or alternatively, the breakdown product of a number of other amino acids is glutamate, and so the cell's available pool of glutamate could be replenished by the breakdown of compounds such as arginine (Goodman & Weiss, 1986), histidine (Polkinghorne & Hynes, 1982) or proline (Arst *et al.*, 1981).

Glutamate is produced from α-ketoglutarate and ammonia by glutamate dehydrogenase enzyme (Sieg & Trotter, 2014). This pathway is not dependent on an Fe/S enzyme but another pathway for glutamate production exists which uses the Fe/S enzyme glutamate synthase (Philpott *et al.*, 2012). A study of yeast has shown that transcripts for glutamate synthase are reduced 20 fold, while glutamate dehydrogenase is increased 4.5 fold when it is grown in iron deficient conditions (Philpott *et al.*, 2012).

Valine is a branched chain amino acid, all of which start production with pyruvate, the product of glycolysis (Chen *et al.*, 2011). Two molecules of pyruvate are converted to 2-acetolactate by acetolactate synthase enzyme (Chen *et al.*, 2011). This is then converted to 2,3-dihydroxy-isovalerate by acetohydroxyacid reductoisomerase, which then becomes 2-keto-isovalerate due to the action of dihyroxyacid dehydratase (Chen *et al.*, 2011). Finally, this is converted to valine by branched-chain amino acid aminotransferase, with the conversion of glutamate to α-ketoglutarate (Chen *et al.*, 2011). The precursor for valine, pyruvate, has been found to be elevated in yeast grown in iron limited conditions due to downregulation of the TCA cycle (Philpott *et al.*, 2012). However, dihydroxyacid dehydratase uses iron as a cofactor (Philpott *et al.*, 2012) and so this could be expected to be downregulated in low-iron conditions, and the

earlier amino acid analysis (chapter 3) showed that valine was reduced in low-iron conditions while glutamate was increased.

5.3.2.2.4 Benzaldehyde, fold change: 0.7, P value: 0.037, SIRIUS score 82%

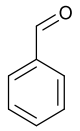

Figure 44: Benzaldehyde.

Benzaldehyde is a chemical used in the fragrance and flavour industries that gives a bitter almond aroma (Lomascolo *et al.*, 2001). It can be produced from phenylalanine, and its production has been reported in bacterial species such as *Lactobacillus plantarum*, and *Pseudomonas putida*, (Nierop Groot & de Bont, 1998) and in fungal species such as the basidiomycete *Trametes suaveolens* (Lomascolo *et al.*, 2001). However, it has been reported that benzaldehyde is toxic to fungal growth (Lomascolo *et al.*, 2001). It has not been studied in *F. venenatum*. The production of benzaldehyde begins with phenylalanine, and this has been reduced by 15% in iron limited conditions (see chapter 3), although it wasn't statistically significant. If phenylalanine was reduced in iron limited conditions, it could be expected that benzaldehyde would be reduced in this growth medium.

5.3.2.3 Nucleic acids

5.3.2.3.1 2-*o*-methyladenosine, fold change: 4.0, P value: 0.006, SIRIUS score: 91%

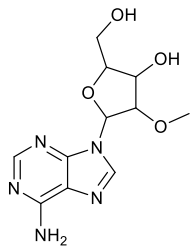

Figure 45: 2-*o*-methyladenosine.

2-*o*-methyladenosine is a nucleoside that has been modified by the addition of a methyl group at the 2'hydroxyl group (Broom & Robins, 1965). 85% of all modified nucleosides are found as part of tRNA molecules, and these can influence protein translation and the metabolism of the cell (Wang *et al.*, 2017). Changes in tRNA modified nucleosides can be part of a response to environmental conditions, stress conditions, starvation, aging and developmental stage and it has been suggested that modifications of tRNA help the cell to respond to environmental stress by influencing the translation of proteins that help to adapt the cell to changing conditions (Wang *et al.*, 2017). A significant increase in 2-*o*-methyladenosine was found in rice plants subjected to salt stress in a study by Wang *et al.* (2017), giving support to this theory. At the same time, transcription of the gene responsible for the modification of adenosine was increased (Wang *et al.*, 2017). The increase in 2-*o*-methyladenosine in iron starved *F. venenatum* may indicate that a similar stress response is working in the fungus.

5.3.2.3.2 Hypoxanthine, fold change: 0.6, P value: 0.016, SIRIUS score: 90%

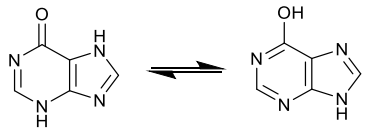

Figure 46: Hypoxanthine.

Hypoxanthine is produced as a break-down product of purine nucleotides (Saint-Marc *et al.*, 2009). The nucleotide inosine monophosphate (IMP) can be broken down to its nucleoside, inosine, by IMP specific nucleotidase (Saint-Marc *et al.*, 2009). The inosine can then be converted to hypoxanthine by purine nucleoside phosphorylase (Saint-Marc *et al.*, 2009). Adenosine can also be converted to inosine by AMP deaminase (Saint-Marc *et al.*, 2009). Results have shown that the level of hypoxanthine has decreased when the fungus was grown in iron limited conditions. As has been discussed in chapter 3 this could be due to a decrease in the availability of precursor molecules that derive from pathways reliant on enzymes that have iron as a cofactor. For example, the purine pathway requires glutamine to convert

phosphoribosyl pyrophosphate to phosphoribosylamine (Zhang *et al.*, 2008), and glutamine is reduced in iron limited conditions (see chapter 3). A depletion of glycolysis intermediates, which are known to be reduced in iron limited conditions (Philpott *et al.*, 2012) could also affect nucleotide biosynthesis as glycolysis supplies the pentose phosphate pathway, which in turn supplies the ribose 5-phosphate needed for purine synthesis (Stincone *et al.*, 2015). This could explain the reduction of hypoxanthine in these results.

5.3.2.4 Cell membrane constituents

5.3.2.4.1 Lysophosphatidylcholine, fold change: 0.3, P value: 0.037, SIRIUS: 76%

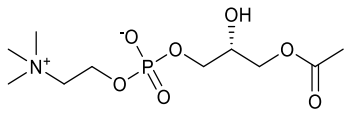

Figure 47: Lysophosphatidylcholine.

Phospholipids are an essential component of membranes in eukaryotic organisms, and are also intermediates for the production of signalling molecules (Cole *et al.*, 2012). Lysophosphatidylcholine is involved with increasing intracellular calcium levels, and has been shown to affect gene expression of multiple proteins in human cells (Yokoyama *et al.*, 2000).

Phospholipid biosynthesis begins with glycerol-3-phosphate which is converted to lysophosphatidic acid by glycerol-3-phosphate acyltransferase (Shindou & Shimizu, 2009). The lysophosphatidic acid is then converted to phosphatidic acid, which can become either diacylglycerol or cytidine diphospho-diacylglycerol (Shindou & Shimizu, 2009). Phospholipids such as phosphatidylcholine and phosphatidylinositol are then made from the cytidine diphospho-diacylglycerol (Shindou & Shimizu, 2009). Alternatively phosphatidylcholine can also be made by another route via diacylglycerol (Shindou &

Shimizu, 2009). Lysophospholipids are produced from phospholipids by a phospholipase enzymes, e.g. phospholipase A_2 can remove the fatty acid from the C2 position of a phospholipid (Voet & Voet, 2004). This conversion can be reversed, for example lysophosphatidylcholine can be converted back to phosphatidylcholine by lysophospholipid acyltransferase (Carman & Han, 2009). A Ca^{2+} dependent phospholipase A_2 has been found in *Tuber borchii*, a species of truffle, and a possible orthologue was indicated in *Gibberella zeae* (the sexual stage of *F. graminearum*) (Köhler *et al.*, 2006).

Results have shown that lysophosphatidylcholine has been reduced in iron limited conditions, which suggests that lipid metabolism may have been impacted by the lack of iron. The precursor for lipid biosynthesis glycerol-3-phosphate is produced from the glycolysis intermediate dihydroxyacetone phosphate by the action of glycerol-3-phosphate dehydrogenase enzyme (Zhang *et al.*, 2018). Since glycolysis is likely to be upregulated in iron-starved conditions, leading to lower levels of glycolysis intermediates (Philpott *et al.*, 2012), this could cause a reduction in lipid biosynthesis.

Alternatively, the levels of lipids could be affected by transcription factors that control the fungal response to iron availability. Lipid biosynthesis has been linked to iron homeostasis and morphology in the ascomycete fungus *Blastomyces dermatitidis* via a GATA transcription factor, *SREB* (siderophore biosynthesis repressor in *Blastomyces*) (Marty *et al.*, 2015). This fungus has the ability to switch its morphology from a filamentous mould to a yeast-like form according to temperature (Marty *et al.*, 2015). GATA transcription factors are involved in the responses of fungi to environmental stimuli such as light, temperature, nitrogen and iron by reducing or increasing gene transcription (Marty *et al.*, 2015). Deletion of this transcription factor prevented the fungus from changing its morphology from yeast to mould, and prevented the suppression of siderophore production when iron was plentiful (Marty *et al.*, 2015). It was found in this study that *SREB* affects the transcription of many genes from a range of processes including those connected with iron and those not connected with iron (Marty *et al.*, 2015). Lipid biosynthesis genes were differentially expressed in *SREB* deletion mutants that reduced

the production of triacylglycerol and ergosterol, but phospholipid levels were not affected (Marty *et al.*, 2015). This has demonstrated that it is possible that lipid biosynthesis in fungi could be affected by iron availability since transcription factors responding to environmental changes such as iron availability can have an effect on a wide range of genes and processes.

5.3.3 Metabolites identified in calcium limited condition

Calcium is used as a signalling molecule, and as such has an effect on a huge number of processes in the cell (Kraus & Heitman, 2003). For example, it can affect gene expression, energy metabolism, endo- and exocytosis, it controls the action of numerous proteins (Cavinder & Trail, 2012), and is known to have a role in stress responses to environmental stimuli (Kraus & Heitman, 2003). A high concentration of calcium at the growing tip has been shown to be important for growth and morphology, due to the coordination of actin filaments, and thereby controlling the exocytosis of vesicles containing cell wall building materials (Takeshita *et al.*, 2017). Calcium exerts its effect on proteins in different ways; when it binds to a protein it can cause the shape to change – thus affecting the function of that protein, or calcium can act via calmodulin (a calcium binding protein) to activate protein kinases which phosphorylate other proteins (Clapham, 2007). Protein phosphorylation gives a negative charge which results in a change in conformation, thus affecting how the protein works (Clapham, 2007). Calmodulin has two domains that bind calcium and target proteins, which can change shape when calcium binds (Hoeflich & Ikura, 2002). This conformational change then allows the calmodulin to alter the active sites of other proteins, remove autoinhibition, or cause proteins to dimerise (Clapham, 2007).

The target proteins of calmodulin perform a number of different functions in the cell, for example: protein kinases; transcription factors; protein phosphatases; motor proteins; and proteins of the cytoskeleton such as actin (Kraus & Heitman, 2003). It is likely, therefore that reducing calcium in the growth medium has disrupted or reduced these functions, and that has resulted in significantly lowering or increasing some of the metabolites identified below.

5.3.3.1 Carnitine pathway

5.3.3.1.1 Acetylcarnitine, fold change: 1.5, P value: 0.01, SIRIUS score: 87%

(see Figure 39) (see above for pathway description)

Acetylcarnitine has been increased significantly in calcium limited conditions. This may indicate that calcium limited has affected energy metabolism as acetylcarnitine is involved in transporting acetyl-CoA from fatty acid metabolism into the mitochondrion, as discussed above (Strijbis *et al.*, 2010).

5.3.3.2 Amino acid metabolism

5.3.3.2.1 Histidine, fold change: 0.7, P value: 0.037, SIRIUS score: 94%

(see *Figure 42*) (see above for pathway description)

Histidine has been reduced in calcium limited conditions, which may indicate that low levels of calcium has disrupted histidine biosynthesis pathway or the supply of precursors required, such as phosphoribosylpyrophosphate, which comes from the pentose phosphate pathway, or the amino acid glutamine.

5.3.3.2.2 Threonylvaline, fold change: 0.2, P value: 0.034, SIRIUS score: 86%

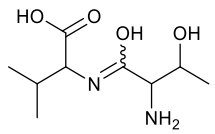

Figure 48: Threonylvaline

Threonylvaline is a dipeptide composed of threonine and valine (Wishart *et al.*, 2018a). The results have shown that its amount has been reduced in calcium limited conditions, this may indicate that calcium-limited medium has affected the breakdown of dipeptides by protease enzymes, or it may show that threonine and valine themselves have been reduced.

There are 5 steps in the biosynthetic pathway for threonine, which starts with aspartate (Farfán & Calderón, 2000). The aspartate is converted to aspartyl phosphate by aspartate kinase (KEGG, 2017) (Kanehisa *et al.*, 2017). This is converted to aspartate semialdehyde by aspartate semialdehyde dehydrogenase (KEGG, 2017) (Kanehisa *et al.*, 2017). Homoserine dehydrogenase then converts this to homoserine, which is then converted to *o*-phospho-homoserine by homoserine kinase (KEGG, 2017) (Kanehisa *et al.*, 2017). The final step is catalysed by threonine synthase, which produces threonine from the *o*-phospho-homoserine (KEGG, 2017) (Kanehisa *et al.*, 2017).

Valine is produced from pyruvate in a series of 5 reactions (Chen *et al.*, 2011). The pyruvate is first converted to 2-acetolactate by acetolactate synthase (Chen *et al.*, 2011). This is then converted to 2,3-dihydroxyisovalerate by acetohydroxyacid reductoisomerase (Chen *et al.*, 2011). The 2,3-dihydroxyisovalerate then becomes 2-ketoisovalerate due to the action of dihydroxyacid dehydratase (Chen *et al.*, 2011). Branched-chain amino-acid aminotransferase then catalyses the final reaction that produces valine from 2-ketoisovalerate (Chen *et al.*, 2011).

5.3.4 Metabolites identified in excess iron conditions

5.3.4.1 Lipid metabolism

5.3.4.1.1 9-oxo-10, 12-Octadecadienoic acid, fold change: 0.67, P value: 0.037, SIRIUS score: 81%

5.3.4.1.2 9-oxo-10, 12-Octadecadienoic acid, fold change: 0.45, P value: 0.016, SIRIUS score: 80%

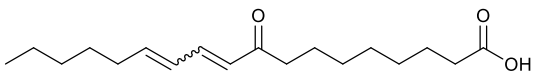

Figure 49: 9-oxo-10, 12-Octadecadienoic acid

In the excess iron condition only two significantly altered metabolites were able to be identified by SIRIUS but they were both assigned the same name. The first had a retention time of 8.9 min, and the second had a retention time of 10.4 min. It is possible that they are isomers but the software couldn't distinguish the difference, highlighting a drawback of using software rather than confirmed identifications using verified standards.

9-oxo-10, 12-Octadecadienoic acid belongs to a class of compounds which are termed oxylipins (Takahashi *et al.*, 2015). It is produced from linoleic acid by an oxidation reaction catalysed by a lipoxygenase enzyme (Zhao *et al.*, 2015), which contains iron as a cofactor (Wadman *et al.*, 2005). These compounds have been previously described in fungi e.g. *Gomphus floccosus* (woolly chanterelle) (Cantrell *et al.*, 2008), *Agaricus bisporus* (portobello mushroom) (Wadman *et al.*, 2005), and plants such as *Solanum melongena* (eggplant) (Zhao *et al.*, 2015), and *Solanum lycopersicum* (tomato) (Takahashi *et al.*, 2015), but they have not previously been reported in *F. venenatum*.

A study by Cantrell *et al.* (2008) investigated the fungicidal properties of 9-oxo-10, 12-Octadecadienoic acid and found that it caused growth inhibition of the plant pathogen *Phomopsis viticola* at higher concentrations (33-333 µL), and it was the most active with *Phomopsis* species, while other fungi were not as sensitive (Cantrell *et al.*, 2008). When it was tested against *F. oxysporum*, 9-oxo-10, 12-Octadecadienoic acid was found to actually stimulate growth at concentrations that were lower than the toxic dose, which is a common effect of some fungicides (Cantrell *et al.*, 2008).

Oxylipin compounds may be able to be used as antibiotics, as was shown in a study by Trapp *et al.* (2015). An extract with antibiotic properties containing 17 oxylipins that was isolated from the plant *Alternanthera brasiliana* was investigated and the separate oxylipins were tested (Trapp *et al.*, 2015). It was found that 9-oxo-10, 12-Octadecadienoic acid, along with many of the other oxylipins tested had antibiotic effects against the Gram-positive bacteria *Bacillus subtilis*, *Micrococcus luteus* and *Staphylococcus aureus* at a dose of 50 µg mL^{-1}

(Trapp *et al.*, 2015). It was suggested, however that the oxylipins could have originated in endophytic bacteria, rather than in the plant itself (Trapp *et al.*, 2015).

Anticancer properties have also been reported for 9-oxo-10, 12-Octadecadienoic acid, which was isolated from *Solanum melongena* (eggplant) (Zhao *et al.*, 2015). The 9-oxo-10, 12-Octadecadienoic acid was identified as the active ingredient in an extract from the calyx of the plant, which had a cytotoxic effect on human ovarian cancer cells. Further investigation showed that the compound had induced apoptosis in the cancer cells (Zhao *et al.*, 2015).

The amount of 9-oxo-10, 12-Octadecadienoic acid has been reduced in the excess iron condition. Oxylipins are known in plants to be involved in stress responses to biotic and abiotic factors and so levels may have been altered due to a stress response to the higher amount of iron (Trapp *et al.*, 2015). Alternatively the production of oxylipins is linked to iron, given that lipoxygenase enzyme contains an iron cofactor (Wadman *et al.*, 2005).

5.3.5 Metabolite differences in other growth conditions

When the fungus was grown in the condition of excess calcium, the statistics indicated very few significant metabolites from which a useful MS/MS spectrum could be produced and therefore these metabolites were not able to be identified with any confidence from the SIRIUS software. This condition therefore appears to have made less changes that were significant to the metabolism of the fungus and these slight effects were unable to be determined.

5.4 Conclusions

The iron limited condition has made the most difference to the metabolism of the fungus, with the largest number of significantly altered compounds compared to the control (347 out of 1617), and the majority of these were found to have increased peak areas (58% increased vs 42% decreased). The metabolites that were identified as significant and that were able to be identified from MS/MS spectra by the SIRIUS software fell into four main areas of cell

chemistry: energy metabolism; amino acid metabolism; purine metabolism, and cell membrane components. Some, but not all of the metabolites have a direct connection to iron, with an enzyme in their pathway that contains iron as a cofactor e.g. lysine. Metabolites with no direct connection with iron may still be indirectly affected due to a pathways such as glycolysis being upregulated or the TCA cycle being downregulated in iron limited conditions and thus reducing the amounts of precursor compounds needed for their production.

The calcium limited condition had 42 significant compounds out of the 1617 compounds found in the samples. Of these 86% were found to have decreased peak areas, compared to 14% that had increased peak areas. This reflects the importance of calcium in the cell, which is known to affect numerous areas of the cells biochemistry including gene transcription and energy metabolism (Cavinder & Trail, 2012). Of the significant compounds, only 3 were able to be identified by SIRIUS from the MS/MS spectra, but these showed that energy metabolism may have been affected with an increase in acetylcarnitine. Amino acid pathways were downregulated in this condition, as histidine was decreased, and the dipeptide threonylvaline was found in reduced amounts which may indicate protein breakdown was affected.

The changes in metabolite profile for *F. venenatum* in iron limited and calcium limited conditions could have implications if this condition was to be used in Quorn production, as alterations in amino acids such as glutamate could affect the flavour of the final product. Glutamate contributes to the savoury umami flavour as monosodium glutamate (MSG), when it is combined with the other umami compounds inosine monophosphate sodium salt (IMP), guanosine monophosphate sodium salt (GMP), and xanthosine monophosphate sodium salt (XMP) (Zhang *et al.*, 2013). Other amino acids can also affect flavour, with aspartate having MSG-like flavour, and arginine, leucine, phenylalanine, and tryptophan having a bitter flavour (Mau *et al.*, 2001). Amino acids could also participate in the Maillard reaction upon heating (Ames, 1998), therefore further investigations could explore this aspect having a direct impact on consumer perception.

The excess iron condition had 110 significantly altered compounds, of which 55% were decreased compared to the control, and 45% were increased. Of these, only one compound was identified by SIRIUS from the MS/MS spectra. This was 9-oxo-10, 12-Octadecadienoic acid which was reduced in these conditions. This compound has not been reported in this organism before, but it has been found in other species of fungi e.g. the basidiomycete *Gomphus floccosus*. It has been suggested in the literature that 9-oxo-10, 12-Octadecadienoic acid has antifungal (Cantrell *et al.*, 2008), antibiotic (Trapp *et al.*, 2015) and anticancer (Zhao *et al.*, 2015) properties, which makes it an interesting compound for further study, especially if it can be produced in *F. venenatum*, given the correct growth conditions.

The excess calcium condition had 58 significantly altered compounds, 66% of which were increased compared to the control, and 34% were decreased. Unfortunately, none of these were identified from the MS/MS spectra by SIRIUS with a score that was above 70%.

5.5 Further work

Since the metabolites were identified by software and online databases, their identities will now have to be confirmed by LC-MS/MS analysis of reference standards. Although metabolite identities described here are a good indication of the true identity, they are considered still tentative in nature.

The results have shown that the metabolite profile of *F. venenatum* has been affected in these different growth conditions, with iron limited having the greatest effect. A further study into how these metabolites affect the properties of the Quorn™ product would be necessary to find out if changing the conditions for food production had an effect on the flavour or quality of the final product and whether this would impart a beneficial or detrimental change. In addition, 9-oxo-10, 12-Octadecadienoic acid is a compound with potentially beneficial properties and so further investigation could lead to discovery of ways to produce it in *F. venenatum*. Mycotoxin production should also be investigated.

Experiments could be reproduced, using concentrated samples to enable better MS/MS fragmentation patterns to be obtained for trace components, leading to further identification of intracellular compounds affected by the changes in the growth medium. The development of the existing databases will undoubtedly also help such investigations.

Finally, the exometabolome could also be investigated, in order to increase our understanding of the biochemistry of the microorganism as affected by changes in the ionic content of the media.

6. Effect of iron cations on *F. venenatum* intracellular proteins

6.1 Introduction

Physicochemical changes in biological systems often affect the production and expression of a range of metabolites and proteins, while techniques developed in recent years enable the monitoring of these effects at the genome, transcriptome, proteome, and metabolome level. Non-targeted proteomic approaches are often used to enable the monitoring of the complete set of proteins present in an individual (or cell, organ, species or entire ecosystem) at a particular developmental stage or when subject to certain environmental conditions (González-Fernández *et al.*, 2010). Such investigations can give insight into the interaction between proteins and metabolites which affect growth, development and cellular activities during the organism's chemical and biological interactions with the environment (González-Fernández *et al.*, 2010).

Studies of *Fusarium* proteomics have concentrated on species such as *F. graminearum,* due to its production of mycotoxins and plant pathogenicity. These studies have aimed to determine how mycotoxin production is related to environmental conditions and how this can help fight plant infections by the fungus. Nivalenol is a type-B trichothecene mycotoxin that is produced in some *Fusarium* species, such as *F. graminearum* (Del Ponte *et al.*, 2012). A study by Pasquali *et al.*, (2013) looked at a nivalenol producing strain of this fungus when it was grown in different conditions designed to allow mycotoxin production; glutamate supplemented medium and agmatine supplemented medium (Pasquali *et al.*, 2013). Results revealed that many proteins expressed in these conditions were related to the stress response, indicating that mycotoxin production is linked to stress, and a large number of the detected proteins were involved with energy and metabolism (Pasquali *et al.*, 2013). Proteins involved in secondary metabolite production and synthesis of the pigment aurofusarin were also detected in these conditions (Pasquali *et al.*, 2013).

Taylor et al., (2008) investigated the *F. graminearum* proteome in order to understand the production of mycotoxins and to potentially find new antifungal agents. The fungus was grown

in nitrogen-limited conditions, which is known to induce trichothecene production (Taylor *et al.*, 2008). The results showed that trichothocene biosynthesis proteins were upregulated in the mycotoxin producing media (Taylor *et al.*, 2008). In addition, over time, proteins related to protein synthesis, primary metabolism and amino acid biosynthesis were downregulated in mycotoxin producing media (Taylor *et al.*, 2008). Proteins that were strongly upregulated over time in mycotoxin producing media included those related to vitamin metabolism (Taylor *et al.*, 2008). Moderately upregulated over time were proteins involved with environmental responses, cellular transport, the cell cycle and production of proteins such as actin and tubulin (Taylor *et al.*, 2008).

Together these studies have demonstrated how external conditions such as substances in the growth medium can cause wide-ranging changes in the many aspects of the metabolism of *Fusarium* species. Proteome studies can yield invaluable information that helps to develop our understanding of these fungi and their interactions with the environment.

The study of the proteome of *F. venenatum* in growth media containing limited and excess iron cations has not been previously reported, and it could reveal information on how the organism changes its biochemistry in response to iron stress. This could lead to the discovery of ways to affect the production of useful proteins or metabolites that could be beneficial in industry, or in the production of Quorn food products. It is also possible that these conditions could lead to the production of compounds such as mycotoxins, which would be detrimental to food production, and this could be revealed if the proteins associated with mycotoxin production are upregulated or downregulated in either condition.

6.1.1 Proteomics investigations of fungi grown in iron deprived conditions

A full proteomics investigation of a *Fusarium* species in iron deprived conditions has not yet been carried out, but a study by Parente *et al.*, (2011) looked at the ascomycete fungus *Paracoccidioides brasiliensis*, which causes the disease paracoccidioidomycosis. This study

used 2D gel electrophoresis, trypsin digestion and mass spectrometry to investigate the proteome (Parente *et al.*, 2011). It was found that 247 proteins were able to be detected that had a difference in abundance between the iron-limited and control conditions, and 96 of these could be identified with 49 upregulated and 47 downregulated (Parente *et al.*, 2011). Iron-starved conditions caused an upregulation of enzymes involved with glycolysis e.g. fructose 1,6-bisphosphate aldolase and glucokinase, while enzymes involved in the TCA cycle e.g. aconitase were downregulated (Parente *et al.*, 2011). Also downregulated were proteins involved with electron transport such as ATP synthase and cytochrome c (Parente *et al.*, 2011).

This was in agreement with the similar investigation by (Shakoury-Elizeh *et al.*, 2010) which also reported a reduction in the TCA cycle and respiration, while there was an increase in glycolysis when *S. cerevisiae* was deprived of iron. A study by Tavsan & Ayar Kayali, (2015) found additional evidence of the downregulation of the TCA cycle in the ascomycete fungus *Trichoderma harzianum* which had decreased levels of citrate, α-ketoglutarate, and fumarate in iron-limited medium.

Fatty acid metabolism was another affected process in iron-limited *Paracoccidioides brasiliensis*, with downregulated proteins such as aldehyde dehydrogenase, 3-hydroxybutyryl CoA dehydrogenase, and carnitine-*o*-acetyltransferase (Parente *et al.*, 2011). Amino acid biosynthesis pathways were also affected with enzymes relating to the pathways of aromatic amino acids, and aspartate being found to be downregulated, while threonine 3-dehydogenase enzyme for the conversion of threonine to glycine was upregulated (Parente *et al.*, 2011). The authors suggest that the metabolism of the fungus is moving away from pathways that contain enzymes reliant on Fe/S cofactors, for example the TCA cycle contains aconitase and succinate dehydrogenase which both require iron (Parente *et al.*, 2011). The results of this study have shown that the biochemistry of ascomycete fungi can be altered in iron deprived conditions, with major pathways being either upregulated or downregulated, especially those with a reliance on iron cofactors (Parente *et al.*, 2011).

6.2 Methods

6.2.1 *Fusarium venenatum* culture

F. venenatum A3/5 (obtained from Quorn Foods) cultures were maintained on oatmeal agar at 4 °C. Starter cultures for each strain were begun by transferring a small piece of hyphae from the edge of the growing fungus into 50 mL Oxoid nutrient broth in a 250 mL baffled conical flask. The starter culture was incubated at 28 °C with shaking at 150 rpm for 3 days. Fifty millilitres of RHM medium and modified RHM medium cultures in 250 mL baffled conical flasks were inoculated using 500 µL of the starter culture, and these were incubated for 3 days at 28 °C with shaking at 150 rpm. RHM medium consisted of potassium dihydrogen phosphate (20 g L^{-1}), ammonium chloride (4.4 g L^{-1}), potassium sulfate (0.3 g L^{-1}), magnesium sulfate heptahydrate (0.25 g L^{-1}), 50% glucose soln. (4 mL L^{-1}), 0.3 g L^{-1} biotin soln. (1 mL L^{-1}), and trace metal soln. (5 mL L^{-1}). The trace metal soln. consisted of iron sulfate heptahydrate (2.8 g L^{-1}), zinc chloride (1 g L^{-1}), manganese chloride tetrahydrate (1 g L^{-1}), copper chloride (0.2 g L^{-1}), cobalt chloride (0.2 g L^{-1}), sodium molybdate (0.2 g L^{-1}), calcium chloride dihydrate (2 g L^{-1}), and citric acid (1.5 g L^{-1}). The modifications to RHM medium were made by altering the trace metal soln. as follows: control (as above); iron-limited - iron sulfate heptahydrate x0; excess iron - iron sulfate heptahydrate x10 (28 g L^{-1}). All RHM cultures were brought to pH 6 using 1 M NaOH solution, before autoclaving and the 50% glucose soln. was autoclaved separately and added to the cultures just before they were inoculated.

The cells from each culture were separated from the broth by centrifugation for 10 min at 3,500 rpm (Beckman Allegra 6R centrifuge). The cell pellets were then lyophilised (Virtis SP Scientific, Sentry 2.0), and the dry cell pellets were frozen in liquid nitrogen and then ground to a fine powder (IKA analytical batch mill).

6.2.2 Protein extraction

The method for protein extraction was based on that described by Pascali *et al.* (2010), with modifications. The first part of the procedure was to extract proteins from the dried cell pellets. 50 mg of dried cells were added to 2 mL lysis buffer, this was vortexed for 10 s, Sonicated with ice for 20 min, and shaken for 20 min. Lysis buffer consisted of 50 mL L^{-1} tris(hydroxymethyl)aminomethane (Tris)-HCl pH 8, 20 g L^{-1} sodium dodecyl sulfate (SDS), 5 mL L^{-1} 2M dithiothreitol (DTT), 800 µL L^{-1} ethylenediaminetetraacetic acid (EDTA), 0.17 g L^{-1} phenylmethane sulfonyl fluoride (PMSF). Samples were then placed in a water bath at 95 °C for 10 min. The tubes were centrifuged for 15 min at 15,000 rpm (Harrier centrifuge) and the supernatant was kept to be pooled later. The resulting pellet was retained, and the same method from the addition of lysis buffer onwards was repeated twice – pooling all 3 supernatants together and finally discarding the pellet.

6.2.3 SDS PAGE

The gels were prepared using the following method: 12% SDS PAGE gels were prepared by making solutions to the following recipes. Resolving gel: 3 mL acrylamide (40%); 4.5 mL dH_2O; 2.5 mL buffer B; 50 µL 10% ammonium persulfate (APS); 10 µL tetramethylethylenediamine (TEMED). Stacking gel: 0.5 mL acrylamide (40%); 2.5 mL dH_2O; 1 mL buffer C; 30 µL 10% APS; 10 µL TEMED. 300 mL of SDS buffer B was prepared by combining 225 mL 2M Tris HCl pH 8.8, 12 mL 10% SDS soln., and 63 mL dH_2O. 300 mL of SDS buffer C was comprised of 150mL 1 M Tris-HCl pH 6.8, 12 mL 10% SDS soln., and 138 mL dH_2O. The resolving gel was added to the glass plates and left to set for approx. 20 min before the stacking gel was added and the comb was inserted, and this was allowed to set for a further 20 min. The SDS running buffer was comprised of 3.039 g L^{-1} Tris-HCl pH 8, 14.4 g L^{-1} glycine, and 10 g L^{-1} SDS. Samples of the raw protein extract were not diluted and were centrifuged at 18,000 rpm for 15 min (Harrier centrifuge) before the loading dye was added. 20 µL of each sample was added to 5 µL SDS loading dye (loading dye consisted of:

4% SDS, 10% 2-mercaptoethanol, 20% glycerol, 0.004% bromophenol blue, 0.125 M Tris-HCl, pH adjusted to 6.8). These were boiled for 10 min and centrifuged at 12,500rpm for 2 min (Fisherbrand bench-top centrifuge) before loading onto the gel. 20 µL of each were loaded onto the gel along with 5 µL of the MW marker. The first gels (Figure 50) were run for 45 min at 180V, the second gels were run for 15 min at 180V.

The gels were stained in the Coomassie Brilliant Blue stain for 10 mins in square petri dishes while being slowly rocked, they were then placed in destain solution overnight. The Coomassie Brilliant Blue stain was comprised of Coomassie Brilliant Blue R250 1 g L^{-1}, 400 mL L^{-1} methanol, and 100 mL L^{-1} acetic acid. The destain solution was comprised of 400 mL L^{-1} methanol, and 100 mL L^{-1} acetic acid.

6.2.4 In – gel trypsin digestion

Each stained protein band from the short gels (Figure 51) was cut out with a clean scalpel. It was then cut into 1x1 mm pieces and transferred to an Eppendorf LoBind microcentrifuge tube. The gel pieces were washed 3x with 200 µL of 100 mM NH_4HCO_3 and 120 µL acetonitrile (ACN) for 15 min at room temperature. The gel pieces were then shrunk by adding 200 µL 100% ACN and vortexed. Once the gel pieces had become white (about 5-10 min) all ACN was removed by pipette. The gel pieces were rehydrated in 100 µL 20 mM DTT for 30 min at 56 °C. The excess liquid was removed by pipette and the gel pieces were shrunk in 200 µL 100% ACN as above.

The gel pieces were then rehydrated by adding 100 µL 55 mM iodoacetamide (IAA) and they were left for 20 min in the dark at room temperature. Excess liquid was removed, and the gel pieces were washed twice with 100 µL 100 mM NH_4HCO_3 and vortexed. The gel pieces were dehydrated with at least 200 µL 100% ACN and vortexed. The ACN was then removed. The samples were dried in a vacuum centrifuge (Christ RVC 2-18) for 5 min to evaporate all ACN.

The digestion was started by adding 30 µL of 20 µg mL^{-1} trypsin solution (Promega Trypsin Gold) and this was allowed to absorb for 20 min on ice. More trypsin was added if needed so that the gel pieces were completely saturated with trypsin solution. After 20 min, 50 µL of 50 mM NH_4HCO_3 was added to completely cover the gel pieces. This was incubated for up to 18 h at 37 °C (overnight).

The peptides were extracted by adding 50 µL 50% (v/v) ACN / 5% (v/v) formic acid, and the tubes were shaken for 30 min. The supernatant was added to another LoBind microcentrifuge tube and the extraction was repeated with 50 µL 83% (v/v) ACN / 0.2% (v/v) formic acid. The supernatants were then pooled, and they were lyophilised (Virtis SP Scientific, Sentry 2.0). Before LC-MS analysis the samples were resuspended in 40 µL of loading buffer (95% dH_2O/5% ACN with 1% tetrafluoroacetic acid (TFA)), and 5 µL injection volume was used.

6.2.5 LC-MS settings

The HPLC used was a Nanoflow Dionex 3000 RSLC system, with a C18 easy spray column (P/N ES803, c18 2 µm, 100A, 75 µm x 50 cm), at a temperature of 50 °C. The trap column was a reverse-phase C18 pepmap 100 trap column (5 µm particles with pore size of 100 Å), maintained at a temperature of 45 °C. The solvents used were buffer A: 95% dH_2O / 5% ACN with 0.1% formic acid, and buffer B: 95% ACN / 5% dH_2O with 0.1% TFA. The flow rate was 300 nL min^{-1}. The chromatographic profile started at 4% buffer B / 96% buffer A. After 3 min this was 8% buffer B / 92% buffer A. After 93 min this was changed to 30% buffer B / 70% buffer A. After 98 min this was 80% buffer B / 20% buffer A. This was held for 10 min before a return to the starting condition, which was continued for 20 min equilibration period.

The data acquisition was performed on a Q-exactive plus system, MS-dd-MS2 (TopN), in data dependent analysis (DDA) mode. The full scan MS^1 was performed at 70,000 MS resolution with an automatic gain control (AGC) of $1e^6$, an injection time of 100 ms, and with a scan range of 375 to 1400 m/z. The MS/MS was performed at 17,500 MS resolution with an

automatic gain control of $1e^5$ with a maximum injection time of 100ms. The isolation window was set to 1.3 m/z, with an underfilled ratio of 0.4%. The dynamic exclusion was set to 15 s, full-width half maximum (FWHM) was 5 s. The Top 10 most abundant ions were selected for MS/MS with a normalized collision energy (NCE) level of 30.

6.2.6 Statistical analysis and protein identification

The Progenesis package is software designed for the statistical analysis of proteomics data (Nonlinear_Dynamics, 2018). The workflow was as follows: the LC-MS files were uploaded, and an alignment of the peaks was carried out. The experimental design was set up to compare the growth conditions in pairs – with the iron-limited medium compared to the control and the excess iron medium compared to the control. Significantly altered peaks were determined as those with an ANOVA p value <0.05 and the number of peaks for investigation was further reduced by choosing only those with a fold change that was greater than 2. Files containing the chosen peaks were then created to be analysed by the Mascot program.

Mascot is a web-based software program that uses a database to search the m/z values of ions and identify the peptide fragments that were created by the trypsin digestion (Matrix_Science, 2018). The settings chosen were: fixed modifications – carbamidomethyl; variable modifications – oxidation (M); peptide charge – 2+, 3+, and 4+; peptide mass tolerance – 25 ppm; MS/MS tolerance – 25 ppm; instrument ESI-TRAP. The genome database for *F. venenatum* in the NCBI database (NCBI, 2018) was converted to a protein sequence and uploaded to Mascot in the FASTA format, for searching. The list of identified proteins was then downloaded from Mascot.

The list of identified proteins from mascot was then analysed by the Progenesis software. This was to remove errors and conflicts in the identification. For example, some peptide fragments were used to identify more than one protein and it had to be decided which protein the fragment was most likely to belong to, and errors were removed. First all peptide fragments with a match

score that was less than 40 and had a number of hits less than 2 were automatically removed. The remaining conflicting peptide fragments were then removed manually from proteins based on a combination of factors e.g. if the mass error was greater, if it had a lower match score, or if it had a lower number of hits. Finally, lists of identified proteins were then created corresponding to proteins up/down regulated in iron-limited conditions compared to the control, and proteins up/down regulated in excess iron conditions compared to the control.

The *F. venenatum* genome sequence from the NCBI database (NCBI, 2018) that was used to identify proteins was not fully annotated with protein names, only locus tags, gene ID, and protein ID numbers were included. The proteins have therefore been given putative identifications using the conserved domain search (CCD, 2018) which is also available from NCBI (NCBI, 2018). This web-based search tool is able to predict the function of a protein by identifying a conserved domain footprint in the sequence (Marchler-Bauer *et al.*, 2011). The conserved domains are used to indicate the similarity of one protein to another and can also indicate evolutionary relationships between proteins (Marchler-Bauer *et al.*, 2011). The database contains information that is based on domain models from 3D structures, and functional sites such as active sites and binding sites for cofactors are included (Marchler-Bauer *et al.*, 2011). The information is joined by evidence such as 3D structures that have been determined experimentally and published (Marchler-Bauer *et al.*, 2011).

6.3 Results and discussion

6.3.1 SDS Gels

(a) (b)

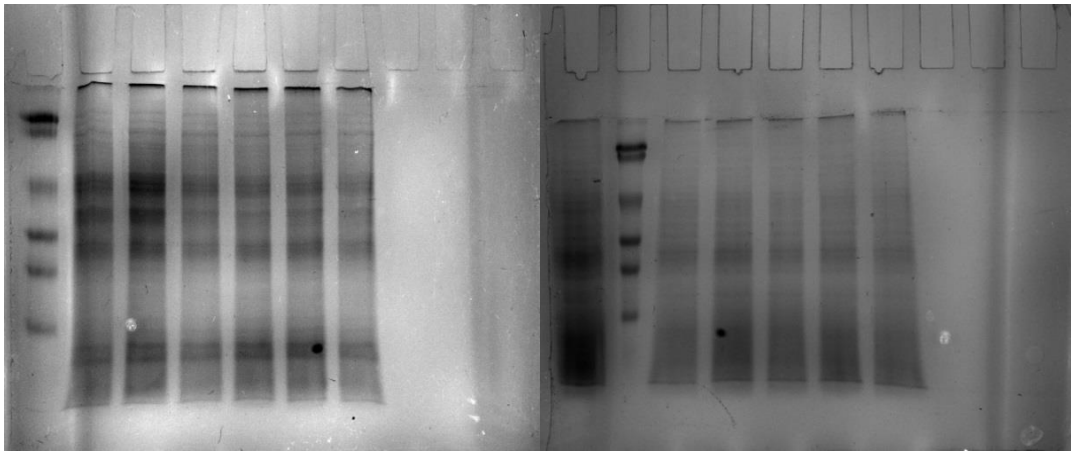

(c)

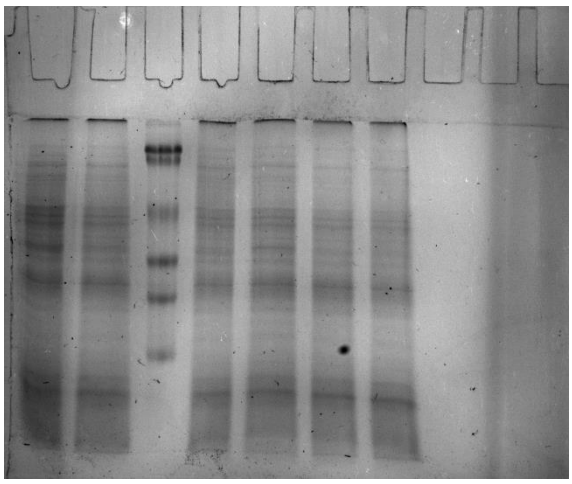

Figure 50: SDS-PAGE gels showing separation of proteins for samples from control cultures. Each separate gel was loaded with samples from 6 replicate cultures, 1a-1f (control), 2a-2f (iron-limited), and 3a-3f (excess iron). Samples were loaded in the following order. (a) Control cultures: marker (Biorad prestained SDS-PAGE standards, low range), 1a, 1b, 1c, 1d, 1e, 1f. (b) Iron-limited cultures: 2a, marker, 2b, 2c, 2d, 2e, 2f. (c) Excess iron cultures: 3a, 3b, marker, 3c, 3d, 3e, 3f. The gels were run for 45 min at 180V.

(a) (b)

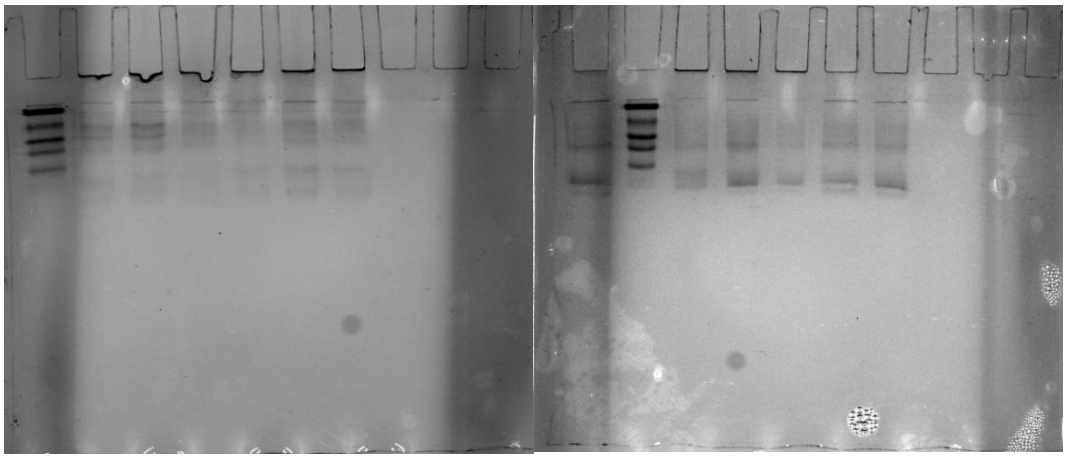

(c)

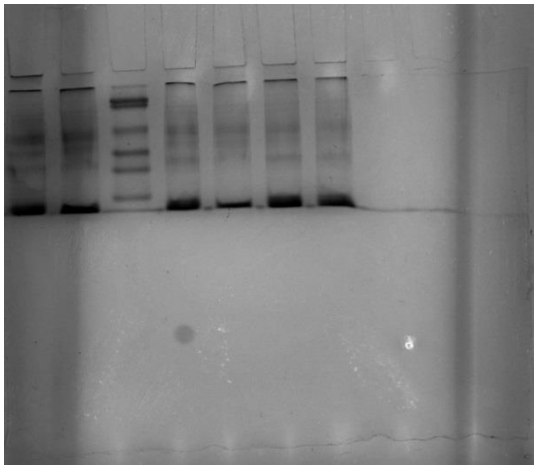

Figure 51: SDS-PAGE gels showing separation of proteins for samples from control cultures. Samples were loaded in the following order. (a) Control cultures: marker (Biorad prestained SDS-PAGE standards, low range), 1a, 1b, 1c, 1d, 1e, 1f. (b) Iron-limited cultures: 2a, marker, 2b, 2c, 2d, 2e, 2f. (c) Excess iron cultures: 3a, 3b, marker, 3c, 3d, 3e, 3f. The gels were run for 15 min at 180V.

6.3.2 Identified proteins

A total of 1226 proteins were observed with changed abundances in the iron limited condition, of which 58% were upregulated and 42% were downregulated. A total of 791 proteins were observed in the excess iron condition, of which 54% were upregulated and 46% were downregulated. The proteins in each list with the highest fold-change were searched in the conserved domain database and organised according to biochemical pathways. The results have shown that a number of diverse biochemical pathways have been affected in both the iron-limited and excess iron media. For example, pathways for amino acids such as tryptophan, leucine and aspartate were downregulated in the iron-limited medium, while pathways for siderophore and possible mycotoxin production were upregulated. Some proteins that form part of oxidative respiration were downregulated in iron-limited conditions but upregulated in the excess iron medium. The medium containing excess iron also affected some of the amino acids pathways with compounds such as ornithine and serine affected by downregulation, and proteins involved with fungal cell wall components and nucleotide metabolism were also downregulated. Upregulated proteins in the excess iron condition included those related to lipid metabolism and signal transduction.

These identifications are still tentative, however, and more analysis would be needed to confirm the identities of these proteins.

Table 5: Proteins up/downregulated in the **limited iron** medium identified using conserved domains.

Locus tag	Conserved domain (NCBI)	Pathway	Up/down regulated	Anova (p)	Fold-change
FVRRES_10100	PRK04346; tryptophan synthase subunit beta; Validated / Trp_syntA; Tryptophan synthase alpha chain	Amino acid metabolism	↓	1.76E-04	10.84
FVRRES_11338	PRK03739; 2-isopropylmalate synthase; Validated	Amino acid metabolism	↓	2.86E-04	9.71
FVRRES_02436	PRK00911; dihydroxyacid dehydratase	Amino acid metabolism	↓	1.18E-09	4.91
FVRRES_05924	AAT_I; Aspartate aminotransferase (AAT) superfamily (fold type I) of pyridoxal phosphate (PLP)-dependent enzymes.	Amino acid metabolism	↓	5.52E-07	4.85
FVRRES_06666	SdaA; L-serine deaminase	Amino acid metabolism	↓	2.65E-05	22.55
FVRRES_06390	LysP; Amino acid permease	Amino acid metabolism	↓	0.01	10.59
FVRRES_07173	Gdh2; NAD-specific glutamate dehydrogenase	Amino acid metabolism	↓	3.11E-03	6.2
FVRRES_13490	LysC; Aspartate kinase	Amino acid metabolism	↓	1.12E-03	5.99

Locus tag	Conserved domain (NCBI)	Pathway	Up/down regulated	Anova (p)	Fold-change
FVRRES_13252	UCR_hinge; Ubiquinol-cytochrome C reductase hinge protein	Respiration	↓	4.41E-03	7.7
FVRRES_07401	COX4; Cytochrome c oxidase subunit IV	Respiration	↓	2.70E-06	5.81
FVRRES_04847	ACH1; Acyl-CoA hydrolase	Respiration	↓	0.02	5.57
FVRRES_10333	AcnA; Aconitase A	Respiration	↓	2.49E-08	5.48
FVRRES_08940	Ferrochelatase	Iron cofactor metabolism	↓	0.05	6
FVRRES_02605	Lipoxygenase	Lipid metabolism	↓	7.12E-08	7.36
FVRRES_09486	Lipase_3; Lipase (class 3).	Lipid metabolism	↓	1.14E-06	7.08
FVRRES_13647	DadA; Glycine/D-amino acid oxidase (deaminating)	Amino acid metabolism	↑	3.90E-03	6.91
FVRRES_05178	Mt_ATP-synt_D; ATP synthase D chain, mitochondrial (ATP5H)	Respiration	↑	0.01	8.1
FVRRES_06588	GH18_chitinase	Fungal cell wall	↑	1.62E-06	8.4

Locus tag	Conserved domain (NCBI)	Pathway	Up/down regulated	Anova (p)	Fold-change
FVRRES_00306	GH16_fungal_CRH1_transglycosylase; glycosylphosphatidylinositol-glucanosyltransferase	Fungal cell wall	↑	9.86E-05	8.99
FVRRES_06504	HET; Heterokaryon incompatibility protein (HET)	Fungal compatibility	↑	2.89E-06	6.81
FVRRES_12631	Isoprenoid_Biosyn_C1; Isoprenoid Biosynthesis enzymes, Class 1	Mycotoxin production	↑	8.94E-10	20.83
FVRRES_09417	TRI12; Fungal trichothecene efflux pump (TRI12)	Mycotoxin transport	↑	2.73E-04	81.76
FVRRES_06752	A_NRPS_SidN3_like; The adenylation (A) domain of siderophore-synthesizing nonribosomal peptide synthetases (NRPS) / AMP-binding; AMP-binding enzyme	siderophore metabolism	↑	3.34E-07	18.1
FVRRES_08875	K_oxygenase; L-lysine 6-monooxygenase (NADPH-requiring)	Siderophore metabolism	↑	3.09E-08	14.71

Table 6: Proteins up/down regulated in the **excess iron** medium, identified using conserved domains.

Locus tag	Conserved domain (NCBI)	Pathway	Up/down regulated	Anova (p)	Fold change
FVRRES_08669	ornithine aminotransferase	Amino acid metabolism	↓	1.03E-06	3.71
FVRRES_06783	Peptidase_S10; Serine carboxypeptidase	Amino acid metabolism	↓	0.02	5.92
FVRRES_03722	Gln-synt_C; Glutamine synthetase, catalytic domain	Amino acid metabolism	↓	0.02	3.69
FVRRES_13122	CM_2; Chorismate mutase type II	Amino acid metabolism	↓	6.40E-04	3.26
FVRRES_02241	PTZ00184; calmodulin; Provisional	Calcium signalling	↓	3.45E-05	2.97
FVRRES_13252	UCR_hinge; Ubiquinol-cytochrome C reductase hinge protein	Respiration	↓	3.96E-04	3.98
FVRRES_04847	ACH1; Acyl-CoA hydrolase	Respiration	↓	4.80E-04	2.79
FVRRES_13496	FBPase; Fructose-1,6-bisphosphatase	Respiration	↓	0.02	2.88
FVRRES_01094	UDPGlcNAc_PPase; UDPGlcNAc pyrophosphorylase	Fungal cell wall	↓	1.19E-03	3.95

Locus tag	Conserved domain (NCBI)	Pathway	Up/down regulated	Anova (p)	Fold change
FVRRES_10322	GH18_chitinase	Fungal cell wall	↓	5.03E-04	3.92
FVRRES_00321	HET; Heterokaryon incompatibility protein (HET)	Fungal compatibility	↓	8.35E-03	3.54
FVRRES_00752	Sod_Cu; Copper/zinc superoxide dismutase (SODC)	Reactive oxygen species protection	↓	1.29E-04	3.54
FVRRES_08940	Ferrochelatase	Iron cofactor metabolism	↓	9.42E-05	4.59
FVRRES_04306	PurK; Phosphoribosylaminoimidazole carboxylase (AIR carboxylase)	Nucleotide metabolism - Purines	↓	1.35E-04	2.9
FVRRES_02940	PRK00885; phosphoribosylamine--glycine ligase / PRK05385; phosphoribosylaminoimidazole synthetase	Nucleotide metabolism - Purines	↓	0.02	2.77
FVRRES_13176	CarA; Carbamoylphosphate synthase small subunit	Nucleotide metabolism - Pyrimidines	↓	0.01	2.89
FVRRES_03220	PTZ00258; GTP-binding protein; Provisional	Signal transduction	↓	1.00E-06	2.88

Locus tag	Conserved domain (NCBI)	Pathway	Up/down regulated	Anova (p)	Fold change
FVRRES_10018	STKc_ERK1_2_like; Serine/Threonine Kinases	Signal transduction	↓	7.21E-03	3.82
FVRRES_01630	CysC; Adenylylsulfate kinase or related kinase	Sulfur metabolism	↓	5.68E-03	3.4
FVRRES_09263	Thr-synth_2; Threonine synthase	Amino acid metabolism	↑	0.04	6.12
FVRRES_00443	Trehalase	Carbohydrate metabolism	↑	6.83E-03	5.71
FVRRES_03742	UCR_14kD; Ubiquinol-cytochrome C reductase complex 14kD subunit	Respiration	↑	1.84E-03	9.25
FVRRES_11620	ATP-synt; ATP synthase	Respiration	↑	0.04	11.16
FVRRES_00444	OSCP; ATP synthase delta (OSCP) subunit	Respiration	↑	0.03	9.07
FVRRES_13835	SQR_TypeC_SdhC; Succinate:quinone oxidoreductase (SQR) Type C subfamily, Succinate dehydrogenase C (SdhC) subunit	Respiration	↑	1.48E-07	7.43
FVRRES_09232	PEMT; Phospholipid methyltransferase	Lipid metabolism	↑	4.31E-06	5.53

Locus tag	Conserved domain (NCBI)	Pathway	Up/down regulated	Anova (p)	Fold change
FVRRES_10003	PssA; Phosphatidylserine synthase	Lipid metabolism	↑	1.54E-06	4.67
FVRRES_05413	LPLAT; Lysophospholipid acyltransferases (LPLATs) of glycerophospholipid biosynthesis	Lipid metabolism	↑	0.05	7.08
FVRRES_01212	PurH; AICAR transformylase/IMP cyclohydrolase PurH	Nucleotide metabolism	↑	5.34E-03	9.92
FVRRES_09437	RagA_like; Rag GTPase, subfamily of Ras-related GTPases, includes Ras-related GTP-binding proteins A and B	Signal transduction	↑	0.04	6.22
FVRRES_01365	PTZ00132; GTP-binding nuclear protein Ran; Provisional	Signal transduction	↑	2.67E-03	5.56

6.3.3 Effect of iron cations on respiration

One of the major pathways that appears to have been downregulated in iron-limited conditions is respiration, with both the tricarboxylic acid (TCA) cycle and the respiratory electron transfer chain having major components that were downregulated. Three proteins with a domain identified as aconitase were downregulated in the iron-limited medium. Aconitase is responsible for the conversion of citrate to isocitrate via aconitate, and it contains an Fe/S cluster as a cofactor (Fazius *et al.*, 2012). Its reliance on iron is a possible reason why this has been downregulated in iron-limited conditions.

Enzymes relating to the electron transfer chain, which also contain iron, have also been identified in the list of downregulated proteins in iron-limited medium, including ubiquinol cytochrome c reductase hinge protein, and cytochrome c oxidase subunit IV. Ubiquinol cytochrome c reductase (cytochrome bc_1) is part of the mitochondrial electron transfer chain, it is responsible for transferring an electron from ubiquinol to cytochrome c, and contains an Fe/S cluster and a haem group (Hunte *et al.*, 2000). The cytochrome c reductase hinge protein is a subunit of cytochrome bc_1 (Hunte *et al.*, 2000). Cytochrome c oxidase is the final electron acceptor of the electron transport chain, it transfers electrons from cytochrome c to oxygen, and also contains a haem group (García-Villegas *et al.*, 2017). Another protein related to respiration has been identified as ATP synthase, which generates ATP (Lancaster, 2002), but it was upregulated in iron-limited conditions, and so this would need to be confirmed by further analysis.

The downregulation of the TCA cycle and electron transfer chain has been observed in iron-limited conditions in other organisms, for example in the study by Parente *et al.*, (2011) of *Paracoccidioides brasiliensis*, and the study by Shakoury-Elizeh *et al.*, (2010) of *Saccharomyces cerevisiae*. The possible implications of downregulating the TCA cycle and the electron transfer chain would be both a lowering of ATP supplies for energy, and a decrease in intermediates that are used in other pathways. For example oxaloacetate that is used in the production of aspartate (Jastrzębowska & Gabriel, 2015), or α-ketoglutarate that is used to

produce lysine (Xu *et al.*, 2006) or glutamate (Sieg & Trotter, 2014). It could therefore be expected that some biosynthetic pathways would be downregulated as a consequence of lower activity of respiration proteins.

In contrast to the results from the iron-limited medium, the excess iron condition led to the upregulation of enzymes involved in oxidative respiration. One of these was succinate quinone oxidoreductase, which is an Fe/S enzyme that belongs to both the TCA cycle, where it converts succinate to fumarate, and to the electron transfer chain (Lancaster, 2002). Ubiquinol cytochrome c reductase 14 kDa subunit, part of cytochrome bc_1, was identified with increased abundance in this condition. However, another subunit of cytochrome bc_1, the ubiquinol cytochrome c reductase hinge protein, was also identified in excess iron conditions as a downregulated protein and so this result would require further confirmation.

Along with these enzymes, ATP synthase which couples the electron transfer chain to ATP production via the proton gradient (Lancaster, 2002) has also been upregulated in excess iron conditions. Together, these results suggest that respiration is upregulated when the fungus has plentiful iron. Since these upregulated enzymes require iron cofactors, they may be upregulated due to the increased availability of iron.

6.3.4 Effect of iron cations on amino acid biosynthesis & metabolism

Results have suggested that a number of enzymes involved with amino acid biosynthesis have been downregulated when the fungus is deficient in iron.

The final enzyme in the tryptophan pathway, tryptophan synthase, was found to have a decreased abundance in this condition (Braus, 1991). Tryptophan is produced in a long pathway that requires the input of intermediates such as glutamine and phosphoribosyl pyrophosphate, and it begins with chorismate from the shikimic acid pathway (Braus, 1991). These intermediates could have been reduced if other pathways have been affected by the iron-limited condition.

The enzyme dihydroxyacid dehydratase, an Fe/S containing enzyme which participates in the biosynthesis of not only leucine but also valine and isoleucine has been downregulated in the iron-deprived medium (Liu *et al.*, 2014). In addition, another enzyme in the leucine biosynthesis pathway, α-isopropylmalate synthase, which produces α-isopropylmalate from α-ketoisovalerate and acetyl-CoA (Ulm *et al.*, 1972), has also been downregulated. Along with dihydroxyacid dehydratase, this pathway also features another enzyme that contains an Fe/S cluster: isopropylmalate isomerase, and so it is possible that this pathway is downregulated in iron-limited conditions in order to preserve iron for more essential processes (Philpott *et al.*, 2012).

The enzyme responsible for the production of aspartate from oxaloacetate, aspartate aminotransferase (Parente *et al.*, 2011), also appears to have been downregulated in the iron-limited medium. This has been suggested by Parente *et al.*, (2011) to be due to a decrease in the substrate for this enzyme, oxaloacetate being decreased in iron-limited conditions, due to downregulation of the iron-requiring enzymes of the TCA cycle. The aspartate pathway links to the pathway for threonine production (Farfán & Calderón, 2000). The first enzyme in the threonine pathway is aspartate kinase (Farfán & Calderón, 2000), and this was also downregulated in iron-limited conditions.

Glutamate dehydrogenase, which produces glutamate from ammonia and α-ketoglutarate (Sieg & Trotter, 2014), was downregulated in iron-limited conditions. It has been suggested previously that this enzyme could be upregulated in iron-limited conditions in order to replace the iron-requiring glutamate synthase enzyme so that glutamate levels are maintained (Philpott *et al.*, 2012). However, that does not appear to have happened in *F. venenatum*, so perhaps glutamate levels are maintained by another route such as the breakdown of other amino acids to glutamate.

Along with enzymes responsible for amino acid synthesis, amino acid transport has also been affected with a downregulation of an amino acid permease, which is used by cells for amino acid uptake for either protein synthesis or for use as a nitrogen source (Helliwell *et al.*, 2001).

An amino acid catabolism pathway also seems to have been affected with the iron-limited medium as serine deaminase, an enzyme responsible for the breakdown of serine to pyruvate was downregulated (Schorsch *et al.*, 2012).

Not all of the identified proteins relating to amino acids were downregulated in iron-limited conditions; some enzymes with a role in amino acid metabolism were upregulated in iron-limited conditions. These were glycine/D-amino acid oxidase, and lysine-6-monoxygenase. D-amino acid oxidase catalyses the oxidation of a variety of D-amino acids to their α-amino acids, which then hydrolyse to become an α-keto acid and ammonia (Gabler & Fischer, 1999). Lysine-6-monoxygenase is involved with siderophore production (Aravind *et al.*, 2010), which is discussed below.

Overall 8 enzymes related to amino acid biosynthesis and metabolism have been identified that are downregulated in iron-limited conditions. A possible reason for this is the presence of iron cofactors in enzymes in their pathways such as isopropylmalate isomerase in the leucine pathway, and in other cases it could be due to a decrease in the supply of the intermediates required for the pathway. These results are in agreement with the previous analysis of amino acids in iron-limited conditions (see chapter 3) which showed that most amino acids, including those discussed here: tryptophan, isoleucine, valine, aspartate, and threonine, had reduced abundance. Interestingly glutamate was found to be increased in iron-limited conditions (see chapter 3) even though glutamate dehydrogenase seems to have been downregulated, but glutamate can be made via different routes including by the breakdown of other amino acids such as arginine (Goodman & Weiss, 1986).

The results have suggested that amino acid biosynthesis has also been affected in the excess iron condition. Ornithine aminotransferase, glutamine synthetase, and chorismate mutase have all been decreased when the medium contained additional iron. Ornithine aminotransferase is part of the pathway for arginine catabolism, and converts ornithine to glutamate-γ-semialdehyde (Weiss & Anterasian, 1977). Glutamine synthetase converts glutamate to glutamine, with the addition of ammonia (Sieg & Trotter, 2014). Chorismate mutase is the

first enzyme in the pathway for the production of both phenylalanine and tyrosine, and converts chorismate into prephenate (Braus, 1991). These results indicate a downregulation of some amino acids pathways when the fungus was supplied with extra iron, although the results of the amino acids analysis (chapter 3) did not show a significant change for these amino acids in excess iron conditions.

In contrast, threonine synthase, the final enzyme for threonine biosynthesis, has been identified as being upregulated in excess iron conditions. It catalyses the production of threonine from its precursor, *o*-phospho-L-homoserine (Ujiie *et al.*, 2017). γ-glutamyl phosphate reductase is the second enzyme in the pathway which produces proline from glutamate (Liang *et al.*, 2014), and this was also upregulated in the excess iron medium.

As well as amino acid metabolism, protein catabolism has also been affected as serine carboxypeptidase was identified as a downregulated protein with excess iron. Serine carboxypeptidase is a proteolytic enzyme which breaks down peptides from the C-terminal peptide bond (Breddam, 1986). They are used to take amino acids from extracellular proteins, can be excreted by fungi into their medium, and they can also be used in the turnover of intracellular proteins (Breddam, 1986).

6.3.5 Iron cofactors in iron-limited conditions

Ferrochelatase is the final enzyme of the biosynthetic pathway for the production of haem, it chelates iron into protoporphyrin IX to produce protohaem, and contains an Fe/S cluster (Ferreira, 1999). Ferrochelatase has been identified in light-sensitive fungi and is thought to play a role in photobiology, (Idnurm & Heitman, 2010). In an investigation by Idnurm & Heitman (2010) it was found to be localised in the mitochondrial membrane and in some fungi e.g. the ascomycete *Neurospora crassa*, and the basidiomycete *Cryptococcus neoformans*, it is linked with responses to light. Porphyrins are reactive molecules that can form radicals, and so it is important that they are regulated (Franken *et al.*, 2013). Idnurm & Heitman, (2010)

explain that porphyrin levels are high in dark conditions, but in response to light ferrochelatase is induced, leading to the production of haem and reduction of porphyrin, as a defence against light-related damage (Idnurm & Heitman, 2010). This enzyme has been downregulated in iron-limited conditions, which could be linked to the decrease in the production of enzymes such as cytochrome c oxidase that require haem to function. A possible consequence of this could be an inability to regulate porphyrin in response to light, which would need to be confirmed by further work. However, a protein with this domain was also identified as being downregulated in the excess iron condition and so this result would need further confirmation.

6.3.6 Siderophore production in iron-limited conditions

Lysine-6-monoxygenase is an enzyme that produces N6-hydroxylysine from lysine by an NADPH-dependent hydroxylation (Aravind *et al.*, 2010), and this was identified as being upregulated in iron-limited conditions. The N6-hydroxylysine is an intermediate in the production of a siderophore, aerobactin (Aravind *et al.*, 2010). Another protein that is upregulated in iron-limited conditions was also identified as being linked to siderophore production, with a domain named as the adenylation domain of siderophore-synthesizing nonribosomal peptide synthetase. Siderophores are iron-chelating molecules produced by fungi so that they can make use of insoluble ferric iron from their environment (Wiebe, 2002b), and so it is likely that their production would be increased in iron-limited conditions. Siderophore production has been previously shown to be increased in *F. venenatum* in iron-limited conditions in a study by Wiebe (2002b).

6.3.7 Carbohydrate metabolism in excess iron conditions

The gluconeogenesis pathway may have been affected in excess iron conditions. The enzyme fructose-1,6-bisphosphatase converts fructose-1,6-bisphosphate to fructose-6-phosphate (Jardon *et al.*, 2008), and this has been found to be downregulated with excess iron. This could

be explained by the result described above that respiration pathways were upregulated in this condition, and so it would be important to supply pyruvate to the TCA cycle rather than using it to produce glucose in gluconeogenesis (Berg *et al.*, 2006).

In the excess iron condition, an upregulated protein was identified as trehalase, the enzyme that breaks down the disaccharide trehalose (Tran *et al.*, 2016). Trehalose is used as an osmoprotectant by *F. venenatum* and has been previously found to be increased in this fungus when it was grown in mycotoxin inducing conditions (Lowe *et al.*, 2010).

6.3.8 Nucleotide biosynthesis in excess iron conditions

The changes to nucleotide biosynthesis appear complex, with a number of enzymes for purine biosynthesis downregulated in excess iron conditions and one enzyme upregulated.

For example, a downregulated protein in the excess iron conditions was identified with two conserved domains that both take part in the purine biosynthetic pathway. One of these domains is phosphoribosylamine glycine ligase (also known as GAR synthase), and the other is phosphoribosylaminoimidazole synthetase. GAR synthase is the second enzyme of the purine biosynthesis pathway, and converts phosphoribosylamine to glycinamide ribonucleotide (GAR) (Zhang *et al.*, 2008). The other identified domain for this protein was phosphoribosylaminoimidazole synthetase (also known as AIR synthase) which converts formylglycinamidine ribonucleotide (FGAM) to 5-aminoimidazole ribonucleotide (AIR) (Zhang *et al.*, 2008). The next enzyme in the same pathway is phosphoribosylaminoimidazole carboxylase (AIR carboxylase), and this has also been downregulated in excess iron conditions. This enzyme converts AIR to carboxyaminoimidazole ribonucleotide (CAIR) (Zhang *et al.*, 2008).

In contrast to this, in excess iron conditions an enzyme for purine nucleotide production was upregulated. The enzyme AICAR transformylase / IMP cyclohydrolase is a bifunctional enzyme which catalyses two reactions of the purine biosynthesis pathway which together

convert 5-aminoimidazole-4-carboxyamide ribonucleotide (AICAR) to inosine monophosphate (IMP) (Zhang *et al.*, 2008).

As well as the pathway for purine biosynthesis, the pyrimidine pathway also appears to have been affected by excess iron conditions. The enzyme carbamoylphosphate synthase II was found to be downregulated in excess iron conditions. This enzyme catalyses the first step in the pyrimidine biosynthesis pathway, in which the hydrogen carbonate ion is converted to carbamoyl phosphate (Nara *et al.*, 2000).

Taken together these results suggest that nucleotide biosynthesis has been impacted by excess iron conditions. This could have an impact on the flavour of the product since the nucleotide monophosphates guanosine monophosphate (GMP); inosine monophosphate (IMP); and xanthosine monophosphate (XMP) along with amino acids such as aspartic acid and glutamic acid are responsible for the savoury umami flavour (Zhang *et al.*, 2013). These nucleotides could have amounts in the excess iron condition that differ from the control condition, thus altering the flavour if this was used in Quorn production.

6.3.9 Effect of iron cations on lipid metabolism

Some of the enzymes that have been identified appear to have a role in lipid metabolism. Long chain Acyl-CoA molecules have a wide variety of functions in the cell including: lipid biosynthesis; fatty acid catabolism; donating fatty acids to signalling molecules; and regulating processes such as vesicle transport, Ca^{2+} release, gene expression and protein kinases (Takagi *et al.*, 2003). Results have identified an acyl-CoA hydrolase enzyme that has been downregulated in iron-limited conditions. Acyl-CoA hydrolase breaks down acyl-CoA to free fatty acids and CoA-SH (Takagi *et al.*, 2003). However, the relationship of this enzyme with iron availability will require confirmation, as another protein with the acyl-CoA hydrolase domain was also identified as downregulated in the excess iron condition. Enzymes which are

linked to fatty acid metabolism were also shown to be affected in iron-limited *P. brasiliensis* in the study by (Parente *et al.*, 2011).

Another enzyme involved in lipid metabolism, lipoxygenase, has been downregulated in iron-limited conditions. This enzyme oxidises polyunsaturated fatty acids, and contains iron (Filippovich *et al.*, 2001). In addition, lipase class 3 was also downregulated, this enzyme belongs to the lipase class of enzymes which break down triglycerides to glycerol and fatty acids (Singh & Mukhopadhyay, 2012). A class 3 lipase was identified in *Neurospora crassa* which is involved in the repair of the plasma membrane (Lopez-Moya *et al.*, 2016). These findings indicate that the iron-limited condition has influenced lipid metabolism, and particularly the breakdown of lipid molecules. One of the enzymes identified, lipoxygenase, would be expected to be directly affected by a lack of iron due to its iron cofactor (Filippovich *et al.*, 2001).

Proteins that have a role in lipid metabolism were identified with increased abundance in excess iron conditions. Lysophospholipid acyltransferase is part of the biosynthesis of glycerophospholipids, in which glycerol-3-phosphate is converted to lysophosphatidic acid, which is converted by a lysophospholipid acyltransferase to phosphatidic acid (Shindou & Shimizu, 2009). Glycerophospholipids are important in both the structure and function of the cell membrane, and also form precursors for other lipid molecules (Shindou & Shimizu, 2009). Another enzyme involved with lipid metabolism is phospholipid methyltransferase, which is involved in the biosynthesis of phosphatidylcholine, by methylation reactions (Kanipes & Henry, 1997). A precursor of phosphatidylcholine is phosphatidylserine, which is produced by phosphatidylserine synthase enzyme (Bae-Lee & Carman, 1984). This enzyme has also been upregulated in excess iron conditions. Upregulation of lipid metabolism may indicate a change in growth or morphology since phospholipids are an important component of cell membranes (Bae-Lee & Carman, 1984), or it could impact other pathways that use lipid molecules as precursors (Shindou & Shimizu, 2009).

6.3.10 Mycotoxin production in iron-limited conditions

One of the upregulated proteins in the iron-limited condition was a protein identified as an isoprenoid biosynthesis enzyme class 1. This is described in the NCBI database as being part of a family of enzymes that can synthesise a variety of products including farnesyl pyrophosphate or other products with an isoprenoid precursor (NCBI, 2018). This could be linked to the production of trichothecene mycotoxins, which are known to be produced in *F. venenatum* in certain growth conditions (O'Donnell *et al.*, 1998). Trichothecene biosynthesis begins with farnesyl pyrophosphate, which is converted to trichodiene by trichodiene synthase (Cardoza *et al.*, 2011). Another protein linked to the trichothecene mycotoxins was also identified. The fungal trichothecene efflux pump was upregulated in iron-limited conditions, and this is responsible for the transport of trichothecenes across membranes (Cardoza *et al.*, 2011). Together these two proteins indicate that trichothecene production could have been increased with conditions of iron-limited, but this would need to be confirmed by analysis of the cultures for the presence of any of these mycotoxins.

6.3.11 Effect of iron cations on fungal cell wall components

A protein labelled as chitinase was found to be increased in iron-limited conditions. This enzyme is responsible for breaking down chitin, which is a major component of the fungal cell wall (Bowman & Free, 2006). Along with this, another enzyme associated with the cell wall was also increased, glycosylphosphatidylinositol glucanosyltransferase, which is responsible for the elongation of 1,3 β-glucan chains (Mouyna *et al.*, 2000).

Two of the identified proteins in excess iron conditions that were downregulated are also linked with the fungal cell wall. The enzyme chitinase, as discussed above, is for chitin break down (Bowman & Free, 2006). UDP-N-acetylglucosamine pyrophosphorylase has also been identified. This enzyme is part of the pathway for the biosynthesis of UDP-N-

acetylglucosamine, the substrate for chitin synthase which produces chitin for the fungal cell wall (Mio *et al.*, 1998).

These results suggest that formation of the cell wall may have been affected in both the iron-limited and excess iron conditions and this could have implications for growth and morphology.

6.3.12 Signal transduction in excess iron conditions

Mechanisms for signal transduction could have been affected in excess iron conditions as both a serine/threonine kinase and a GTP-binding protein have been identified as being downregulated. Serine/threonine kinases phosphorylate the serine and threonine residues of target proteins in order to regulate a variety of cellular functions (Park *et al.*, 2011). GTP-binding proteins, or GTPases act as molecular switches as part of signalling pathways; when they are bound to GTP they are switched on, and when they are bound to GDP they are switched off (Harris, 2011).

In contrast, a protein which has been identified as a GTPase, and another described as a GTP-binding nuclear protein have been identified with increased abundance in the excess iron condition. In fungi such as *Aspergillus niger* and *Saccharomyces cerevisiae*, GTPases are involved in many functions including morphogenesis, organisation of the cytoskeleton and membrane-trafficking (Harris, 2011).

Calcium signalling could also have been affected as the calcium-binding protein calmodulin has also been indicated in the results as a protein with decreased abundance in excess iron conditions. Calmodulin binds Ca^{2+} and interacts with a large number of proteins, taking part in many activities in the cell (Hoeflich & Ikura, 2002).

These signalling molecules may be involved in many pathways in the cell (Harris, 2011), and since these signalling molecules potentially have such wide-ranging effects, a change in

abundance in these signalling molecules could indicate that excess iron is affecting many areas of the cell's biochemistry.

6.3.13 Protection from reactive oxygen species in excess iron conditions

The enzyme Cu, Zn superoxide dismutase has been decreased in the excess iron condition. This enzyme protects the fungus from harmful reactive oxygen species (ROS) by converting superoxide radicals to hydrogen peroxide and oxygen (Thirach *et al.*, 2007). Cu Zn superoxide dismutase is localised to the cytoplasm and it is suggested that it is used to protect the fungus from external ROS (Thirach *et al.*, 2007).

6.3.14 Sulfur metabolism in excess iron conditions

One of the enzymes in sulfur metabolism, adenylyl sulfate kinase has been decreased in the excess iron condition. Sulfate is first combined with ATP to create adenylyl sulfate by ATP sulfurylase, and the adenylyl sulfate is converted to phosphoadenylyl sulfate by adenylyl sulfate kinase (Thomas & Surdin-Kerjan, 1997). This suggests that sulfate metabolism could have been affected, and this could have an impact on the production of the sulfur amino acids cysteine and methionine.

6.3.15 Heterokaryon compatibility in low and excess iron conditions

The heterokaryon compatibility protein was identified as one of the upregulated proteins in the iron-limited medium. This protein is responsible for the recognition of 'self' when fungal hyphae meet, since their cells can fuse and mix cytoplasm, forming heterokaryons (cells with nuclei of different types) (Saupe, 2000). In contrast, this protein was downregulated in excess iron conditions. These results suggest that this process is affected by iron availability.

6.4 Conclusions

This is the first study of untargeted proteomics of *F. venenatum* in conditions of altered iron availability and it has revealed that the growth of *F. venenatum* in conditions of limited and excess iron has produced an effect on some major pathways of the biochemistry of the fungus.

Respiration appears to have been downregulated in the iron-limited condition but upregulated in the excess iron condition. This could be due to enzymes in the TCA cycle and the electron transfer chain requiring Fe/S clusters. A protein involved with iron cofactors, ferrochelatase was downregulated in both the iron-limited and excess iron conditions. Amino acid metabolism was also affected in both conditions, when compared to the control. Pathways for the biosynthesis of some amino acids were downregulated in both the iron-limited and excess iron conditions. Sulfur metabolism was also affected in the excess iron condition, which may affect sulfur-containing amino acids.

In addition, nucleotide biosynthesis seems also to have been affected, with proteins downregulated in both purine and pyrimidine pathways when the fungus was subjected to the excess iron medium. Lipid metabolism was suggested to be affected in both the excess iron condition, with upregulated proteins involved with phospholipid pathways, and the iron-limited conditions with lipoxygenase and lipase enzymes downregulated.

In iron-limited conditions, results have indicated that mycotoxin production may have been upregulated, with isoprene biosynthesis enzymes having increased abundance, along with a trichothecene transport protein. Siderophore production may also have been upregulated in iron-limited conditions.

Alongside these major changes to the biochemistry, it was also found that synthesis of compounds relating to the fungal cell wall e.g. chitin, may have been affected, with a downregulation in excess iron conditions, and upregulation in iron-limited conditions. A protein involved with heterokaryon compatibility was downregulated in excess iron conditions and upregulated in iron-limited conditions.

Signal transduction pathways have also been affected in excess iron conditions, with calmodulin showing downregulation, and different GTP binding proteins showing both upregulation and downregulation.

6.5 Further work

The protein identifications are based on a search of their conserved domains, which has given an indication of their functions. Further analysis will therefore be required to confirm their identity and to validate the results. Experiments should be repeated so that extracts can be concentrated to give a better chance for MS/MS analysis to be successful. Targeted analysis of proteins of interest could also be carried out with prior purification of proteins by column chromatography for more accurate confirmation of their identity.

However, the results have indicated many areas of interest that could lead to further study. For example, the amount of iron in the medium could be used to affect the production of amino acids and nucleotides as a way of affecting the flavour of the Quorn product, since the results have shown an effect on these pathways.

Some of the proteins identified in the iron-limited condition were related to mycotoxin production, which suggests that this process could be upregulated if the fungus was deprived of iron. It would therefore be necessary to analyse the cells and supernatant of these cultures for the presence of mycotoxins so that this result can be confirmed. If this was confirmed, then further work could be undertaken to find out exactly how iron relates to mycotoxin production and how this could be used to control this process.

7. Investigation of *F. venenatum* growth in recycled growth medium

7.1 Introduction

The fermentation of microorganisms in industry is a costly process that requires huge amounts of water input, and generates a significant volume of used effluent that must be treated and disposed of (Hsiao *et al.*, 1994). Wastewater disposal requires a dedicated treatment facility, which comes at a considerable investment (Hsiao *et al.*, 1994). The cost to the business can also rise over time, as regulations change and restrictions on wastewater increase (Hsiao *et al.*, 1994). The ability to recycle some of the wastewater produced by fermentation could therefore be of significant economic benefit to industry (Hsiao & Glatz, 1996).

The current wastewater treatment system at Quorn™ foods uses a deep-shaft aerobic airlift fermenter that is buried underground and is approximately 80 m deep. The 20-30 m^3 of wastewater that is generated per fermenter per hour is treated by the microbial population in the wastewater treatment fermenter. After solids are removed and disposed of, it is then clarified leaving clean water that meets regulatory requirements to be disposed directly in the River Tees (Figure 52). This process costs the company a figure in the low millions per year, which could be reduced if it were possible to recycle the fermenter waste.

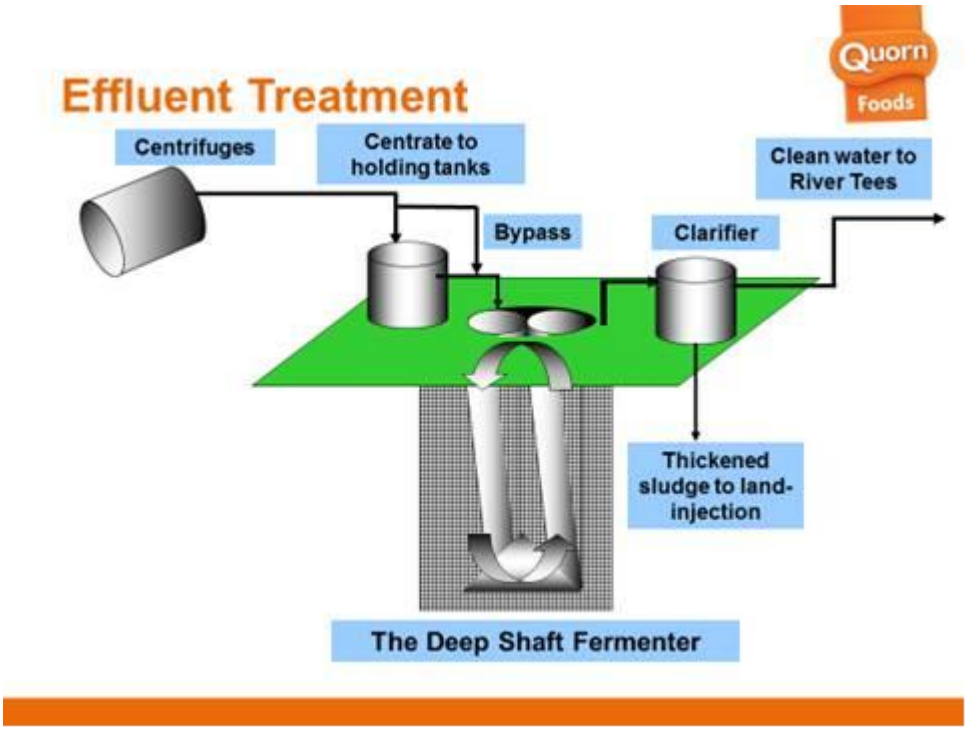

Figure 52: Current treatment process for the wastewater produced by F. venenatum fermentation for Quorn production. (Diagram reproduced with kind permission from Quorn foods).

As well as reducing the cost of wastewater treatment and disposal, the recycling of fermenter effluent could have other benefits. The effluent will still contain unused nutrients that the organism can take advantage of in the second fermentation, thus allowing savings to be made in the inputs of essential nutrients such as the nitrogen and carbon sources (Wang *et al.*, 2012). Recycling the fermenter effluent could therefore have a dual benefit of reducing waste and saving money from the treatment process, and also decreasing expenditure on the main nutrient inputs to the fermenter. This could therefore have a very positive impact on the economic viability of production.

The reuse of growth medium for the fermentation of *F. venenatum* has not been researched before. However, previous studies into the use of recycled medium for the growth of other microorganisms have investigated how to achieve growth and productivity while reducing wastewater and reducing the waste of growth medium components.

For example, a study by Babu and Panda (1991) used recycled growth medium for growth of penicillin amidase producing *E. coli*. The used broth was analysed to determine the amounts of nutrients such as nitrogen, sulfur, phosphorous, calcium, magnesium, and iron, and these were then replenished up to the initial concentrations in the fresh medium (Babu & Panda, 1991). The use of recycled medium was repeated for 8 consecutive batch cultures, at a number of ratios of fresh medium to recycled medium (Babu & Panda, 1991). It was and found that the growth rate of the bacterium increased with increased ratios of recycled media for 3 consecutive fermentations. At higher recycle ratios, the specific growth rate reached a maximum at a certain batch number, for example at a ratio of 0.8 the optimum batch number was 5. In addition, it was hypothesised that the recycled broth could contain a factor that was responsible for the observed increases in growth (Hsiao & Glatz, 1996). Further investigation showed that an isolate that tested positive for protein was present, and that adding this residue to the fermentation at low concentrations increased penicillin amidase production and reduced the lag time for growth (Hsiao & Glatz, 1996). The authors conclude that the recycling process enabled them to reuse between 40-60% of the broth, and that extracellular proteins present in the used medium could influence penicillin amidase production, although other factors may be present (Babu & Panda, 1991).

Hsiao & Glatz (1996) investigated recycled medium in the production of L-lysine in *Corynebacterium glutamicum*. After the L-lysine was recovered by cation exchange, the used broth was analysed for its content of major ions, sugar, amino acids, and ammonium (Hsiao & Glatz, 1996). Glucose, citric acid, and minerals were then added to replenish the correct amounts (Hsiao & Glatz, 1996). A medium was then produced that was composed of 75% used culture broth, and this process was repeated for 3 consecutive fermentations (Hsiao &

Glatz, 1996). They were able to show that in all cases results closely matched the control, which showed that the recycled medium had not caused any inhibition of L-lysine production (Hsiao & Glatz, 1996). It was also shown that the production of organic acid metabolites (pyruvate, acetate and lactate) did increase with each reuse of the broth but that these did not inhibit the growth of the bacteria, showing that the level of build-up of metabolites in this process did not pose a problem (Hsiao & Glatz, 1996).

Another similar investigation looked at lactic acid production by *Lactobacillus delbrueckii* (Ye *et al.*, 1996). The lactic acid becomes inhibitory in this process and so it was removed before the spent broth had essential nutrients replaced and was used for 3 repeat fermentations at a ratio of 75% spent/fresh broth (Ye *et al.*, 1996). The results showed that the use of the recycled broth did not cause any significant decrease in performance, and a high biomass and product yield were achieved with an efficient use of the medium (Ye *et al.*, 1996).

Microbial lipid fermentation in *Trichosporon cutaneum* CX1 with wastewater recycling was investigated by Wang *et al.* (2012). Six repeated batch fermentations of the yeast were carried out using waste broth, after the cells had been separated by either centrifugation or flocculation (Wang *et al.*, 2012). Results showed that recycling of the medium made no difference to the lipid production for the first 5 fermentations and lipid production remained almost constant, but lipid production was decreased in the 6^{th} successive reuse of the broth (Wang *et al.*, 2012). The dry cell mass decreased with each successive broth recycle fermentation, whereas in the control only a negligible decrease was seen; the reason for this is suggested to be a decreased cell viability with successive batches (Wang *et al.*, 2012). As an explanation of this, it is suggested that there was an accumulation of metabolites in the recycled broth from earlier fermentations, which inhibited the growth and metabolism of the bacteria (Wang *et al.*, 2012). The use of this method reduced at least 70% of the wastewater that would otherwise have required disposal (Wang *et al.*, 2012).

Together these studies have shown the potential for using recycled broth in the growth of microorganisms, which indicates that it is likely that recycled medium can be used successfully in *F. venenatum* production.

As previous studies have discussed, there may be substances in the used culture medium that are detrimental to growth or product formation (Hsiao *et al.*, 1994). These could be problematic, as they will build up further during the second fermentation (Hsiao *et al.*, 1994). Therefore, in order to reduce any build-up of harmful metabolites, the used medium will first be treated with activated carbon. Activated carbon has been investigated previously for the removal of organic substances such as amino acids from wastewater, and it is successful in removing small nitrogenous compounds from drinking water (Cermakova *et al.*, 2017). The capacity of the activated carbon to adsorb compounds depends on a number of factors that include the pore structure of the carbon (adsorbant) and the properties of the compound (adsorbate) such as polarity, functional groups and molecular weight (Xiao *et al.*, 2014). A study by Xiao *et al.*, (2014) showed that activated carbon was able to remove amino acids from peanut meal hydrolysate, but the efficacy of their removal depended on the properties of each amino acid (Xiao *et al.*, 2014). For example, the removal of acidic and basic amino acids depended on pH but the aromatic amino acids were less affected by pH (Xiao *et al.*, 2014).

The first aim of this experiment was to develop a method for the treatment of used medium with activated carbon so that the build-up of any compounds that could be harmful to growth can be minimised. The success of this method was judged by analysing the amino acids and nucleotide levels in the treated broth. The second aim was then to test the feasibility of using this treated recycled culture medium for the growth of *F. venenatum*. The investigation included measuring the biomass to determine growth and investigating any effects on the morphology of the organism.

7.2 Methods

7.2.1 Initial cultures to produce used culture medium

In order to produce a sufficient quantity of used culture supernatant 2 1 L RHM medium cultures were grown in baffled conical flasks that were incubated for 3 days at 28 °C, with shaking at 150 rpm. The RHM medium consisted of potassium dihydrogen phosphate (20 g L^{-1}), ammonium chloride (4.4 g L^{-1}), potassium sulfate (0.3 g L^{-1}), magnesium sulfate heptahydrate (0.25 g L^{-1}), 0.3 g L^{-1} biotin soln. (1 mL L^{-1}), trace metal soln. (5 mL L^{-1}), and dH_2O. The trace metal soln. consisted of iron sulfate heptahydrate (2.8 g L^{-1}), zinc chloride (1 g L^{-1}), manganese chloride tetrahydrate (1 g L^{-1}), copper chloride (0.2 g L^{-1}), cobalt chloride (0.2 g L^{-1}), sodium molybdate (0.2 g L^{-1}), calcium chloride dihydrate (2 g L^{-1}), citric acid (1.5 g L^{-1}), and dH_2O. After autoclaving, 20 mL 50% glucose solution was added to each. The cultures were each inoculated with 10 mL of starter culture (50 mL Oxoid nutrient broth in a 250 mL baffled conical flask, inoculated with fungus from a solid oatmeal agar culture and incubated at 28 °C with shaking at 150 rpm for 3 days).

7.2.2 Purification of spent media using activated charcoal

The cultures were centrifuged at 3,500 rpm for 10 min, (Beckman Allegra 6R centrifuge) and the supernatant was filtered (Whatman paper filters) to remove the hyphae. The filtered supernatants were then combined. 1 L of this was then treated by adding 50 g activated carbon and mixing for 10 min at 20 °C in a shaking incubator. This was then filtered to remove the carbon (Whatman paper filters), and the carbon treated used medium was then tested for reducing sugar and ammonium content.

7.2.3 Analysis of carbon treated used medium

After the used medium was treated with activated carbon, it was tested for reducing sugar content and ammonium content so that these could be replenished by the appropriate amounts.

In order to determine the efficacy of the treatment in removing biologically important molecules, the amino acid and nucleotide content were also analysed in the supernatant before and after the carbon treatment.

7.2.3.1 Determination of reducing sugars

The amount of reducing sugar was measured using DNS (Dinitrosalicylic acid) reagent. The DNS reagent was prepared by first dissolving 600 g of potassium sodium tartrate in 1 L dH_2O, and dissolving 20 g 3,5-Dinitrosalicylic acid in 400 mL dH_2O. These 2 solutions were combined and dH_2O was added to increase the volume to 2L. Six identical samples were taken from the carbon treated used medium and diluted to 1/20 with dH_2O. One millilitre of each diluted sample was then added to a test tube with 1 mL of DNS and 2 mL of dH_2O. The tubes were then placed in boiling water for 10 min. Sixteen millilitres of dH_2O was then added to each tube, and the absorbance of each solution was measured at 540 nm. Calibration standards were prepared using a glucose solution and were subjected to the same method.

7.2.3.2 Determination of ammonia

The ammonium content of the carbon treated used medium was measured using an ammonia assay kit (Sigma). This is a fluorometric method based on the reaction of *o*-phthalaldehyde with ammonium ions. Six identical samples of the carbon treated used medium were diluted to 1/100 using dH_2O and 10 µL of each were added to 90 µL working reagent (ammonia assay buffer (90µL), reagent A (4 µL), reagent B (4 µL) in a 96 well plate. The fluorescence was measured using a plate reader, with an excitation wavelength of 360 nm and emission wavelength of 500 nm. Calibration standards were prepared using a solution of ammonium chloride and were measured in the same way.

7.2.3.3 Determination of nucleotides

The nucleotide content was determined by HPLC analysis. Samples of carbon treated and untreated culture supernatant were concentrated prior to analysis by freeze drying 2 mL and adding 100 µL dH_2O to each. The reconstituted samples were then filtered using a 13 mm 0.22 µm nylon filter (chromatography direct). The analysis was carried out on a Dionex Ultimate 3000 UHPLC (Dionex, Sunnyvale, CA). The HPLC system used an AmG C18 column (3x 150mm, 3 µm particle size) with AmG guard column. The column temperature was maintained at 17 °C, and the flow rate was a constant 0.5 mL min^{-1}, with an injection volume of 3 µL. Buffer A was 30 mM phosphate buffer (3.733 g L^{-1} potassium phosphate monobasic, 0.444 g L^{-1} potassium phosphate dibasic, 15 mL L^{-1} 1 M triethylammonium acetate, 1 mL L^{-1} 99.9% LC-MS grade formic acid). The pH of buffer A was adjusted to 5.3 using 50% NaOH solution. Buffer B was 100% HPLC grade methanol. The buffers were used in the UHPLC with the following gradient system: 5 min equilibration period with 0% B, 0-16 min 0% B, 16-18 min 30% B, 18-22 min 75% B, 25-28 min 0% B.

7.2.3.4 Determination of amino acids

The amino acid content was determined by GC-MS. Six 2 mL aliquots of the treated and untreated supernatant were lyophilised (Virtis SP Scientific, Sentry 2.0) and weighed to determine the dry mass. Five hundred microliters of dH_2O were added to each sample. The presence of amino acids in the samples then was determined by gas chromatography-mass spectrometry (GC-MS) using the materials and method supplied with the Phenomenex EZ:Faast™ amino acids kit (Phenomenex). A Zebron ZB-AAA GC column (10 mm x 250 um x 0.25 mm) was used with a GC sampler 80 (Agilent Technologies) injector. A standard split injection mode and a 2 µL injection volume was used with the injector temperature set at 250 °C and the split ratio at 15:1. The oven programme had an initial temperature of 110 °C for 1 min followed by a ramp of 30 °C min^{-1} up to 320 °C, which was held for 2 min. The carrier gas was helium with a 1.5 mL min^{-1} constant flow. The solvent delay was 1 min. The

total ion count (TIC) scanning mode was used with an m/z range of 45-460, and a gain factor of 2. Results were calculated from 6 repeats of each condition and quantitation was performed using the formula below:

$$Amount\ AA\ (nmol/g) = \frac{Area\ AA/_{Area\ norvaline}}{Rf\ x\ mass\ (g)}\ x\ amount\ norvaline\ (nmol)$$

7.2.4 Preparation of recycled medium cultures

Six 50 mL cultures were prepared for each of the following conditions: control conditions; 50% recycled medium; and 100% recycled medium. The control cultures were prepared using RHM medium, with the same composition of the initial cultures above, and these cultures were sterilised by autoclaving.

The carbon treated recycled medium was nutrient replenished by adding the same constituents as the RHM medium, in the same amounts. The amount of ammonium chloride added was reduced to 1.77 g L^{-1} based on the calculated residual ammonium present, so that the final ammonium concentration was the same as that of fresh RHM medium. The 50% recycled medium was prepared by mixing fresh RHM medium with the replenished used medium. The 50% and 100% recycled medium cultures were sterilised using syringe filters (Millex 0.22 µm, Merck Millipore). Before inoculation, all cultures had 50% glucose solution added. The fresh RHM cultures and the 50% recycled cultures had 1 mL 50% glucose solution added. The 100% recycled cultures had a reduced amount of 50% glucose solution added (791 µL), taking into account the residual glucose in the used medium calculated from the DNS assay. All cultures were inoculated with 500 µL of Oxoid nutrient broth starter culture, as above, and incubated for 3 days at 28 °C, with shaking at 150 rpm.

A second experiment was conducted using the same methodology as above, however in this instance the recycled media were autoclaved rather than filter sterilised. Since these cultures were made up using a different batch of the used medium, the glucose and ammonia were tested again, and the amounts added to the recycled medium were 0.48 g L^{-1} ammonium chloride, and 992 µL 50% glucose was added to each 50 mL culture of 100% recycled medium.

7.2.5 Determination of dry mass of cells

The cultures were centrifuged at 3,500 rpm for 10 min (Beckman Allegra 6R centrifuge), the supernatant was removed, and the cell pellets were lyophilised (Virtis SP Scientific, Sentry 2.0) and weighed. The dry mass is reported as the proportion of dry cell mass to the mass of the whole culture.

7.2.6 Statistical tests

The statistical tests were carried out using SPSS. The data were tested for normal distribution using the Shapiro-Wilk test. The data were then compared using the Mann Whitney U test for non-parametric data.

7.3 Results & Discussion

7.3.1 Effectiveness of the carbon treatment to remove amino acids and nucleotides from the used medium

The amino acid analysis showed that the carbon treatment was successful in reducing the total amino acids amount by 30%, and this was a statistically significant result ($P<0.05$). The majority of the individual amino acids also showed statistically significant decreases ($P<0.05$), with some showing 100% decreases, although alanine, glycine, valine, proline, lysine and histidine did not show a significant change (Figure 53 & Figure 54). The method has therefore

been reasonably successful at reducing the amino acid content of the supernatant, but further development of the method would be needed in order to completely remove all of the amino acids. This could include changes to the pH, as this is known to affect the removal of amino acids depending on their properties (Xiao *et al.*, 2014). The amount of carbon added, the temperature and the duration of mixing could also have an effect.

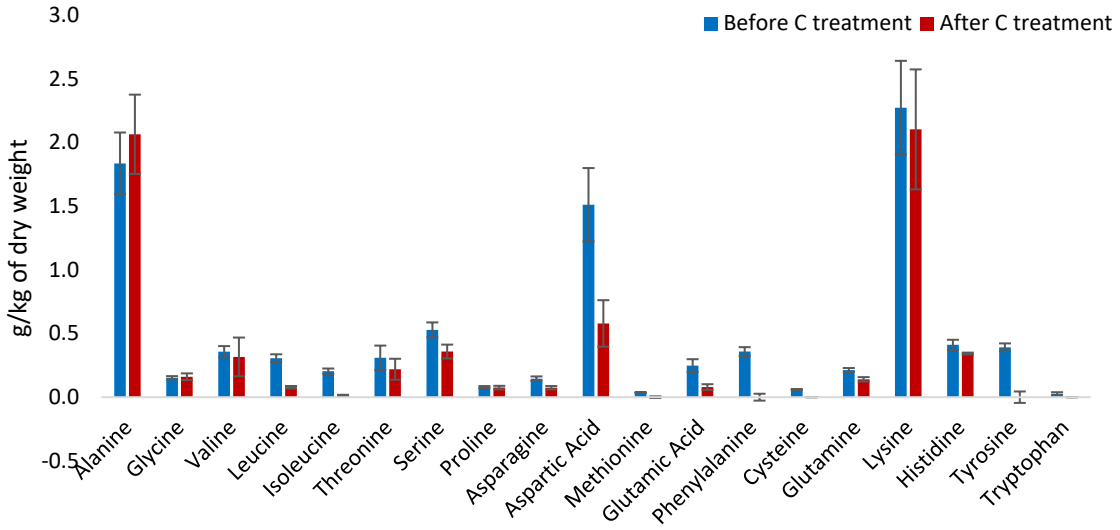

Figure 53: Amount of each free amino acid in the untreated culture supernatant compared to the carbon treated culture supernatant (g kg^{-1} of dry weight). Error bars represent one standard deviation. Results based on 6 repeat cultures for each condition. Results shown were statistically significant ($P<0.05$), except for alanine, glycine, valine, proline, lysine, and histidine.

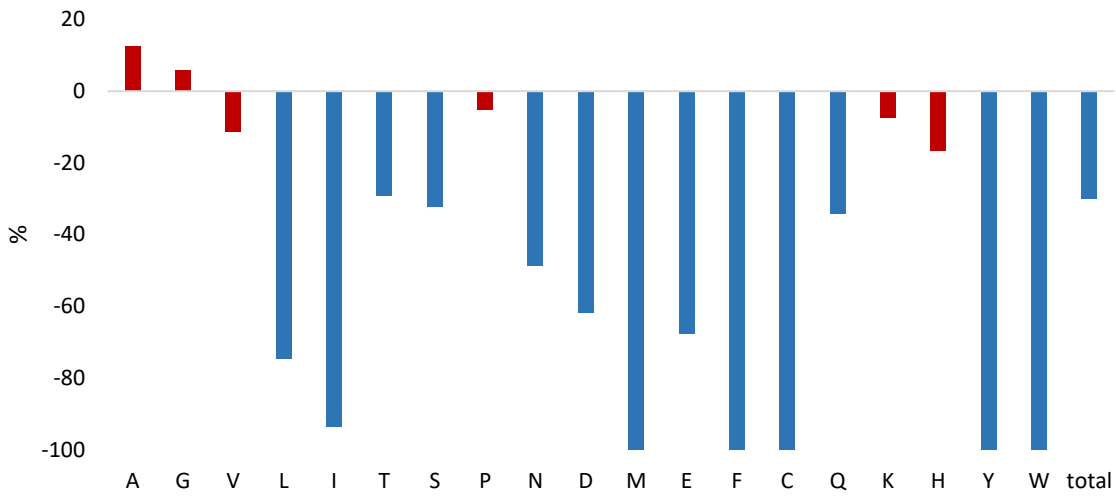

Figure 54: Differences in amino acid amounts in F. venenatum when grown in iron-limited conditions. Percentage change compared to the control. A) alanine G) glycine V) valine L) leucine I) isoleucine T) threonine S) serine P) proline N) asparagine D) aspartic acid M) Methionine E) glutamic acid F) phenylalanine C) Cysteine Q) glutamine K) lysine H) histidine Y) tyrosine W) tryptophan. Note: changes seen in alanine, glycine, valine, proline, lysine, and histidine (shaded red) were not found to be statistically significant.

The removal of nucleotides by the treatment has been more successful; the nucleotides analysis showed that the carbon treatment reduced all of the measurable nucleotides by 100%. The method was therefore able to completely remove all of the nucleotides from the supernatant.

7.3.2 Changes in dry mass for cultures grown in recycled medium

Similar patterns in growth were observed for both the filter sterilised and autoclaved spent media. For the cultures that were sterilised by filtration, an increase in dry mass over the control was observed of 44% for the 50% recycled cultures and 77% for the 100% recycled cultures (Figure 55a). These results were very highly statistically significant ($p < 0.001$). For the cultures that were autoclaved, there was a 29% increase in dry mass over the control for

the 50% recycled cultures, and a 90% increase for the 100% recycled cultures (Figure 55b). Again, these results are also very highly statistically significant ($p < 0.001$).

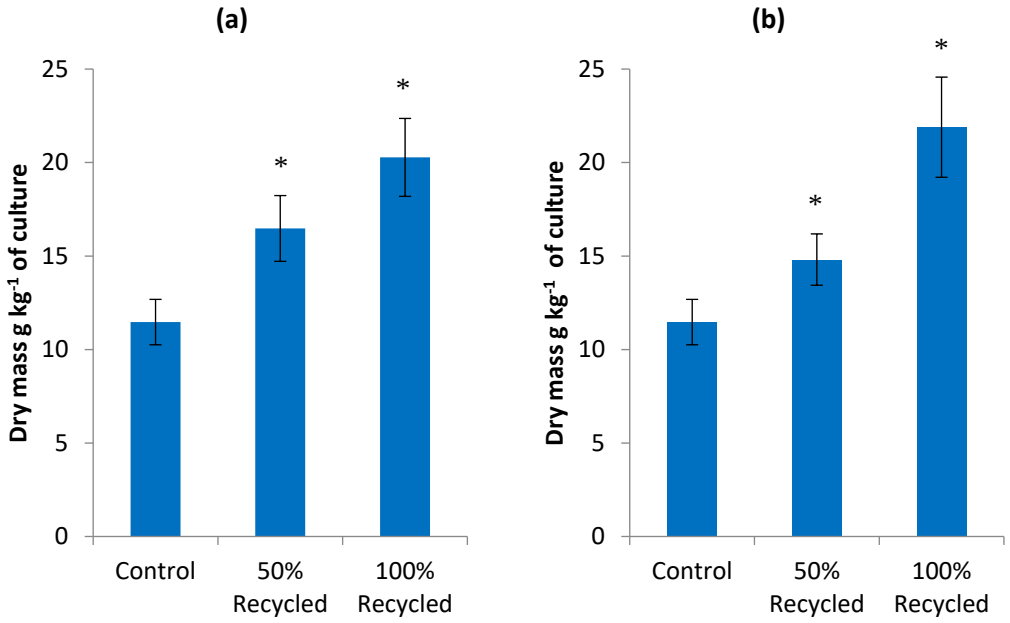

Figure 55: Average dry mass of cell pellet (g kg^{-1} of culture) from cultures grown with carbon treated used culture medium. (a) Biomass results for the recycled media that were sterilised by filtration. Error bars represent 1 standard deviation. Average is based on 6 repeat cultures for the control and 50% recycled conditions, and 5 repeat cultures for the 100% recycled condition. (b) Biomass results for the recycled media that were sterilised by autoclave. Error bars represent 1 standard deviation. Average is based on 6 repeat cultures for all conditions. * indicates statistical significance.

The carbon treated used medium allowed the growth of the fungus, and significantly increased ($P<0.05$) the biomass in both sets of results, suggesting the presence of factor(s) in the used medium that is/are encouraging the growth of the fungus. As discussed above, a previous study found that a protein-containing extract from the used medium was able to encourage the production of penicillin amidase by *E. coli* and to reduce the lag time of growth (Babu &

Panda, 1991). The authors also indicated that the extract could have contained other factors, as well as the protein, that positively influenced the bacterium (Babu & Panda, 1991). In the present study, it is unlikely to be a protein growth factor as the effect was seen both when the medium was filtered and when it was autoclaved, which would have denatured the protein. However, it may be that the fungus is able to use residual amino acids or digested protein as a nitrogen source for growth, as results have shown that not all the amino acids were removed from the carbon treatment. Alternatively, the level of trace metals was not measured prior to making the medium and these were replenished by adding the same amount to the used medium as fresh, and so it could be that the recycled broth had a higher level of metal ions, which affected growth. However, this will require some additional investigation as results from previous experiments showed that increasing the levels of iron and calcium did not have a significant effect on the biomass although the average for excess calcium was higher than the control (see chapter 3), while other earlier cultures did show some significant increases with limited iron, excess iron and excess calcium (see chapter 2). Other metal ions may also have had an effect, but they have not been investigated here. It is not possible on these results alone to explain how this has happened, and so further work would need to be undertaken to determine how the increased growth was caused.

7.3.3 Changes in morphology of cultures grown in recycled medium

The results have shown that the morphology has been significantly affected by the recycled medium, as shown by changes in the number of tips and the growth unit ‘G’ (Table 7). The number of tips was reduced with very high statistical significance ($P<0.001$) in all of the conditions, with the greatest percentage decrease (-38%) in the autoclaved 100% recycled medium (Figure 56). The growth unit ‘G’ was also affected, with very highly significant increases ($P<0.001$) in all but the filtered 50/50 recycled medium, and the greatest percentage increase (70%) in the autoclaved 100% medium (Figure 57). The length of the hyphae did not show any significant changes in any of the recycled media (Figure 58).

Table 7: Statistical significance and % change comparing each recycled medium with the control. The P value was calculated using the Mann Whitney U test, as the data were not normally distributed.

	Tips		length		G	
Condition	P value	% change	P value	% change	P value	% change
Filtered 50/50	0.00175	-20	0.29	-1.9	0.06096	22.0
Filtered 100%	0.00026	-22	0.63	5.8	0.00003	38.8
Autoclaved 50/50	0.00005	-26	0.43	-1.8	0.00004	29.8
Autoclaved 100%	0.00000	-38	0.66	2.8	0.00000	70.2

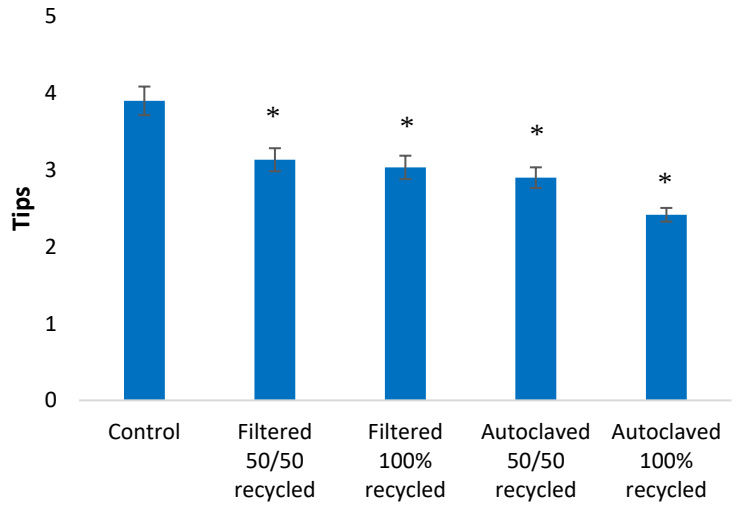

Figure 56: Number of growing tips for recycled medium cultures compared to the control. Average number of tips was calculated from 60 measurements, 10 from each of 6 cultures for each treatment. Error bars represent one standard error. * indicates statistical significance.

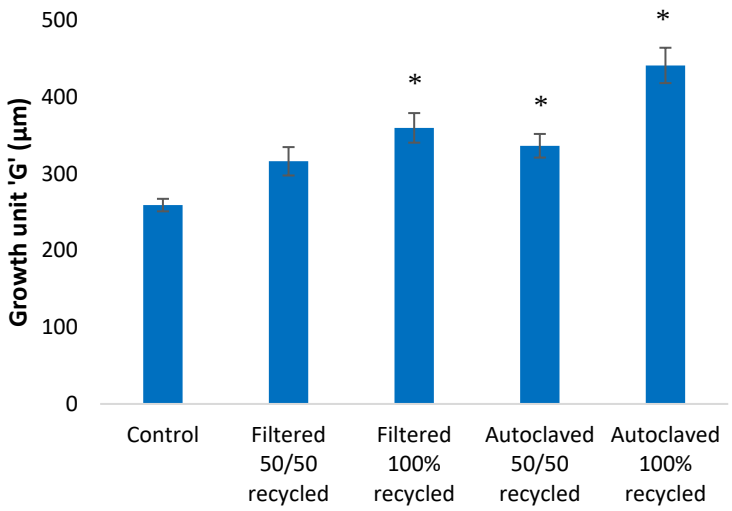

Figure 57: Hyphal Growth Unit (G) (µm) (G = total hyphal length ÷ number of tips) for recycled medium cultures compared to the control. Average G was calculated from 60 measurements, 10 from each of 6 cultures for each treatment. Error bars represent one standard error. * indicates statistical significance.

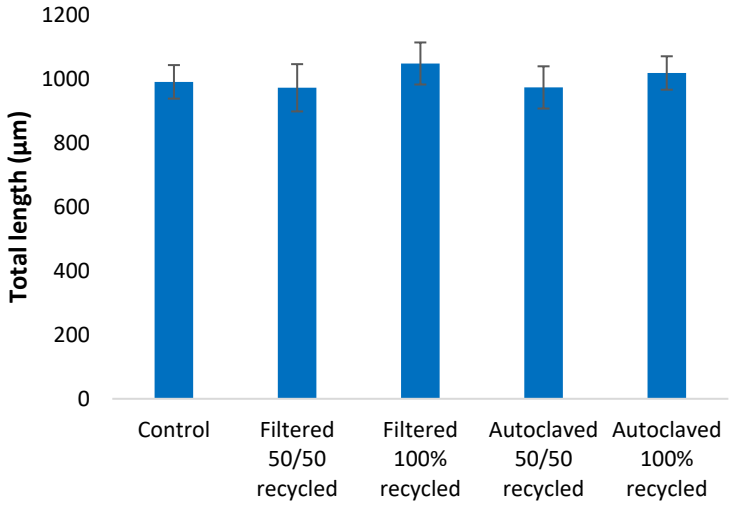

Figure 58: Total length of hyphae for recycled medium cultures compared to the control. Total length was calculated from 60 measurements, 10 from each of 6 cultures for each treatment. Error bars represent one standard error. These results were not statistically significant.

These results have shown that the branching frequency has been affected in all of the recycled media. It is hard to explain at this point, why the recycled medium caused this effect, but it is known that the amounts of iron and calcium ions affect the morphology (see chapter 2) and previous studies have shown that calcium in particular affects branching, with more branches formed in media with a lower calcium concentration (Robson *et al.*, 1991b). It could be that the recycled medium had increased ion concentrations due to ions that were not fully depleted by the first fermentation, and the recycled broth was replenished by adding the full amount. This could be significant for the growth of *F. venenatum* because the branching could affect the texture of the food product. Furthermore, as has been discussed previously (see chapter 2) the production of *F. venenatum* for Quorn is hampered by the appearance of variant strains with excessive branching that normally cause the fermenter to be shut down (Wiebe *et al.*, 1992). If the recycled medium is able to reduce branching, then there may be a factor in the recycled medium that could act to delay the onset of the mutants.

7.4 Conclusions

The results have given a good indication that recycled medium would be successful for cultivation of *F. venenatum*, and it may even be possible to increase the biomass produced. However, the morphology was affected, with a decrease in branching and a lower 'G' value, which could have implications for the texture of the final product. The use of activated carbon to reduce organic compounds in the medium was successful at reducing most amino acids and completely eliminated nucleotides.

While the results have indicated that the use of recycled medium would be successful for Quorn™ production, the used medium that was investigated here would differ from the used centrate from the industrial production of Quorn™ due to differences between the two processes. Batch cultures were used here which supply all of the nutrients and glucose that the fungus needs in the medium at the start, whereas the Quorn™ fermentation process uses a nutrient-unlimited glucose-stat continuous culture (Simpson *et al.*, 1998). After the fermentation but before centrifugation, the industrial process includes a step in which the biomass is heated to 65 °C for 25-30 min to reduce the RNA content, this could also change the composition of the centrate that would be used for recycling. It would be important therefore to carry out further similar experiments using the actual centrate from Quorn™ production in order to confirm these results.

The ability to recycle the fermenter effluent could have positive implications for Quorn™ as it would reduce their expenditure on wastewater treatment at the same time as reducing some of the nutrients used, increase the sustainability and profitability of the process. A reduction in water use could also be useful if the company were to start Quorn™ production in areas with less easily available water or a more expensive water supply.

7.5 Further work

These exploratory investigations lend themselves to substantial future research which would aim to further understand the impact of recycling on the morphology and growth of the organism.

As discussed above, any further experiments would need to begin by testing the effects of recycling the centrate from the industrial production of Quorn™ in order to confirm the results shown here when only batch cultures were used.

Future experimental designs could then incorporate the fractionation of the used media to groups of components in order to isolate potential compounds that are responsible for the observed effects. Such investigations could include the use of prep HPLC to purify, fractionate, concentrate and add back individual fractions in small volume cultures and this would be complemented by analysis of the proteome and metabolome to identify key metabolic effects.

Amino acids were not completely removed by the carbon treatment, and so further development of the carbon treatment method should be carried out, along with further analysis to ensure that as many of the small organic molecules are removed as possible that could build-up and affect growth. The use of ion exchange resins is of particular interest as they are traditionally used in the industry for the removal of ionic species such as amino acids and organic acids. The used medium could also be tested without the carbon treatment, as it could be a more cost-effective process if beneficial effects can be found even when expensive activated carbon is not used.

The next steps for the investigation of the fungus would be an analysis of the metabolome and proteome when it is grown in the recycled medium so that any changes in its biochemistry that would affect aspects such as flavour or texture of the product can be revealed. This analysis could also help to find out why the recycled medium has increased the biomass. A full analysis of the treated recycled medium would also be necessary to find out what metal ions, proteins

or other metabolites are present at higher levels and which could have affected the biomass and morphology. These could then be investigated individually in modified media.

It would also be extremely important to identify if these conditions had caused the production of mycotoxins, as the fungus is known to be capable of mycotoxin production (O'Donnell *et al.*, 1998), but under the normal production conditions it does not (Wiebe, 2004). It is possible that the altered conditions of growth when recycled medium is used could have increased mycotoxin production, which might require yet further investigations on cause and effect relationships.

8. Conclusions & further work

8.1 The effect of cation modified media on the biochemistry of *F. venenatum*

Growing cultures of *F. venenatum* in media with limited iron has made significant changes to its biochemistry. Amino acid analysis revealed that the total free amino acids were reduced by 31% when the iron-limited culture was compared to the control, and the majority of individual amino acids were also significantly reduced. Conversely, the amount of glutamic acid was increased in iron-limited conditions. These changes were seen without any significant decreases to the biomass produced by the fungus. The other changes to the media did not show so many significant results, with only an increase in histidine seen in excess iron medium, and an increase in glycine in the calcium-limited medium.

These changes to amino acid levels were further supported by the results of the metabolome and proteome analyses. The results of the metabolome analysis again showed that the greatest effect was seen in the iron-limited cultures, with the most compounds that were significantly altered. Amino acids were among the significantly altered metabolites, and the proteome analysis identified proteins from amino acid pathways in both the iron-limited and excess iron cultures, with 8 enzymes that belong to amino acid biosynthesis pathways showing reduced abundance in the iron-limited cultures, and others were decreased in the excess iron medium.

The reason for these changes to amino acid metabolism in iron-limited conditions is likely to be a result of enzymes that require iron cofactors e.g. those that contain an Fe/S cluster being downregulated. This effect has been described in fungi previously by other authors (Philpott *et al.*, 2012), (Shakoury-Elizeh *et al.*, 2010). Amino acid biosynthesis could be expected to be directly affected by this affect as some pathways contain iron-requiring enzymes e.g. dihyroxyacid dehydratase in the synthesis of branched chain amino acids or homoaconitase in lysine biosynthesis.

Other pathways were also affected by iron-limited conditions. The proteomics analysis indicated that proteins involved in respiration were downregulated in iron-limited conditions

but upregulated in the excess iron condition. This is also possibly a result of these proteins having iron as a cofactor. A reduction in the TCA cycle or the electron transfer chain in iron-limited cultures could also have indirectly affected other biochemical processes including amino acid biosynthesis as the supply of ATP would be reduced, or the amounts of intermediates needed as precursors for these compounds would be decreased.

In addition to amino acid metabolism and respiration, the results of the proteome analysis also showed changes to diverse pathways in the iron-limited medium, this included lipid biosynthesis, cell wall synthesis, siderophore production, and two proteins associated with mycotoxins were also observed to be upregulated. In the excess iron medium, pathways that were affected included nucleotide biosynthesis, lipid biosynthesis, signal transduction, and sulfur metabolism.

These biochemical changes could be significant for Quorn™ production as changes in amino acid and nucleotide biosynthesis could affect the savoury umami flavour of the product by altering the levels of glutamate and aspartate along with the flavour active nucleotides IMP, GMP, and XMP (Zhang *et al.*, 2013). Other amino acids also contribute to flavour, for example arginine and leucine have a bitter flavour while alanine and glycine give a sweet flavour (Mau et al., 2001). Amino acids could also participate in the Maillard reaction upon heating which produces further flavour compounds (Ames, 1998). Since the results have also shown that these changes can be brought about without significantly decreasing the biomass, these results could potentially offer a way for Quorn™ producers to develop new growth media that result in better flavour for their food products.

8.2 The effect of cation modified media on the morphology of *F. venenatum.*

Changes to the iron and calcium content of the medium had significant effects on the morphology of the fungus. In the iron-limited medium after 2 days of growth the hyphae are longer and had a larger G value. The number of growing tips was lower in iron-limited cultures

after 4 days and 8 days of culture, but it was higher after 2 days of culture in calcium-limited medium. Growth in a 1 L fermenter with greater control of pH and aeration gave a very similar result with a significant increase in length and G value compared to the control, but no significant change in the number of tips when the fungus was grown in iron-limited medium.

These results could be significant in Quorn™ production as the morphology of the fungus could affect the quality and texture of the final product. Knowledge of how the morphology changes in response to substances in the medium will help Quorn™ producers understand how to achieve the best possible conditions for growth that give an optimum product.

8.3 The effect of recycled medium on the biomass and morphology of *F. venenatum*.

The analysis of cultures grown in carbon treated recycled medium showed the potential for using this type of medium for Quorn™ production. The biomass showed significant increases for both 50% and 100% recycled medium. The morphology was affected, however with a significant decrease in branching, which may affect the final product.

These results could be significant for Quorn™ producers as an increase in biomass at the same time as reducing the amount of wastewater that requires expensive treatment would increase profitability. The environmental sustainability of the process would also be improved with less wastewater being released back into the environment.

8.4 Further work

The results discussed here have indicated great potential for modifying the metabolism and morphology of *F. venenatum* by altering the metal cations supplied in the medium. However, several investigations are necessary to further understand how these changes have been brought about.

Firstly, given that the growth conditions used here were based on batch fermentation in either conical flasks or 1 L fermenters, it would be necessary to extend this investigation to the use

of cation modified medium in continuous fermentation conditions in an air-lift fermenter which would more closely model the process used for producing Quorn™ in industry.

The compounds identified in the metabolomics investigation require further analysis for confirmation of their identity, this could be done by analysing reference standards by LC-MS/MS and comparing fragmentation patterns. The analysis could also be repeated with more concentrated samples to allow better MS/MS fragmentation for more reliable results. Similarly, the proteins identified in the proteomics results also require confirmation, and this should also involve analysis of more concentrated samples, along with purified target proteins to achieve more reliable identifications.

The extracellular metabolome and proteome could also be analysed in the same way, to reveal how these growth conditions affect the metabolites and proteins that are secreted into the medium.

The metabolome and proteome data could be complimented by an analysis of the transcriptome which may be able to reveal more information on which genes are upregulated/downregulated in each condition and this would help to explain changes in the proteome and metabolome.

The results indicated that iron-limited cultures had the greatest effect on the biochemistry and morphology of the fungus but only 2 conditions were tested, it would therefore be of interest to try the experiment again with a range on iron concentrations which could reveal the threshold of iron that causes these changes. This information could be of use if Quorn™ producers wanted to use this effect to improve the cultivation of the organism for food production. The investigation of the effect of metal ions in the medium could also be extended to other metals such as magnesium as this could also have an effect on the biochemistry of the fungus, and it has previously been found to have an effect on mycotoxin production (Pinson-Gadais *et al.*, 2008)

The changes to amino acid metabolism described here could have an effect on the flavour of the final product and so further investigation into how amino acid amounts impact the flavour, particularly the umami flavour or Maillard reaction products could be carried out. This could include an investigation of consumer preferences.

Food safety is of course of utmost importance, and any investigation into optimising *F. venenatum* production for Quorn™ would need to include an analysis of mycotoxin production. It is not known how changing the iron or calcium content of the medium impacts mycotoxin production, but the proteomics results did indicate that proteins related to mycotoxins may have been upregulated in the iron-limited medium. This would need further analysis to confirm whether the mycotoxins were actually produced in this condition.

Changes to the morphology seen in these results may affect the quality and texture of the final product and so further investigation of how differences in the length or branching of the hyphae affect the material properties of the product would be useful in determining whether these growth conditions could be beneficial or detrimental.

The use of recycled medium was shown to be successful in increasing the biomass, but it is not yet known how this was caused. This would require an investigation into the components of the recycled media that may be increased or decreased after the initial fermentation. Analysis of the metabolites, proteins and metal ions present in the recycled medium would therefore need to be carried out, and an investigation of how these affect the fungus would then follow.

9. References

Abadjieva, A., Pauwels, K., Hilven, P. & Crabeel, M. (2001). A new yeast metabolon involving at least the two first enzymes of arginine biosynthesis: acetylglutamate synthase activity requires complex formation with acetylglutamate kinase. *Journal of Biological Chemistry.* 276:46, 42869-42880.

Ames, J. M. (1998). Applications of the Maillard reaction in the food industry. *Food Chemistry.* 62:4, 431-439.

Aravind, L., de Souza, R. F. & Iyer, L. M. (2010). Predicted class-I aminoacyl tRNA synthetase-like proteins in non-ribosomal peptide synthesis. *Biology Direct.* 5:1, 48-48.

Arst, H. N., Jones, S. A. & Bailey, C. R. (1981). A method for the selection of deletion mutations in the L-proline catabolism gene cluster of *Aspergillus nidulans*. *Genetical Research.* 38:2, 171-195.

Babu, P. S. R. & Panda, T. (1991). Effect of recycling of fermentation broth for the production of penicillin amidase. *Process Biochemistry.* 26:1, 7-14.

Bae-Lee, M. S. & Carman, G. M. (1984). Phosphatidylserine synthesis in *Saccharomyces cerevisiae*. Purification and characterization of membrane-associated phosphatidylserine synthase. *Journal of Biological Chemistry.* 259:17, 10857-10862.

Bailão, E. F. L. C., Borges, C. L., Bailão, A. M., de Almeida Soares, C. M., Parente, A. F. A., Parente, J. A., Silva-Bailão, M. G., de Castro, K. P., Kmetzsch, L., Staats, C. C. *et al.* (2012). Metal acquisition and homeostasis in fungi. *Current Fungal Infection Reports.* 6:4, 257-266.

Bayry, J., Aimanianda, V., Guijarro, J. I., Sunde, M. & Latgé, J.-P. (2012). Hydrophobins-unique fungal proteins. *PLoS Pathogens.* 8:5, 1-4.

Bedair, M. & Sumner, L. W. (2008). Current and emerging mass-spectrometry technologies for metabolomics. *Trends in Analytical Chemistry.* 27:3, 238-250.

Bedekovics, T., Li, H. Q., Gajdos, G. B. & Isaya, G. (2011). Leucine biosynthesis regulates cytoplasmic iron-sulfur enzyme biogenesis in an Atm1p-independent manner. *Journal of Biological Chemistry.* 286:47, 40878-40888.

Beluhan, S. & Ranogajec, A. (2011). Chemical composition and non-volatile components of Croatian wild edible mushrooms. *Food Chemistry.* 124:3, 1076-1082.

Berg, J. M., Tymoczko, J. L. & Stryer, L. (2006). *Biochemistry.* 6th edn. New York, N.Y: W. H. Freeman

Berka, R. M., Nelson, B. A., Zaretsky, E. J., Yoder, W. T. & Rey, M. W. (2004). Genomics of *Fusarium venenatum*: An alternative fungal host for making enzymes. *Applied Mycology and Biotechnology.* 4:C, 191-203.

Bertrand, S., Azzollini, A., Schumpp, O., Bohni, N., Schrenzel, J., Monod, M., Gindro, K. & Wolfender, J.-L. (2014). Multi-well fungal co-culture for de novo metabolite-induction in time-series studies based on untargeted metabolomics. *Molecular BioSystems.* 10:9, 2289-2298.

Böcker, S. & Dührkop, K. (2016). Fragmentation trees reloaded. *Journal of Cheminformatics.* 8:1, 1-26.

Böcker, S., Letzel, M. C., Lipták, Z. & Pervukhin, A. (2009). SIRIUS: decomposing isotope patterns for metabolite identification. *Bioinformatics.* 25:2, 218-224.

Bowman, S. M. & Free, S. J. (2006). The structure and synthesis of the fungal cell wall. *Bioessays.* 28:8, 799-808.

Brakhage, A. A. & Schroeckh, V. (2011). Fungal secondary metabolites – Strategies to activate silent gene clusters. *Fungal Genetics and Biology.* 48:1, 15-22.

Brand, A. & Gow, N. A. R. (2009). Mechanisms of hypha orientation of fungi. *Current Opinion in Microbiology.* 12:4, 350-357.

Braus, G. H. (1991). Aromatic amino acid biosynthesis in the yeast *Saccharomyces cerevisiae*: a model system for the regulation of a eukaryotic biosynthetic pathway. *Microbiological Reviews.* 55:3, 349-370.

Breddam, K. (1986). Serine carboxypeptidases. A review. *Carlsberg Research Communications.* 51:2, 83-128.

Broom, A. D. & Robins, R. K. (1965). The Direct Preparation of 2'-O-Methyladenosine from Adenosine. *Journal of the American Chemical Society.* 87:5, 1145-1146.

Brown, D. W., Butchko, R. A. E., Baker, S. E. & Proctor, R. H. (2012). Phylogenomic and functional domain analysis of polyketide synthases in *Fusarium*. *Fungal Biology.* 116:2, 318-331.

Browne, R. A. & Brindle, K. M. (2007). ^{1}H NMR-based metabolite profiling as a potential selection tool for breeding passive resistance against *Fusarium* head blight (FHB) in wheat. *Molecular Plant Pathology.* 8:4, 401-410.

Brownridge, P. & Beynon, R. J. (2011). The importance of the digest: Proteolysis and absolute quantification in proteomics. *Methods.* 54:4, 351-360.

Brzywczy, J., Sieńko, M., Kucharska, A. & Paszewski, A. (2002). Sulphur amino acid synthesis in *Schizosaccharomyces pombe* represents a specific variant of sulphur metabolism in fungi. *Yeast.* 19:1, 29-35.

Cañas, B., Piñeiro, C., Calvo, E., López-Ferrer, D. & Gallardo, J. M. (2007). Trends in sample preparation for classical and second generation proteomics. *Journal of Chromatography A.* 1153:1, 235-258.

Cantrell, C. L., Case, B. P., Mena, E. E., Kniffin, T. M., Duke, S. O. & Wedge, D. E. (2008). Isolation and Identification of Antifungal Fatty Acids from the Basidiomycete *Gomphus floccosus*. *Journal of Agricultural and Food Chemistry.* 56:13, 5062-5068.

Cardoza, R. E., Malmierca, M. G., Hermosa, M. R., Alexander, N. J., McCormick, S. P., Proctor, R. H., Tijerino, A. M., Rumbero, A., Monte, E. & Gutiérrez, S. (2011). Identification of Loci and Functional Characterization of Trichothecene Biosynthesis Genes in Filamentous Fungi of the Genus *Trichoderma*. *Applied and Environmental Microbiology.* 77:14, 4867-4877.

Carman, G. M. & Han, G.-S. (2009). Regulation of phospholipid synthesis in yeast. *Journal Of Lipid Research.* April Supplement:2009, S69.

Cavinder, B., Hamam, A., Lew, R. R. & Trail, F. (2011). Mid1, a mechanosensitive calcium ion channel, affects growth, development, and ascospore discharge in the filamentous fungus *Gibberella zeae*. *Eukaryotic Cell.* 10:6, 832-841.

Cavinder, B. & Trail, F. (2012). Role of Fig1, a component of the low-affinity calcium uptake system, in growth and sexual development of filamentous fungi. *Eukaryotic Cell.* 11:8, 978-988.

CCD (2018) Conserved Domain Database https://www.ncbi.nlm.nih.gov/ (Accessed: 7/12/18)

Cermakova, L., Kopecka, I., Pivokonsky, M., Pivokonska, L. & Janda, V. (2017). Removal of cyanobacterial amino acids in water treatment by activated carbon adsorption. *Separation and Purification Technology.* 173:330-338.

Chen, X., Nielsen, K. F., Borodina, I., Kielland-Brandt, M. C. & Karhumaa, K. (2011). Increased isobutanol production in *Saccharomyces cerevisiae* by overexpression of genes in valine metabolism. *Biotechnology for Biofuels.* 4:1, 21.

Cherest, H., Davidian, J. C., Thomas, D., Benes, V., Ansorge, W. & Surdin-Kerjan, Y. (1997). Molecular characterization of two high affinity sulfate transporters in *Saccharomyces cerevisiae*. *Genetics.* 145:3, 627-635.

Clapham, D. E. (2007). Calcium signaling. *Cell.* 131:6, 1047-1058.

Claus, J. & Chavarría-Krauser, A. (2012). Modeling regulation of zinc uptake via ZIP transporters in yeast and plant roots. *PLoS One.* 7:6, 1-11.

Cole, L. K., Vance, J. E. & Vance, D. E. (2012). Phosphatidylcholine biosynthesis and lipoprotein metabolism. *Biochimica et Biophysica Acta (BBA) - Molecular and Cell Biology of Lipids.* 1821:5, 754-761.

Cottrell, J. S. (2011). Protein identification using MS/MS data. *Journal of Proteomics.* 74:10, 1842-1851.

Cox, P. W. & Hooley, P. (2009). Hydrophobins: New prospects for biotechnology. *Fungal Biology Reviews.* 23:1, 40-47.

Cuero, R. & Ouellet, T. (2005). Metal ions modulate gene expression and accumulation of the mycotoxins aflatoxin and zearalenone. *Journal of Applied Microbiology.* 98:3, 598-605.

Cuero, R., Ouellet, T., Yu, J. & Mogongwa, N. (2003). Metal ion enhancement of fungal growth, gene expression and aflatoxin synthesis in *Aspergillus flavus*: RT-PCR characterization. *Journal of Applied Microbiology.* 94:6, 953-961.

de Paulo Martins, V., Dinamarco, T. M., Curti, C. & Uyemura, S. A. (2011). Classical and alternative components of the mitochondrial respiratory chain in pathogenic fungi as potential therapeutic targets. *Journal of Bioenergetics & Biomembranes.* 43:1, 81-88.

De Vos, R. C. H., Moco, S., Lommen, A., Keurentjes, J. J. B., Bino, R. J. & Hall, R. (2007). Untargeted large-scale plant metabolomics using liquid chromatography coupled to mass spectrometry. *Nature Protocols.* 2:4, 778.

Deacon, J. W. (2009). *Fungal Biology.* 4th edn. E.B.L. Available at: http://northumbria.eblib.com/patron/FullRecord.aspx?p=428109 (Accessed: 8th April 2015)

Del Ponte, E. M., Garda-Buffon, J. & Badiale-Furlong, E. (2012). Deoxynivalenol and nivalenol in commercial wheat grain related to *Fusarium* head blight epidemics in southern Brazil. *Food Chemistry.* 132:2, 1087-1091.

Desjardins, A. E. & Proctor, R. H. (2007). Molecular biology of *Fusarium* mycotoxins. *International Journal of Food Microbiology.* 119:1, 47-50.

Dijksterhuis, J. & Molenaar, D. (2013). Vesicle trafficking via the Spitzenkörper during hyphal tip growth in *Rhizoctonia solani*. *Antonie Van Leeuwenhoek International Journal of General and Molecular Microbiology.* 103:4, 921-931.

Donofrio, N. M., Oh, Y., Lundy, R., Pan, H., Brown, D. E., Jeong, J. S., Coughlan, S., Mitchell, T. K. & Dean, R. A. (2006). Global gene expression during nitrogen starvation in the rice blast fungus, *Magnaporthe grisea*. *Fungal Genetics and Biology.* 43:9, 605-617.

Dührkop, K., Scheubert, K. & Böcker, S. (2013). Molecular Formula Identification with SIRIUS. *Metabolites.* 3:2, 506-516.

Dührkop, K., Shen, H., Meusel, M., Rousu, J. & Böcker, S. (2015). Searching molecular structure databases with tandem mass spectra using CSI:FingerID. *Proceedings of the National Academy of Sciences.* 112:41, 12580-12585.

Edlayne, G., Simone, A. & Felicio, J. D. (2009). Chemical and biological approaches for mycotoxin control: a review. *Recent Patents on Food, Nutrition & Agriculture.* 1:2, 155-161.

El-Sayed, A. S. A., Yassin, M. A., Khalaf, S. A., El-Batrik, M., Ali, G. S. & Esener, S. (2015). Biochemical and pharmacokinetic properties of PEGylated cystathionine γ-lyase from *Aspergillus carneus* KF723837. *Journal of Molecular Microbiology and Biotechnology.* 25:5, 301-310.

Elleuche, S. & Poggeler, S. (2010). Carbonic anhydrases in fungi. *Microbiology.* 156:1, 23-29.

Farfán, M. a.-J. & Calderón, I. L. (2000). Enrichment of threonine content in *Saccharomyces cerevisiae* by pathway engineering. *Enzyme and Microbial Technology.* 26:9–10, 763-770.

Fazius, F., Shelest, E., Gebhardt, P. & Brock, M. (2012). The fungal α-aminoadipate pathway for lysine biosynthesis requires two enzymes of the aconitase family for the isomerization of homocitrate to homoisocitrate. *Molecular Microbiology.* 86:6, 1508-1530.

Feldmann, H. (2012). *Yeast molecular and cell biology.* 2nd edn. Available at: http://ebookcentral.proquest.com/lib/northumbria/detail.action?docID=1023291 (Accessed: 12th May 2017)

Ferreira, G. C. (1999). Ferrochelatase. *The International Journal of Biochemistry & Cell Biology.* 31:10, 995-1000.

Festa, R. A. & Thiele, D. J. (2011). Copper: An essential metal in biology. *Current Biology.* 21:21, R877-R883.

Filippovich, S., Rybakov, Y., Afanasieva, T., Bachurina, G., Lukina, G., Ezhova, I., Nosova, A., Artjushkina, T., Sineokii, S. & Kritskii, M. (2001). Characterization of Lipoxygenase from Fungi of the Genus *Mortierella*. *Applied Biochemistry and Microbiology.* 37:5, 473-479.

Franken, A., Werner, E., Haas, H., Lokman, B., Hondel, C., Ram, A., Weert, S. & Punt, P. (2013). The role of coproporphyrinogen III oxidase and ferrochelatase genes in heme biosynthesis and regulation in Aspergillus niger. *Applied Microbiology and Biotechnology.* 97:22, 9773-9785.

Franken, J., Kroppenstedt, S., Swiegers, J. H. & Bauer, F. F. (2008). Carnitine and carnitine acetyltransferases in the yeast *Saccharomyces cerevisiae*: a role for carnitine in stress protection. *Current Genetics.* 53:6, 347.

Gabler, M. & Fischer, L. (1999). Production of a new D-amino acid oxidase from the fungus *Fusarium oxysporum*. *Applied and Environmental Microbiology.* 65:8, 3750-3753.

García-Villegas, R., Camacho-Villasana, Y., Shingú-Vázquez, M. Á., Cabrera-Orefice, A., Uribe-Carvajal, S., Fox, T. D. & Pérez-Martínez, X. (2017). The Cox1 C-terminal domain is a central regulator of cytochrome oxidase biogenesis in yeast mitochondria. *Journal of Biological Chemistry.* 292:26, 10912.

Geiser, D. M., del Mar Jiménez-Gasco, M., Kang, S., Makalowska, I., Veeraraghavan, N., Ward, T. J., Zhang, N., Kuldau, G. A. & O'Donnell, K. (2004). FUSARIUM-ID v. 1.0: A DNA sequence database for identifying *Fusarium*. *European Journal of Plant Pathology.* 110:5, 473-479.

Gerke, J., Bayram, Ö. & Braus, G. H. (2012). Fungal S-adenosylmethionine synthetase and the control of development and secondary metabolism in *Aspergillus nidulans*. *Fungal Genetics and Biology.* 49:6, 443-454.

Gold, N. D., Gowen, C. M., Lussier, F.-X., Cautha, S. C., Mahadevan, R. & Martin, V. J. J. (2015). Metabolic engineering of a tyrosine-overproducing yeast platform using targeted metabolomics. *Microbial Cell Factories.* 14:73, 1-16.

Gong, L., Jiang, Y. & Chen, F. (2015). Molecular strategies for detection and quantification of mycotoxin-producing *Fusarium* species: a review. *Journal of the Science of Food and Agriculture.* 95:9, 1767-1776.

González-Fernández, R., Prats, E. & Jorrín-Novo, J. V. (2010). Proteomics of Plant Pathogenic Fungi. *Journal of Biomedicine and Biotechnology.* 2010, 1-36.

Goodman, I. & Weiss, R. L. (1986). Control of arginine metabolism in *Neurospora crassa*. Role of feedback inhibition. *Journal of Biological Chemistry.* 261:22, 10264-10270.

Gottschalk, C., Barthel, J., Engelhardt, G., Bauer, J. & Meyer, K. (2007). Occurrence of type A trichothecenes in conventionally and organically produced oats and oat products. *Molecular Nutrition and Food Research.* 51:12, 1547-1553.

Grandhi, K. (2015) Quorn Foods agrees sale to Monde Nissin for £550m http://www.ibtimes.co.uk/quorn-foods-agrees-sale-monde-nissin-550m-1521937 (Accessed: 07/12/2016)

Grimm, L. H., Kelly, S., Krull, R. & Hempel, D. C. (2005). Morphology and productivity of filamentous fungi. *Applied Microbiology and Biotechnology.* 69:4, 375-384.

Hallen, H. E. & Trail, F. (2008). The L-Type calcium ion channel Cch1 affects ascospore discharge and mycelial growth in the filamentous fungus *Gibberella zeae* (Anamorph *Fusarium graminearum*). *Eukaryotic Cell.* 7:2, 415-424.

Hansen, F. T., Sørensen, J. L., Giese, H., Sondergaard, T. E. & Frandsen, R. J. N. (2012). Quick guide to polyketide synthase and nonribosomal synthetase genes in *Fusarium*. *International Journal of Food Microbiology.* 155:3, 128-136.

Harris, S. D. (2011). Cdc42/Rho GTPases in fungi: variations on a common theme. *Molecular Microbiology.* 79:5, 1123.

Helliwell, S. B., Losko, S. & Kaiser, C. A. (2001). Components of a Ubiquitin Ligase Complex Specify Polyubiquitination and Intracellular Trafficking of the General Amino Acid Permease. *The Journal of Cell Biology.* 153:4, 649-662.

Hernandez-Montes, G., Diaz-Mejia, J. J., Perez-Rueda, E. & Segovia, L. (2008). The hidden universal distribution of amino acid biosynthetic networks: a genomic perspective on their origins and evolution. *Genome Biology (Online Edition).* 9:R95, R95.

Hestbjerg, H., Nielsen, K. F., Thrane, U. & Elmholt, S. (2002). Production of trichothecenes and other secondary metabolites by *Fusarium culmorum* and *Fusarium equiseti* on common laboratory media and a soil organic matter agar: An ecological interpretation. *Journal of Agricultural and Food Chemistry.* 50:26, 7593-7599.

Hidayat, B. J., Wiebe, M. G. & Eriksen, N. T. (2007). Phosphate-limited continuous flow cultures of *Fusarium venenatum* A3/5 and production of acid phosphatase. *Enzyme and Microbial Technology.* 40:4, 902-907.

Hildonen, S., Halvorsen, T. G. & Reubsaet, L. (2014). Why less is more when generating tryptic peptides in bottom-up proteomics. *Proteomics.* 14:17-18, 2031-2041.

Hoeflich, K. P. & Ikura, M. (2002). Calmodulin in Action: Diversity in Target Recognition and Activation Mechanisms. *Cell.* 108:6, 739-742.

Hosseini, S. M., Khosravi-Darani, K., Mohammadifar, M. A. & Nlkoopour, H. (2009). Production of mycoprotein by *Fusarium venenatum* growth on modified vogel medium. *Asian Journal of Chemistry.* 21:5, 4017-4022.

Hsiao, T. & Glatz, C. E. (1996). Water reuse in the L lysine fermentation process. *Biotechnology and Bioengineering.* 49:3, 341-347.

Hsiao, T., Glatz, C. E. & Glatz, B. A. (1994). Broth recycle in a yeast fermentation. *Biotechnology and Bioengineering.* 44:10, 1228-1234.

Hunte, C., Koepke, J., Lange, C., Roßmanith, T. & Michel, H. (2000). Structure at 2.3 Å resolution of the cytochrome bc1 complex from the yeast *Saccharomyces cerevisiae* co-crystallized with an antibody Fv fragment. *Structure.* 8:6, 669-684.

Huss, M. J., Campbell, C. L., Jennings, D. B. & Leslie, J. F. (1996). Isozyme variation among biological species in the *Gibberella fujikuroi* species complex (*Fusarium* section *Liseola*). *Applied and Environmental Microbiology.* 62:10, 3750.

Hussein, H. S. & Brasel, J. M. (2001). Toxicity, metabolism, and impact of mycotoxins on humans and animals. *Toxicology.* 167:2, 101-134.

Idnurm, A. & Heitman, J. (2010). Ferrochelatase is a conserved downstream target of the blue light-sensing White collar complex in fungi. *Microbiology (Reading, England).* 156:Pt 8, 2393-2407.

Ingold, C. T. (1984). *The Biology of Fungi.* 5th edn. London: Hutchinson

Ito, M., Sato, I., Koitabashi, M., Yoshida, S., Imai, M. & Tsushima, S. (2012). A novel actinomycete derived from wheat heads degrades deoxynivalenol in the grain of wheat and barley affected by *Fusarium* head blight. *Applied Microbiology and Biotechnology.* 96:4, 1059-1070.

Jackson, S. L. & Heath, I. B. (1993). Roles of calcium ions in hyphal tip growth. *Microbiological Reviews.* 57:2, 367-382.

Jardon, R., Gancedo, C. & Flores, C.-L. (2008). The Gluconeogenic Enzyme Fructose-1,6-Bisphosphatase Is Dispensable for Growth of the Yeast *Yarrowia lipolytica* in Gluconeogenic Substrates. *Eukaryotic Cell.* 7:10, 1742.

Jastrzębowska, K. & Gabriel, I. (2015). Inhibitors of amino acids biosynthesis as antifungal agents. *Amino Acids.* 47:2, 227-249.

Jennings, D. H. (1996). *Fungal biology : understanding the fungal lifestyle.* Oxford: Bios

Jennings, M. L. & Cui, J. (2012). Inactivation of *Saccharomyces cerevisiae* sulfate transporter Sul2p: use it and lose it. *Biophysical Journal.* 102:4, 768-776.

Jewett, M. C., Hofmann, G. & Nielsen, J. (2006). Fungal metabolite analysis in genomics and phenomics. *Current Opinion in Biotechnology.* 17:2, 191-197.

Kanehisa, M., Furumichi, M., Tanabe, M., Sato, Y. & Morishima, K. (2017). KEGG: new perspectives on genomes, pathways, diseases and drugs. *Nucleic Acids Research.* 45:D1, D353-d361.

Kanehisa, M. & Goto, S. (2000). KEGG: kyoto encyclopedia of genes and genomes. *Nucleic Acids Research.* 28:1, 27-30.

Kanehisa, M., Sato, Y., Kawashima, M., Furumichi, M. & Tanabe, M. (2016). KEGG as a reference resource for gene and protein annotation. *Nucleic Acids Research.* 44:D1, D457-462.

Kanipes, M. I. & Henry, S. A. (1997). The phospholipid methyltransferases in yeast. *Biochimica et Biophysica Acta (BBA)/Lipids and Lipid Metabolism.* 1348:1, 134-141.

Kaplan, C. D. & Kaplan, J. (2009). Iron acquisition and transcriptional regulation. *Chemical Reviews.* 109, 4536-4552.

Kaur, J. & Bachhawat, A. K. (2007). Yct1p, a novel, high-affinity, cysteine-specific transporter from the yeast *Saccharomyces cerevisiae*. *Genetics.* 176:2, 877-890.

KEGG (2017) KEGG pathways http://www.genome.jp/kegg/ (Accessed: 16/6/17)

Kim, Y.-T., Lee, Y.-R., Jin, J., Han, K.-H., Kim, H., Kim, J.-C., Lee, T., Yun, S.-H. & Lee, Y.-W. (2005). Two different polyketide synthase genes are required for synthesis of zearalenone in *Gibberella zeae*. *Molecular Microbiology.* 58:4, 1102-1113.

King, R., Brown, N. A., Urban, M. & Hammond-Kosack, K. E. (2018). Inter-genome comparison of the Quorn fungus *Fusarium venenatum* and the closely related plant infecting pathogen *Fusarium graminearum*. *BMC Genomics.* 19:1, 269.

King, R., Urban, M., Hammond-Kosack, M. C. U., Hassani-Pak, K. & Hammond-Kosack, K. E. (2015). The completed genome sequence of the pathogenic ascomycete fungus *Fusarium graminearum*. *BMC Genomics.* 16:1, 1-21.

Kishore, G., Sugumaran, M. & Vaidyanathan, C. S. (1976). Metabolism of DL (±) phenylalanine by *Aspergillus niger*. *Journal of Bacteriology.* 128:1, 182-191.

Klötzel, M., Gutsche, B., Lauber, U. & Humpf, H.-U. (2005). Determination of 12 type A and B trichothecenes in cereals by liquid chromatography−electrospray ionization tandem mass spectrometry. *Journal of Agricultural and Food Chemistry.* 53:23, 8904-8910.

Köhler, G. A., Brenot, A., Haas-Stapleton, E., Agabian, N., Deva, R. & Nigam, S. (2006). Phospholipase A2 and Phospholipase B activities in fungi. *Biochimica et Biophysica Acta (BBA) - Molecular and Cell Biology of Lipids.* 1761:11, 1391-1399.

Kosman, D. J. (2003). Molecular mechanisms of iron uptake in fungi. *Molecular Microbiology.* 47:5, 1185-1197.

Kraus, P. R. & Heitman, J. (2003). Coping with stress: calmodulin and calcineurin in model and pathogenic fungi. *Biochemical and Biophysical Research Communications.* 311:4, 1151-1157.

Lancaster, C. R. D. (2002). Succinate:quinone oxidoreductases: an overview. *BBA - Bioenergetics.* 1553:1, 1-6.

Lara, M., Blanco, L., Campomanes, M., Calva, E., Palacios, R. & Mora, J. (1982). Physiology of ammonium assimilation in *Neurospora crassa*. *The Journal of Bacteriology.* 150:1, 105.

Larive, C. K., Barding, G. A. & Dinges, M. M. (2015). NMR spectroscopy for metabolomics and metabolic profiling. *Analytical Chemistry.* 87:1, 133.

Lehrstuhl-Bioinformatik (2018) SIRIUS https://bio.informatik.uni-jena.de/software/sirius/ (Accessed: 26/11/18)

Leslie, J. F. & Summerell, B. A. (2006). *The Fusarium laboratory manual*. Oxford: Blackwell Publishing

Li, M., Chen, T., Gao, T., Miao, Z., Jiang, A., Shi, L., Ren, A. & Zhao, M. (2015). UDP-glucose pyrophosphorylase influences polysaccharide synthesis, cell wall components, and hyphal branching in *Ganoderma lucidum* via regulation of the balance between glucose-1-phosphate and UDP-glucose. *Fungal Genetics and Biology.* 82:C, 251-263.

Liang, X., Dickman, M. B. & Becker, D. (2014). Proline biosynthesis is required for endoplasmic reticulum stress tolerance in *Saccharomyces cerevisiae*. *Journal of Biological Chemistry.* 289:40, 27794-27806.

Lin, X., Alspaugh, J. A., Liu, H. & Harris, S. (2014). Fungal morphogenesis. *Cold Spring Harbor perspectives in medicine.* 5:2, a019679.

Lipschutz, J. H. & Mostov, K. E. (2002). Exocytosis: The Many Masters of the Exocyst. *Current Biology.* 12:6, R212-R214.

Liu, G., Zhang, M., Chen, X., Zhang, W., Ding, W. & Zhang, Q. (2015). Evolution of threonine aldolases, a diverse family involved in the second pathway of glycine biosynthesis. *Journal of Molecular Evolution.* 80:2, 102-107.

Liu, X., Wang, J., Xu, J. & Shi, Jr. (2014). FgIlv5 is required for branched-chain amino acid biosynthesis and full virulence in *Fusarium grammearum*. *Microbiology-SGM.* 160:4, 692-702.

Lomascolo, A., Asther, M., Navarro, D., Antona, C., Delattre, M. & Lesage-Meessen, L. (2001). Shifting the biotransformation pathways of L -phenylalanine into benzaldehyde by *Trametes suaveolens* CBS 334.85 using HP20 resin. *Letters in Applied Microbiology.* 32:4, 262-267.

Lopez-Moya, F., Kowbel, D., Nueda, M. J., Palma-Guerrero, J., Glass, N. L. & Lopez-Llorca, L. V. (2016). *Neurospora crassa* transcriptomics reveals oxidative stress and plasma membrane homeostasis biology genes as key targets in response to chitosan. *Molecular BioSystems.* 12:2, 391-403.

Lowe, R. G. T., Allwood, J. W., Galster, A. M., Urban, M., Daudi, A., Canning, G., Ward, J. L., Beale, M. H. & Hammond-Kosack, K. E. (2010). A Combined ^{1}H nuclear magnetic resonance and electrospray ionization mass spectrometry analysis to understand the basal metabolism of plant-pathogenic *Fusarium* spp. *Molecular Plant-Microbe Interactions.* 23:12, 1605-1618.

MacPherson, S., Larochelle, M. & Turcotte, B. (2006). A fungal family of transcriptional regulators: the zinc cluster proteins. *Microbiology and Molecular Biology Reviews.* 70:3, 583-604.

Maggio-Hall, L. A., Lyne, P., Wolff, J. A. & Keller, N. P. (2008). A single acyl-CoA dehydrogenase is required for catabolism of isoleucine, valine and short-chain fatty acids in *Aspergillus nidulans*. *Fungal Genetics and Biology.* 45:3, 180-189.

Marchler-Bauer, A., Lu, S., Anderson, J. B., Chitsaz, F., Derbyshire, M. K., Deweese-Scott, C., Fong, J. H., Geer, L. Y., Geer, R. C., Gonzales, N. R. *et al.* (2011). CDD: a Conserved

Domain Database for the functional annotation of proteins. *Nucleic Acids Research.* 39:Database issue, D225.

Marty, A. J., Broman, A. T., Zarnowski, R., Dwyer, T. G., Bond, L. M., Lounes-Hadj Sahraoui, A., Fontaine, J., Ntambi, J. M., Keleş, S., Kendziorski, C. *et al.* (2015). Fungal Morphology, Iron Homeostasis, and Lipid Metabolism Regulated by a GATA Transcription Factor in *Blastomyces dermatitidis* (*B. dermatitidis* SREB). 11:6, e1004959.

Marzluf, G. A. (1997). Molecular genetics of sulfur assimilation in filamentous fungi and yeast. *Annual Review of Microbiology.* 51:1, 73-96.

Matheus, N., Hansen, S., Rozet, E., Peixoto, P., Maquoi, E., Lambert, V., Noël, A., Frédérich, M., Mottet, D. & Tullio, P. (2014). An Easy, Convenient Cell and Tissue Extraction Protocol for Nuclear Magnetic Resonance Metabolomics. *Phytochemical Analysis.* 25:4, 342-349.

Matrix_Science (2018) Mascot http://www.matrixscience.com/search_form_select.html (Accessed: 12/12/18)

Mau, J.-L., Lin, H.-C. & Chen, C.-C. (2001). Non-volatile components of several medicinal mushrooms. *Food Research International.* 34:6, 521-526.

Metlin (2017) Metlin https://metlin.scripps.edu/landing_page.php?pgcontent=mainPage (Accessed: 21/11/17)

Meyer, V., Arentshorst, M., Flitter, S. J., Nitsche, B. M., Kwon, M. J., Reynaga-Peña, C. G., Bartnicki-Garcia, S., van den Hondel, C. A. M. J. J. & Ram, A. F. J. (2009). Reconstruction of signaling networks regulating fungal morphogenesis by transcriptomics. *Eukaryotic Cell.* 8:11, 1677-1691.

Miech, R. P. & Parks, R. E. (1965). Adenosine triphosphate: guanosine monophosphate phosphotransferase. *The Journal of Biological Chemistry.* 240, 351-357.

Miller, J. D. & Blackwell, B. A. (1986). Biosynthesis of 3-acetyldeoxynivalenol and other metabolites by *Fusarium culmorum* HLX 1503 in a stirred jar fermentor. *Canadian Journal of Botany.* 64:1, 1-5.

Miller, J. D. & MacKenzie, S. (2000). Secondary metabolites of *Fusarium venenatum* strains with deletions in the Tri5 gene encoding trichodiene synthetase. *Mycologia.* 92:4, 764-771.

Minenko, E., Vogel, R. F. & Niessen, L. (2014). Significance of the class II hydrophobin FgHyd5p for the life cycle of *Fusarium graminearum*. *Fungal Biology.* 118:4, 385-393.

Mio, T., Yabe, T., Arisawa, M. & Yamada-Okabe, H. (1998). The eukaryotic UDP-N-acetylglucosamine pyrophosphorylases. Gene cloning, protein expression, and catalytic mechanism. *Journal of Biological Chemistry.* 273:23, 14392.

Moss, M. O. & Thrane, U. (2004). *Fusarium* taxonomy with relation to trichothecene formation. *Toxicology Letters.* 153:1, 23-28.

Mouyna, I., Fontaine, T., Vai, M., Monod, M., Fonzi, W. A., Diaquin, M., Popolo, L., Hartland, R. P. & Latge, J. P. (2000). Glycosylphosphatidylinositol-anchored glucanosyltransferases play an active role in the biosynthesis of the fungal cell wall. *Journal of Biological Chemistry.* 275:20, 14882-14889.

Nakari-Setälä, T., Aro, N., Ilmén, M., Muñoz, G., Kalkkinen, N. & Penttilä, M. (1997). Differential expression of the vegetative and spore-bound hydrophobins of *Trichoderma reesei*: Cloning and characterization of the hfb2 gene. *VTT Publications.* 254, 1-15.

Nara, T., Hshimoto, T. & Aoki, T. (2000). Evolutionary implications of the mosaic pyrimidine-biosynthetic pathway in eukaryotes. *Gene.* 257:2, 209-222.

NCBI (2018) National Center for Biotechnology Information (US) https://www.ncbi.nlm.nih.gov/ (Accessed: 12/12/18)

Netz, D. J. A., Mascarenhas, J., Stehling, O., Pierik, A. J. & Lill, R. (2014). Maturation of cytosolic and nuclear iron–sulfur proteins. *Trends in Cell Biology.* 24:5, 303-312.

Nguyen, Q.-T., Merlo, M. E., Medema, M. H., Jankevics, A., Breitling, R. & Takano, E. (2012). Metabolomics methods for the synthetic biology of secondary metabolism. *FEBS Letters.* 586:15, 2177-2183.

Nielsen, K. F. & Larsen, T. O. (2015). The importance of mass spectrometric dereplication in fungal secondary metabolite analysis. *Frontiers in microbiology.* 6:71, 1-15.

Nierop Groot, M. N. & de Bont, J. A. M. (1998). Conversion of Phenylalanine to Benzaldehyde Initiated by an Aminotransferase in *Lactobacillus plantarum*. *Applied and Environmental Microbiology.* 64:8, 3009.

Nonlinear_Dynamics (2018) Progenesis QI for proteomics http://www.nonlinear.com/progenesis/qi-for-proteomics/how-it-works/ (Accessed: 11/12/18)

O'Donnell, K., Cigelnik, E. & Casper, H. H. (1998). Molecular phylogenetic, morphological, and mycotoxin data support reidentification of the Quorn mycoprotein fungus as *Fusarium venenatum*. *Fungal Genetics and Biology.* 23:1, 57-67.

Panagiotou, G., Christakopoulos, P. & Olsson, L. (2005a). The influence of different cultivation conditions on the metabolome of *Fusarium oxysporum*. *Journal of Biotechnology*. 118:3, 304-315.

Panagiotou, G., Christakopoulos, P., Villas-Boas, S. G. & Olsson, L. (2005b). Fermentation performance and intracellular metabolite profiling of *Fusarium oxysporum* cultivated on a glucose–xylose mixture. *Enzyme and Microbial Technology.* 36:1, 100-106.

Panagiotou, G., Kekos, D., Macris, B. J. & Christakopoulos, P. (2003). Production of cellulolytic and xylanolytic enzymes by *Fusarium oxysporum* grown on corn stover in solid state fermentation. *Industrial Crops & Products.* 18:1, 37-45.

Papagianni, M. (2004). Fungal morphology and metabolite production in submerged mycelial processes. *Biotechnology Advances.* 22:3, 189-259.

Parente, A. F. A., Bailao, A. M., Borges, C. L., Parente, J. A., Magalhaes, A. D., Ricart, C. A. O. & Soares, C. M. A. (2011). Proteomic Analysis Reveals That Iron Availability Alters the Metabolic Status of the Pathogenic Fungus *Paracoccidioides brasiliensis. PLoS One.* 6:7, e22810.

Park, G., Servin, J. A., Turner, G. E., Altamirano, L., Colot, H. V., Collopy, P., Litvinkova, L., Li, L., Jones, C. A., Diala, F.-G. *et al.* (2011). Global Analysis of Serine-Threonine Protein Kinase Genes in *Neurospora crassa*. *Eukaryotic Cell.* 10:11, 1553-1564.

Pasquali, M., Giraud, F., ric, Lasserre, J. P., Planchon, S., Hoffmann, L., Bohn, T. & Renaut, J. (2010). Toxin Induction and Protein Extraction from *Fusarium* spp. Cultures for Proteomic Studies. *Journal of Visualized Experiments.* 36, e1690.

Pasquali, M., Serchi, T., Renaut, J., Hoffmann, L. & Bohn, T. (2013). 2D difference gel electrophoresis reference map of a *Fusarium graminearum* nivalenol producing strain. *Electrophoresis.* 34:4, 505-509.

Patro, K., Basak, U., Mohapatra, A. & Gupta, N. (2014). Development of new medium composition for enhanced production of L-asparaginase by *Aspergillus flavus*. *Journal of Environmental Biology.* 35:1, 295-300.

Peñalosa-Ruiz, G., Aranda, C., Ongay-Larios, L., Colon, M., Quezada, H. & Gonzalez, A. (2012). Paralogous ALT1 and ALT2 retention and diversification have generated catalytically active and inactive aminotransferases in *Saccharomyces cerevisiae* (alanine aminotransferase diversification). *PLoS One.* 7:9, 1-13.

Pera, L. M. & Callieri, D. A. (1997). Influence of calcium on fungal growth, hyphal morphology and citric acid production in *Aspergillus niger*. *Folia Microbiologica.* 42:6, 551-556.

Phenomenex *EZ:Faast User Manual: EZ:Faast for free (Physiological) Amino Acid Analysis by GCMS.* Phenomenex. Available at: https://www.phenomenex.com/Home/TechnicalDocuments (Accessed: 14/5/15)

Philpott, C. C., Leidgens, S. & Frey, A. G. (2012). Metabolic remodeling in iron-deficient fungi. *Biochimica et Biophysica Acta.* 1823:9, 1509-1520.

Philpott, C. C. & Protchenko, O. (2008). Response to Iron Deprivation in *Saccharomyces cerevisiae*. *Eukaryotic Cell.* 7:1, 20.

Pinson-Gadais, L., Richard-Forget, F., Frasse, P., Barreau, C., Cahagnier, B., Richard-Molard, D. & Bakan, B. (2008). Magnesium represses trichothecene biosynthesis and modulates Tri5, Tri6, and Tri12 genes expression in *Fusarium graminearum*. *Mycopathologia.* 165:1, 51-59.

Polkinghorne, M. A. & Hynes, M. J. (1982). L-histidine utilization in *Aspergillus nidulans*. *Journal of Bacteriology.* 149:3, 931.

Postic, J., Cosic, J., Vrandecic, K., Jurkovic, D., Saleh, A. A. & Leslie, J. F. (2012). Diversity of *Fusarium* Species Isolated from Weeds and Plant Debris in Croatia. *Journal of Phytopathology.* 160:2, 76-81.

Prakash, P., Namasivayam, S. K. R., Swetha, S. & Bavani, L. (2015). Evaluation of insecticidal activity of *Fusarium venenatum* metabolites againstsf-21 cell lines. *International Journal of ChemTech Research.* 7:4, 2029-2033.

Puig, S., Askeland, E. & Thiele, D. J. (2005). Coordinated remodeling of cellular metabolism during iron deficiency through targeted mRNA degradation. *Cell.* 120:1, 99-110.

Putri, S. P., Yamamoto, S., Tsugawa, H. & Fukusaki, E. (2013). Current metabolomics: Technological advances. *Journal of Bioscience and Bioengineering.* 116:1, 9-16.

Rafferty, J. L., Siepmann, J. I. & Schure, M. R. (2011). Retention mechanism for polycyclic aromatic hydrocarbons in reversed-phase liquid chromatography with monomeric stationary phases. *Journal of Chromatography A.* 1218:51, 9183-9193.

Robson, G. D., Wiebe, M. G. & Trinci, A. P. J. (1991a). Involvement of Ca^{2+} in the regulation of hyphal extension and branching in *Fusarium graminearum* A3/5. *Experimental Mycology.* 15:3, 263-272.

Robson, G. D., Wiebe, M. G. & Trinci, A. P. J. (1991b). Low calcium concentrations induce increased branching in *Fusarium graminearum*. *Mycological Research.* 95:5, 561-565.

Rodríguez, J. M., Ruíz-Sala, P., Ugarte, M. & Peñalva, M. A. (2004). Fungal metabolic model for type I 3-methylglutaconic aciduria. *The Journal of Biological Chemistry.* 279:31, 32385.

Royer, J. C., Christianson, L. M., Yoder, W. T., Gambetta, G. A., Klotz, A. V., Morris, C. L., Brody, H. & Otani, S. (1999). Deletion of the trichodiene synthase gene of *Fusarium venenatum*: two systems for repeated gene deletions. *Fungal Genetics and Biology.* 28:1, 68-78.

Saint-Macary, M. E., Barbisan, C., Gagey, M. J., Frelin, O., Beffa, R., Lebrun, M. H. & Droux, M. (2015). Methionine biosynthesis is essential for infection in the rice blast fungus *Magnaporthe oryzae*. *PLoS One.* 10:4, 1-22.

Saint-Marc, C., Pinson, B., Coulpier, F., Jourdren, L., Lisova, O. & Daignan-Fornier, B. (2009). Phenotypic consequences of purine nucleotide imbalance in *Saccharomyces cerevisiae*. *Genetics.* 183:2, 529.

Saupe, S. J. (2000). Molecular Genetics of Heterokaryon Incompatibility in Filamentous Ascomycetes. *Microbiology and Molecular Biology Reviews.* 64:3, 489.

Scholtmeijer, K., Janssen, M. I., Gerssen, B., de Vocht, M. L., van Leeuwen, B. M., van Kooten, T. G., Wösten, H. A. & Wessels, J. G. (2002). Surface modifications created by using engineered hydrophobins. *Applied and Environmental Microbiology.* 68:3, 1367-1373.

Schorsch, C., Köhler, T., Andrea, H. & Boles, E. (2012). High-level production of tetraacetyl phytosphingosine (TAPS) by combined genetic engineering of sphingoid base biosynthesis and L-serine availability in the non-conventional yeast *Pichia ciferrii*. *Metabolic Engineering.* 14:2, 172-184.

Shakoury-Elizeh, M., Protchenko, O., Berger, A., Cox, J., Gable, K., Dunn, T. M., Prinz, W. A., Bard, M. & Philpott, C. C. (2010). Metabolic response to iron deficiency in *Saccharomyces cerevisiae*. *Journal of Biological Chemistry.* 285:19, 14823-14833.

Shakoury-Elizeh, M., Tiedeman, J., Rashford, J., Ferea, T., Demeter, J., Garcia, E., Rolfes, R., Brown, P. O., Botstein, D. & Philpott, C. C. (2004). Transcriptional remodeling in response to iron deprivation in *Saccharomyces cerevisiae*. *Molecular Biology of the Cell.* 15:3, 1233.

Shimizu, M., Fujii, T., Masuo, S. & Takaya, N. (2010). Mechanism of de novo branched-chain amino acid synthesis as an alternative electron sink in hypoxic *Aspergillus nidulans* cells. *Applied and Environmental Microbiology.* 76:5, 1507-1515.

Shindou, H. & Shimizu, T. (2009). Acyl-CoA: Lysophospholipid Acyltransferases. *Journal of Biological Chemistry.* 284:1-5.

Sieg, A. G. & Trotter, P. J. (2014). Differential contribution of the proline and glutamine pathways to glutamate biosynthesis and nitrogen assimilation in yeast lacking glutamate dehydrogenase. *Microbiological Research.* 169: , 709-716.

Simpson, D. R., Withers, J. M., Wiebe, M. G., Robson, G. D. & Trinci, A. P. J. (1998). Mutants with general growth rate advantages are the predominant morphological mutants to be isolated from the Quorn® production plant. *Mycological Research.* 102:2, 221-227.

Singh, A. & Mukhopadhyay, M. (2012). Overview of Fungal Lipase: A Review. *Applied Biochemistry and Biotechnology.* 166:2, 486-520.

Smedsgaard, J. & Nielsen, J. (2005). Metabolite profiling of fungi and yeast: from phenotype to metabolome by MS and informatics. *J Exp Bot.* 56:410, 273-286.

Son, H.-S., Hwang, G.-S., Kim, K. M., Kim, E.-Y., van den Berg, F., Park, W.-M., Lee, C.-H. & Hong, Y.-S. (2009). ^{1}H NMR-based metabolomic approach for understanding the fermentation behaviors of wine yeast strains. *Analytical Chemistry.* 81:3, 1137-1145.

Song, Z., Cox, R. J., Lazarus, C. M. & Simpson, T. J. (2004). Fusarin C biosynthesis in *Fusarium moniliforme* and *Fusarium venenatum*. *ChemBioChem.* 5:9, 1196-1203.

Stincone, A., Prigione, A., Cramer, T., Wamelink, M. M. C., Campbell, K., Cheung, E., Olin-Sandoval, V., Grüning, N.-M., Krüger, A., Tauqeer Alam, M. *et al.* (2015). The return of metabolism: biochemistry and physiology of the pentose phosphate pathway. *Biological Reviews.* 90:3, 927-963.

Strieker, M., Tanović, A. & Marahiel, M. A. (2010). Nonribosomal peptide synthetases: structures and dynamics. *Current Opinion in Structural Biology.* 20:2, 234-240.

Strijbis, K., Vaz, F. M. & Distel, B. (2010). Enzymology of the carnitine biosynthesis pathway. *Life.* 62:5, 357-362.

Suzuki, T. & Iwahashi, Y. (2012). Comprehensive gene expression analysis of type B trichothecenes. *Journal of Agricultural and Food Chemistry.* 60:37, 9519-9527.

Takagi, M., Yamakawa, H., Watanabe, T., Suga, T. & Yamada, J. (2003). Inducible expression of long-chain acyl-CoA hydrolase gene in cell cultures. *Molecular and Cellular Biochemistry.* 252:1, 379-385.

Takahashi, H., Kamakari, K., Goto, T., Hara, H., Mohri, S., Suzuki, H., Shibata, D., Nakata, R., Inoue, H., Takahashi, N. *et al.* (2015). 9-Oxo-10(E),12(Z),15(Z)-Octadecatrienoic Acid Activates Peroxisome Proliferator-Activated Receptor α in Hepatocytes. *Lipids.* 50:11, 1083-1091.

Takeshita, N., Evangelinos, M., Zhou, L., Serizawa, T., Somera-Fajardo, R. A., Lu, L., Takaya, N., Nienhaus, G. U. & Fischer, R. (2017). Pulses of Ca^{2+} coordinate actin assembly and exocytosis for stepwise cell extension. *Proceedings of the National Academy of Sciences of the United States of America.* 114:22, 5701-5706.

Tavsan, Z. & Ayar Kayali, H. (2015). The Variations of Glycolysis and TCA Cycle Intermediate Levels Grown in Iron and Copper Mediums of *Trichoderma harzianum*. *Applied Biochemistry and Biotechnology.* 176:1, 76-85.

Taylor, R. D., Saparno, A., Blackwell, B., Anoop, V., Gleddie, S., Tinker, N. A. & Harris, L. J. (2008). Proteomic analyses of *Fusarium graminearum* grown under mycotoxin-inducing conditions. *Proteomics.* 8:11, 2256-2265.

Tchuenbou-Magaia, F. L., Norton, I. T. & Cox, P. W. (2009). Hydrophobins stabilised air-filled emulsions for the food industry. *Food Hydrocolloids.* 23:7, 1877-1885.

Theodoridis, G., Gika, H. G. & Wilson, I. D. (2008). LC-MS-based methodology for global metabolite profiling in metabonomics/metabolomics. *Trends in Analytical Chemistry.* 27:3, 251-260.

Thirach, S., Cooper, J. C. R., Vanittanakom, P. & Vanittanakom, N. (2007). The Copper, Zinc Superoxide Dismutase Gene of *Penicillium marneffei*: Cloning, Characterization, and Differential Expression During Phase Transition and Macrophage Infection. *Medical Mycology.* 45:5, 409-417.

Thomas, D. & Surdin-Kerjan, Y. (1997). Metabolism of sulfur amino acids in *Saccharomyces cerevisiae*. *Microbiology and Molecular Biology Reviews.* 61:4, 503.

Tran, L. M., Bang, S. H., Yoon, J., Kim, Y.-H. & Min, J. (2016). Effect of acid trehalase (ATH) on impaired yeast vacuolar activity. *Enzyme and Microbial Technology.* 93-94:44-50.

Trapp, M. A., Kai, M., Mithöfer, A. & Rodrigues-Filho, E. (2015). Antibiotic oxylipins from Alternanthera brasiliana and its endophytic bacteria. *Phytochemistry.* 110:C, 72-82.

Trinci, A. P. J. (1994). Evolution of the Quorn myco-protein fungus, *Fusarium graminearum* A3/5. *Microbiology.* 140:9, 2181-2188.

Tylová, T., Kolařík, M. & Olšovská, J. (2011). The UHPLC-DAD fingerprinting method for analysis of extracellular metabolites of fungi of the genus *Geosmithia* (Acomycota: Hypocreales). *Analytical and Bioanalytical Chemistry.* 400:9, 2943-2952.

Ujiie, Y., Tanaka, W., Hanaoka, K., Harada, R., Kayanuma, M., Shoji, M., Murakawa, T., Ishida, T., Shigeta, Y. & Hayashi, H. (2017). Molecular mechanism of the reaction specificity

in threonine synthase: importance of the substrate conformations. *Journal of Physical Chemistry B.* 121:22, 5536-5543.

Ulm, E. H., Bohme, R. & Kohlhaw, G. (1972). α-Isopropylmalate Synthase from Yeast: Purification, Kinetic Studies, and Effect of Ligands on Stability. *The Journal of Bacteriology.* 110:3, 1118.

Valo, H. K., Laaksonen, P. H., Peltonen, L. J., Linder, M. B., Hirvonen, J. T. & Laaksonen, T. J. (2010). Multifunctional hydrophobin: Toward functional coatings for drug nanoparticles. *ACS Nano.* 4:3, 1750-1758.

van Maris, A. J. A., Luttik, M. A. H., Winkler, A. A., van Dijken, J. P. & Pronk, J. T. (2003). Overproduction of threonine aldolase circumvents the biosynthetic role of pyruvate decarboxylase in glucose-limited chemostat cultures of *Saccharomyces cerevisiae*. *Applied and Environmental Microbiology.* 69:4, 2094-2099.

Vaniya, A. & Fiehn, O. (2015). Using fragmentation trees and mass spectral trees for identifying unknown compounds in metabolomics. *Trends in Analytical Chemistry.* 69:52-61.

Vasavada, A. B. & Hsieh, D. P. (1988). Effects of metals on 3-acetyldeoxynivalenol production by *Fusarium graminearum* R2118 in submerged cultures. *Applied & Environmental Microbiology.* 54:4, 1063-1065.

Villas-Boas, S. G., Hojer-Pedersen, J., Akesson, M., Smedsgaard, J. & Nielsen, J. (2005). Global metabolite analysis of yeast: evaluation of sample preparation methods. *Yeast.* 22:14, 1155-1169.

Voet, D. & Voet, J. G. (2004). *Biochemistry.* 3rd ed.. edn. New York Chichester: Wiley

Vogel, H. J. (1956). A convenient growth medium for *Neurospora* (medium N). *Microbial Genetics Bulletin.* 13, 42-44.

Wadman, M. W., van Zadelhoff, G., Hamberg, M., Visser, T., Veldink, G. A. & Vliegenthart, J. F. G. (2005). Conversion of linoleic acid into novel oxylipins by the mushroom *Agaricus bisporus*. *Lipids.* 40:11, 1163-1170.

Wang, Y., Li, D., Gao, J., Li, X., Zhang, R., Jin, X., Hu, Z., Zheng, B., Persson, S. & Chen, P. (2017). The 2′- O -methyladenosine nucleoside modification gene OsTRM13 positively regulates salt stress tolerance in rice. *Journal of Experimental Botany.* 68:7, 1479-1491.

Wang, Y., Liu, W. & Bao, J. (2012). Repeated batch fermentation with water recycling and cell separation for microbial lipid production. *Frontiers of Chemical Science & Engineering.* 6:4, 453-460.

Weiss, R. L. & Anterasian, G. P. (1977). Control of arginine metabolism in *Neurospora*. Induction of ornithine aminotransferase. *Journal of Biological Chemistry.* 20, 6974-6980.

Wiebe, M. G. (2002a). Myco-protein from *Fusarium venenatum*: a well-established product for human consumption. *Applied Microbiology and Biotechnology.* 58:4, 421-427.

Wiebe, M. G. (2004). Quorn™ myco-protein - Overview of a successful fungal product. *Mycologist.* 18:1, 17-20.

Wiebe, M. G. (2002b). Siderophore production by *Fusarium venenatum* A3/5. *Biochemical Society Transactions.* 30:4, 696-698.

Wiebe, M. G., Blakebrough, M. L., Craig, S. H., Robson, G. D. & Trinci, A. P. J. (1996a). How do highly branched (colonial) mutants of *Fusarium graminearum* A3/5 arise during Quorn® myco-protein fermentations? *Microbiology.* 142:3, 525-532.

Wiebe, M. G., Robson, G. D., Oliver, S. G. & Trinci, A. P. J. (1996b). pH oscillations and constant low pH delay the appearance of highly branched (colonial) mutants in chemostat cultures of the Quorn® myco- protein fungus, *Fusarium graminearum* A3/5. *Biotechnology and Bioengineering.* 51:1, 61-68.

Wiebe, M. G., Robson, G. D. & Trinci, A. P. J. (1998). Peptone changes the timing and accumulation of morphological mutants of the Quorn® myco-protein fungus *Fusarium graminearum* A3/5 in glucose-limited chemostat cultures. *FEMS Microbiology Letters.* 169:1, 23-28.

Wiebe, M. G., Robson, G. D., Trinci, A. P. J. & Oliver, S. G. (1992). Characterization of morphological mutants generated spontaneously in glucose-limited, continuous flow cultures of *Fusarium graminearum* A3/5. *Mycological Research.* 96:7, 555-562.

Wiebe, M. G. & Trinci, A. P. J. (1991). Dilution rate as a determinant of mycelial morphology in continuous culture. *Biotechnology and Bioengineering.* 38:1, 75-81.

Winkelmann, G. (2007). Ecology of siderophores with special reference to the fungi. *BioMetals.* 20:3, 379-392.

Wishart, D. S. (2008). Quantitative metabolomics using NMR. *TrAC Trends in Analytical Chemistry.* 27:3, 228-237.

Wishart, D. S., Feunang, Y. D., Marcu, A., Guo, A. C., Liang, K., Vázquez-Fresno, R., Sajed, T., Johnson, D., Li, C., Karu, N. *et al.* (2018a). HMDB 4.0: the human metabolome database for 2018. *Nucleic Acids Research.* 46:D1, D608-D617.

Wishart, D. S., Feunang, Y. D., Marcu, A., Guo, A. C., Liang, K., Vázquez-Fresno, R., Sajed, T., Johnson, D., Li, C., Karu, N. *et al.* (2018b) Human Metabolome Database - valylglutamate http://www.hmdb.ca/metabolites/HMDB0029126#identification (Accessed: 19/11/18)

Xiao, C., Zheng, L., Su, G. & Zhao, M. (2014). Effect of solution p H and activated carbon dosage on the decolourization ability, nitrogen components and antioxidant activity of peanut meal hydrolysate. *International Journal of Food Science & Technology.* 49:12, 2571-2577.

Xiao, J. F., Zhou, B. & Ressom, H. W. (2012). Metabolite identification and quantitation in LC-MS/MS-based metabolomics. *Trends in Analytical Chemistry.* 32, 1-14.

Xie, Q.-N., Jia, L.-J., Wang, Y.-Z., Song, R.-T. & Tang, W.-H. (2017). High-resolution gene profiling of infection process indicates serine metabolism adaptation of *Fusarium graminearum* in host. *Science Bulletin.* 62:11, 758-760.

Xu, H., Andi, B., Qian, J., West, A. H. & Cook, P. F. (2006). The α-aminoadipate pathway for lysine biosynthesis in fungi. *Cell Biochemistry and Biophysics.* 46:1, 43-64.

Xu, Q., Liu, J., Song, H., Zou, T., Liu, Y. & Zhang, S. (2013). Formation mechanism of volatile and non-volatile compounds in peptide–xylose Maillard reaction. *Food Research International.* 54:1, 683-690.

Ye, K., Jin, S. & Shimizu, K. (1996). Cell recycle and broth reuse fermentation with cross-flow filtration and ion-exchange resin. *Journal of Chemical Technology and Biotechnology.* 66:3, 223-226.

Yin, W. & Keller, N. P. (2011). Transcriptional regulatory elements in fungal secondary metabolism. *The Journal of Microbiology.* 49:3, 329-339.

Yokoyama, K., Shimizu, F. & Setaka, M. (2000). Simultaneous separation of lysophospholipids from the total lipid fraction of crude biological samples using two-dimensional thin-layer chromatography. *Journal Of Lipid Research.* 41:1, 142-147.

Zabriskie, T. M. & Jackson, M. D. (2000). Lysine biosynthesis and metabolism in fungi. *Natural Product Reports.* 17:1, 85-97.

Zhang, C., Meng, X., Gu, H., Ma, Z. & Lu, L. (2018). Predicted Glycerol 3-phosphate dehydrogenase homologs and the glycerol kinase GlcA coordinately adapt to various carbon sources and osmotic stress in *Aspergillus fumigatus*. *G3: Genes, Genomes, Genetics.* 8:7, 2291-2299.

Zhang, Y., Morar, M. & Ealick, S. (2008). Structural biology of the purine biosynthetic pathway. *Cellular and Molecular Life Sciences.* 65:23, 3699-3724.

Zhang, Y., Venkitasamy, C., Pan, Z. & Wang, W. (2013). Recent developments on umami ingredients of edible mushrooms - A review. *Trends in Food Science and Technology.* 33:2, 78-92.

Zhao, B., Tomoda, Y., Mizukami, H. & Makino, T. (2015). 9-Oxo-(10E,12E)-octadecadienoic acid, a cytotoxic fatty acid ketodiene isolated from eggplant calyx, induces apoptosis in human ovarian cancer (HRA) cells. *Journal of Natural Medicines.* 69:3, 296-302.

Zhao, G., Hou, L., Yao, Y., Wang, C. & Cao, X. (2012). Comparative proteome analysis of *Aspergillus oryzae* 3.042 and *A. oryzae* 100–8 strains: Towards the production of different soy sauce flavors. *Journal of Proteomics.* 75:13, 3914-3924.

Zheng, D., Zhang, S., Zhou, X., Wang, C., Xiang, P., Zheng, Q., Xu, J.-R. & Lee, Y.-W. (2012). The FgHOG1 Pathway Regulates Hyphal Growth, Stress Responses, and Plant Infection in *Fusarium graminearum*. *PLoS One.* 7:11, 1-12.

Zinedine, A., Soriano, J. M., Moltó, J. C. & Mañes, J. (2007). Review on the toxicity, occurrence, metabolism, detoxification, regulations and intake of zearalenone: An oestrogenic mycotoxin. *Food and Chemical Toxicology.* 45:1, 1-18.